

Stratigraphy, Depositional Systems, Diagenesis, and Stable Isotope  
Geochemistry of the Paradise Formation (Late Mississippian), Big  
Hatchet Mountains, Hidalgo County, New Mexico

by

David J. Sivils, B.S., M.S.

Geotechnical  
Information Center

Submitted in Partial Fulfillment  
of the Requirements for the Degree of  
Doctor of Philosophy in Geology

Department of Earth and Environmental Sciences  
New Mexico Institute of Mining and Technology

Socorro, New Mexico

December, 1997

**NMIMT**  
**Library**  
**SOCORRO, NM**

MAY 14 1998

This work is dedicated to my family and to Dr. David V. LeMone, professor, mentor, friend, and colleague, who inspired me and kindled my interest in carbonates.

## ACKNOWLEDGMENTS

First and foremost I would like to thank my parents, Dr. Jimmy C. Sivils and Marcia E. Sivils for their unwavering financial and emotional support throughout the duration of this project. I would like to thank my advisor, Dr. D.B. Johnson, for his support, encouragement, numerous suggestions and conversations throughout the duration of this project. To my other committee members, Dr.'s. Charles Chapin, Andy Campbell, Peter Mozley, and Bill Chavez, for their time and suggestions helping me improving this dissertation. For help in editing and greatly improving the readability of to this work and improving my ability with the written word, my thanks to Randy Scasny, and to Dana Rowan of Texaco for a final go through and spelling check.

I would like to thank the following organizations for their financial support: New Mexico Bureau of Mines and Mineral Resources, New Mexico Geological Society, ARCO Oil and Gas Company, Unocal Oil and Gas Company's science and technology division, and the Houston Geological Society.

For input and stimulating conversations about the Paradise Formation and geology in general I express my thanks to Dr. Gus Armstrong of the United States Geological Survey, and Dr. Frank Kottlowski of the New Mexico Bureau of Mines and Mineral Resources.

I would like to express my gratitude to those individuals who helped me with the fieldwork to Ed Fry, Mark Lambert, Bruce Hallett, Chris Beck, and my brother Steve.

Finally, I would like to express my thanks all my friends who have helped me through this in many ways.

## Table of Contents

List of Figures .....	x
List of Tables and Equations .....	xvi
Abstract.....	xvii
Introduction.....	1
Purpose.....	1
Location .....	1
Big Hatchet Mountains .....	4
Geologic Setting .....	4
Methods of Study.....	8
Field .....	8
Laboratory.....	8
Petrography.....	8
Clastic Rocks .....	9
Carbonate Rocks.....	9
Cathodoluminescence Petrography .....	10
Stable Isotopes.....	10
Previous Work .....	12
Stratigraphic.....	12
Isotopic.....	13
Stratigraphy.....	15
Lithostratigraphy.....	17

Lithostratigraphy .....	17
Horse Pasture Canyon Section.....	17
New Well draw Section.....	17
Chaney Canyon Section.....	19
Lithostratigraphy: Synopsis.....	19
Lithofacies .....	27
Carbonates .....	27
Lime Mudstone Lithofacies .....	27
Bryozoan-Brachiopod Wackestone Lithofacies.....	29
Pelmatozoan-Brachiopod Packstone Lithofacies.....	30
Abraded Grainstone Lithofacies .....	32
Oolitic Grainstone Lithofacies.....	33
Dolomudstone Lithofacies.....	34
Siliciclastics.....	35
Sandstone Lithofacies.....	35
Siltstone Lithofacies .....	35
Terrigenous Mudstone Lithofacies .....	37
Diversity.....	39
Biotic Diversity and Environmental Analysis .....	39
Other Measures of Environmental Stability.....	40
Bias, Biotic Diversity and the Rock Record.....	40
Diversity in the Paradise Formation .....	41
Diversity Trends and Lithofacies.....	47

Environmental Interpretations .....	50
Previous Environmental Interpretation .....	50
Lithofacies Interpretations .....	50
Disseminated Detrital Quartz .....	50
Carbonate Lithofacies .....	51
Lime Mudstone Lithofacies .....	51
Bryozoan-Brachiopod Wackestone Lithofacies .....	53
Pelmatozoan-Brachiopod Packstone Lithofacies .....	55
Abraded Skeletal Grainstone Lithofacies .....	57
Oolitic Grainstone Lithofacies .....	58
Dolomudstone Lithofacies .....	58
Detrital Clastic Lithofacies .....	60
Siltstone Lithofacies .....	60
Sandstone Lithofacies .....	61
Terrigenous Mudstone Lithofacies .....	61
Facies Patterns .....	62
Vertical Facies Patterns .....	62
Lateral Facies Patterns .....	64
Depositional Models .....	64
Modern Carbonate Depositional Systems .....	67
Bahamas .....	67
Bahamas and the Paradise Formation.....	67
Persian Gulf .....	69

Persian Gulf and the Paradise Formation .....	70
Conceptual Models for Carbonate Deposition .....	72
Epeiric Sea, Clear Water Carbonate Depositional Model .....	74
Carbonate Ramps.....	75
Punctuated Aggradational Cycles (PAC).....	78
Depositional Systems and The Paradise Formation .....	79
Detrital Clastics .....	80
Cyclicality .....	85
Cycle Duration.....	86
Causal Mechanisms of Paradise Cyclicality.....	89
Global Comparisons .....	92
Cyclicality in the Paradise Formation: Synthesis .....	93
Diagenesis.....	94
Diagenetic Features.....	94
Neomorphism .....	94
Neomorphic Textures in the Paradise Formtion.....	95
Aggrading Neomorphic Textures and Matrix.....	97
Aggrading Neomorphism in the Paradise Formation .....	97
Micritization .....	97
Micritization in the Paradise Formation .....	100
Dissolution.....	101
Dissolution in the Paradise Formation.....	101
Compaction.....	101

Calcite Cements .....	105
Low-Magnesium Sparry Calcite Cements .....	106
Ferroan Sparry Calcite Cements .....	109
Dolomitization .....	110
Dolomitization Models .....	112
Silicification and Silica Cements .....	113
Silicification .....	113
Silica Cements .....	114
General Paragenesis .....	117
Integration of Diagenesis and Lithofacies .....	117
Porosity and Permeability .....	119
Stable Isotopes .....	120
Approach .....	120
Data .....	121
Data Distribution, Interpretation and Models .....	124
Water Composition .....	133
Carbonate Component Isotopic Data .....	136
Stable Isotopes and Diagenesis: Synthesis .....	142
Conclusions and Summary .....	144
References Cited .....	149
Appendices .....	161
A-Detailed Graphic Stratigraphic Sections .....	161
Measured Section Legend .....	162



Horse Pasture Canyon Measured Section Big Hatchet Mountains, Hidalgo County, New Mexico .....	163
New Well draw Measured Section Big Hatchet Mountains, Hidalgo County, New Mexico .....	169
Chaney Canyon Measured Section Big Hatchet Mountains, Hidalgo County, New Mexico .....	176
B-Detailed Written Descriptions of Stratigraphy .....	177
Horse Pasture Measured Section, Big Hatchet Mountains .....	178
New Well Draw Measured Section, Big Hatchet Mountains .....	183
Chaney Canyon Measured Section, Big Hatchet Mountains .....	192
C-Thin Section Point Count Data .....	194
D-Diversity Data .....	202
E-Stable Isotope Data .....	207
Vita .....	209

Data Disk in Pocket

## LIST OF FIGURES

Figure 1	Generalized location map of the southwestern United States and northern Mexico showing the known distribution of the Paradise Formation.....	2
Figure 2	Map showing the location of the Big Hatchet Mountains and the locations of measured sections used in this study .....	3
Figure 3	Generalized stratigraphic column for the Big Hatchet Mountains. Figure also shows the relationship of the Paradise Formation to both the underlying Escabrosa Group and the overlying Horquilla Limestone .....	5
Figure 4	Generalized geologic and tectonic history chart for southwestern New Mexico and the surrounding region. Note time of Paradise deposition in relation to ongoing tectonic events in the region .....	6
Figure 5	Age and correlation chart for the Paradise Formation .....	15
Figure 6	View Looking North-Northwest of the Paradise Formation in the Big Hatchet Mountains. Photograph shows the very distinctive weathering profile and coloration of the Paradise. Lower white line marks the contact with the underlying Escabrosa Group. The upper white dashed line marks the contact with the overlying Horquilla Limestone .....	16
Figure 7	Simplified geologic map of Horse Pasture Canyon region showing the location of measured section .....	18
Figure 8	Simplified geologic map of New Well draw region showing the location of measured section.....	19
Figure 9	Simplified geologic map of the Chaney Canyon region showing the location of measured section.....	21
Figure 10	Generalized stratigraphic column of the Paradise Formation from the Big Hatchet Mountains divided into three informal members. Member boundaries are shown and dashed lines. See Text for descriptions of each member .....	23
Figure 11	Outcrop photograph of the Paradise Formation showing typical sheet-like bedding geometries.....	24

Figure 12 Correlation between Paradise Formation members in the Big Hatchet Mountains. Note the similarity between member thickness and basic lithologies at each section.....	25
Figure 13 Generalized stratigraphic cross section of the Paradise Formation showing members and the overall continuity of the members across the known distribution of the Paradise.....	26
Figure 14 Photomicrograph of a typical lime mudstone from the Paradise Formation.....	27
Figure 15 Field photograph of the lime mudstone lithofacies in the Paradise Formation....	28
Figure 16 Photomicrograph of a typical bryozoan-brachiopod wackestone lithofacies from the Paradise Formation .....	30
Figure 17 Photomicrograph of a typical pelmatozoan-brachiopod packstone lithofacies from the Paradise Formation .....	31
Figure 18 Photomicrograph of a typical abraded grainstone lithofacies. Note the high degree of overpacking evident in this sample. This is typical of this lithofacies throughout the Paradise Formation.....	32
Figure 19 Photomicrograph of oolitic grainstone lithofacies from the Paradise Formation. The radial fibrous internal fabric of the ooids is clearly visible. This is characteristic of all the ooids from the Paradise.....	34
Figure 20 Ternary plot of sandstones from the Paradise Formation. All data points plot directly on the Q pole of the diagram. Multiple data points plotting on the Q pole are plotted above the pole.....	36
Figure 21 Quartz sandstone from the Paradise Formation. In this example, the sandstone is composed entirely of detrital quartz, which is cemented with quartz overgrowths. Also present is a detrital zircon, labeled Z on the image.....	37
Figure 22 Photomicrograph of a typical siltstone from the Paradise Formation. The dark grains are peloidal material. Light red to pink intergranular regions are sparry calcite.....	38

Figure 23 Plots of relative diversity with respect to stratigraphic position. Note the overall consistency of the data sets before and after correcting for transported grains.....	42
Figure 24 Diagram of an idealized carbonate cycle in the Paradise Formation showing the general pattern of variation in biotic diversity through a cycle with respect to lithology. Diversity curve represents average values for each lithofacies.....	49
Figure 25 Graphic illustration of an ideal cycle from the Paradise Formation. Sea level curve indicate relative water depths, and shows the shallowing-upwards character of the cycles .....	63
Figure 26 Vertical lithofacies relationship of the single occurrence of dolomudstone in the Paradise Formation at Horse Pasture Canyon section. The dolomite is the capping unit of cycle number 4. ....	65
Figure 27 Interpretative depositional cross section of the Paradise Formation at any given point in time showing the lateral distribution of facies presented in Figure 25. Measured sections used in this study can be located at any point along the section at any point in time. Symbols correspond to those used in Figure 25 and those in Appendix A.....	66
Figure 28 Simplified facies map off of Andros Island, Bahamas.....	68
Figure 29 Simplified facies map for the Persian Gulf. Area shown is offshore Qatar. The overall trend is one of increasing lime mud and terrigenous mud as waters become deeper, reflecting less winnowing toward the center of the basin.....	71
Figure 30 Paleogeographic map showing the general configuration of the Pedregosa basin during the deposition of the Paradise Formation. The paleogeographic position is similar to the present day Persian Gulf, with prevailing winds from the North-Northeast.....	73
Figure 31 Theoretical model for carbonate deposition in an epicontinental sea proposed by Irwin, 1965 and Shaw, 1964 .....	74
Figure 32 Subdivisions of a carbonate ramp and associated facies.....	77
Figure 33 Interpretative depositional cross section of the Paradise Formation at any given point in time showing the lateral distribution of facies presented in Figure 25.	

Section shows the development of a very shallowly, eastward dipping ramp during Paradise time. .... 81

Figure 34 Idealized carbonate ramp illustrating the general concept of cyclic and reciprocal sedimentation. During relative highstands in sea level detrital clastics are trapped in a shoreward position. Following a relative drop in sea level the clastics migrate across the exposed shelf and are distributed in the basin by marine current and wave action..... 83

Figure 35 Interpretive depositional cross sections illustrating cyclic and reciprocal sedimentation in the Paradise Formation. The top illustration depicts deposition during a relative highstand in sea level. The lower illustration depicts deposition during the subsequent relative lowstand in sea level. During this phase is when the detrital clastics are distributed across the shelf and into the basin..... 84

Figure 36 Sequence stratigraphic hierarchy established for the Paradise Formation. Higher order sequences reflect cyclic sedimentation governed by glacioeustasy and local tectonism. Lower order sequences reflect depositional patterns governed by regional and continental tectonics related to the assemblage of Pangea..... 88

Figure 37, A and B Examples of two types of microspar development in the Paradise Formation. Example A shows patches forming in a lime mudstone. Example B shows microspar developing along the boundaries between skeletal material and micritic matrix ..... 98

Figure 38 Photomicrograph showing development of pseudospar in an oolitic wackestone. Clearly visible in the lower image are patches of micrite floating in the pseudospar ..... 99

Figure 39 Photomicrograph of well developed micritic rim on a gastropod. Subsequent dissolution of the gastropod shell left an outer and inner micritic rim in the original shape of the mollusk. Fracturing of outer rim suggests early compaction following dissolution, but prior to cementation ..... 100

Figure 40 Ooid with original aragonitic nucleus dissolved and replaced by pore-filling ferroan spar cement. This figure also shows the preservation of the ooid's internal fabric indicating the ooid was originally precipitated as calcite ..... 102

Figure 41 Plot of the range of intergranular volumes (porosity) from the main carbonate rock types in the Paradise Formation. Intergranular volume is calculated as the percent sparry calcite filling intergranular void space based on the total volume of rock. .... 104

Figure 42 Plot showing the stratigraphic distribution of freshwater cements in the Paradise Formation. Break at 72 meters does not correspond to any recognizable stratigraphic division, or surface..... 107

Figure 43 Photomicrograph of an oolitic grainstone showing freshwater, isopachous, sparry calcite cements on ooids with the pore spaces between the isopachous cements filled with ferroan calcite cement..... 108

Figure 44 Photomicrograph of abraded grainstone showing ferroan calcite,(stained blue) pore-filling cement with a poikilotopic texture. Also apparent in this image is evidence of early compaction, resulting in the crushing and interpenetration of grains prior to cementation. .... 108

Figure 45 Photomicrograph of a replacement dolomite. Dolomite is replacing a lime mudstone..... 111

Figure 46 Silica cemented quartz sandstone from the Paradise Formation. Faint dust rings are present on some of the grains indicating the boundary between the grain and the quartz overgrowth ..... 115

Figure 47 Generalized paragenetic sequence for the Paradise Formation showing relationship of diagenesis to lithofacies in the Paradise Formation. Note lighter shading indicates some uncertainty of timing and overlap of features..... 118

Figure 48 Isotopic distribution of whole rock samples from the Paradise Formation..... 122

Figure 49 Distribution of whole rock isotopic values from this study compared to published Mississippian isotopic data ..... 123

Figure 50 Isotopic distribution showing possible alteration trend assuming a single diagenetic event ..... 125

Figure 51 Plot showing the separation of data into two fields based on the stratigraphic order of the data..... 127

Figure 52 Plot showing the relationship between rock type and isotopic composition..... 129

Figure 53 Plot showing the stratigraphic distribution of stable isotopes from the Horse Pasture Canyon measured section. Noted on the plot is the division between fields 1 and 2 on Figure 51 ..... 131

Figure 54 Isotopic distribution from the Paradise Formation with a meteoric calcite line. This line indicates the equilibrium oxygen value between calcite and water (~-6‰)..... 134

Figure 55 Temperature and  $\delta^{18}\text{O}$  ( $\text{H}_2\text{O}$ ) SMOW relationship for the Paradise Formation calculated using an equilibrium calcite value of -6‰ and the fractionation equation for calcite-water of Friedman and O'Neil, 1977..... 134

Figure 56 Distribution of carbonate components with respect to whole rock isotopic data. 138

Figure 57 Distribution of carbonate components and their respective host sample. In all instances the components are altered to some degree from the host material ..... 138

Figure 58 Plot showing the distribution of Mississippian brachiopods from published sources as compared to those analyzed from the Paradise Formation..... 139

Figure 59 Photomicrograph taken under cathodoluminescence of a brachiopod shell showing the degree of fracturing and shell degradation assumed as the cause of isotope exchange between diagenetic fluids and brachiopods ..... 140

## LIST OF TABLES AND EQUATIONS

Table 1 Statistical data from relative diversity of member A .....	45
Table 2 Statistical data from relative diversity of member B.....	46
Table 3 Statistical data from relative diversity of member C.....	47
Table 4 Typical durations associated with common sequence stratigraphic orders of cyclicality.....	87
Equation 1. Calcite-water fractionation equation of Friedman and O'Neil (1977).....	133



## ABSTRACT

The Paradise Formation is exposed in a distinctive thin belt along the eastern flank of the Big Hatchet Mountains. It is a mixed carbonate-clastic sequence situated between the underlying Lower Mississippian Escabrosa Group and the overlying Pennsylvanian/ Permian Horquilla Limestone. The Paradise measures 130 meters in thickness and can be informally divided into three distinctive members that are traceable not only in the Big Hatchets but over the known extent of the formation. Each member is composed of a limited number of distinctive lithofacies, which are repeated in some 30 coarsening upward cycles ranging from 2 to 12 meters in thickness. Although the average biotic diversity is rather uniform diversity does vary greatly at the meter scale. These wide variations of in diversity are consistent with the cyclic nature of sedimentation reflected in the vertical development of lithofacies. Interpretations of lithofacies coupled with relative biotic diversity data suggest that deposition of the Paradise Formation occurred on a shallowly dipping carbonate ramp. Carbonate and detrital clastic sedimentation was controlled by relative changes in sea level. Paleogeographic reconstructions and the presence of eolian derived quartz sands and silts redeposited in a marine setting suggest arid conditions existed during Paradise time. The best modern analog for the Paradise is the Persian Gulf, both in regard to facies types and their distribution as well as the overall geographic setting.

Glacioeustasy acted as the primary control on sea level during Paradise time and governed sedimentation patterns and development of cycles within the Paradise Formation. Three scales of cycles have been identified within the Paradise forming a

sequence stratigraphic hierarchy or a single 2<sup>nd</sup> order cycle, three 3<sup>rd</sup> order cycles consisting of the three members and 30 4<sup>th</sup>/5<sup>th</sup> order scale cycles. The high frequency 4<sup>th</sup>/5<sup>th</sup> order cycles are of similar duration to coeval cycles described from the Black Warrior Basin and from Britain. The influence of eustasy also acted to control the distribution of coarse-grained detrital clastics through cyclic reciprocal sedimentation.

Diagenesis significantly altered the sediments and rocks of the Paradise Formation. Two types of sparry calcite cements are recognizable, a low-magnesium calcite spar and a ferroan calcite spar. The low-magnesium spar cement is restricted to the lower part of the section, while the ferroan cement is found throughout the section. Petrographic and compaction data suggest that the low-magnesium calcite cements are early and likely reflect freshwater diagenesis, while the ferroan cements are most likely formed later during burial diagenesis of the Paradise at a depth of at least 600 m. Water compositions derived from isotopic data are compatible with both of these interpretations, and suggest that the low-magnesium calcite spar was precipitated from waters with an isotopic composition of  $-4\text{‰}\delta^{18}\text{O}(\text{H}_2\text{O})$  SMOW, and that the ferroan spar was precipitated from waters with an isotopic composition of  $-1\text{‰}\delta^{18}\text{O}(\text{H}_2\text{O})$  SMOW. Dolomitization and silicification are extremely rare in the Paradise. All of these diagenetic processes acted to reduce the porosity and permeability of the Paradise to near zero effectively rendering the Paradise useless as a reservoir for any type of fluid. The pervasive nature of diagenesis is recognizable in the stable isotopic signatures of whole rock and carbonate components. Even carbonate components composed of more stable low-magnesium calcite, such as brachiopods, show effects of diagenesis and isotopic alteration. Isotopic data from the lower Paradise indicates that several diagenetic events

acted on the sediments. The isotopic pattern developed in the lower Paradise is consistent with the cyclic nature of the Paradise.

The most interesting findings about the Paradise Formation in the Big Hatchet Mountains, is how significant cyclicity was during Paradise time in governing patterns of sedimentation. And that these cycles can be correlated worldwide indicating how influential and important eustasy was during the Late Mississippian.

## **INTRODUCTION**

### **Purpose**

Compared to the Early Mississippian there is a limited amount of Late Mississippian strata preserved across North America (Cook et. al., 1975). This small volume of preserved strata limits our ability to evaluate eustasy and the paleogeography during the Late Mississippian in North America. One region that can provide additional information about the Late Mississippian is the Pedregosa basin located in the southwestern United States and Northern Mexico. Preserved in this enigmatic Late Paleozoic basin is the little studied Paradise Formation (Late Mississippian), which is the focus of this study. It provides an excellent opportunity to evaluate not only the depositional systems and paleogeography of the region during Late Mississippian time, but also cyclic sedimentation in southwestern North America during the latest Mississippian.

### **Location**

The Paradise Formation is limited in areal distribution to southeastern Arizona, southwestern New Mexico and Northern Mexico (Figure 1). Of the 12 known locations eight are surface outcrops, and four are oil and gas tests in the region that have reported penetrating the Paradise. Following reconnaissance geology and gathering of basic stratigraphic data from all known outcrops, the exposures located in the Big Hatchet Mountains, Hidalgo County, New Mexico (Figure 2) were chosen for this study. These outcrops represent the thickest preserved occurrences of the Paradise. The large exposures of the Paradise in the Big Hatchets are ideal for selecting well exposed, structurally simple, closely spaced stratigraphic sections.

**Key to locations**

**Outcrops**

- 1) Pedregosa Mountains, Arizona
- 2) Blue Mountains, Arizona
- 3) Northern Peloncillo Mountains, New Mexico
- 4) Klondike Hills, New Mexico
- 5) Northern Animas Mountains, New Mexico
- 6) Big Hachet Mountains, New Mexico
- 7) Sierra de Palomas, Chihuahua, Mexico
- 8) Bavispe, Sonora, Mexico

**Oil and Gas Tests**

- 9) PEMEX Chinos #1, Chihuahua, Mexico
- 10) PEMEX Centauro #1, Chihuahua, Mexico
- 11) Humble #1 State "BA", Sec. 25, T32S, R16W, New Mexico
- 12) Cockrell #1 Playas, Sec. 14, T30S, R17W, New Mexico

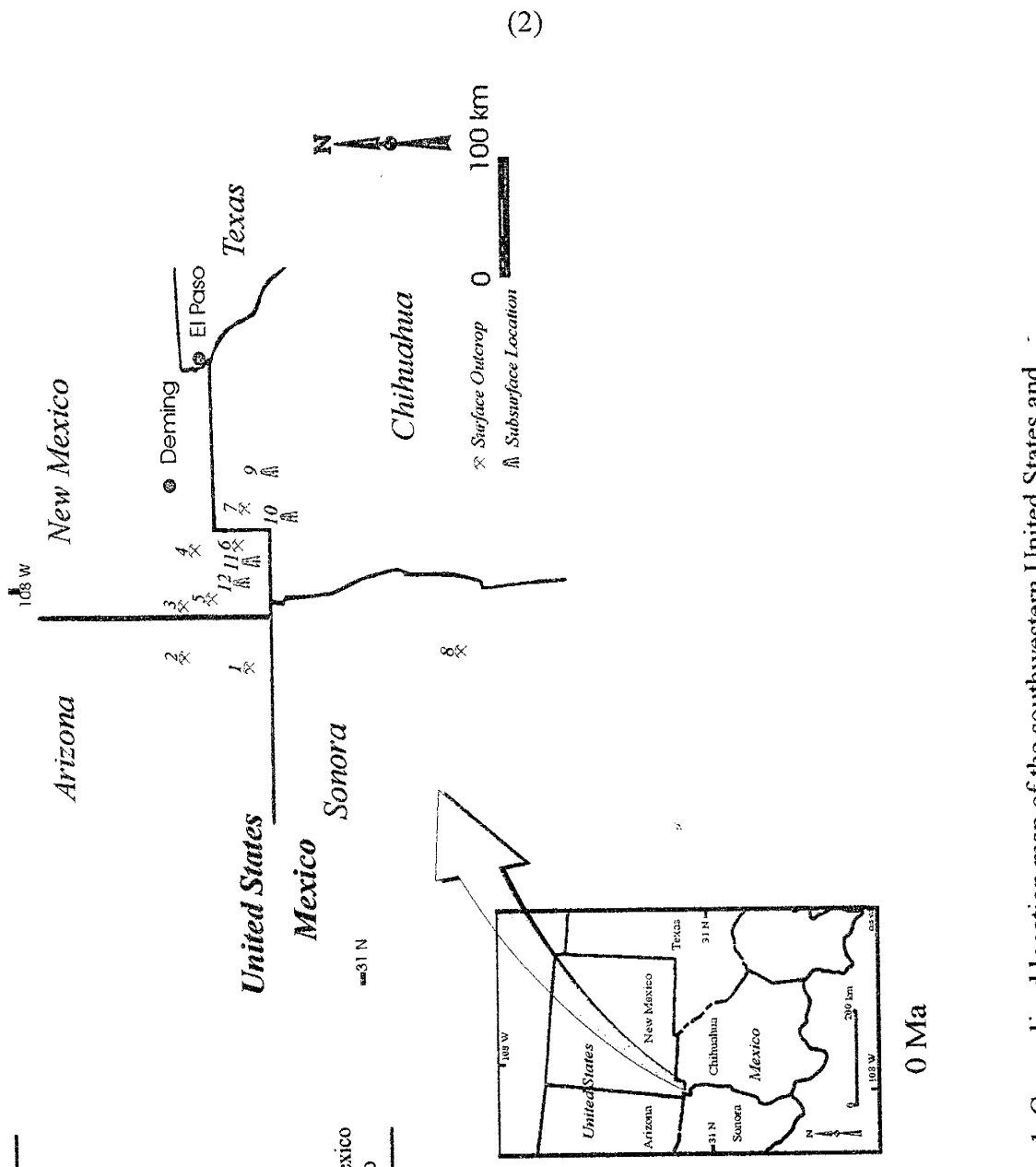


Figure 1. Generalized location map of the southwestern United States and northern Mexico showing the known distribution of the Paradise Formation.

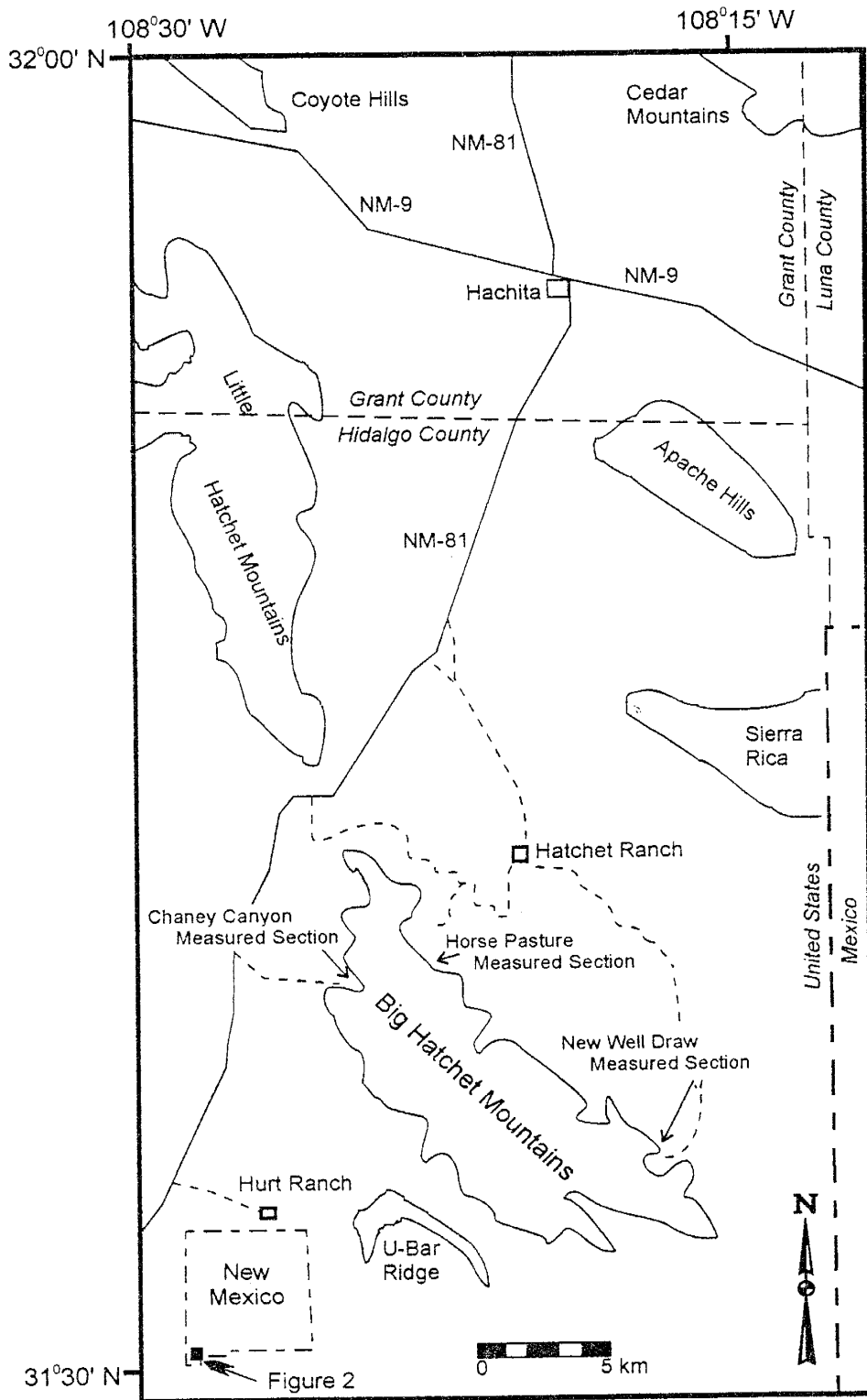


Figure 2. Map showing the location of the Big Hatchet Mountains and the locations of measured sections used in this study.

## **Big Hatchet Mountains**

The Big Hatchet Mountains form a northwest to southeast trending range located in the bootheel region of far southwestern New Mexico. Strata in the range strike northwest and dip to the south–southwest. The bulk of the Paradise Formation crops out as a distinctive, orangish-tan, slope-forming band along the eastern flank of the Big Hatchet Mountains. Additional outcrops are located along the northern rim of the Big Hatchets and along the southern side of Chaney Canyon on the western side of the range.

### **Geologic Setting**

The Big Hatchet Mountains lie within the southern extent of the Basin and Range Province, and act as the northern terminus of the Boca Grande structural trend, which originates in northern Mexico (Brown, 1986). This trend of uplifts is also referred to as the Hidalgo uplift (Seager and Mack, 1986).

The most complete stratigraphic section in southwestern New Mexico is exposed in the Big Hatchet Mountains. The section begins in Precambrian igneous and metamorphic rocks and terminates in Tertiary sediments (Figure 3).

Prior to the deposition of the Paradise Formation the region was tectonically quiet (Figure 4). During Paradise time the region was affected by the early stages of the Ouachita-Marathon orogeny (Figure 4; Ross, 1979; Kluth and Coney, 1981), and the Pedregosa basin began to form. The Pedregosa basin is a relatively poorly understood basin. Kottowski (1958) originally introduced the term Pedregosa trough for the thick, northwest trending accumulations of Late Paleozoic carbonates. This was described later as the Pedregosa basin (Kottowski, 1959) on the basis of thick (>760 m) of

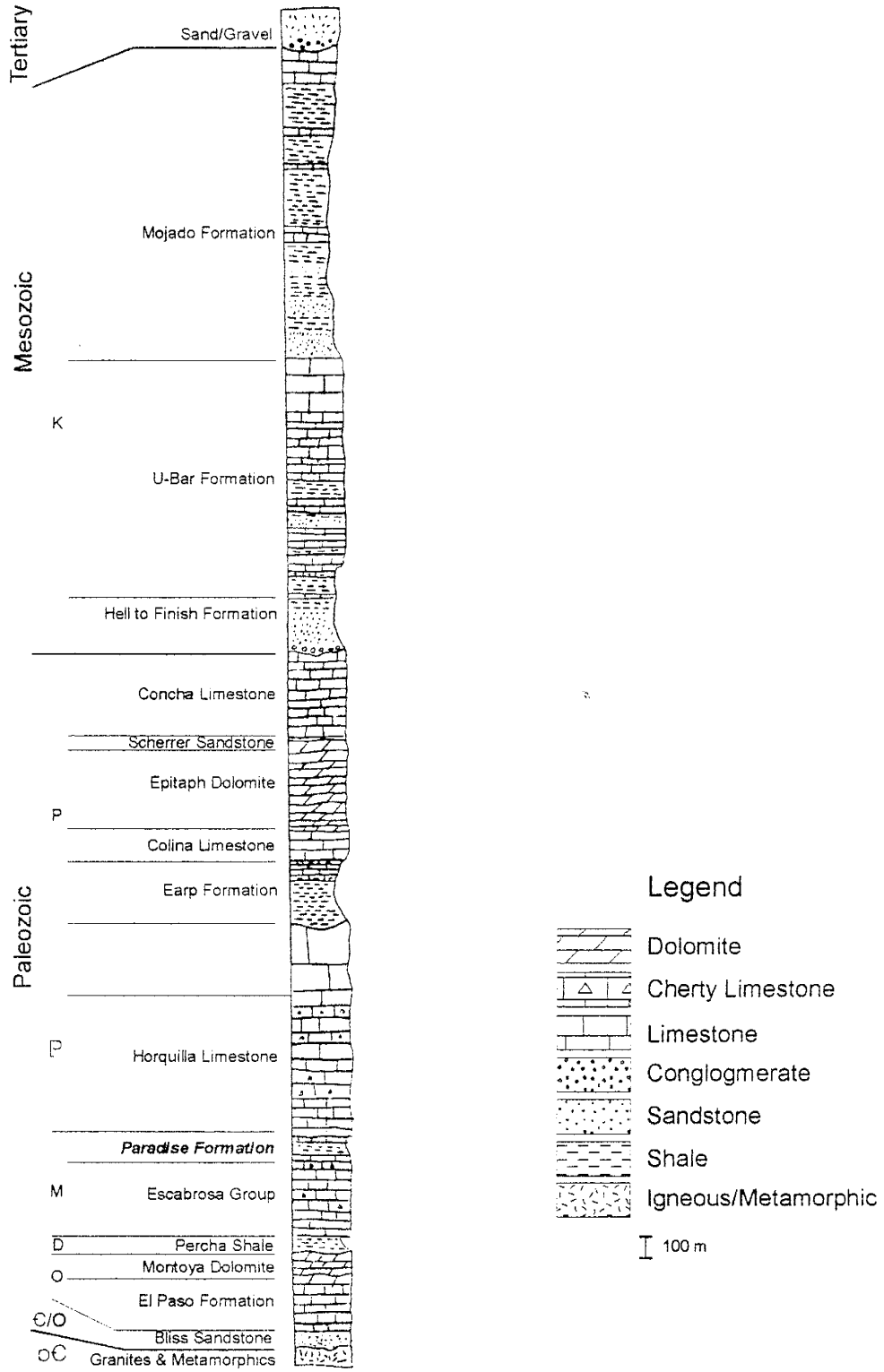


Figure 3. Generalized stratigraphic column for the Big Hatchet Mountains. Figure also shows the relationship of the Paradise Formation to both the underlying Escabrosa Group and the overlying Horquilla Limestone. (Data compiled from Zeller, 1965.)



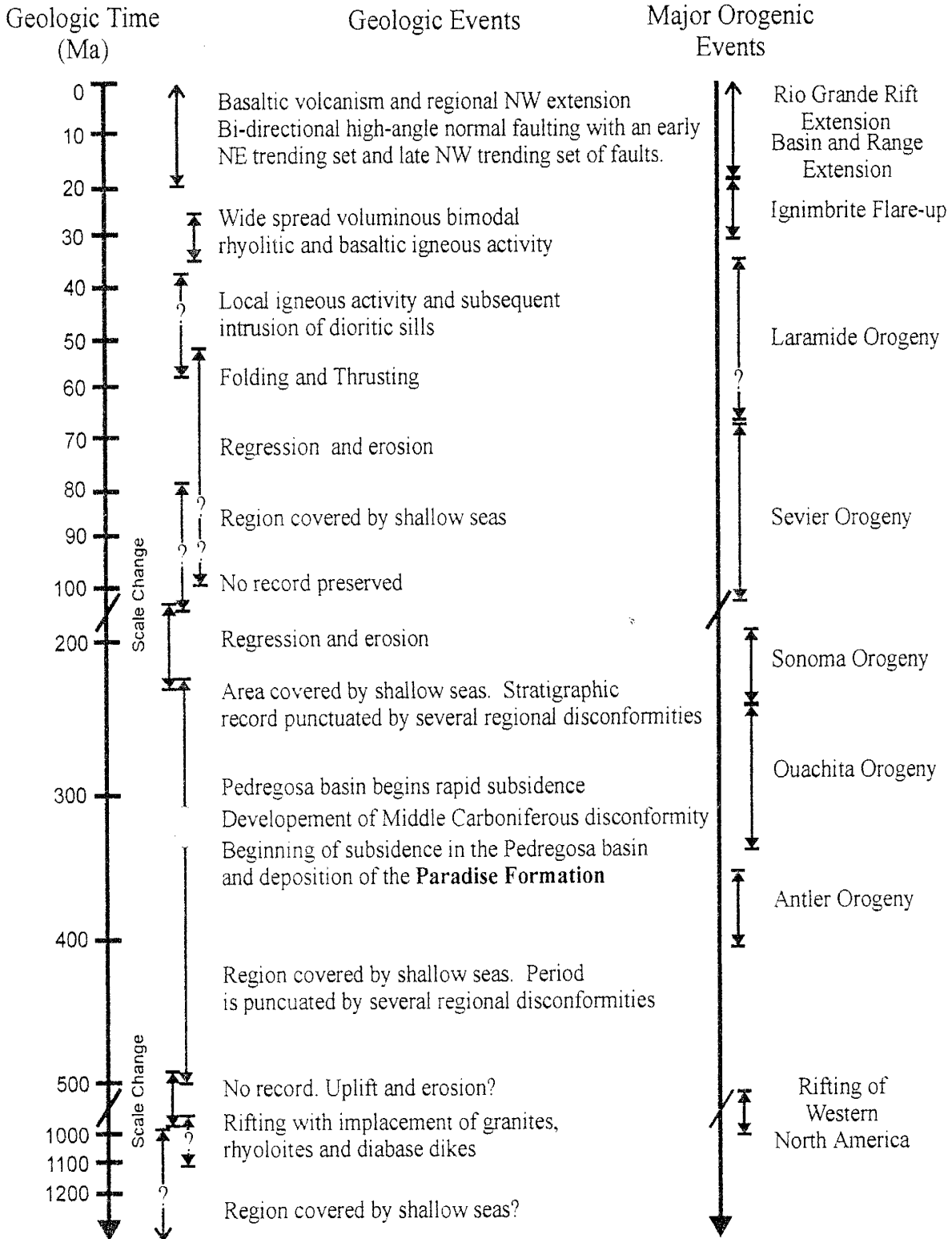


Figure 4. Generalized geologic history chart for southwestern New Mexico and the surrounding region. Note time of Paradise deposition in relation to ongoing tectonic events.

Pennsylvanian strata. Kottlowski (1965) later expanded the definition of the Pedregosa basin to include strata as old as Mississippian.

The Paradise Formation was deposited in a carbonate dominated depositional system that developed along the margins of the incipient Pedregosa basin. Following the deposition of the Paradise Formation, the region was subjected to several significant tectonic events (Figure 4). These began with the main pulses of the Late Paleozoic Ouachita–Marathon orogeny related to the final assembly of Pangea (Thomas, 1977, 1983, Ross, 1979; Kluth and Coney, 1981). Compressional forces related to this orogeny caused a dramatic deepening of the Pedregosa basin along with uplift of surrounding structural elements, the Florida–Moyotes uplift to the north of the basin (Kluth and Coney, 1981). Although there is no direct evidence of a foreland-like uplift to the south of the Pedregosa basin, Thompson and Jacka (1981) and Handschy et al. (1987) and Ye et al. (1996) indicate that one existed. This uplift, the Magdalena-Sierra de Nido Uplift, is to the south of the Sierra El Tigre in Sonora, Mexico. The location is based largely on the southern-most exposures of middle to late Paleozoic strata, which are strikingly similar to the middle and late Paleozoic strata exposed in the Big Hatchet region (Imlay, 1936; Devery, 1979; Holcomb, 1979). A rapid increase in subsidence related to the Ouachita–Marathon orogeny during the Early Pennsylvanian (Morrowan) (Ye et al., 1996) resulted in the burial of the Paradise under several kilometers of sediments during the Late Paleozoic, including more than a kilometer of Horquilla Limestone (Pennsylvanian/ Permian) (Zeller, 1965; Thompson et al., 1977).

## **METHODS OF STUDY**

### **Field**

Following a reconnaissance of the Big Hatchet Mountains, selected stratigraphic sections of the Paradise Formation were measured, described, and collected. Detailed stratigraphic columns of each section are located in Appendix A. Written descriptions of measured sections are included in Appendix B.

Hand samples for laboratory analyses were collected from every bed. Multiple samples were collected from beds greater than one meter in thickness and from beds with demonstrable changes in lithology. In addition to sampling the beds, data pertaining to bedding orientations, bedding geometries, sedimentary structures, and major fossil groups were recorded in the field. Colors were also recorded in the field using the GSA Color Chart.

### **Laboratory**

Standard petrographic thin sections were prepared from samples. In addition to thin sections, thick sections and/or the matching billets from thin sections were polished and labeled for isotopic analyses (see section on stable isotopes below). Point count and stable isotope data derived from this study are archived in digital form on 3.5" 1.44 MB MS-DOS<sup>®</sup> formatted diskettes included with this study (back pocket). The README.TXT file included on the diskette contains instructions for accessing these data.

### **Petrography**

Samples collected for petrographic analyses were cataloged and described. Thin sections of each sample were examined using a petrographic microscope. To facilitate

cathodoluminescence petrography and staining, cover slips were not placed on thin sections. To maintain statistically valid representation of each sample, a minimum of 350 points per slide were counted. These counts permitted comparisons between samples for classification and paleoenvironmental interpretations.

### ***Clastic Rocks***

Mineralogical components, sedimentary structures, fabrics, and textures were identified and described for detrital clastic rocks. After each thin section was counted, data were plotted on ternary diagrams and classified using the sandstone classification of Folk (1980).

### ***Carbonate Rocks***

Several techniques were used to classify carbonate rocks and to describe their diagenetic history. Thin sections were stained to facilitate identification of carbonate minerals. Methods for staining are described by Dickson (1966).

The grain-bulk method (Dunham, 1963; Flügel, 1982) was used in order to determine the modal composition of each sample. This method is used to estimate the bulk volume of each constituent by including voids within grains and any void filling material as part of the grain. This is more useful than the weight percent method (Flügel, 1982) for examining the relative abundances of framework grains, which are critical for depositional and paleoenvironmental interpretations.

In conjunction with point counting, petrographic determinations of porosity, carbonate grain relations, presence of lime mud, sorting, degree of packing, dolomitization, non-carbonate grains, bioturbation, geopetal structures, laminations, biotic diversity, sedimentary structures, textures, and cements were also evaluated.

After each thin section was point-counted and described, it was classified using both the Dunham (1962) and Folk (1962) carbonate rock classifications.

### **Cathodoluminescence Petrography**

Cathodoluminescence petrography was used to identify carbonate grains and cements, and to evaluate diagenesis. Cathodoluminescence photomicrographs and sketches of thin and thick sections were used in mapping the distribution of luminescent and non-luminescent components and to select regions for isotopic sampling.

### **Stable Isotopes**

Micromilling was used to sample carbonate material for stable isotope analyses of oxygen and carbon (Prezbindowski, 1980; Meyers and Lohmann, 1985; Popp et al., 1986). Carbonate material was collected from ooids, brachiopods, pelmatozoans, lime mud, cements, and whole rock samples. Sample sites on carbonate grains (e.g., brachiopods) and cements were determined by the combination of optical petrography, cathodoluminescence, and staining methods. These analyses were done on the presumption that they would correlate with relatively pristine carbonate grains and to select coeval generations of cements (Popp et al., 1986; Veizer et al., 1986; Aldis et al., 1988; Rush and Chafetz, 1990).

Powdered samples were reacted with 100% phosphoric acid at 25°C to evolve carbon dioxide gas. The evolved gas was processed through a Finnigan Matt Delta E™ gas-ratio mass spectrometer to determine the  $\delta^{18}\text{O}$  and  $\delta^{13}\text{C}$  values of each sample with respect to the Pee Dee Belemnite (PDB) standard. Oxygen values are also reported with respect to standard mean ocean water (SMOW; McCrea, 1950; Craig, 1957). Carbonate

standards NBS-20, and an in-house carbonate standard, Mexican Calcite, were randomly run as checks on the phosphoric acid batch, the precision and accuracy of sample preparation techniques, and mechanical systems.

## PREVIOUS WORK

### Stratigraphic

Although Mississippian strata in the Big Hatchet Mountain area were first reported in 1904 by Ransome, the Paradise Formation was not formally recognized in the Big Hatchet Mountains until 1955 by Packard. This was 30 years after the description of the type section in the Chiricahua Mountains of southeastern Arizona by Stoyanow (1926). Since Packard's study, little attention has been paid to the Paradise. The first major work done on the Paradise following Packard was by Zeller (1958, 1965). Zeller included a discussion of the Paradise in the Big Hatchet Mountains, drawing heavily on information from Packard (1955).

In addition to Zeller's (1965) memoir on the Big Hatchet Mountains, a variety of studies have included some mention of the Paradise Formation. Works by Armstrong (1962, 1978), Armstrong et. al. (1979), Armstrong, Mamet, and Repetski (1980), Armstrong and Mamet (1978, 1988), Bahling (1979), Kottlowski (1963, 1965, 1969), Thompson and Jacka (1978), Wilkening (1984), and Frenzel et al. (1988) all include brief descriptions and comments on the Paradise in the Big Hatchet Mountains. None of these reports are detailed, nor do any of them address the diagenesis of the Paradise. They tend to be similar to earlier studies, focusing on the basic lithostratigraphy, general depositional environments, and correlation of the Paradise. Limited descriptions of the Paradise Formation in the Big Hatchet Mountains are also given in several geologic maps (Zeller, 1958, 1975; Drewes, 1991).

There have been some limited biostratigraphic studies of the Paradise Formation. Some of these are parts of the aforementioned larger studies. Several studies have used microfossils for biostratigraphic control on the Paradise in the Big Hatchet Mountains. Armstrong and Mamet (1988) worked out the foraminiferal zonation of the Paradise. Their conclusions supported the results drawn by the macrofossil studies. As part of a

study of the lower Horquilla Limestone in the Big Hatchet Mountains, Wilkening (1984) examined the conodont fauna of the upper Paradise and determined it to be essentially barren. This is consistent with a report of a barren conodont zone in the type section of the Paradise (Norby, 1971). Thompson and Jacka (1981) noted that the foraminiferal zones of the uppermost Paradise, on the western side of the Big Hachets in Chaney Canyon, indicate a Chesterian age for the Paradise. Zeller (1965) presented a listing of microfossils from the Paradise he credited to Elias. Zeller also discussed the biostratigraphic significance of the fauna and used it to correlate the section in the Big Hatchet Mountains to both the type section in Arizona and age equivalent strata in eastern New Mexico and west Texas.

Along with the published reports listed above, there are several unpublished reports that include information about the Paradise Formation. New Mexico Bureau of Mines and Mineral Resources Open-file Report 312 (Bayless and Schwarzer, 1987) reported the results of a geochemical study of the Lower Paleozoic section in the Big Hatchet Mountains. This includes a suite of samples from outcrops of the Paradise at Mescal Canyon. United States Geological Survey Open-file Reports 88-450-B (Butler, 1988), 88-450-M (Butler, 1989), and 93-248 (Butler, 1993) all discuss the potential of hydrocarbon resources in the Pedregosa basin region. These reports give brief descriptions of the Paradise, as well as the source and reservoir rock potential of the Paradise.

### **Isotopic**

Previous work employing variations in isotopic composition with respect to stratigraphic position can be divided into two categories: those dealing with recent sediments and rocks, and those dealing with ancient rocks. These studies have investigated the correlation and diagenetic evolution of stratigraphic intervals. Studies related to cyclicity and the effects of diagenesis using modern geologic materials include



those by Allan and Matthews (1977, 1982) on the effects of meteoric waters and exposure surfaces in Barbados, West Indies. Lohmann (1988) reviewed the various applications of stable isotope data. These include the utility of stable isotopes in understanding meteoric diagenetic systems, and their application to defining exposure surfaces.

Studies of ancient stratigraphic intervals are much more numerous. Typically, these studies dealt with correlation problems and those problems related to cyclic sedimentation (Magaritz and Turner, 1982; Adlis et al., 1988; Algeo et al., 1991).

Isotopic studies related to carbonate components and their applications to revealing secular changes in the isotopic composition of seawater are numerous. This chain of research has its roots in a pioneering study by Lowenstam (1961). This study reported on the ability of brachiopods to preserve the isotopic signature of the seawater in which they lived through geologic time. Since Lowenstam's study, there have been a multitude of studies related to evaluating biotic and abiotic carbonate grains as a means to study the isotopic evolution of sea water (Keith and Weber, 1964; Veizer and Hoefs, 1976; Brand and Veizer, 1981; Brand, 1982; Dickson et al., 1991; Bates and Brand, 1991).

## STRATIGRAPHY

Biostratigraphic studies indicate that the Paradise ranges in age from Meramecian to Chesterian, with the bulk of the section being Chesterian in age (Figure 5; Packard, 1955; Zeller, 1965; Wilkening, 1984; Armstrong and Mamet, 1988). Consequently, the Paradise Formation in the Big Hatchet Mountains represents deposition during the latest stages of the Mississippian.

In the Big Hatchet Mountains, the Paradise Formation rests conformably on the Hachita Formation of the Escabrosa Group, and is disconformably overlain by the Horquilla Limestone (Pennsylvanian/Permian). The Paradise ranges in thickness from 95 m (Packard, 1955) to over 130 m (this report and Armstrong, personal comm., 1994).

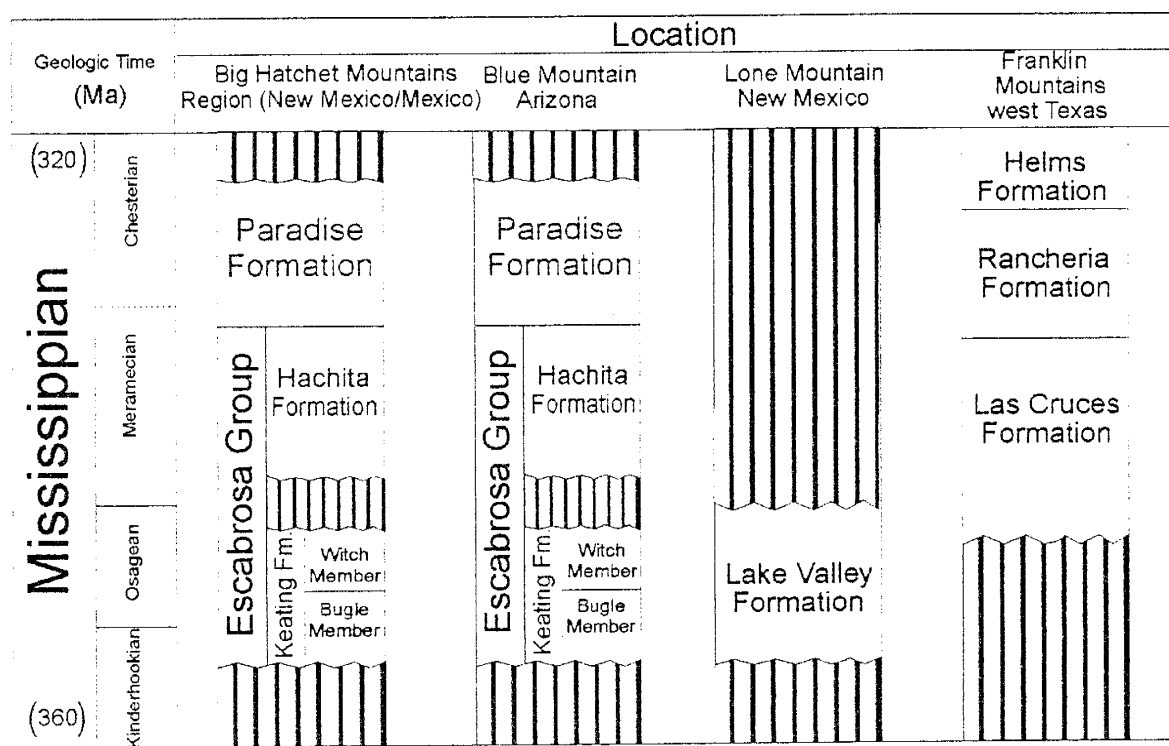


Figure 5. Age and correlation diagram for the Paradise Formation. (Data from Armstrong, 1962, Zeller, 1965, Pratt, 1967, and Armstrong and Mamet, 1988.)

The Paradise Formation is characterized by its distinctive orangish-tan weathering, mixed carbonate-clastic sequence of rocks. Carbonate rocks include grainstones, packstones, wackestones, and lime mudstones. Detrital clastic rocks consist of sandstones, siltstones, and shales. Typically, these rocks are thinly bedded and are slope formers (Figure 6).

Two complete sections and a single partial detailed stratigraphic section of the Paradise Formation were measured and sampled for depositional, diagenetic, and isotopic analysis. The complete sections are located on the eastern flank of the Big Hatchet

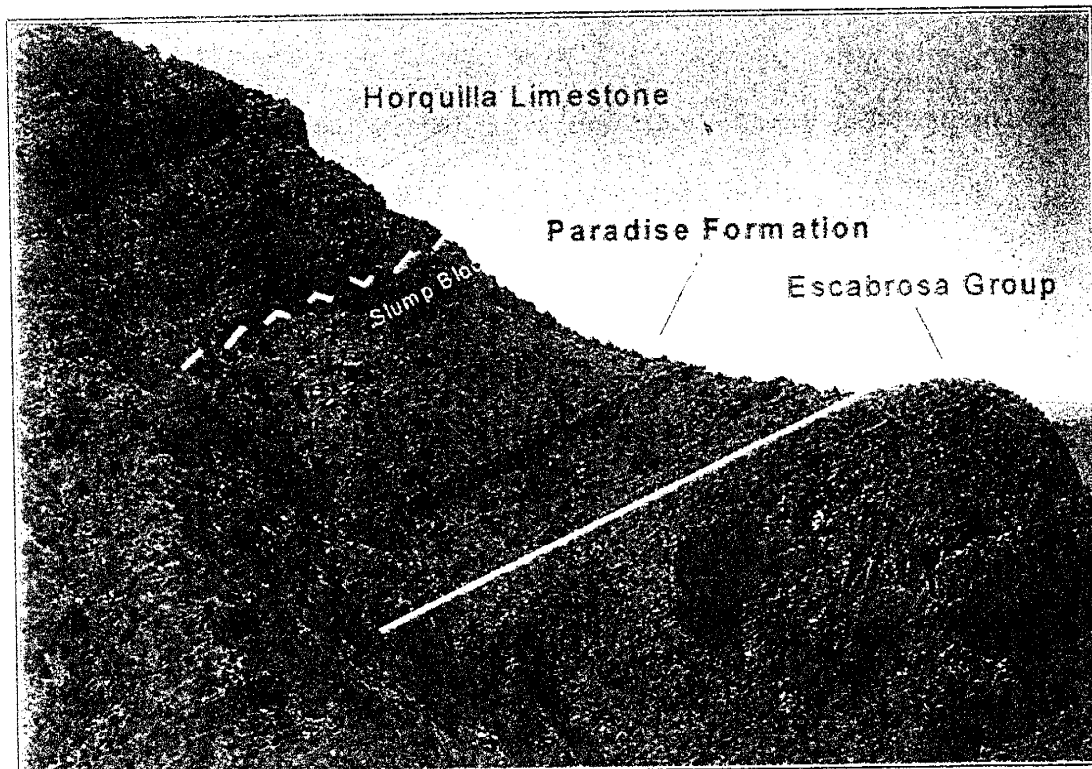


Figure 6. View looking North-Northwest of the Paradise Formation in the Big Hatchet Mountains. Photograph shows the very distinctive weathering profile and coloration of the Paradise. Lower white line marks the contact with the underlying Escabrosa Group. The upper white dashed line marks the contact with the overlying Horquilla Limestone. (Photo location Mescal Canyon.)

Mountains approximately 8 km apart. The northern section is located just south of Horse Pasture Canyon, and the southern section is located just north of New Well Canyon. Both of the sections selected are located in structurally simple areas and are more than 90% exposed. The partial section was measured on the western side of the Big Hatchet Mountains in upper Chaney Canyon.

### **Lithostratigraphy**

This discussion is divided into two parts. The first part describes the stratigraphy and stratigraphic relationships of the Paradise Formation. The second part describes lithofacies and their environmental interpretation.

#### **Horse Pasture Canyon Section**

The Horse Pasture Canyon section is located (Figure 7) in sec. 33 T30S R15W, Hidalgo County, New Mexico. The Paradise Formation is 128.9 m thick at this location. The contact with the underlying Escabrosa Group is sharp and conformable. The contact is placed between the last chert-rich crinoidal grainstones of the Escabrosa and the finer-grained, cross-bedded grainstones of the Paradise. The contact with the overlying Horquilla Limestone is sharp and disconformable. There is no angularity between the formations or evidence for karsting at this location. This contact is placed just below the first medium-gray, thick-bedded packstones and grainstones encountered along the traverse.

#### **New Well Draw Section**

New Well draw is a term introduced in this study to define the location of the section exposed in a small draw just north of the entrance to New Well Canyon. The

# Explanation Geologic Units

- Qal** Gravel and Sand (Recent)—Alluvial deposits in fans and drainages.
- IP-Ph** Horquilla Limestone (Pennsylvanian-Permian)—Medium-gray, cliff forming, fossiliferous limestones. Beds commonly contain distinctive black chert.
- Mp** Paradise Formation (Upper Mississippian)—Olive-gray to orangish weathering limestones and siltstones. Sandstones and shales are also common.
- Me** Escabrosa Group (Lower Mississippian)—Massive, light- to dark-gray crinoidal limestones with pinkish-gray and orange chert.
- Dp** Percha Shale (Devonian)—Medium-gray to pale yellowish-gray clay and shale. Rare interbedded siltstones. Usually covered and poorly exposed.
- Om** Montoya Group (Ordovician)—Light-gray, fine-grained cherty brachiopod bearing dolomites.
- Oe** El Paso Formation (Ordovician)—Light-gray to light brownish gray limestone and dolomitic limestones containing brown nodular chert.

## Map Symbols

- Strike and dip of bedding C.I. = 40 feet
- Line of measured section
- Fault, ball on down thrown side 305 m (~ 1000')
- Formation contact

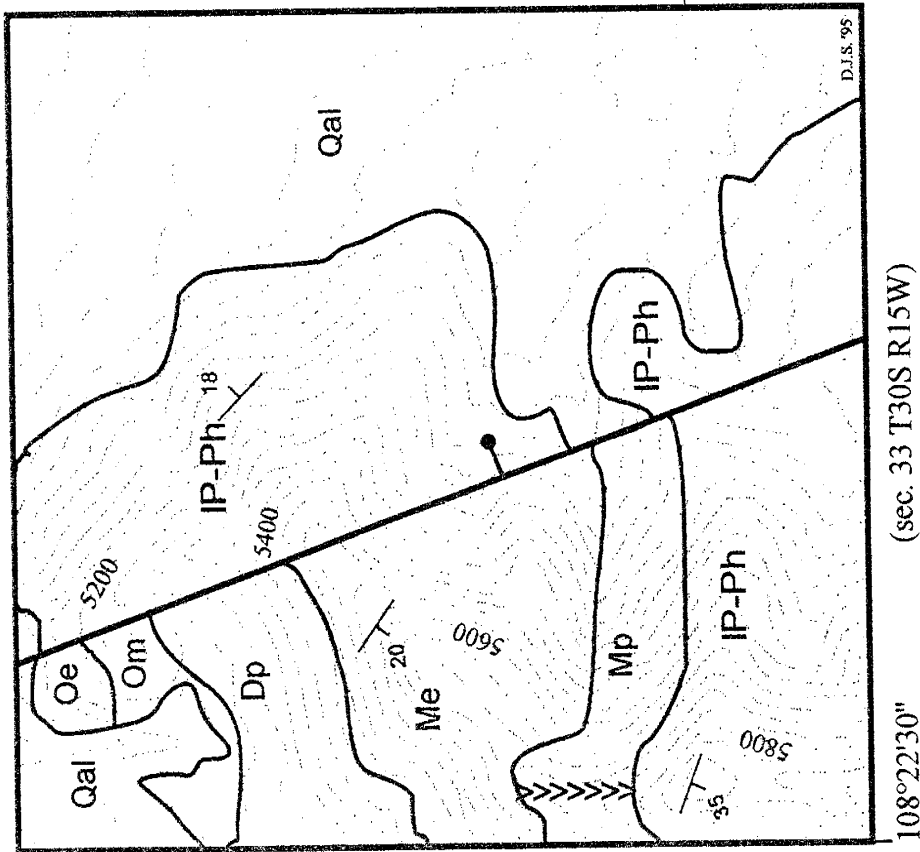
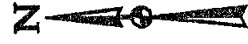


Figure 7. Simplified geologic map of Horse Pasture Canyon region showing location of measured section.

New Well draw section is located (Figure 8) in sec. 29 T31S R14W, Hidalgo County, New Mexico. The Paradise Formation is 133.5 m at this location. The lower contact is placed where thin-bedded, silty grainstones overlie chert rich crinoidal grainstones of the Escabrosa Group. The upper contact at New Well draw is a distinctive erosional disconformity that marks the upper boundary of the Paradise with the medium gray, cherty carbonates of the Horquilla Limestone. Moderate karstification of the uppermost limestone beds in the Paradise indicates a period of subaerial exposure following the deposition of the Paradise.

### **Chaney Canyon Section**

The Chaney Canyon section is located in sec. 30 T31S R14W, Hidalgo County, New Mexico (Figure 9). This is only a partial stratigraphic section consisting of the upper 21 m of the Paradise Formation. This portion of the Paradise is very similar to the uppermost part of the section measured at Horse Pasture Canyon.

The upper contact with the Horquilla Limestone is placed where the slope-forming, silty, dolomitic, lime mudstones of the uppermost Paradise give way to thick-bedded, light-gray chert bearing limestones of the lower Horquilla Limestone. The contact is sharp and has the appearance of being conformable. The nature of the lower contact at this location is unknown, because it is not exposed.

### **Lithostratigraphy: Synopsis**

Stratigraphically the Paradise Formation, as described and measured in the Big Hatchet Mountains, is very consistent over some 8 km. Basic lithologies, macrofossils, and stacking patterns are essentially identical at each location. Bed geometries in each section are sheet-like with some being slightly wedge-shaped. They have sharp upper

# Explanation

## Geologic Units

**Qal** Gravel and Sand (Recent)—Alluvial deposits in fans and drainages.


**IP-Ph** Horquilla Limestone (Pennsylvanian-Permian)—Medium-gray, cliff forming, fossiliferous limestones. Beds commonly contain distinctive black chert.


**Mp** Paradise Formation (Upper Mississippian)—Olive-gray to orangish weathering limestones and siltstones. Sandstones and shales are also common.

**Me** Escabrosa Group (Lower Mississippian)—Massive, light-to dark-gray crinoidal limestone with pinkish-gray to orange chert.


## Map Symbols

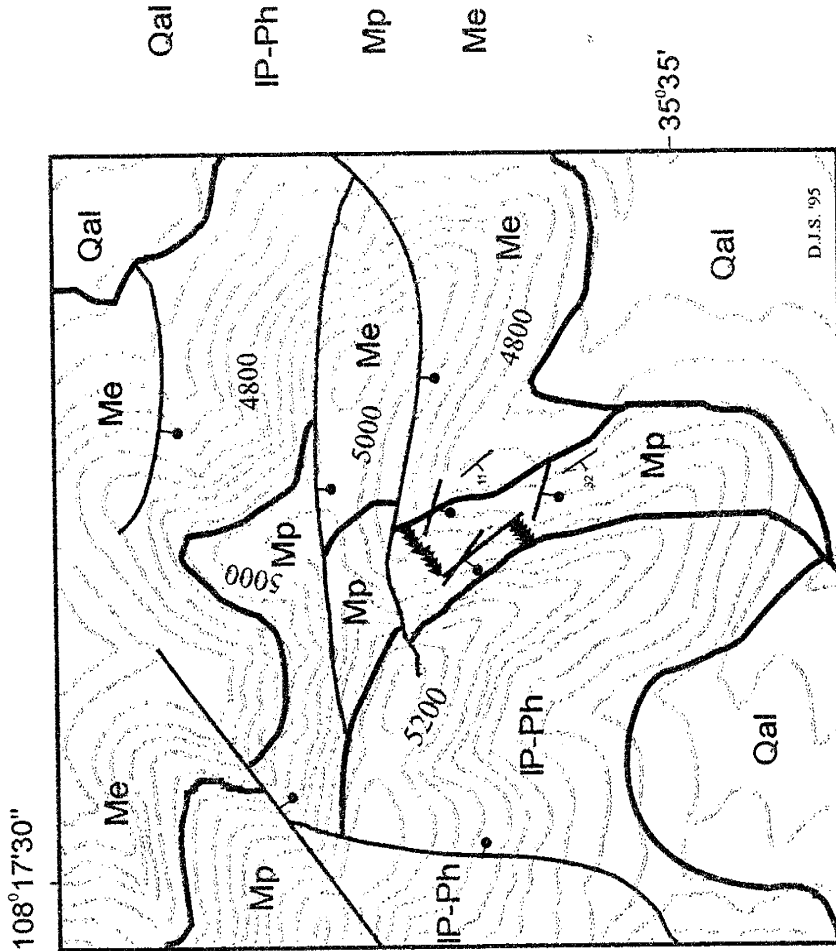
 Strike and dip of bedding

 Line of measured section

 Fault, ball on down thrown side

 Formation contact

C.I. = 40 feet  
 500 m (~1640')



(sec. 29 T31SR14W)

Figure 8. Simplified geologic map of New Well draw showing the location of measured section.

# Explanation

## Geologic Units

Gravel and Sand (Recent)—Alluvial deposits of fans and drainages.

Horquilla Limestone (Pennsylvanian-Permian)—Medium-gray, cliff forming, fossiliferous limestones. Beds commonly contain distinctive black chert.

Paradise Formation (Upper Mississippian)—Olive-gray to orangish weathering limestones and siltstones. Sandstones and shales are also common.

Escabrosa Group (Lower Mississippian)—Massive, light- to dark-gray crinoidal limestones.

Qal

P-Ph

Mp

Me

## Map Symbols

45 Strike and dip of bedding

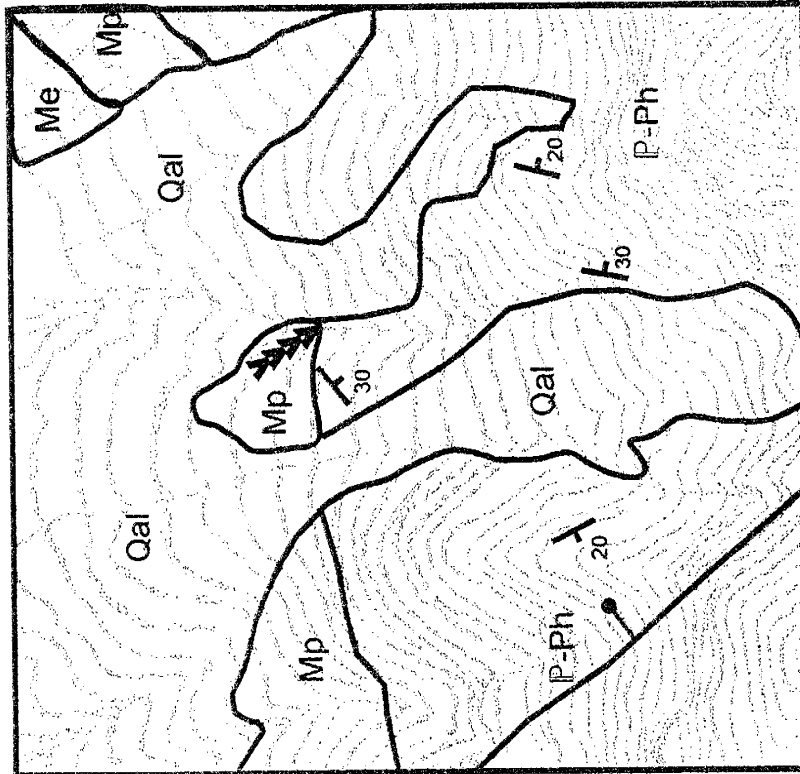
Line of measured section

Fault, ball on down thrown side

Formation contact



C.I. = 40 feet 500 m (~1640')



(NW 1/4 sec. 6 T31S R15W)

Figure 9. Simplified geologic map of the Chaney Canyon region showing location of measured section.



and lower contacts. The primary difference in the sections is the nature of the upper contact with the overlying Horquilla Limestone. At the southern location, in New Well draw, this contact is irregular and distinctly disconformable showing signs of subaerial exposure and subsequent karsting. At Horse Pasture Canyon and Chaney Canyon, the upper contact is sharp and does not appear to represent a surface of significant exposure or karstification.

The Paradise Formation in the Big Hatchet Mountains is divisible into three informal members. These are designated member A, member B and member C in stratigraphic order from oldest to youngest (Figure 10).

Member A is characterized by thin- to- medium-bedded, ledgy carbonates, with few interbedded detrital clastic units. The beds are sheet-like to slightly prism-shaped in geometry (Figure 11).

Member B represents the middle portion of the stratigraphic interval. The beds in this member are thin- to- thick-bedded. The most distinctive feature of this member is an increase in shaly intervals. This increase in shales causes this member to weather into more of a slope. As in member A, bed geometries are sheet-like.

Member C, the uppermost part of the Paradise Formation, is similar in character to member A since both are dominated by carbonates (Figure 11). A decrease in mud-rich carbonates and in finer-grained detrital clastics is coupled with a return to thin- to- medium-bedded ledge forming units. Bed geometries in member C are also sheet-like. There is a slight increase in silt and sand-sized detrital clastic material in member C. These sandstones and siltstones form resistant ledges capping carbonates.

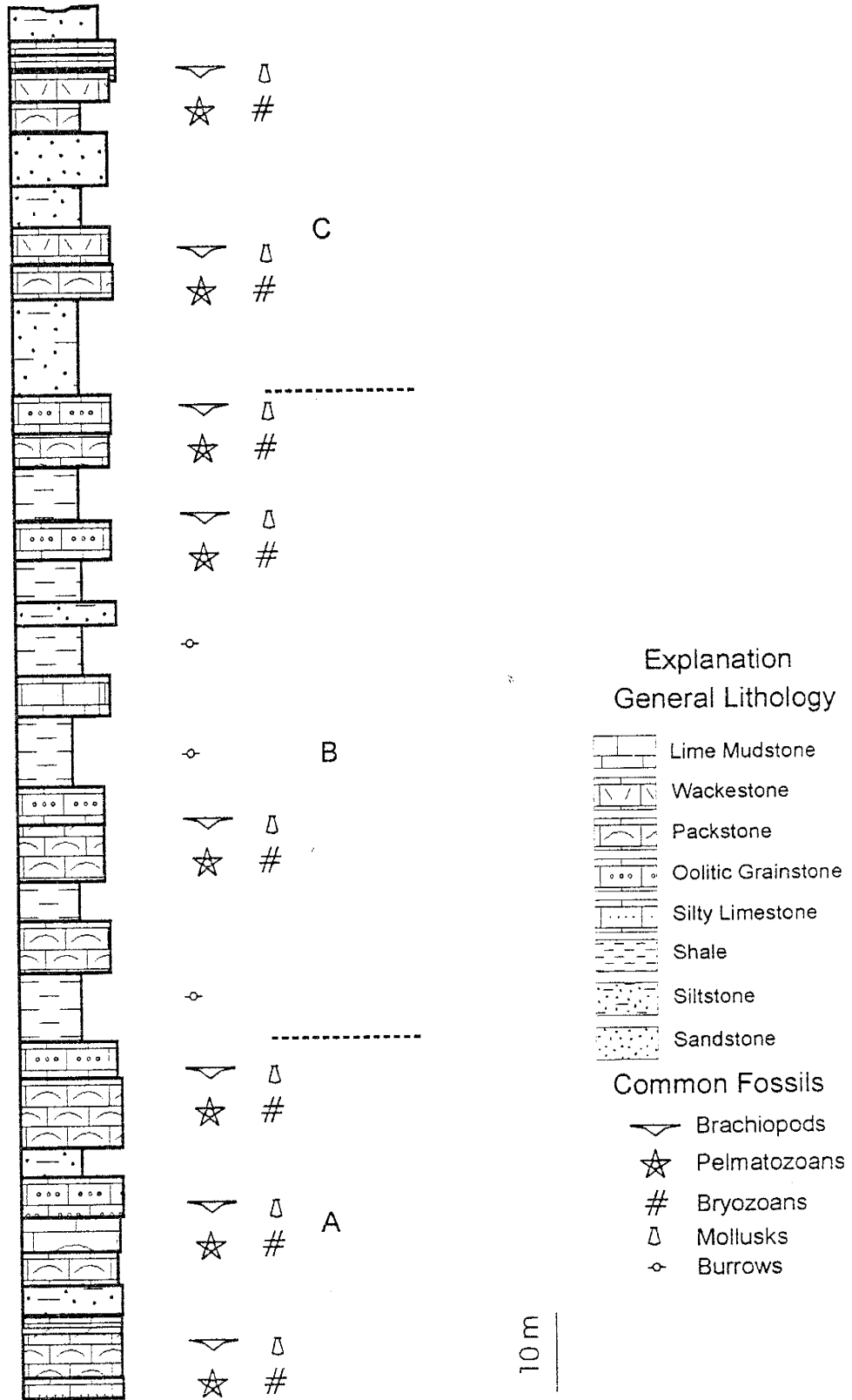


Figure 10. Generalized stratigraphic column of the Paradise Formation from the Big Hatchet Mountains divided into three informal members. Member boundaries are shown as dashed lines. See text for descriptions of each member.

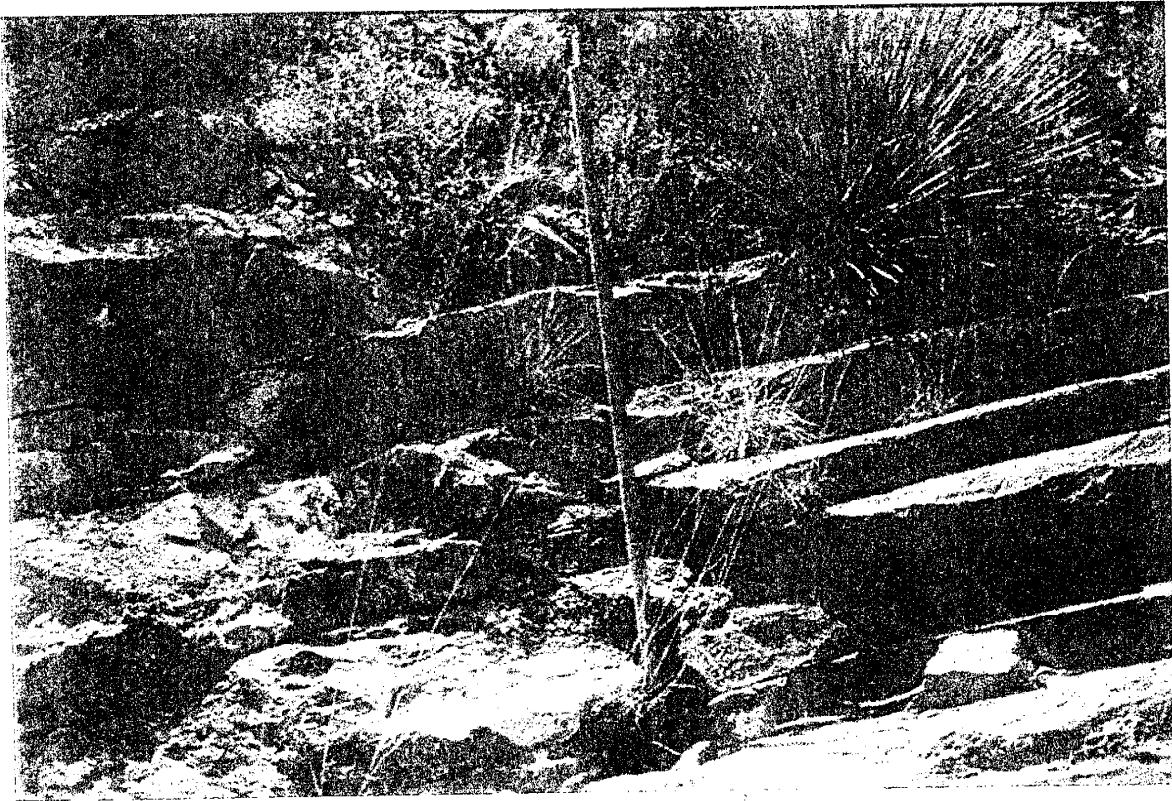


Figure 11. Outcrop photograph of the Paradise Formation showing typical sheet-like bedding geometries. (This basic bedding style persists throughout the entire stratigraphic interval. Photograph from Member A, New Well draw measured section. Jacob's staff is 1.5 m in height.)

Each member described above is consistent across the study area (Figure 12). This consistency is also found at the bed level, with only a slight thickening of beds to the south. Reconnaissance work on other sections shows that these members are traceable across the known distribution of the Paradise Formation (Figure 13). In general, this consistency of stratigraphic architecture may reflect fundamental stability in the overall tectonic setting of the region and related sedimentation during Paradise time. Figure 13 also indicates that during Paradise time the depocenter of the Pedregosa basin was in a position to the East of the Big Hatchet Mountains. This basin configuration is consistent with coeval deeper water facies of the Helms and Rancheria formations of Eastern New Mexico and west Texas (Yurewicz, 1977; Madden, 1984).

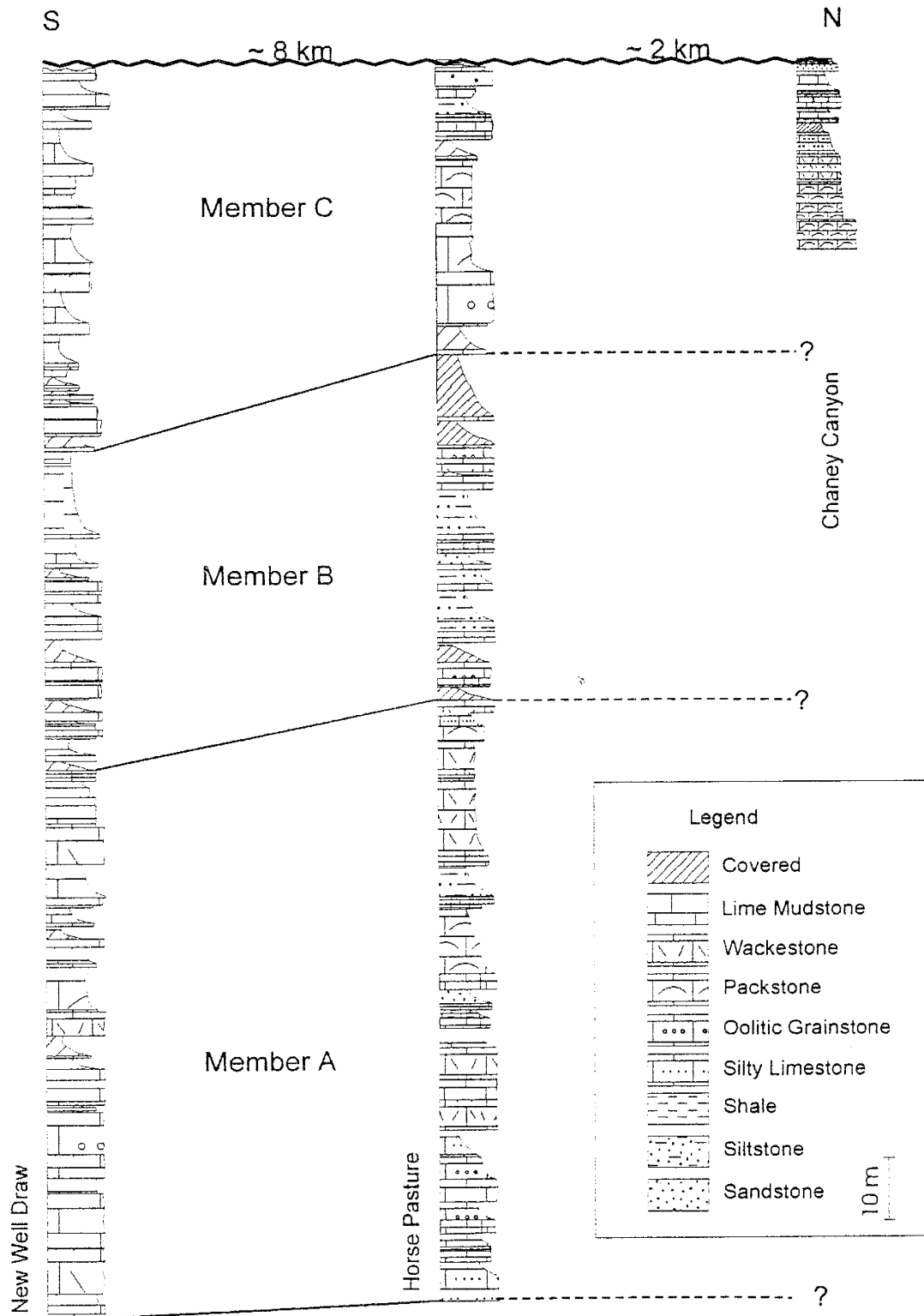


Figure 12. Correlation between Paradise Formation Members in the Big Hatchet Mountains. Note the similarity between member thickness and basic lithologies at each section..

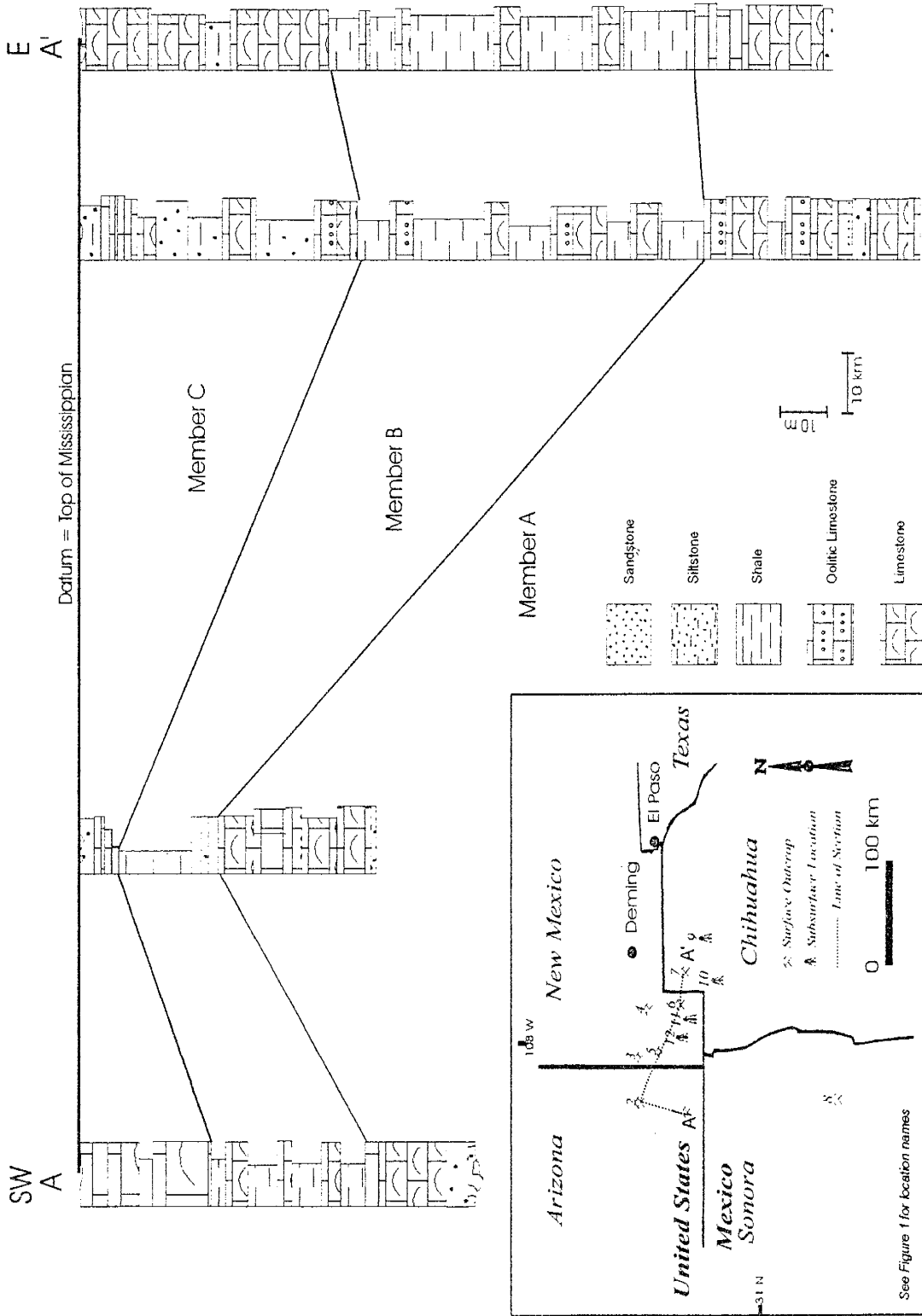


Figure 13. Generalized stratigraphic cross section of the Paradise Formation showing members and the overall continuity of the members across the known distribution of the Paradise.

## LITHOFACIES

This section defines individual lithofacies found within the Paradise Formation. Two distinctive groups of lithofacies are present in the Paradise and are grouped into carbonate lithofacies and siliciclastic lithofacies. Each lithofacies name is derived from the most distinctive characteristic of that lithofacies.

### Carbonates

#### Lime Mudstone Lithofacies

Lime mudstones are the least abundant carbonate rock type found in the Paradise Formation. This lithofacies occurs most often within the middle member, member B, of the Paradise. Typically, lime mudstones are sheet-like in geometry, and are structureless to finely laminated (Figure 14). The homogenized nature of the majority of lime mudstones is due to intense bioturbation by infaunal organisms.

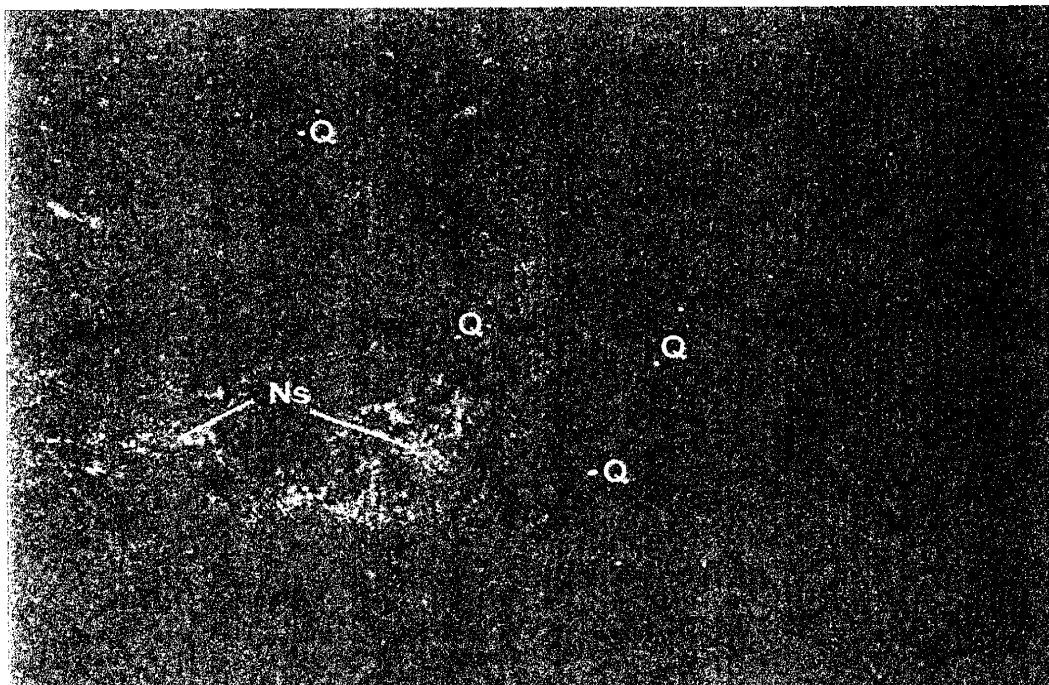


Figure 14. Photomicrograph of a typical lime mudstone from the Paradise Formation. (Q-dentate quartz, Ns-neomorphic spar. Field of view approximately 5.5 mm).

Fossils are rare in this lithofacies. When encountered, they are dominated by minute fragments of brachiopods and bryozoans. In rare instances small pelmatozoan columnals are present. In addition to hardparts of invertebrates preserved in the lime mudstones, several burrows are common to this lithofacies. In outcrop (Figure 15) and thin section, the burrows are ovate in shape, filled with lime mud, and readily apparent. In addition to the generic "burrow", three distinct species of ichnofossils are identifiable in the lime mudstone lithofacies.

*Planolites* sp., simple, wandering, circular-to-ovate shaped, feeding burrows are commonly found in the lime mudstone lithofacies. *Chondrites* sp. is the second identifiable ichnofossil found in the Paradise Formation. *Chondrites* are viewed as

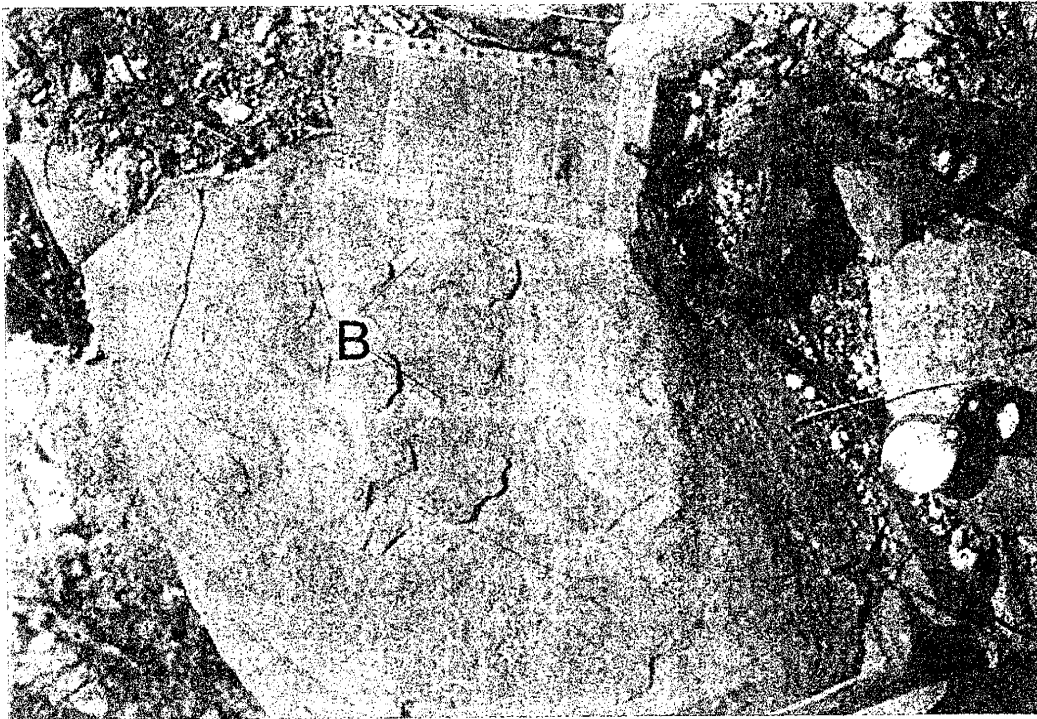


Figure 15. Field photograph of the lime mudstone lithofacies in the Paradise Formation. (Clearly visible in this photograph are meandering mud-filled burrows, labeled B. Photograph from member B, at New Well draw measured section).

circular- to- ellipsoidal- shaped, mud-filled spots in outcrop. The third is *Zoophycos* sp. *Zoophycos* burrows are spiral-shaped, sperite-filled, feeding traces. They appear as feathered fan shapes when exposed along bedding planes.

Variable amounts of detrital quartz are common in the lime mudstone lithofacies. The amount of detrital quartz ranges from less than 1% to nearly 50% of the framework grains. The quartz grains are angular to subangular and range from 0.002 mm to 0.06 mm in diameter. Where detrital quartz makes up several percent of the rock, it is disseminated throughout the sample.

Staining with Alizarin Red-S and potassium ferricyanide for carbonate mineral species indicated that the lime mudstones are composed exclusively of low magnesium calcite. Typically the lime mudstones exhibit varying degrees of aggrading neomorphism (Figure 14).

### **Bryozoan-Brachiopod Wackestone Lithofacies**

Wackestones are widely distributed throughout the Paradise Formation. Bioclastic constituents are poorly sorted. Biotic grains consist of bryozoans, brachiopods, pelmatozoan debris, foraminifera, trilobites, and rare mollusks (Figure 16). In addition to whole fossils, there is a high percentage of broken biotic grains. Grain degradation is most likely the result of bioturbation of the muddy substrate by infaunal feeders. In addition to the biotic grains found in this lithofacies, peloidal grains are also present.

The micritic matrix commonly shows signs of aggrading neomorphism (see diagenesis section, Page 95). The neomorphism is typically restricted to the boundary



between the matrix material, the micrite, and the carbonate grain, whether biotic or abiotic (Figure 16).

Detrital silt-sized and very fine-grained, sand-sized quartz ranging from 0.03 to 0.05 mm in size is also found as a common constituent in this lithofacies. As in the lime mudstone lithofacies, the detrital quartz in this lithofacies is subrounded to subangular in shape.

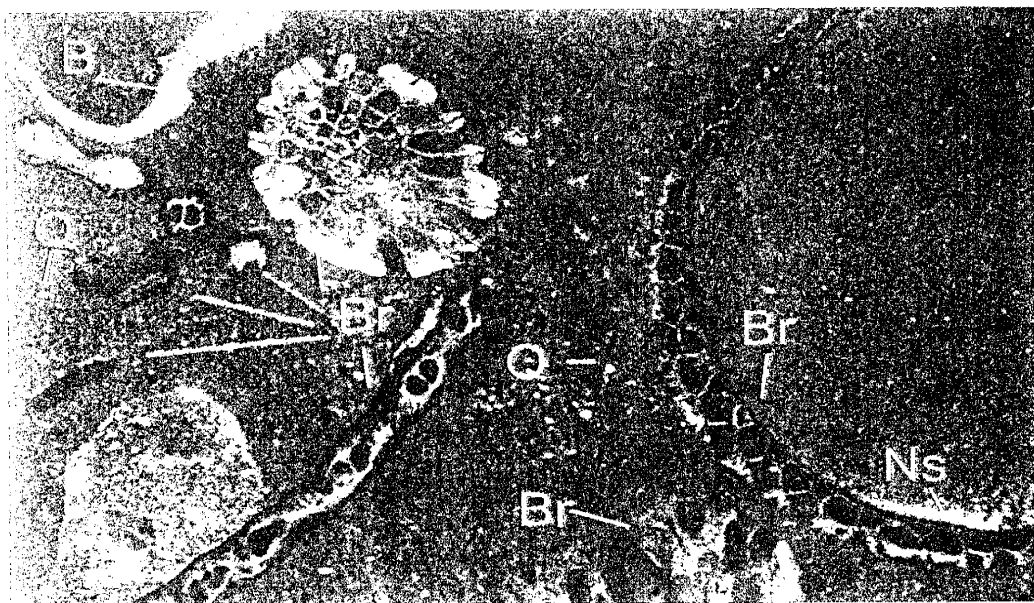


Figure 16. Photomicrograph of a typical bryozoan-brachiopod wackestone lithofacies from the Paradise Formation. (Br-bryozoan, B-brachiopod, Q-detrital quartz, Ns-neomorphic spar. Field of view approximately 6.00 mm)

#### Pelmatozoan-Brachiopod Packstone Lithofacies

This is the second most abundant lithofacies in the Paradise Formation. Although the rock types grouped into this lithofacies may contain varying amounts of sparry calcite cement, this lithofacies is typified by mud-rich rocks (Figure 17). Biotic grains consist of pelmatozoans, brachiopods, bryozoans, mollusks, and rare Foraminifera. Abiotic

carbonate grains in this lithofacies include intraclasts, peloids, and minor ooids. Some of the biotic grains show minor amounts of abrasion and well developed micritic rims.

Micritic matrix is present and shows signs of aggrading neomorphism. Sparry calcite cement is found filling intergranular pore space and void spaces within carbonate grains (see section on diagenesis).

Detrital quartz silt is also present in this lithofacies. It is identical to the silts present in the lime mudstone and the bryozoan-brachiopod wackestone lithofacies. The grains range in size from 0.03 to 0.05 mm and are subrounded to angular in shape. The detrital quartz occurs as individual grains and forms millimeter thick laminae. The upper and lower boundaries of these laminae vary from sharp to gradational with the adjacent carbonate.

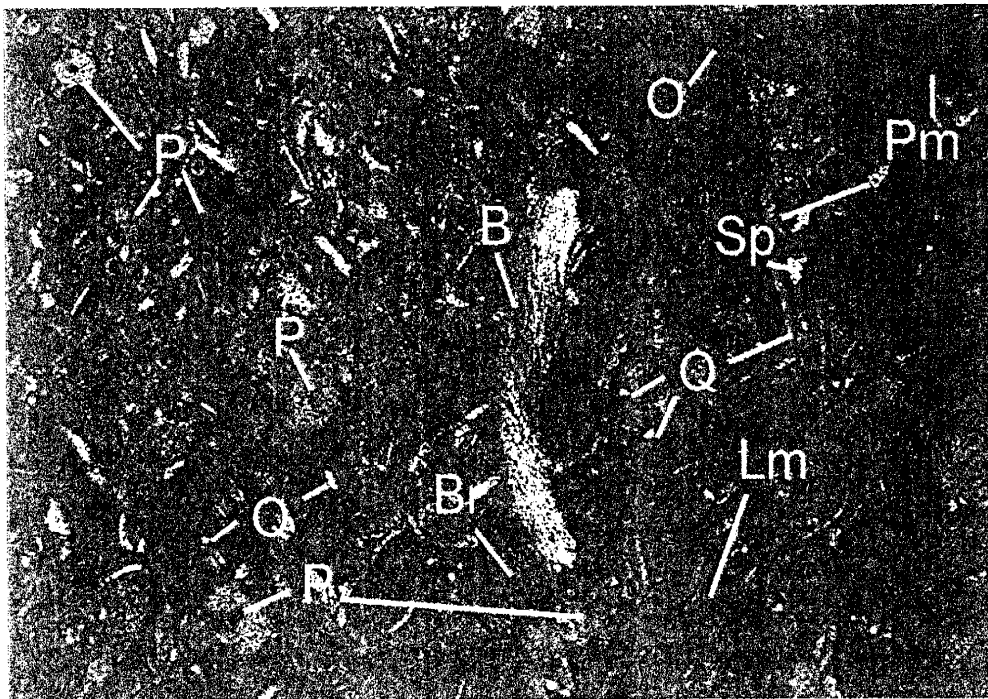


Figure 17. Photomicrograph of a typical pelmatozoan-brachiopod packstone lithofacies from the Paradise Formation. (P-pelmatozoan, Pm pelmatozoan with micritic rim, B-brachiopod, Br-bryozoan, O-ooid, Q-detrital quartz, Lm-lime mud, Sp-sparry calcite cement. Field of view approximately 6.00 mm).

### Abraded Grainstone Lithofacies

This is most common lithofacies in the Paradise Formation. It is dominated by accumulations of highly abraded biotic grains dominated by pelmatozoan debris (Figure 18). In addition, abraded brachiopod and bryozoan fragments are common. Rare mollusk fragments dominated by bivalves are locally present. The biotic grains are well sorted, and in many cases, show significant over packing. Brachiopod and bivalve

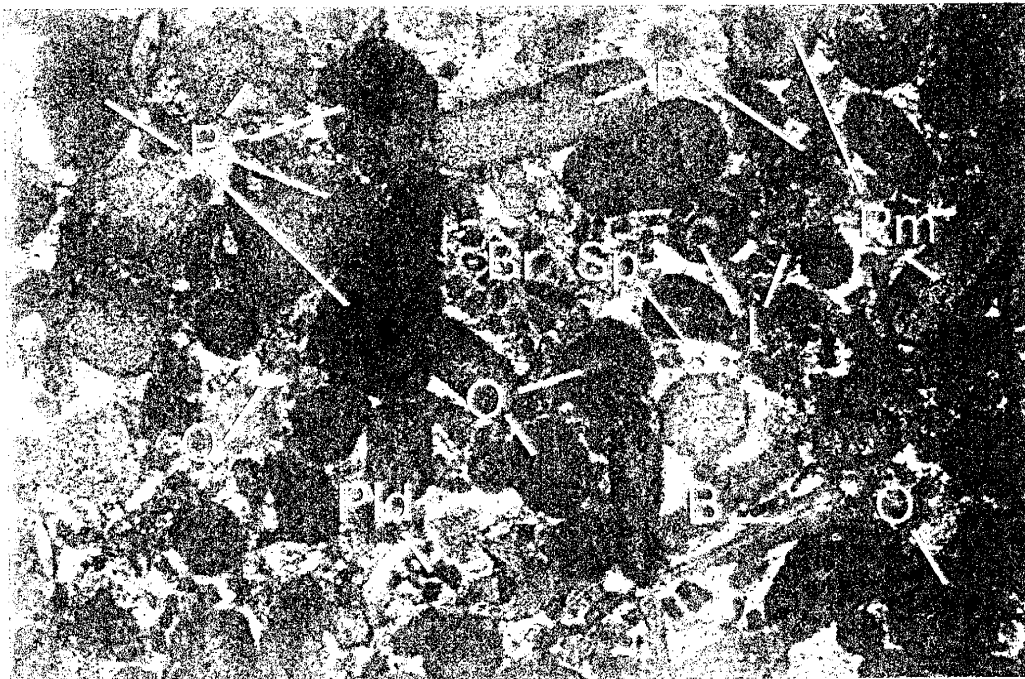


Figure 18. Photomicrograph of typical abraded grainstone lithofacies. Note the high degree of overpacking evident in this sample. This is typical of this facies throughout the Paradise Formation. (P-pelmatozoan, B-brachiopod, Br-bryozoan, Pm-pelmatozoan with micritic rim, O-ooid, I-intraclast, Pld-peloidal material, Q-detriral quartz, Sp-sparry calcite cement. Field of view approximately 6.00 mm)

fragments are consistently disarticulated and commonly broken. The majority of biotic grains are heavily micritized. Micritization is most evident on pelmatozoan debris

(Figure 18). In addition to the biotic grains in this lithofacies, ooids and intraclasts are common framework grains.

Intergranular pore spaces are completely filled with pore-filling, sparry calcite cements virtually eliminating porosity and permeability. Micritic material is conspicuously absent from this lithofacies.

### **Oolitic Grainstone Lithofacies**

Carbonate grains in the oolitic grainstone lithofacies are dominantly, if not entirely, ooids. Ooids in the Paradise Formation range in size from 0.2 mm to 1.0 mm, averaging 0.5 mm in diameter. The ooids are well sorted and exhibit a packed-to-over packed texture. Intergranular pore space is completely occluded by pore-filling sparry calcite cement and isopachous sparry cements (Figure 19). Further discussion of the cements is covered in the section on diagenesis.

Ooid nuclei include of a variety of materials from detrital quartz to broken and abraded ooids. The most typical nuclei are biotic fragments, with the majority being pelmatozoan debris. In cases where nuclei were composed of less stable grains, the original grains were dissolved leaving a mold that has been subsequently filled with sparry calcite cement.

The surrounding cortex commonly consists of four to six coatings. These coatings are composed of dark concentric rings separated by radially oriented calcite (Figure 19). Very few of the ooids have less than three coatings and are similar to what Carrozzi (1989) describes as superficial ooids. Although many of the ooids show some micritization along the outer margins, their primary fabric is well preserved.

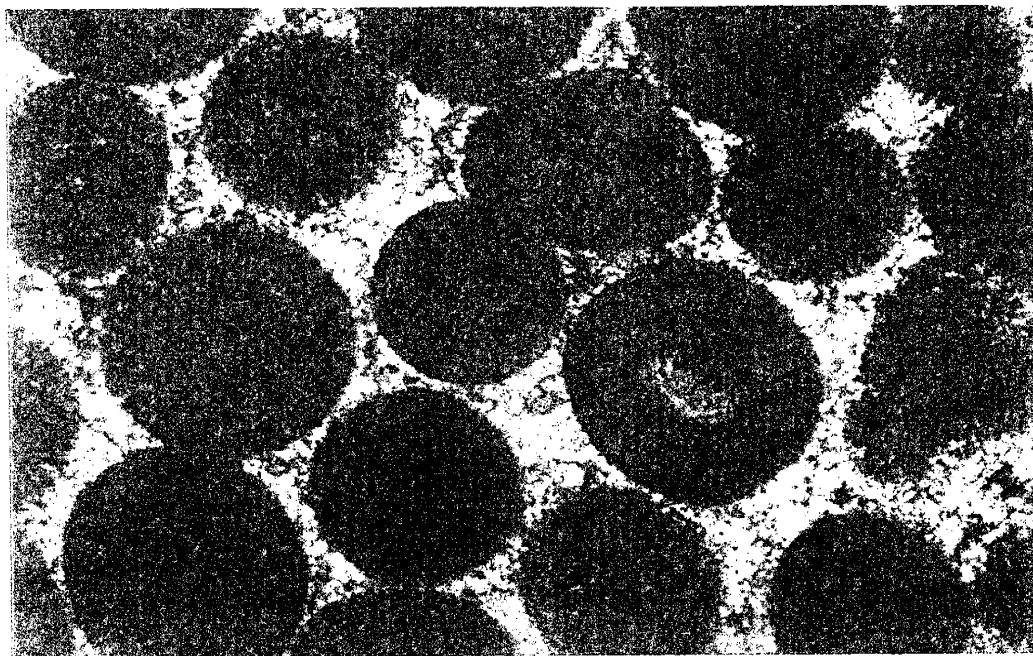


Figure 19. Photomicrograph of oolitic grainstone lithofacies from the Paradise Formation. The radial fibrous internal fabric of the ooids is clearly visible. This is characteristic of all the ooids from the Paradise. (Field of view approximately 3.00 mm).

### Dolomudstone Lithofacies

There is only a single example of this lithofacies observed in the Paradise Formation, located in the northern stratigraphic section located at Horse Pasture Canyon (Appendix A, Page 158). The dolomudstone lithofacies is present as a thin, yellowish orange colored, microcrystalline, dolomite bed. The bed is structureless and devoid of fossils. A significant amount of quartz silt is present throughout the dolostones. Small, spar-filled features similar to what are commonly referred to as birdseye, or fenestral structures, are distributed throughout.

## **Siliciclastics**

### **Sandstone Lithofacies**

Sandstones are distributed throughout the entire stratigraphic interval represented by the Paradise Formation. They occur as tan- to- orangish weathering beds that range from 0.3 m to 1.0 m in thickness. Typically, sandstones are found capping the abraded grainstone or oolitic grainstone lithofacies. The sandstones vary from being massive with no apparent sedimentary structures to containing small-scale ripple cross-laminations. Identifiable fossil fragments are rare in this lithofacies. When present, the fossils are broken and severely abraded. The most common identifiable fossil fragments in sandstones are brachiopods and pelmatozoans.

The sandstone lithofacies is composed of subrounded to subangular, detrital quartz grains ranging from 0.05 to 0.12 mm in diameter. The sandstones are compositionally supermature with quartz as the principal detrital grain present (Figure 20). The quartz is extremely well sorted in all of the samples. The only accessory mineral observed in the sandstones is zircon. Zircons are present in all of the sandstone samples examined for this study. The framework grains are cemented by quartz overgrowths (Figure 21) and by pore-filling sparry calcite.

### **Siltstone Lithofacies**

The siltstone lithofacies is found throughout the Paradise Formation. In outcrop it forms thin (< 0.5 m), orangish, weathering units, which either cap grainstone lithofacies, or are found intercalated with the grainstones. Primary sedimentary structures in the siltstones are small-scale ripple cross-laminations, horizontal laminations, and burrows.

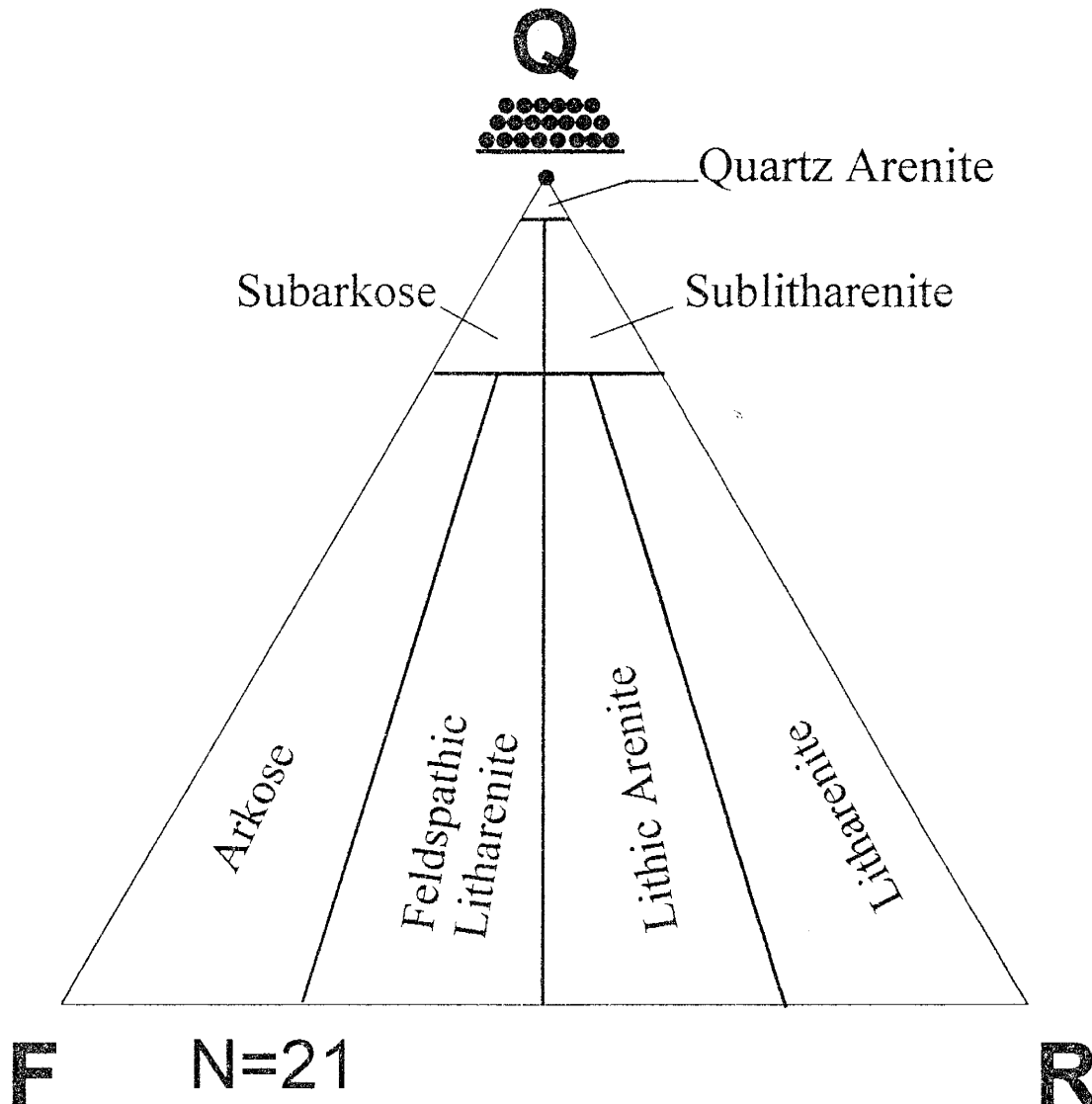


Figure 20. Ternary plot of sandstones from the Paradise Formation. All data points plot directly on the Q pole of the diagram. Multiple data points on the Q pole are plotted above the pole. Q—monocrystalline quartz, F—feldspars, R—rock fragments including chert (Sandstone classification of Folk, 1980).

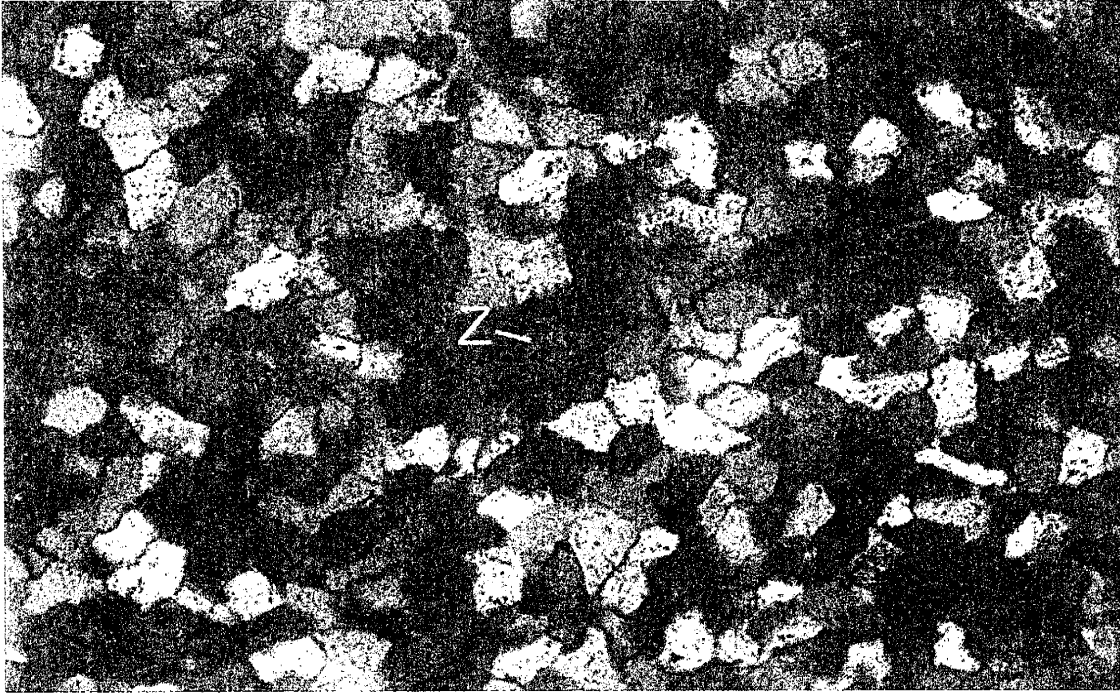


Figure 21. Quartz sandstone from the Paradise Formation. In this example, the sandstone is composed entirely of detrital quartz, which is cemented with quartz overgrowths. Also present is a detrital zircon labeled Z on the image. (Field of view approximately 3.00 mm)

They are composed of tabular and angular, 0.005 mm quartz silt. Marine fossils and peloidal material are associated with the detrital quartz (Figure 22). Common fossils in the siltstone lithofacies include brachiopods, mollusks, bryozoans, and pelmatozoan debris. They are similar to those found in the marine sandstone lithofacies, and are disarticulated, broken, and highly abraded. Intergranular cementing material is a sparry calcite.

#### **Terrigenous Mudstone Lithofacies**

The terrigenous mudstone lithofacies is composed of homogeneous shales, and shales exhibiting moderate fissility. The mudstone lithofacies is most common in the B



member of the Paradise Formation. Commonly, the terrigenous mudstone lithofacies is covered or it is poorly exposed, forming distinctive slopes between the more resistant

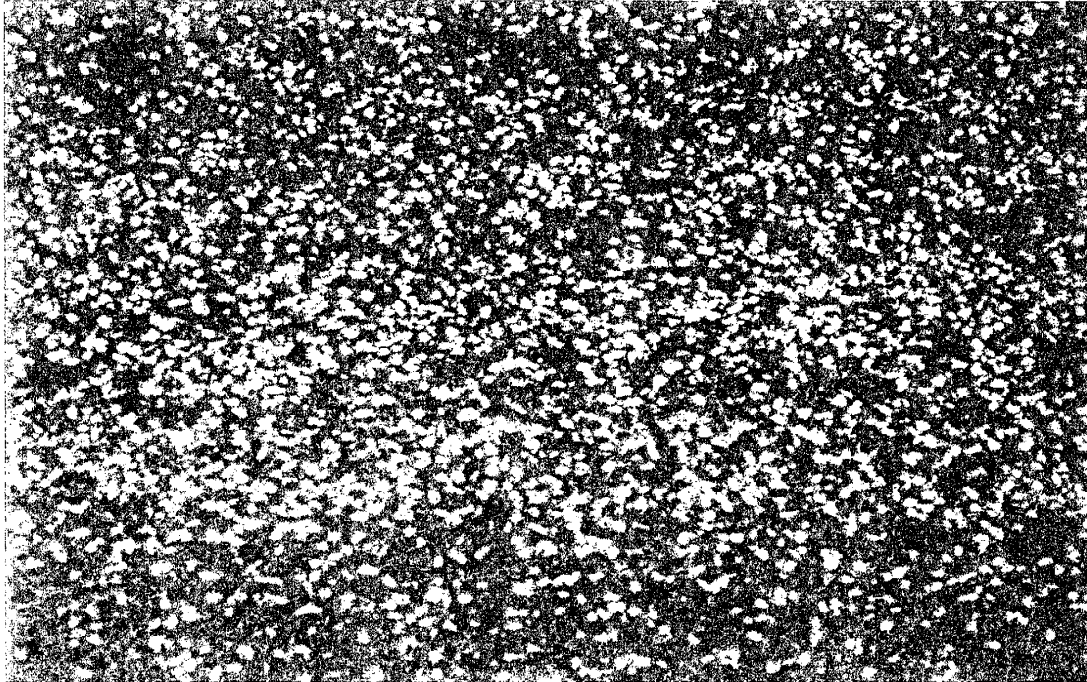


Figure 22. Photomicrograph of a typical siltstone from the Paradise Formation. The dark colored grains are peloidal material mixed with the quartz. Pinkish intergranular areas are stained calcite. (View is approximately 6.5 mm)

carbonate units. When exposed, the mudstones are deeply weathered and retain no primary sedimentary structures. Macrofossils are rare in these units, but when found are typically diminutive brachiopods or bryozoan fragments. Disaggregation of the mudstones also produced minor amount of fossil debris and quartz silt.

Although *Zoophycos* sp. were not observed in any of the measured sections, well developed *Zoophycos* sp. traces were observed in the terrigenous mudstone lithofacies just south of the New Well draw location. These occur in a shaly sequence correlated with the middle member of the Paradise in the New Well draw measured section.

## DIVERSITY

### **Biotic Diversity and Environmental Analysis**

Biotic analysis of marine organisms can be used as a tool for evaluating modern and ancient marine environments, but must conform to uniformitarian principles (Heckle, 1972). One useful measure of biota in marine environments is biotic diversity. Biotic diversity is defined, herein, as the total number of dissimilar taxa. The utility of biotic diversity is its sensitivity to environmental stability. In general, the greater the stability of an environment, the higher the biotic diversity.

Environmental stability encompasses a wide range of factors including, but not limited to, substrate, nutrient supply, water agitation, water turbidity, oxygenation, temperature, salinity, and position relative to the photic zone. Using the salinity distribution of modern fossilizable organisms as one example of stability, Heckle demonstrates (1972, figure 3) that in stable marine environments, virtually all major groups (phyla and classes) will be represented. As stability (salinity in this case) decreases, there is a systematic reduction in the representatives of these major groups, and total biotic diversity declines. When a comparison of diversities is made, the sample with a greater relative biotic diversity represents the more stable environment.

In modern environments, pelmatozoans, bryozoans, foraminifera, and brachiopods represent stenohaline taxa (restricted to normal marine salinity). A crucial assumption is that the salinity tolerance of organisms has remained constant with respect to geologic time. Environmental tolerances of species may have changed with time. An understanding of these tolerances must be established for each individual taxon, making it difficult to evaluate the environmental requirements of extinct organisms. However,

Wilson (1975), Wilson and Jordon (1983) and Enos (1983) all suggest that in ancient carbonate-dominated depositional systems the presence of brachiopods, pelmatozoans, and bryozoans, by themselves or together is indicative of normal marine conditions.

### **Other Measures of Environmental Stability**

In modern biotas, relative abundance (a comparison of the number of individuals in a single taxon) is also a reasonably reliable indicator of environmental stability. High relative abundance is typical of unstable environments. Similarly, measures of relative size (within individuals in a single taxon) are also useful as indicators of environmental stability, with larger specimens correlating with more stable conditions. In the rock record it is difficult, if not impossible, to assess relative abundance and relative size. Biotic diversity may be established from either outcrop or thin section analyses, and comparable results are achieved when comparisons are made using either method (Smosna and Warshauer, 1978).

### **Bias, Biotic Diversity and the Rock Record**

One concern regarding the use of biotic diversity as a tool in evaluating depositional environments relates to the issue of preservational bias. Because only a small percentage of the original taxa in any environment are preserved, analyses of biotic diversity must rely on only a sample of the total original taxa. Laporte (1968) argues that by using changes in the number of preserved taxa (relative diversity), proportional representation of the original biota is achieved, reducing or nullifying the effects of preservation.

Another consideration relates to the possibility of postmortem transport of biotic components from their original environment by wave or current action. In carbonates

postmortem transport is a minor concern. As noted by Laporte (1968), carbonates form in situ and are typically preserved at or near their point of origin. It is this correspondence of carbonate production and minimal carbonate grain transport that results in the coincidence of biofacies and lithofacies in carbonates. Exceptions to this are related to varying hydrodynamic properties among certain carbonate grains in a biofacies. In particular, Foraminifera and pelmatozoan fragments have high intragranular porosities making their effective densities considerably less than those for calcite. Consequently, these grains may be selectively transported by wave or current action and deposited as hydrodynamic buildups or as sheet-like concentrations.

#### **Diversity in the Paradise Formation**

Samples from the Paradise Formation were evaluated with respect to diversity by tabulating the number of different identifiable taxa in thin section (Appendix D). The most common fossils in the Paradise are brachiopods and pelmatozoans. They are present throughout the entire stratigraphic interval at each location studied. Plotting the total biotic diversity from each stratigraphic section of the Paradise shows overall trends in diversity with respect to stratigraphic position (Figure 23, *A* and *D*). At the meter scale, there are large changes in diversity from zero or one to three or higher. These variations in biotic diversity repeat in a regular manner throughout each stratigraphic interval. Comparing relative diversity data from Horse Pasture Canyon and New Well draw sections shows a similar average relative diversity of four along depositional strike, suggesting similar environmental conditions existed along depositional strike.

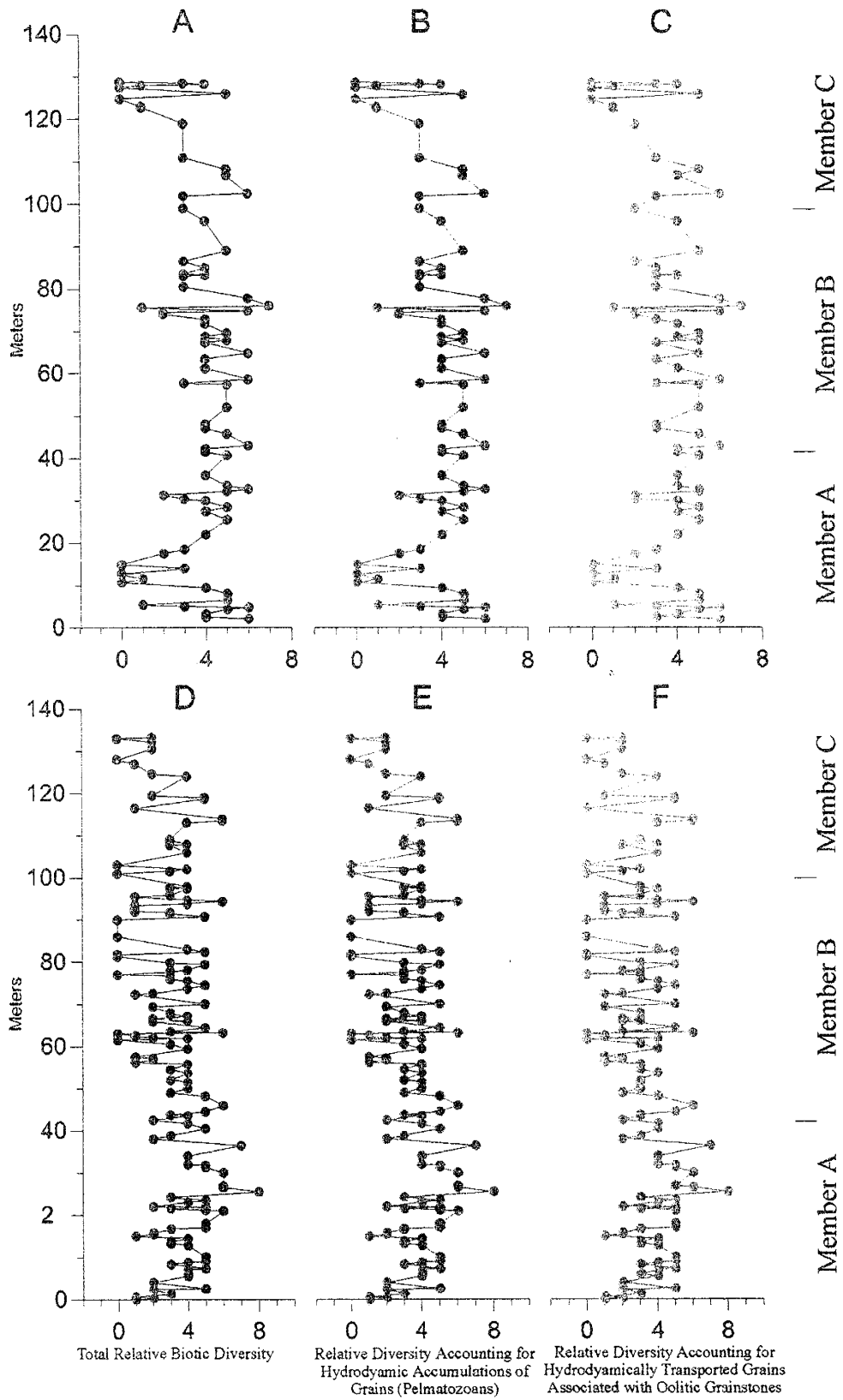


Figure 23. Plots of relative diversity with respect to stratigraphic position. Note the overall consistency of the data sets before and after correcting for transported grains. (Plots (A, B, C) are from Horse Pasture Canyon, plots (D, E, F) are from New Well draw).

The diversity data presented in Figure 23, includes all biotic elements tabulated from each unit sampled. Using all of the biota may be misleading as indicated in the preceding discussion relating to postmortem transport of some carbonate grains. A critical review of these data is needed to identify biotic elements suspected of being subject to selective transportation. Removing suspect carbonate grains from the data set might result in more representative trends of relative diversity. In the Paradise Formation, the most likely grains to undergo postmortem transport are pelmatozoan fragments and foraminiferal tests. Finding these grains in high concentrations in grainstones suggests transport and accumulation by wave or current action. This is especially true in crinoidal grainstones, where 75–100% of the framework grains are pelmatozoan debris. Additionally, the presence of Foraminifera or pelmatozoan debris associated with oolitic grainstones may indicate transport of these biotic grains by wave or current action into the oolitic shoals. Foraminifera are present, but in low numbers. They are also found in mud-rich rocks suggesting they are most likely in situ. There is no change in relative diversity trends when excluding pelmatozoan-rich grainstones by using a minimum cutoff of 75% for pelmatozoan debris (Figure 23, *B* and *E*). Also, removing suspect grains from oolitic grainstones resulted in only minor changes in the trends (Figure 23, *C* and *F*). This suggests that the original data sets accurately reflect stratigraphic variations in relative diversity of the Paradise.

Throughout the stratigraphic interval examined at each location, biotic diversity consistently varied over a wide range, but with an average slope of zero for a best-fit line through the data suggesting long-term environmental stability. This is true not only with respect to time, but also with respect to space. There is little difference in the data

between the Horse Pasture Canyon and New Well draw sections, indicating that environmental conditions were consistent along depositional strike.

Dividing the diversity data into three parts based on the three stratigraphic members (Figure 23) provides a way to evaluate changes in relative diversity in smaller segments. It also provides a framework to compare changes in diversity between stratigraphic sections.

Member A, the lowermost member, represents approximately the lower 42 meters of the Paradise Formation in each section. Statistically the two sections are similar, with Horse Pasture Canyon having a slightly higher mean biotic diversity (Table 1), suggesting somewhat more stable environmental conditions at that location. Using the standard deviation of the data as a measure of variability the data suggest that overall environmental conditions varied in a similarly manner at each location. The slightly higher standard deviation at Horse Pasture Canyon may indicate that environmental conditions fluctuated more there than they did at New Well draw.

At Horse Pasture Canyon the initial diversity is relatively high and then declines, whereas at New Well draw the initial diversity is relatively low and then increases (Figure 23 *A* and *D*). At New Well draw the basal Paradise is a silty, oolite bearing grainstone. Additional carbonate grains include intraclasts, peloidal material, and pelmatozoan debris. This association of carbonate grains, and the lack of lime mud, indicates relatively high wave or current action and is consistent with the development of a shoal or shoreface. The basal grainstones at Horse Pasture Canyon are similar to the grainstones at New Well draw, suggesting they too were deposited in a region of high wave or current action. The differences observed between the two sections above these

basal grainstone units are an increase in relative diversity at New Well draw suggesting establishment of more stable environmental conditions, and a decrease in diversity at Horse Pasture Canyon, suggesting increasing restriction. These changes in biotic diversity are consistent with the progression of lithofacies at each section. At New Well draw, the lithofacies remain matrix-poor indicating more agitated waters and show an overall increase in the relative diversity. At Horse Pasture Canyon, the lithofacies progress into a thin, silty, dolomitic unit suggesting the development of highly restricted supratidal conditions responsible for the decrease in diversity. This difference between

Table 1. Statistical data for relative diversity of member A (lower Paradise Formation)

<b>N=60</b>	<b>New Well draw</b>	<b>Horse Pasture Canyon</b>
Mean	3	4
Mode	3	4
Standard Deviation	1.6	1.8

the two sections may reflect a subtle deepening of water between them.

The relative diversity in member B of the Paradise Formation shows considerable variation between the two sections (Figure 23, *A* and *D*). Although the trends of the data are essentially identical, there are wider fluctuations at New Well draw than at Horse Pasture Canyon. The New Well draw section also has a larger number of samples with low relative diversity. Despite these apparent differences in the data plots, (Figure 23 *A* and *D*), the biotic diversity between the sections is statistically very similar with comparable mean values (Table 2). Similar to member A, the standard deviations of the data in member B indicate wide fluctuations in the diversity at each location and varied



in a similar manner at both locations. The similarity between the standard deviation of these data and those in member A also suggests that relative diversity, hence environmental conditions, varied in a similar fashion in each member.

In member B, the larger mean diversity at Horse Pasture Canyon, compared to the New Well draw section, suggests that slightly more stable conditions existed at Horse Pasture Canyon during member B time.

The relative diversity in the uppermost part of the Paradise Formation equivalent to member C is similar in each section (Figure 23, *A* and *D*). Each section shows a declining trend in diversity near the top of the sections. The similarity in these trends suggests an overall decline in environmental stability as deposition of the Paradise was coming to a close.

Table 2. Statistical data for relative diversity of member B (middle Paradise Formation)

<b>N=72</b>	<b>New Well draw</b>	<b>Horse Pasture Canyon</b>
Mean	3	4
Mode	3	3
Standard Deviation	1.7	1.4

Higher mean diversity at Horse Pasture Canyon in member C (Table 3) once again suggests that overall, more stable conditions existed at that location during the end of Paradise deposition. The same standard deviation of the data between each section in this member indicates that the magnitude of environmental variability varied in a similar fashion at each location. The higher standard deviation of these data compared to those of members A and B indicates that there were greater fluctuations in relative biotic

diversity, and changing environmental conditions during member C time. This, in conjunction with the lower mean values in member C, might reflect decreasing environmental stability during the waning stages of Paradise deposition.

Table 3. Statistical data for relative diversity of member C (upper Paradise Formation)

<b>N=29</b>	<b>New Well draw</b>	<b>Horse Pasture Canyon</b>
Mean	2	3
Mode	2	3
Standard Deviation	2.0	2.0

The preceding discussions evaluated the relative diversity of each member of the Paradise Formation and compared the two sections. From these data the following generalizations can be made. At the meter scale relative biotic diversity varied greatly reflecting changing environmental conditions. For the lower two members these fluctuations were of similar magnitude. In the upper member the gradual decline in relative diversity, and greater degree of fluctuation in relative diversity reflects decreasing environmental stability towards the end of Paradise deposition during the waning stages of Late Mississippian time.

### **Diversity Trends and Lithofacies**

Using lithostratigraphic and petrographic data, an idealized cycle for the Paradise Formation can be constructed (Figure 24; Figure 25, Page 64). Variations in relative biotic diversity corresponding to vertical position within the cycle are plotted against an ideal cycle (Figure 24). This curve is based on averages in relative diversity calculated for each lithofacies. The lime mudstone and oolitic grainstone lithofacies contain few biotic grains compared to the total volume of the rock. This small number of biotic

grains reduces the statistical accuracy of the lower and upper portion of this curve. The overall shape of the curve accurately reflects variations in biotic diversity with respect to any given cycle regardless of any reduction in statistical accuracy.

The pattern of changing relative diversity with respect to a cycle should be repeated time after time in a cyclic stratigraphic sequence. Such a pattern could be a valuable aide in defining cycles. In the Paradise Formation, this is not necessarily the case. Using changing patterns in relative diversity from the Paradise as an indicator of cyclicity produces a lower number of cycles than defined based on lithostratigraphy and petrography. The reason for this discrepancy may lie within the cycles themselves. Cycles in the Paradise can vary significantly from the ideal cycle depicted in Figure 24. Many of the cycles found in the Paradise are missing one or more of the lithofacies found in the idealized cycle. The end result of these variations may be to mask a cycle. If the upper portions of a cycle are not developed, the higher diversity portions might be missing resulting in placing the lower diversity lithofacies of two cycles stratigraphically on top of each other, making the two cycles appear as a single, thicker cycle using diversity data. Whereas, based upon field relationships, the boundaries separating cycles are more distinctive. The variations in cycles and their potential causes are discussed in greater detail in the chapter on cyclicity.

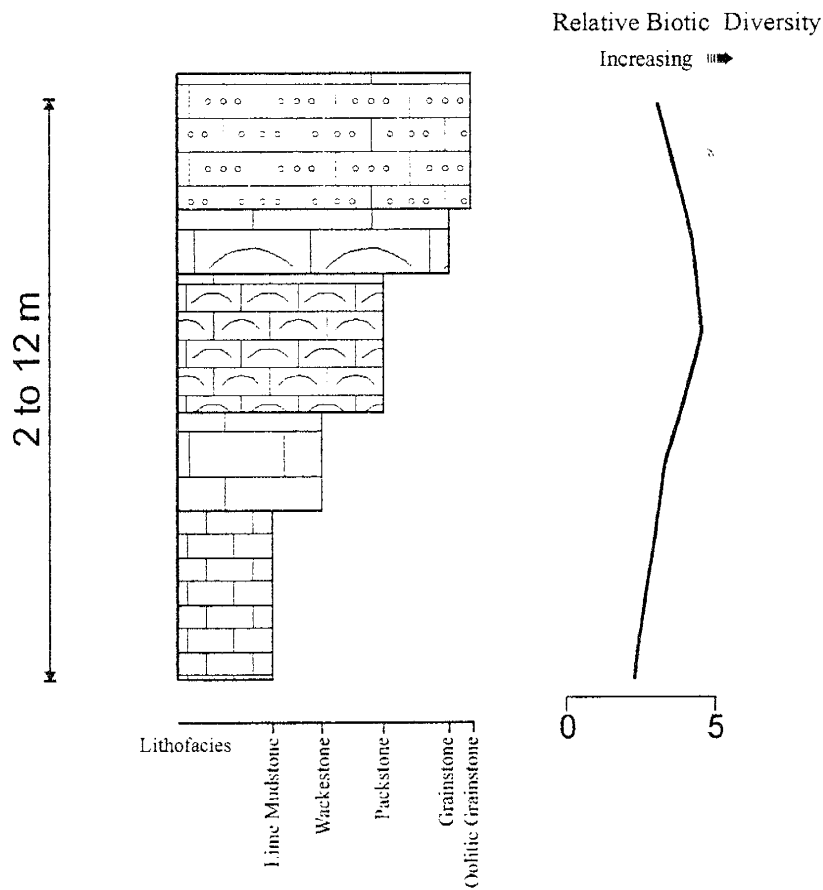


Figure 24. Diagram of an idealized carbonate cycle in the Paradise Formation showing the general pattern of variation in biotic diversity through a cycle with respect lithology. Diversity curve represents average values for each lithofacies.

## **ENVIRONMENTAL INTERPRETATIONS**

This section focuses on environmental interpretations of the lithofacies.

Environmental interpretations of these lithofacies are presented in the same order as they were described, which approximates their observed stratigraphic relationships. All of the environmental data and interpretations are integrated into an idealized depositional sequence for the Paradise Formation. This idealized depositional sequence is compared to both modern and ancient carbonate depositional models.

### **Previous Environmental Interpretation**

The Paradise Formation has not been assigned or placed into any depositional model or compared to any modern analogs of carbonate systems. Previous interpretations are limited to suggesting that deposition of the Paradise occurred on a shallow to very shallow marine carbonate platform (Packard, 1955). Zeller (1965) and Armstrong and Mamet (1988) accepted this depositional framework.

### **Lithofacies Interpretations**

#### **Disseminated Detrital Quartz**

In addition to the carbonate grains and matrix, there is some fraction of disseminated detrital quartz present in each of the carbonate lithofacies. This quartz is discussed here to avoid repetition in the following sections. The quartz is silt-sized and found as angular to tabular shaped grains. The size, shape, and distribution of the detrital quartz is similar and consistent with windblown quartz silts described from the Pennsylvanian of the Pedregosa and Orogrande basins (Soreghan, 1993) and the Permian in southwestern North America (Fisher and Sarnthein, 1988). These silts are also very

similar in size and shape to modern windblown silts found in the sediments of the Atlantic Ocean derived from North Africa (Fisher and Sarnthein, 1988).

The similarities of windblown silts described from modern eolian environments, and from other formations in the rock record to those found in the Paradise Formation, suggest that the silts in the Paradise have an eolian origin. Currently accepted paleogeographic plate reconstructions for the Late Mississippian (Ross and Ross, 1987b) place the study area within the tradewind belts at latitudes where dry desert conditions similar to present day North Africa may have developed. Consistent winds in the trade wind latitudes would be able to disperse the silt-sized material in suspension over wide regions, where they eventually settled out and were incorporated into the carbonate sediments.

## **Carbonate Lithofacies**

### **Lime Mudstone Lithofacies**

The information derived from various skeletal grains and sedimentary structures observed in this lithofacies suggests the lime mudstone lithofacies formed offshore below wave base in waters, which were capable of supporting a marine biota. Bottom sediments may have varied from well oxygenated to oxygen-poor as suggested by the benthic biota, bioturbation, and the ichnofossils *Chondrities* sp. and *Zoophycos* sp..

The presence of the ichnofossils *Chondrities* sp. and *Zoophycos* sp. indicate deposition offshore, in quiet water (Seilacher, 1967; Gall, 1983; Ekdale, 1988). *Chondrities* sp. and *Zoophycos* sp. may also indicate reduced oxygen levels within bottom sediments with the organisms generating these traces requiring a connection to well oxygenated sea water (Ekdale, 1985; 1988). The reduced ichno-diversity associated

with oxygen-poor sediments acts to preserve some sedimentary structures, rather than obliterate them from the sediments. In the Paradise Formation there is a coincidence with lime mudstone beds that have preserved laminations and the presence of *Chondrites* sp. and *Zoophycos* sp., suggesting low ichno-diversity and low oxygen settings. The presence of homogenized matrix material, minute skeletal fragments, and pellets in some of the lime mudstones also suggest intense bioturbation by infaunal organisms within well oxygenated, organic-rich sediments in these examples.

The overwhelming predominance of lime mud suggests a lack of winnowing and that deposition likely occurred in quiet water. Lime mud accumulations in quiet water can occur either offshore, below wave base, or in relatively shallow water in a protected lagoonal setting. The carbonate grain types and primary sedimentary structures recognized in this lithofacies may occur in either depositional setting. The presence of peloidal material suggests three possible origins. They may represent preserved fecal matter. Alternatively, the peloids may be small intraclasts, and their small size obscures the origin of the grain. Intraclasts like these may be swept offshore from shallower, more shoreward positions (Wilson, 1969). A third alternative is the complete micritization of carbonate grains. If the peloids are either micritized grains or intraclasts, there should be a range of shapes and sizes. If the peloids have a fecal origin, they should all be approximately the same shape and size. The consistent size and shape of the peloidal material in this lithofacies suggests that they are fecal pellets. In shallow, protected lagoons, preservation of fecal pellets may be attributed to slightly elevated temperatures (Lees, 1975). Fecal pellets may also be preserved in deep, quiet water settings below

wave base, where agitation is insufficient to break them apart (Wilson, 1975). If lithification is early, the pellets will retain their original shape.

Brachiopods and bryozoans, the chief biotic components in this lithofacies, are considered both in modern marine environments Heckle (1972), and in the geologic record, to represent more open, normal marine conditions (Wilson, 1975, Wilson and Jordan, 1983; Enos, 1983). Bryozoans are found as various sized fragments.

Brachiopods are found as fragments and as whole, disarticulated shells. It does not appear that either of these groups of fossils are in life position. This may indicate either shoreward or seaward transport of the grains from their place of origin by strong wave or current action. Alternatively, they may represent low diversity *in situ* death assemblages where the skeletal grains were disturbed postmortem by infaunal burrowing organisms. This situation may also occur either in a protected lagoon or in deeper water offshore. The brachiopods and bryozoans suggest a more normal, open-marine environment.

#### **Bryozoan-Brachiopod Wackestone Lithofacies**

The information derived from the various components in this lithofacies suggest deposition could have occurred either offshore in open-marine waters or in a protected lagoon. The high biotic diversity and biotic associations in this lithofacies suggest deposition occurred in waters capable of supporting a robust, normal marine, benthic biota.

The presence of large volumes of lime mud indicates quiet water conditions existed during deposition. As is the case with the lime mudstone lithofacies, large volumes of lime mud can accumulate in quiet-water either offshore below fair-weather wave base or in relatively shallow water in protected lagoons.



Peloidal material is present, but rare. These peloids vary in size and shape suggesting that they are either micritized carbonate grains, or small intraclastic material. The small size and nondescript shapes of the peloids precludes further identification. Peloidal material formed by micritization of grains, or those composed of diminutive intraclasts, may be present in offshore waters or in lagoonal waters. In either of these settings, the peloids may be formed *in situ* or be swept in by currents.

There is a significant increase in overall biotic diversity in this lithofacies compared to the lime mudstone lithofacies. This relatively high biotic diversity suggests environmental conditions were relatively more stable than during deposition of the lime mudstone lithofacies. The most common biotic elements in this lithofacies are brachiopods and bryozoans. A significant portion of the remaining biotic elements are pelmatozoans. Bryozoans and pelmatozoans are filter feeding organisms and require a certain degree of current activity to survive. Their presence suggests the depositional setting was in a position where mild currents were able to sustain such communities, but were not strong enough to winnow lime mud. Fossils are commonly found whole with the exception of pelmatozoans, which quickly disarticulate upon death. In both present day environments (Heckle, 1972) and the ancient (Wilson and Jordan, 1983; Enos, 1983), the association of brachiopods, bryozoans, and pelmatozoans suggests stable, normal marine conditions. The presence of these biotic elements in this material is interpreted to suggest deposition occurred in open, normal marine conditions rather than in a protected lagoonal setting where waters deviate from normal marine conditions.

The homogenized nature of the matrix and variety of broken skeletal fragments suggest intense bioturbation. Such a high degree of bioturbation suggests well

oxygenated, organic-rich bottom sediments and is not indicative of any specific depositional setting.

### **Pelmatozoan Packstone Lithofacies**

The information derived from components in the pelmatozoan packstone lithofacies suggest deposition of this lithofacies occurred offshore above storm wave base in moderately agitated, open circulation waters. The biotic associations suggest stable, normal marine conditions similar to the brachiopod-bryozoan wackestone lithofacies. Associated with the biotic grains are small numbers of ooids. The minor amount of ooids (<25%) suggests that they are allochthonous and formed in an adjacent, higher energy facies suitable for creating ooids (Folk, 1962).

A decrease in the volume of lime mud relative to carbonate grains in this lithofacies suggests increased wave or current action to a level capable of winnowing matrix material, likely above storm weather wave base. It is possible for currents to be generated in shallow, protected lagoons, but their effects on winnowing lime mud is negligible. In these settings there is little chance that the mud can be swept out of the lagoon. When mud is stirred by water agitation in such settings the mud is moved and redeposited in the same environment with no winnowing. It is more likely that stronger currents, such as those found offshore in open waters, would result in the winnowing of matrix material.

Biotic diversity is relatively high and comparable to the brachiopod-bryozoan wackestone lithofacies. The most common biotic component is pelmatozoans. Brachiopods and bryozoans are commonly associated with the pelmatozoans. This biotic association suggests stable normal marine conditions existed during deposition of this

lithofacies (Wilson and Jordan, 1983; Enos, 1983). There is some micritization of skeletal grains. The micritization tends to be restricted to pelmatozoan fragments where, in some instances, entire columnals have been micritized and are recognizable only by their shape.

Ooids make up a very small proportion of the carbonate grains in this lithofacies when compared to the bulk volume of carbonate grains. Although ooids typically form in highly agitated water, they are known to form in quiet-water settings. Quiet-water ooids tend to be small (0.05 to 0.15 mm), with few poorly developed laminae, and have a radial structure (Flügel, 1982). The ooids in these rocks do have a radial-fibrous structure, averaging 0.5 mm in size. The low numbers of well-developed ooids suggest that the ooids are allogenic, and were transported by wave or current action into this mud-rich quieter water setting.

Intraclasts are present, but they make up a small percentage of the bulk rock volume (<25%). According to Folk (1962) intraclasts, if present, are the most important carbonate grain type. Because their presence implies deposition in shallow water, with a lowered wave base or an increase in local tectonism. Intraclastic material in this lithofacies varies in size and shape. In many cases the intraclasts have an identifiable skeletal grain core that is coated with an earlier lithified lime mud, suggesting transport from another location. Some of the intraclasts are composed of dark, nondescript micritic material of unknown origin. These more obscure intraclasts could have been swept into this lithofacies by currents, or they may represent highly micritized carbonate grains.

### **Abraded Skeletal Grainstone Lithofacies**

The environment of deposition of this lithofacies was most likely in shallow, normal marine waters in a region under constant water agitation by wave and current action.

The complete lack of matrix material and abraded skeletal fragments indicate constant water agitation by wave and current action. Even though the grains are highly abraded, transport of the grains into this lithofacies is not likely. Laporte (1968) argues that carbonates form *in situ* and are typically preserved at or near their point of origin, resulting in the coincidence of biofacies and lithofacies. Exceptions to this are related to varying hydrodynamic properties among certain carbonate grains in a biofacies. In particular, Foraminifera and pelmatozoan fragments have high intragranular porosities making their effective densities considerably less than those for crystalline calcite. Consequently, these grains may be selectively transported by wave or current action and deposited as hydrodynamic buildups or as sheet-like concentrations.

A specific subtype of the abraded grainstone lithofacies is composed dominantly (>75%) of pelmatozoan debris. Typically, high concentrations of pelmatozoan debris form above fair-weather wave base in regions of constant water agitation. The high concentrations of pelmatozoans grains in the Paradise Formation are likely the result of selective transport and hydrodynamic concentration of grains.

In addition to the biotic grains in this lithofacies, ooids are typically present. The moderate to high water agitation suggested by the abrasion of biotic grains could possibly result in ooid formation. The low percentage of ooids (<25%) with respect to the total

carbonate grain volume suggests transport of the ooids into this lithofacies by wave or current action, rather than *in situ* generation of the ooids (Folk, 1962).

Intraclasts are also found in this lithofacies, but make up less than 25% of the total bulk grain volume. Their presence also argues for moderate to strong water agitation, and shallow water conditions (Folk, 1962).

### **Oolitic Grainstone Lithofacies**

The environment of deposition for the oolitic grainstones lithofacies is in a region of shoaling well above wave base where waters are under constant agitation. The development of large volumes of ooids and the development of cross-stratification indicate constant, high water agitation by waves and/or currents. Water salinities and temperatures were most likely elevated and contributed to the generation of oolites (Lees, 1975). Basal contacts with the underlying facies range from sharp and erosional to gradational, suggesting that the ooids formed as mobile shoals or sheets in shallow water and migrated across the shelf. The rare occurrence of normal marine fauna such as, brachiopods, bryozoans, and pelmatozoans in this lithofacies suggests that these grains were transported into the higher salinity waters, where the oolitic shoals were forming, from adjacent environments where more normal marine conditions existed.

### **Dolomudstone Lithofacies**

The suggested environment of deposition for this lithofacies is supratidal. The microcrystalline texture of the dolomite and the presence of fenestral structures and rip-up clasts are typical of supratidal conditions (Wilson, 1975). Of these features, the fenestral structures are most indicative of supratidal conditions (Shinn, 1983). Formation of fenestral fabric is the result of gas bubbles from the putrefaction of organic matter

trapped within the sediments. The presence of rip-up clasts may indicate intense current activity possibly from storm events that ripped up and redeposited lithified, or partially lithified carbonate sediments. Rip-up clasts also form from desiccation cracks on the exposed surface of supratidal or intertidal environments. Rip-up clasts formed by exposure have a distinctive concave up shape in cross section. The rip-up clasts observed in this lithofacies are small (<4cm), show some indications of being curved, and are found in discrete layers. These characteristics are most similar to rip-ups formed through desiccation, rather than by storm events. This interpretation is consistent with the notion that the region was arid during Paradise time (Kottowski, 1965; Sivils and Johnson, 1993).

In arid regions dolomites are commonly associated with evaporites, such as in the Persian Gulf; Shark Bay, Australia; and to some degree in the Bahamas. Even though paleogeographic evidence suggests that the Pedregosa basin region was arid during Paradise time, there is a lack of associated evaporites in the Paradise Formation. This lack of evaporites associated with the dolomites in the Paradise suggests that these dolomites formed in a setting similar to the modern Coorong Lagoon. Coorong Lagoon is a region of coastal lagoons and ephemeral coastal lakes situated along the arid southern coast of Australia. In this setting, early dolomitization of aragonite and the precipitation of primary dolomite takes place in the mixed-water environments of coastal ephemeral lakes and in the coastal lagoons (Alderman, 1959). Despite the aridity of the region and high rates of evaporation there is an absence of evaporites. This lack of evaporite deposition is likely due to the reflux of brines forming in the lagoons and lakes mixing with seaward flowing groundwater (Morrow, 1982b). Another possibility is that

these dolomites were originally precipitated as lime muds in a supratidal setting, and were subsequently diagenetically altered to dolomite. This also would explain the lack of associated evaporites. With the little data available neither of these scenarios can be ruled out.

## **Detrital Clastic Lithofacies**

### **Siltstone Lithofacies**

The siltstone lithofacies was deposited in an eolo-marine depositional environment. Eolo-marine is a term used by Fisher and Sarnthein (1988) for sediments whose depositional history includes an eolian part and a marine part. The size, shape and compositional maturity of the quartz in these siltstones, the presence of rare detrital mica, and the complete lack of a clay-sized fraction are characteristic of windblown detrital quartz.

Fossils are present, but rare in these siltstones. Typical fossils present are bivalves, gastropods, brachiopods, pelmatozoan, and bryozoans. Bivalves and gastropods are not necessarily indicators of a marine setting, while the brachiopods, pelmatozoans, and bryozoans are indicators of marine settings (Wilson and Jordan, 1983). In addition to skeletal fragments in the siltstones circular burrows are relatively common.

Pellets are also common in this lithofacies. The pellets are found dispersed within the lithofacies as well as making up discrete laminae.

Various sedimentary structures are present in the siltstone lithofacies. Sedimentary structures include ripple laminations, small trough cross-bedding, and horizontal lamination, typical of water laid sediments (Allen, 1984).

All of the information from the detrital quartz in the siltstones, including the size, shape, associated detrital grains, and maturity is consistent with eolian derived silts. The presence of marine fossils strongly suggests a final marine depositional setting for the siltstones.

### **Sandstone Lithofacies**

An eolo-marine depositional environment is also suggested for the sandstone lithofacies. The sandstones are texturally and compositionally supermature. Surface textures and shapes of the quartz grains, associated rare mica grains, and distinctive lack of clay-sized detrital fraction are consistent with an eolian origin for the quartz (Kransley and Trusty, 1985; Fisher and Sarnthein, 1988). Biota present includes brachiopods and pelmatozoans. Burrowing by infaunal organisms is also common in this lithofacies.

Sedimentary structures in the sands consist of small-scale ripples and oscillation ripples. The type and scale of these sedimentary structures is consistent with those formed in water-laid sediments (Allen, 1984). These structures combined with marine fossils indicates that final deposition of the sands was in a marine setting.

### **Terrigenous Mudstone Lithofacies**

The probable environment of deposition for this lithofacies was in a deep, open-marine setting. The presence of small fossil fragments and a variety of ichnofossils, including *Zoophycos* sp. indicates that waters during deposition were hospitable to biota. The scarcity of large, identifiable, fossil material makes it difficult to accurately assess environmental conditions. The high content of quartz silt present in this lithofacies was likely delivered by eolian processes, with the source of silt being inland or coastal dunes.



Due to limited outcrops and preservation of the Paradise Formation the only known preserved facies are marine, with the single exception of the dolomudstones described herein. This limitation makes the identification of any known potential point sources, such as a fluvial system, for the delivery of clay-sized detritus by fluvial and/or deltaic systems during Paradise time virtually impossible. However, it is common for terrigenous muds to be deposited in a basin by lateral transport (Burchette and Wright, 1992). This could mean that the shales were derived from a fluvial system far removed from the Big Hatchet region and swept into the area by lateral marine currents. Some of the clay-sized material in the terrigenous muds, along with the very fine quartz silt, was likely delivered to the basin by prevailing winds as eolian sediments.

### **Facies Patterns**

The vertical and lateral relations of the lithofacies are discussed in this section. Once these relationships are established they will be used to develop a depositional model and to evaluate cyclic sedimentation in the Paradise Formation.

#### **Vertical Facies Relationships**

Lithofacies exhibit a repetitious vertical pattern throughout the entire stratigraphic interval suggesting cyclic sedimentation. Vertical boundaries separating the different lithofacies are sharp and distinct. Each succession of lithofacies is a coarsening-upwards sequence. These sequences begin with either a terrigenous mudstone (shale) or a lime mudstone culminating in one of the coarser grained lithofacies, such as an oolitic grainstone. In some instances, cycles are capped with either a sandstone or a siltstone (Figure 25). Some thirty of these coarsening-upward sequences were identified in the Paradise Formation's stratigraphic interval. Commonly, these packages of rock are

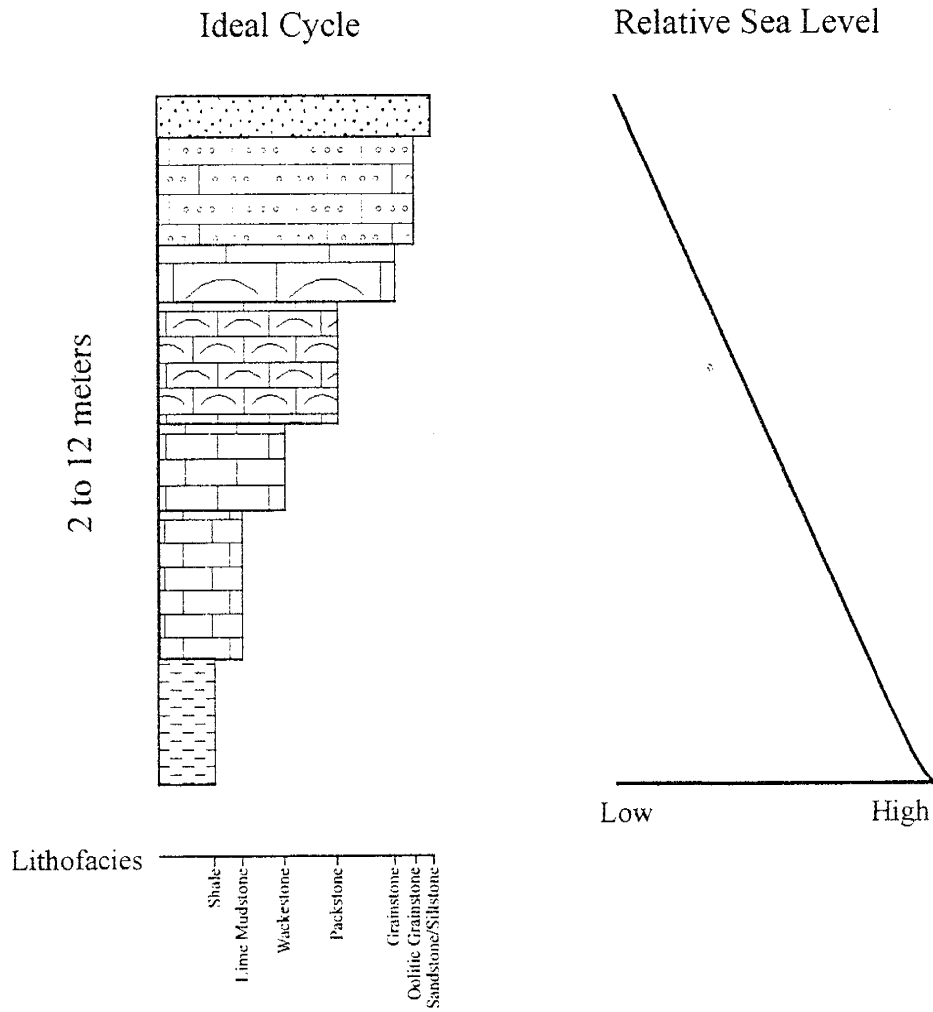


Figure 25. Graphic illustration of an ideal cycle from the Paradise Formation. Sea level curve indicates relative water depths, and shows the shallowing-upwards character of a cycle. (See symbol key in Appendix A)

missing one or more lithofacies. The missing lithofacies may happen at any place within the ideal succession; however, the grainstones capping cycles or coarse-grained detrital clastic lithofacies are the most commonly missing lithofacies. The causes for missing lithofacies are addressed in the discussion on cyclicity.

There is a single occurrence of dolomite in the Horse Pasture Canyon section. Since this is the only observed occurrence of this lithofacies in the Paradise Formation in the Big Hatchet Mountains, it was left out of the ideal shallowing-upwards sequence. In an ideal sequence from the Paradise, the dolomitic mudstone would occur between two lime mudstone facies. In this position, the dolomudstone is acting as the cap, or top of the lower cycle, and as the flooding surface of the next cycle (Figure 26).

### **Lateral Facies Relationships**

Tracing lithofacies laterally in the field revealed remarkable uniformity in the lithofacies, with a subtle thickening of lithofacies from north to south. Although all of the units show some degree of increasing thickness in a southerly direction, thickening is most prevalent in the fine-grained lime mudstone and shale lithofacies (Figure 12). The one exception to this is found at Horse Pasture Canyon. In this section a single, thin, dolomitic unit in the lowermost part of member A is traceable to the north for several miles, but thins to zero thickness toward the south and is completely absent in the New Well draw section.

## **DEPOSITIONAL MODELS**

Using the vertical and lateral facies relationships established for the Paradise Formation an idealized depositional cross section can be constructed (Figure 27) in

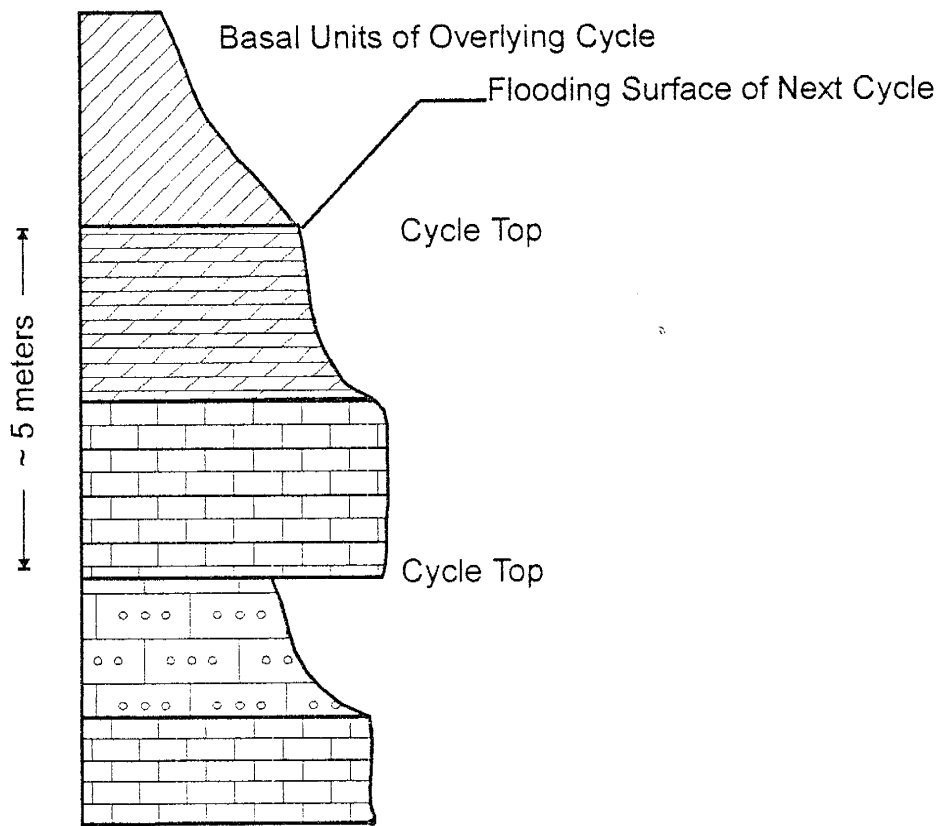


Figure 26. Vertical lithofacies relationship of the single occurrence of dolomudstone in the Paradise Formation at Horse Pasture Canyon section. The dolomite is the capping unit of cycle number 4. Graphic shows weathering profile (See symbol key in Appendix A)

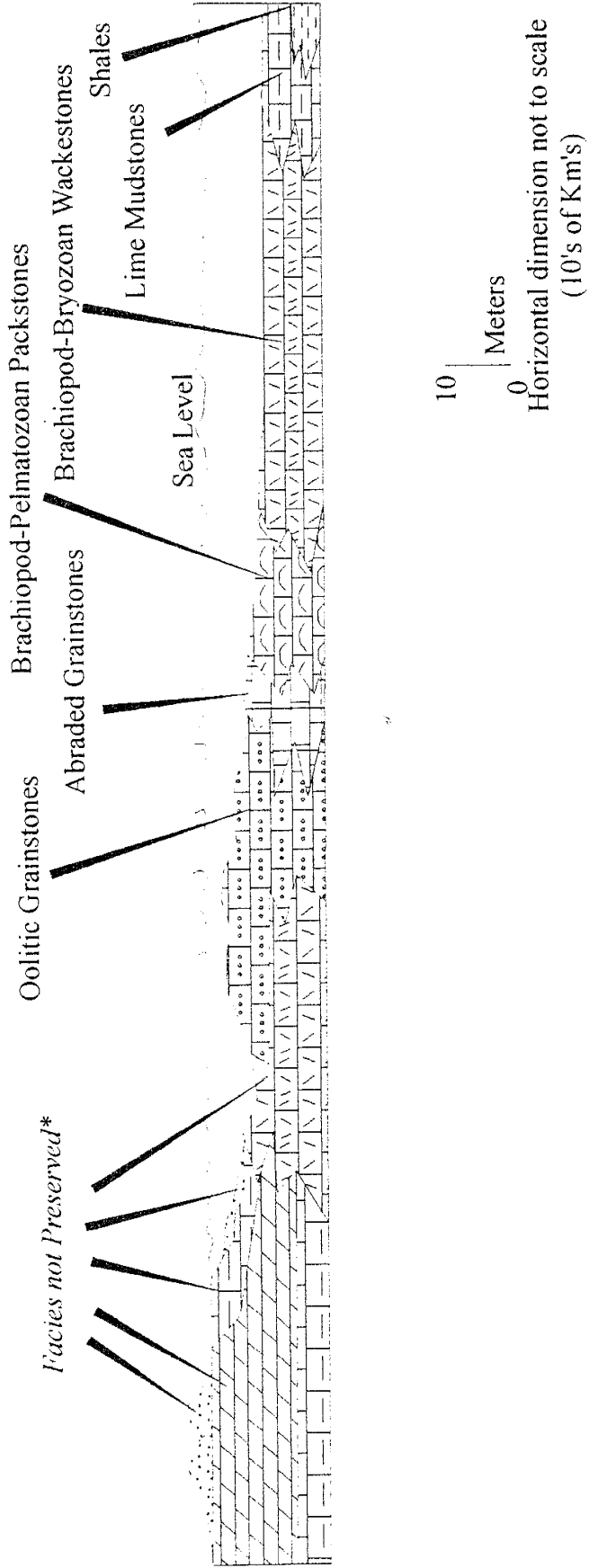


Figure 27. Interpretative depositional cross section of the Paradise Formation at any given point in time showing the lateral distribution of facies presented in Figure 25. Symbols correspond to those used in Figure 25 and those in Appendix A. (\*There is a single occurrence of dolomitic lime mudstone in the Horse Pasture Canyon Section)

order to aid in assessing what carbonate environments were present during the deposition of the Paradise. This idealized cross section is compared to modern carbonate depositional models and systems.

### **Modern Carbonate Depositional Systems**

It is appropriate to examine modern carbonate depositional systems that can act as analogs for the rock record. Of the modern carbonate systems currently active, two of them, the Bahamas and the Persian Gulf, provide the wide range of environments and lithofacies most appropriate for this study.

#### **Bahamas**

The Bahamas are a series of isolated carbonate platforms of various sizes. The platforms are rimmed by coral reefs and with well-developed ooid sand shoals (Figure 28) forming in regions of higher energy. Shoreward of these ooid sand shoals and reefs are carbonate sands, grapestones, and highly pelleted lagoonal lime muds. Increasing restriction within the lagoonal setting also results in the development of magnesium-rich carbonate muds which laterally change to dolomitic tidal flats (Purdy, 1963; Bathurst, 1975). There is little progradation of carbonate facies in the Bahamas. Changes in relative sea level primarily control the distribution of facies in a manner similar to punctuated aggradational cycles (Goodwin and Anderson, 1985).

#### ***Bahamas and the Paradise Formation***

There is a reasonable correlation between many of the lithofacies described from the Paradise Formation and those currently found in the Bahamas. Both have oolitic and bioclastic grainstones, mud-rich sediments, and lime mudstones. The presence of the trace fossils *Zoophycos* sp. and *Condrities* sp. in the lime mudstones of the Paradise

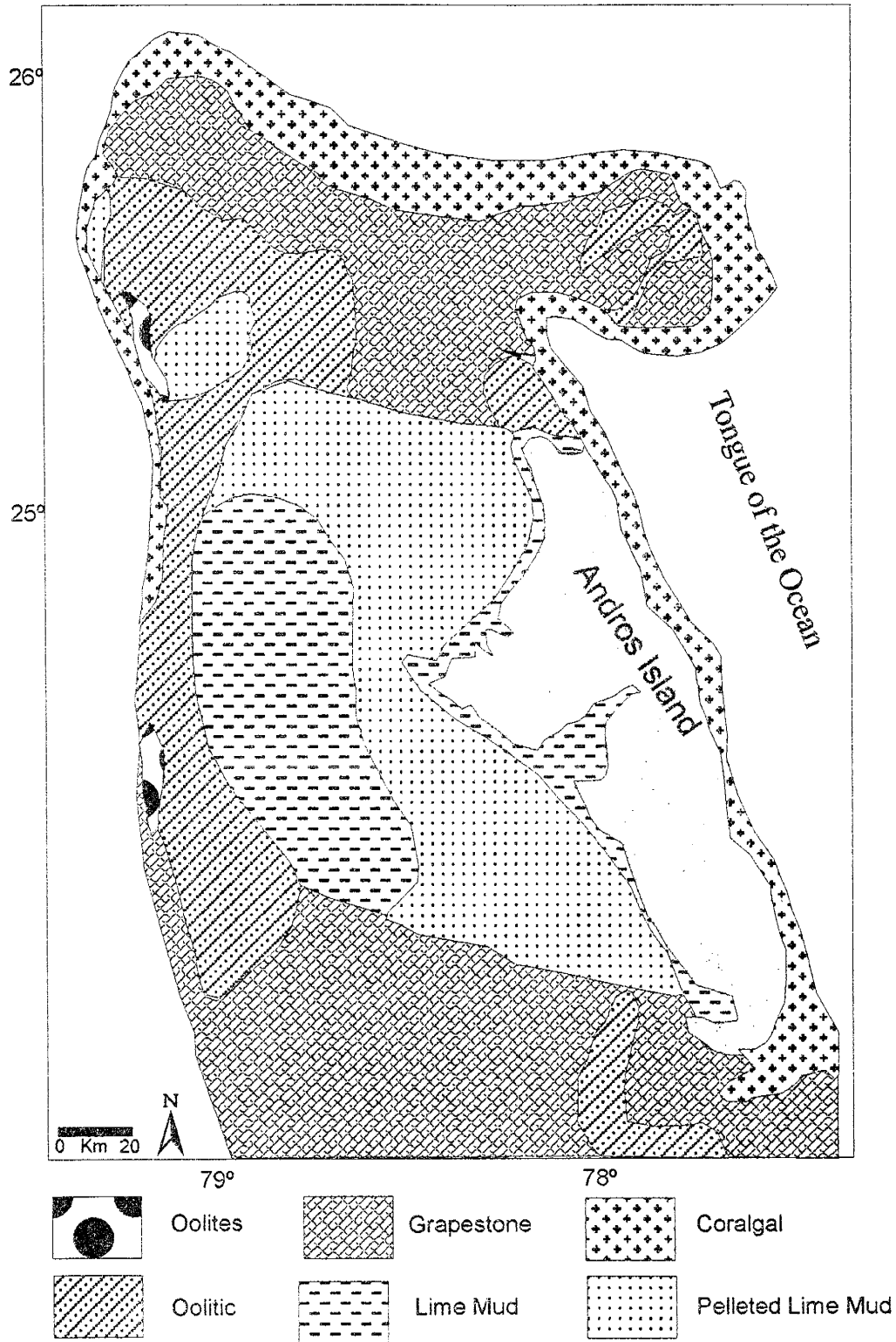


Figure 28. Simplified facies map off of Andros Island, Bahamas (Redrawn from Purdy, 1963)

restrict those lime mudstones to offshore waters, whereas the lime mudstones currently being deposited in the Bahamas are more restricted in nature and represent lagoonal deposition. This difference makes the lateral facies changes between the Paradise and the Bahamas incompatible. Even though the dominant style of sedimentation in the Bahamas is aggradational, the lateral facies changes can be used to compare the overall pattern of facies distributions. In the Bahamas there is a lateral facies relationship from reefs or oolitic shoals to finer-grained, more restricted lagoonal facies. In the Paradise there is a lateral change of facies from finer-grained offshore carbonates to more grain-rich lithofacies culminating in oolitic or bioclastic grainstones, essentially the opposite from the Bahamas. All of these facies represent deposition in normal marine waters. This contradiction in facies associations and environmental setting makes the Bahamas a poor modern analog for the Mississippian during Paradise time in the Pedregosa basin.

### **Persian Gulf**

The Persian Gulf region is an example of a modern shallowly dipping carbonate ramp with maximum water depths of 80-100 m (Harris, 1995), and has even been referred to as a modern analog for an epicontinental sea (Heckle, 1972). The basin is asymmetric with the deepest portion along the northern margin of the basin. Freshwater from several intermittent fluvial systems enter the gulf at its northern terminus (Wilson and Jordan, 1983). Waters in the Persian Gulf have elevated salinities, up to 45‰ in the open gulf water, due to high rates of evaporation in the hot and dry climate of the region and partial restriction from the Indian Ocean (Bathurst, 1975; Wilson and Jordan, 1983). Carbonate sedimentation patterns along the western margin of the Persian Gulf follow well-developed facies belts.



The best examples of the development of facies belts are found off the Qatar Peninsula (Figure 29). There the development of facies belts reflects changing water depth and water energy. From shallow to deeper water these facies include, grainstones, angular molluscan grainstones, molluscan wackestones to packstones, argillaceous wackestones, and lime mudstones (Bathurst, 1975; Wilson and Jordan, 1983). In addition to these facies, there is the development of oolitic and reef facies in the shallowest waters (Heckle, 1972). In the Persian Gulf there are well-developed supratidal primary dolomites with associated evaporites.

#### *Persian Gulf and the Paradise Formation*

There is a good correlation between the facies in the Persian Gulf and those identified in the Paradise Formation. Both have oolitic and bioclastic grainstones, mud-rich facies, lime mudstones, and shales. Primary differences between the two are the dominance of mollusks and the presence of patch reefs in the modern Persian Gulf. During the Mississippian, or even the Paleozoic, the environmental niche currently occupied by mollusks was taken by brachiopods. As far as the absence of reefs, the Mississippian is not known as a time of reef building, but rather one dominated by the development of oolitic shoals. Not only is there a good correlation between facies found in the Persian Gulf and those in the Paradise Formation, but also the distribution of facies in the Persian Gulf is compatible with the distribution of lithofacies proposed for the Paradise. The distribution of facies in the Persian Gulf is one of a shoreward decrease in carbonate mud beginning in deeper water shales and carbonate muds to increasing grain-rich sediments as waters shallow in a shoreward direction. This distribution is essentially identical to that proposed for the Paradise (Figure 27). In addition to the lithofacies and

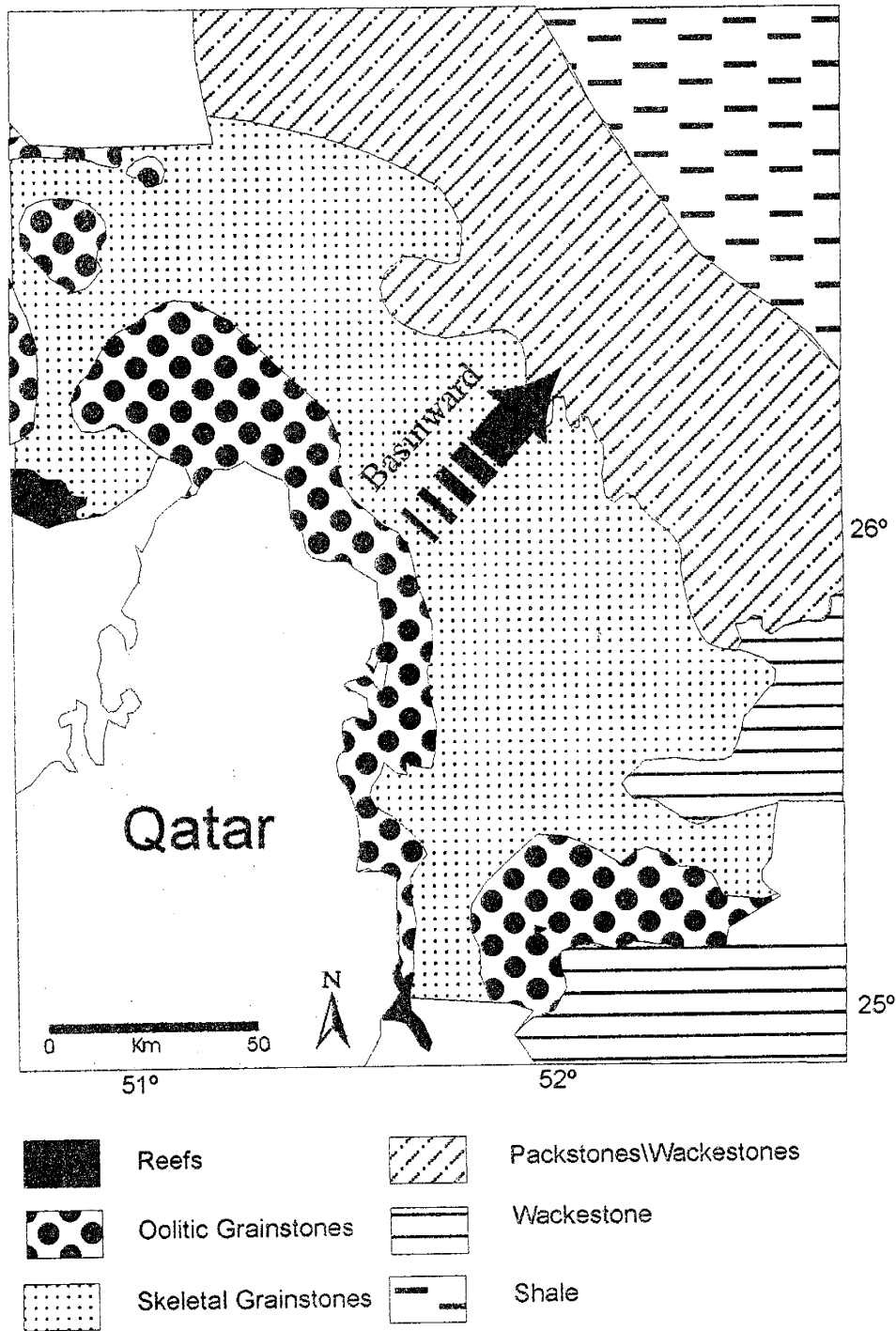


Figure 29. Simplified facies map for the Persian Gulf. Area shown is offshore Qatar. The overall trend is one of increasing lime mud and terrigenous mud as waters become deeper, reflecting less winnowing toward the center of the basin. (Figure redrawn from Bathurst, 1975)

their distribution, the geographic location of the Persian Gulf at low latitudes in an arid region with elevated temperatures, and the development of eolian sands that are incorporated into marine sediments, are remarkably similar to the proposed paleogeographic setting for the Paradise (Figure 30). All of these similarities make the Persian Gulf an ideal modern analog for the Mississippian during Paradise time in the Pedregosa basin.

### **Conceptual Models for Carbonate Deposition**

Carbonate deposition produces two general vertical facies patterns. These patterns exhibit either an asymmetrical facies relationship, such as A-B-C-A-B-C, or a symmetrical facies relationship such as A-B-C-B-A, where A, B, and C represent different carbonate facies. Within asymmetrical patterns there are two basic successions, a fining-upward package and a coarsening-upward package (Wilson, 1975). The means by which either a coarsening or a fining shallowing-upward sequence may be produced is based on two general concepts for carbonate sedimentation. One concept uses a more gradualistic approach and the combination of vertical aggradation and basinward progradation of carbonate facies, producing the classic basinward prograding sedimentary wedge. The second concept relies upon vertical accretion of sediments within a given accommodation space with the vertical variation in facies related to changing environmental conditions associated with aggradation.

These two basic concepts for carbonate sedimentation and the production of shallowing-upward carbonate depositional sequences are illustrated by three general models of carbonate depositional systems. These models are the epeiric sea, or clear water carbonate model, originally proposed by Shaw (1964) and Irwin (1965); the

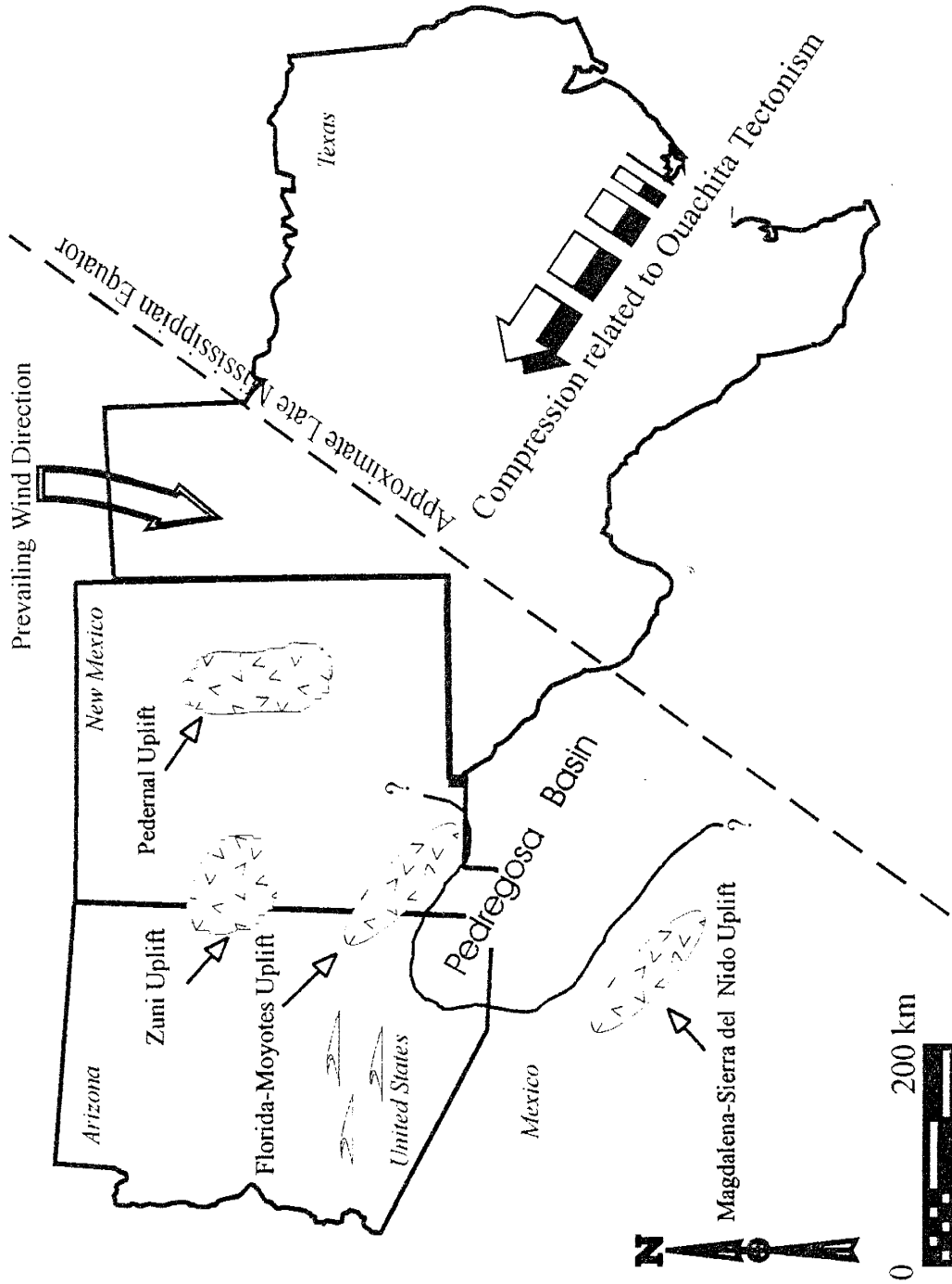


Figure 30. Paleogeographic map showing the general configuration of the Pedregosa basin during the deposition of the Paradise. Paleogeographic position is similar to the present day Persian Gulf, with prevailing winds from the North-Northeast. (Data from Ross and Ross, 1987a, 1988; Ye et al., 1996)

carbonate ramp model first popularized by Ahr (1973); and the punctuated aggradational cycle, or PAC, model of Goodwin and Anderson (1985). The epeiric sea and carbonate ramp models are based on Waltherian ideas and encompass both the aggradation and the lateral progradation, or basinward migration of facies. The PAC model is a non-Waltherian model that is based the vertical accretion of facies in a given accommodation space created following a rapid rise in sea level.

### Epeiric Sea, Clear Water Carbonate Depositional Model

The epeiric sea, clear water carbonate model put forth by Shaw (1964) and Irwin (1965) is based on changes in water energy and environmental restriction in basins with very gently sloping depositional surfaces (Figure 31). These basins extend hundreds to thousands of kilometers in width and have slopes on the order of 0.04m/km (Irwin, 1965). Typically, clear water carbonate sedimentation occurs in a basin that receives only a limited amount of detritus. Carbonate deposition along this gently dipping surface is governed primarily by water energy and chemistry. Changes in water chemistry are related to the shoreward restriction of normal marine waters (Shaw, 1964).

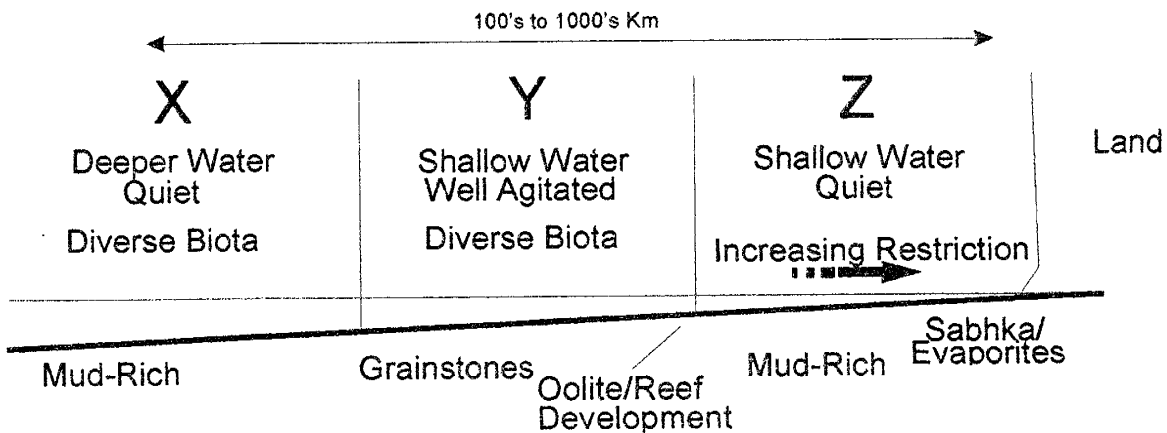


Figure 31. Theoretical model for carbonate deposition in an epicontinental sea proposed by Irwin, 1965 and Shaw, 1964.

Shaw's general model of clear water sedimentation begins at the energy margin of an epeiric sea, where maximum wave energy intersects the sea bottom (Shaw 1964, figure 8-2). In this high-energy region, carbonate sediments such as reefs and grain-rich shoals form. As water depth shallows in a landward direction, water energy is dissipated by friction along the sediment-water interface. Along with the dissipation of wave energy there is also an increase in the volume of lime mud. Landward of the limit of tidal action there is net evaporation of sea water causing increasing restriction, and a decline in biotic diversity.

Further landward in marginal marine settings, high evaporation leads to an increase in magnesium-rich muds and the formation of evaporites. Depending upon the climatic conditions there may be some dilution of high-salinity marine waters near the shoreline by precipitation and fresh water input by fluvial systems. This dilution of higher salinity marine waters may reduce or halt the precipitation of evaporites and magnesium-rich sediments.

Irwin (1965) also proposed a model for the deposition of carbonates in a clear water setting. He subdivided the clear water model into three environmental zones labeled X, Y, and Z based upon water energy. Each zone is characterized by sedimentary facies, or sedimentation zones. These zones reflect the carbonate grain types, biotic relationships, and matrix related to differences in water energy (Irwin, 1965, figure 5). The outermost X zone represents quiet water environments, typically below fair-weather wave base where fine-grained sediments accumulate. The Y zone represents the region of highest energy equivalent to the energy margin of Shaw (1964). This zone is characterized by the development of oolitic shoals or reefs, and it is a region of

accumulations of grain-rich carbonate skeletal sands. Quiet, shallow waters and mud-rich sediments characterize the innermost Z zone. Wave and current action in zone Z is limited to wind driven currents. This zone is characterized by a restricted biota and it is where both evaporites and magnesium-rich sediments are deposited. As with Shaw's (1964) depiction of the clear-water carbonate model, with changing climatic conditions, there can be dilution of high-salinity marine waters near the shoreline (Z zone) by precipitation and freshwater supplied by fluvial systems. This dilution of higher salinity marine waters may reduce or halt the precipitation of evaporites and magnesium-rich sediments.

There are no modern examples of large epeiric seas prevalent in the geologic record. A modern carbonate system used as analogs to epeiric seas and clear-water carbonate sedimentation is Florida Bay (Shaw, 1964). The main difference between this modern depositional system and a true epeiric sea is in the scale of the basins. Florida Bay is several orders of magnitude smaller than an epeiric sea. Heckle (1972) applied Irwin's clear water carbonate sedimentation model to modern carbonate systems active in the Persian Gulf and the Bahamas. Heckle demonstrated that the sedimentation patterns predicted by Irwin in epicontinental basins could readily be applied to smaller basins.

### **Carbonate Ramps**

Ahr (1973) introduced the concept of carbonate ramps as a depositional model for ancient carbonates. In general, carbonate ramps are categorized as either a homoclinal dipping ramp or a distally steeped ramp. The slope on a carbonate ramp can vary widely from near 0 degrees to very high slopes (Burchette and Wright, 1992). Carbonate ramps can be divided into four sections, each with a distinctive style of sedimentation. These

are the basin, outer ramp, below fair-weather wave base; the mid-ramp, which is dominated by high-energy wave action; and the inner ramp, where lagoonal to supratidal deposition occurs (Figure 32; Ahr, 1973; Burchette and Wright, 1992). The outer ramp setting is dominated by laminated to mildly ripple laminated carbonate muds with a component of quartz silt, and can also be dominated by terrigenous mudstones. The outer ramp is typically composed of bioturbated or laminated lime or terrigenous mudstones. These may be interbedded with storm deposits. The mid-ramp setting is dominated by coarse-grained, cross-laminated sediments, which are affected by storms. The inner ramp setting is composed of a wider variety of sediments. These include bioclastic and oolitic grainstones, packstones, wackestones. As the ramp becomes more restricted landward, lagoonal lime muds, sabkha deposits, and evaporitic sediments are deposited (Burchette and Wright, 1992). The transitions between these facies are gradational, and the facies may either aggrade, prograde, or develop in a combination of aggradation and progradation across the ramp. As relative sea level changes, a series of ramps will

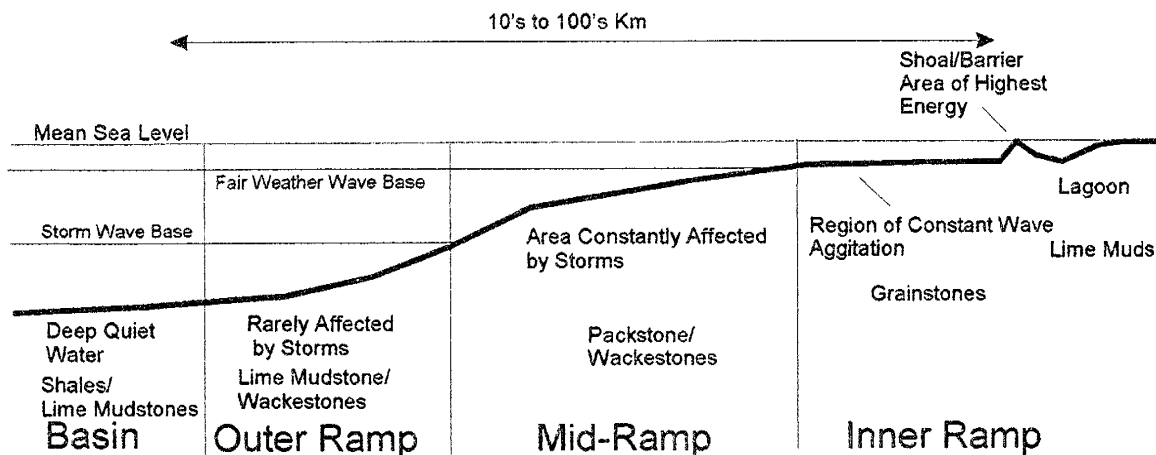


Figure 32. Subdivisions of a carbonate ramp and associated facies. (After Burchette and Wright, 1992).



develop resulting in a stacked set of similar cycles.

Wilson (1974, 1975) continued to develop the carbonate ramp model by dividing the basic ramp into nine distinctive facies belts, each characterized by a variety of standard microfacies (Wilson, 1975, figure 12-1). Each standard microfacies is defined by a specific set of sedimentologic characteristics. These characteristics include matrix material, sedimentary structures, and carbonate grain type. There are some 24 standard microfacies. Not every facies belt or standard microfacies need be present in a given depositional system. The width, presence, or absence of any number of facies belts and standard microfacies is a function of ramp profile and depositional slope (Wilson 1975).

### **Punctuated Aggradational Cycles (PAC)**

Goodwin and Anderson (1985) introduced an alternative to the more Waltherian carbonate depositional models. They proposed the punctuated aggradational cycle, or PAC. This model relies on the allocyclic succession of facies through vertical aggradation to produce not only a shallowing-upward carbonate package, but also time-stratigraphic units. In Goodwin and Anderson's model, PAC sedimentation is controlled by abrupt rises in relative sea level. These changes in relative sea level are governed by a combination of glacial eustasy and subsidence, producing available accommodation space on the order of one to five meters. The PAC model assumes that the carbonate sediments generated are uniform and sheet-like forming one to five meter thick cycles. A PAC may be composed of a single facies or a succession of shallowing-upward facies with no basinward progradation of facies. Variations in facies are governed by autocyclic processes, as accommodation space is reduced by net aggradation of

sediments. Facies can either remain the same or start with fine-grained sediments that become more grain-rich as accommodation space is reduced by aggradation.

### **Depositional Systems and The Paradise Formation**

The lithofacies sequences defined in the Paradise Formation are dominantly sheet-like and occur as 2 to 12 meter thick, shallowing-upward cycles that are essentially identical over the study area suggesting a uniform depositional surface. Trends in the overall thickness of the Paradise Formation (Figure 13, Page 26) suggest that the depositional surface of the Paradise was most likely an easterly to southeasterly gently dipping carbonate system with a depocenter to the east of the Big Hatchet Mountains. The presence of coeval deeper water facies preserved in the Helms and Rancheria formations (Yurewicz, 1977; Madden, 1984) found in Eastern New Mexico and west Texas also support this basin configuration.

Taking these factors into account, the uniform nature of the Paradise Formation in the Big Hatchets and the overall stratigraphic relationship of the Paradise, it is possible to suggest a depositional setting. The stacking of similar depositional sequences is consistent with either carbonate deposition attributed to PAC sedimentation (Goodwin and Anderson, 1985), or successive sequences of carbonates deposited on a carbonate ramp following repeated changes in relative sea level. This indicates that each of the sedimentary sequences in the Paradise represent the amount of accommodation space created following a rapid rise in relative sea level. In such a situation, the vertical changing of lithofacies is most likely driven by autocyclic environmental changes as accommodation space is reduced by the aggradation of carbonate sediments. Once filled it is possible to have some minor basinward progradation and minor interfingering of

facies. Subsequent environmental changes related to water depth and agitation within these settings makes it common for skeletal debris and ooids to be swept across the ramp as sheets (Burchette and Wright, 1992). This is consistent with the uniform nature of the oolitic and abraded grainstone lithofacies of the Paradise. It is possible that there was significant basinward progradation of carbonate sediments during Paradise time. This is a typical occurrence during highstands of relative sea level in carbonate systems (Calvet et al., 1990). If large-scale progradation did occur it was likely at a position east of the Big Hatchet Mountains, in to a deeper water setting where the Helms and Rancheria formations were being deposited (see page 24).

The most likely depositional setting for the Paradise was on a gently, eastward dipping, carbonate ramp (Figure 33). Within this setting, variations in relative sea level acted as the primary control on carbonate sedimentation. These changes in relative sea level acted to produce a series of similar cycles of carbonates.

### **Detrital Clastics**

Up to this point only the carbonates have been discussed with regard to depositional setting during Paradise time. In the Paradise Formation, there is a significant amount of coarse-grained detrital clastics. The observed distribution of these coarser-grained detrital clastics within the vertical facies sequences is similar, if not identical, to sedimentation patterns related to cyclic and reciprocal sedimentation from the Pennsylvanian in the Orogrande Basin of New Mexico (Wilson, 1967) and the Pedregosa basin (Soreghan, 1993), and on the Permian basin of west Texas (Wilson, 1975). Cyclic and reciprocal sedimentation is a process which produces a carbonate-clastic cycle that is arranged with a lower carbonate part and an upper clastic part. Each



part of the carbonate-clastic cycle reflects significant changes in deposition that have been related to changes in relative sea level (Figure 34; Wilson, 1967, 1975). When a relative rise in sea level results in the strandline moving landward, effectively expanding the available area on the shelf for carbonate production and trapping detrital clastics in a near shore position. This effectively increases carbonate production and produces the carbonate part of a cycle. As relative sea level begins to fall, the shelf area is reduced and carbonate production shifts basinward. After relative sea level has dropped exposing the inner shelf, the detrital clastics trapped in a shoreward position are able to migrate across the shelf to the strandline where they are distributed by marine currents in the basin. This produces the capping clastic portion of a cycle. Repeated changes in relative sea level produce stacks of carbonate-clastic cycles, thus the term reciprocal. If the source of detrital clastics changes with time or is not present during lowstands in relative sea level, pure carbonate cycles are produced.

The presence of detrital capped cycles throughout the entire stratigraphic interval suggests that this manner of sedimentation was active during the duration of time represented by the Paradise Formation. These sandstones and siltstones have characteristics indicating both eolian and marine origins. This suggests that the quartz was originally transported across the exposed shelf as eolian dunes during relative lowstands in sea level. Once the dunes reached the strandline, the quartz was assimilated into the marine setting and was redistributed by marine currents over the carbonates (Figure 35).

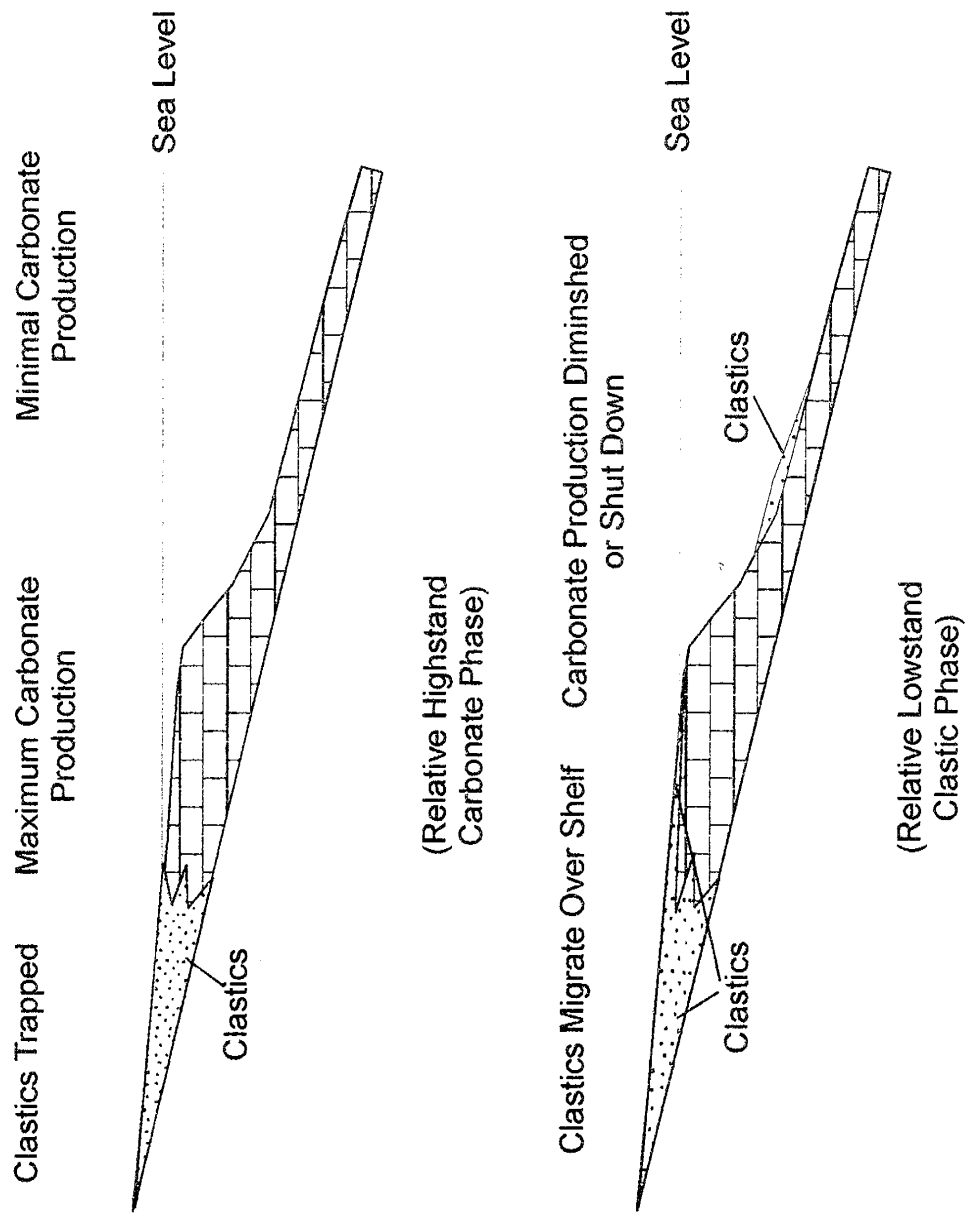


Figure 34. Idealized carbonate ramp illustrating the general concept of cyclic and reciprocal sedimentation. During relative highstands in sea level detrital clastics are trapped in a shoreward position. Following a relative drop in sea level the clastics migrate across the exposed inner shelf and are distributed in the basin by current and wave action. (After Wilson, 1975) (Note this is idealized ramp model, and does not reflect the geometry of the proposed ramp for the Paradise Formation.)

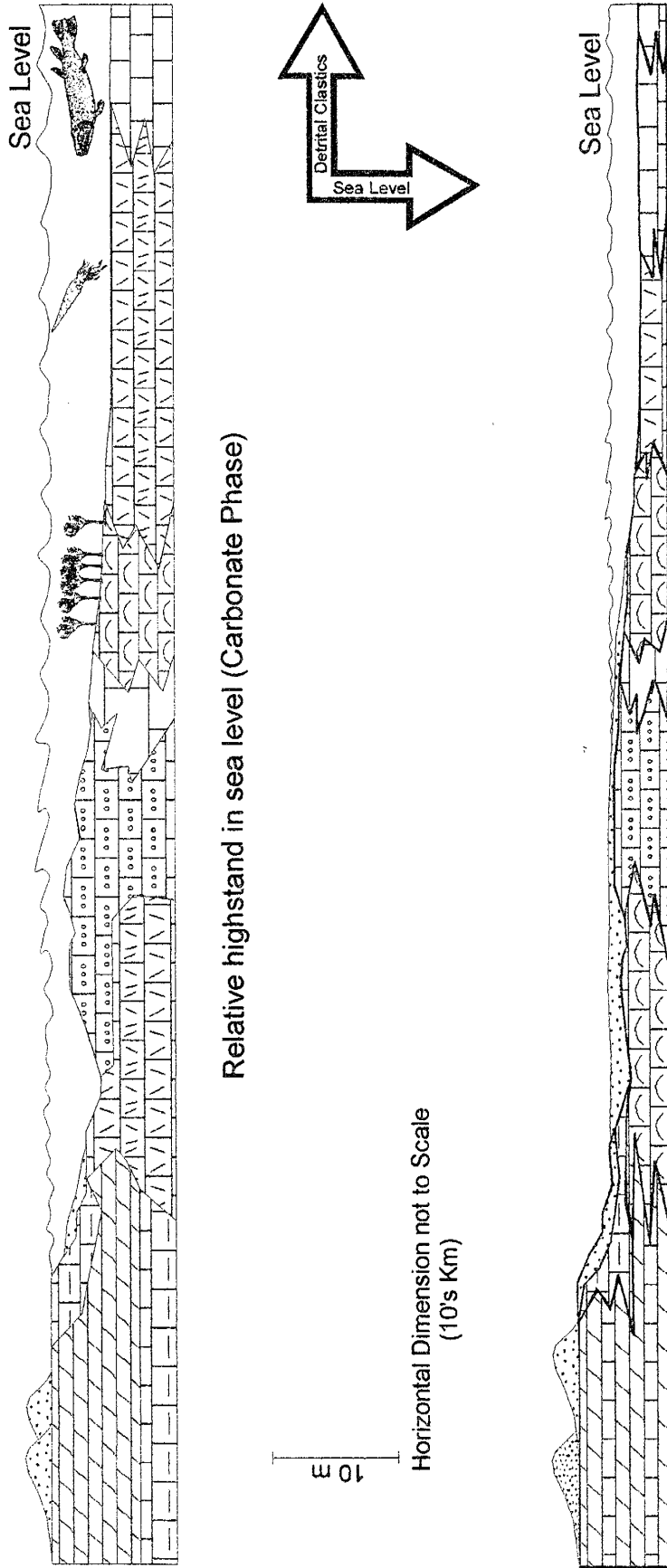


Figure 35. Interpretive depositional cross sections illustrating cyclic and reciprocal sedimentation in the Paradise Formation. The top illustration depicts deposition during a relative highstand in sea level. The lower illustration depicts deposition during the subsequent relative lowstand in sea level. During this phase is when the detrital clastics are distributed across the shelf and basin.

## CYCLICITY

The repeated patterns of lithofacies, and the cyclic reciprocal sedimentation identified in the Paradise Formation, suggest that cyclic sedimentation was active throughout Paradise time. Data from lithostratigraphic and petrographic analyses identified a maximum of 30 small-scale cycles, ranging from 2 to 12 meters in thickness. These cycles average 4 meters in thickness, with the majority of cycles being less than 7 meters in thickness. Thicker cycles, those 7 meters and greater, are most common in the middle member of the Paradise. Approximately the same number of cycles were identified at both Horse Pasture Canyon, 26 cycles, and New Well draw, 30 cycles (Appendix A). The different number of preserved cycles at each section reflects the amount of section preserved at each location. The removal of cycles by erosion means the number of preserved cycles is a minimum. Each of the aforementioned cycles is a shoaling, asymmetrical, coarsening-upward cycle (Figure 25).

Using the vertical distribution of lithofacies, and lithofacies interpretations, a sequence for the construction of a cycle can be established, beginning with a flooding surface. The coarse-grained facies capping a cycle represent such a surface. Following each flooding event the carbonate factory on the shelf is pushed shoreward resulting in a significant reduction in carbonate production. The deep water facies of each cycle is represented by the lime mudstone or shale lithofacies that record initial deposition on the flooding surface. Once the available accommodation space on the shelf is filled by sediment aggradation, the facies begin to prograde basinward.



### Cycle Duration

Using basic stratigraphic data from the Paradise Formation, the average duration of a cycle is easily estimated. This requires, however, an assumption basic to all studies of cyclicity, that each cycle represents approximately an equal amount of time. The assumption that each cycle represents an equal amount of time can be supported by the fact that a majority of the cycles are of similar thickness, and by assuming that the rate of carbonate production was similar for each cycle. Data for calculating the cycle duration includes the number of identified cycles and the amount of geologic time represented by the strata in question (Reid and Dorobek, 1993). The amount of relative geologic time represented by the Paradise is approximately 15 Ma (personal comm. Armstrong, 1994). Using the Chesterian as a proxy for the Paradise, the Decade of North American Geology (DNAG; Palmer, 1983) time scale can be used to determine the uncertainty associated with the duration of the Paradise. The uncertainty associated with the duration of the Chesterian is approximately 6%. A 6% error translates to  $\pm 1$  Ma, giving a range of 14 to 16 Ma for the duration of the Paradise. Using the 30 small-scale cycles deposited between 14 to 16 Ma of time, the average duration of a cycle is calculated by dividing 14 Ma and 16 Ma by 30. Rounding this value to the nearest 100 k.y. results in an average duration of 500 k.y. per cycle. Because the number of preserved cycles represents a minimum, the average duration of those cycles is a maximum for any given cycle. Under currently accepted sequence stratigraphic terminology (Table 4) described in Miall (1990), it is possible to classify these small-scale cycles as 4<sup>th</sup>/5<sup>th</sup> order.

Table 4. Typical durations associated with sequence stratigraphic orders. (After Miall, 1990).

Sequence Duration	Cycle Order
200 to 500 m.y.	First Order
10 to 100 m.y.	Second Order
1 to 10 m.y.	Third Order
< 1 m.y.	Fourth Order
< 1 m.y. (0.01-0.2 m.y.)	Fifth Order

The range in duration of the cycles in the Paradise Formation are similar to those of coeval cyclothems in England described by Ramsbottom (1979). In addition to these cyclothems, Ramsbottom also described slightly longer cycles he termed mesothems. Each mesothem consists of a number of cyclothems. Within the Chesterian there are approximately three mesothems, or medium scale cycles (Ramsbottom, 1979; Saunders et al., 1979).

By treating each of the three stratigraphic members in the Paradise as a cycle, similar in scale to Ramsbottom's mesothems, and by considering the entire Paradise to be a sequence, a hierarchy of cycles can be established. Assuming a duration of approximately 5 Ma for each medium scale cycle, and by using the value of  $15 \pm 1$  Ma for the duration of the entire Paradise, further refinement and classification of sequences is possible. The medium-scale cycles are classified as 3<sup>rd</sup> order, and the entire stratigraphic interval represents a 2<sup>nd</sup> order cycle (Figure 36). This hierarchy of cycles relates the deposition of the Paradise to a sequence stratigraphic framework.

# PARADISE FORMATION



2<sup>nd</sup> Order  
Duration ~ 15 m.y.

## MEMBERS



3<sup>rd</sup> Order  
Duration ~ 5 m.y.

### Meter-Scale Cycles



4<sup>th</sup>/5<sup>th</sup> Order  
2-12 m in Thickness  
Duration ~5 k.y.

Figure 36. Sequence stratigraphic hierarchy established for the Paradise Formation. Higher order sequences reflect cyclic sedimentation governed by glacioeustasy and local tectonism. Lower order sequences reflect depositional patterns governed by regional and continental tectonics related to the assemblage of Pangea.

### Causal Mechanisms of Paradise Cyclicity

The processes driving cyclic sedimentation and the development of sedimentary sequences are not well understood. The probable causes for the cycles listed in Table 4 include: 1<sup>st</sup> order, major eustatic changes related to the assemblage or breakup of continents; 2<sup>nd</sup> order, eustatic changes related to spreading rates along mid-ocean ridge systems; 3<sup>rd</sup> order, eustatic changes related to spreading rates and continental glacial activity; and 4<sup>th</sup> and 5<sup>th</sup> order, eustatic changes related to Milankovitch glacioeustatic cycles (Miall, 1990). Regional and local tectonics must also be considered in evaluating mechanisms for controlling cyclic sedimentation particularly in discrete basins.

In the Paradise Formation, the 2<sup>nd</sup> order cycles may be explained by eustatic changes related to large-scale tectonism associated with the assemblage of Pangea and the earliest stages of the Ouachita orogeny. Large-scale tectonic events, such as these, cause a change in the volume of the oceans and affect an eustatic change. Additionally, uplifts in the region related to the Ouachita orogeny might have impacted the amount of detritus deposited in the Pedregosa basin during Paradise time. Third-order cycles in the Paradise are also likely the result of large-scale regional tectonism coupled with glacial activity (Miall, 1990). The primary mechanism for generating the 4<sup>th</sup>/5<sup>th</sup> order cycles was eustatic and related to the waxing and waning of glaciers. High frequency cyclicity attributed to glacioeustasy is explained by changes in the earth's orbit parameters. These parameters are collectively known as Milankovitch cycles and are thought to be the primary cause of climatic changes. Milankovitch cycles are governed by variations in three components: the Earth's orbital eccentricity, the Earth's tilt, and the Earth's wobble. These three components act in an additive or subtractive fashion depending

upon if they are in phase or out of phase. Of the three, eccentricity controls cycles ranging from 100 k.y. to just over 400 k.y. (Imbrie and Imbrie, 1979; Weedon, 1991).

The calculated duration of the high-frequency cycles in the Paradise are comparable to, but less than, those reported for recent Milankovitch-driven cycles. The duration of ancient Milankovitch cycles is unknown, however, several workers (Berger and Loutre, 1989; Schwarzacher, 1991; Weedon, 1991) suggest that ancient Milankovitch cycles were longer. Evidence for widespread continental glaciation during the Mississippian also supports glacioeustasy as the cause for high-frequency cyclicity (Crowell, 1978; Caputo and Crowell, 1985; Ross and Ross, 1987a; 1988).

Not all of the cycles observed in the Paradise Formation are complete. There may be several causes for generating incomplete cycles. These causes include changes in rates of sedimentation, abrupt changes in accommodation space, or the removal of upper portions of a cycle during the subsequent regression.

Local tectonism is a reasonable way to change the rate of sedimentation and modify accommodation space. At the onset of Paradise deposition, the Ouachita orogeny was influencing the Pedregosa basin and surrounding region. Prominent uplifts in the region, such as the Zuni-Defiance and Pedernal uplifts, were emerging (Armstrong, 1962; Armstrong et al., 1980). In addition to uplifts in the Pedregosa basin region, Lisenbee et al. (1979) cite evidence for large-scale Late Mississippian faulting associated with the early stages of Ouachita orogeny in the Sandia and Manzano mountains in north-central New Mexico. Tectonism related to the Ouachita-Marathon orogeny also affected the Pedregosa basin during Paradise time through uplift and subsidence. Ye et al. (1996) argue that the Pedregosa basin actually began to form during the Morrowan. However,

the deeper water carbonates and shales of the coeval Rancheria and Helms formations distributed across eastern New Mexico and western Texas (Yurewicz, 1977, Madden, 1984) and the eastward thickening of the Paradise Formation strongly suggest that the Pedregosa basin actually began to form during the Chesterian. The depocenter of this early Pedregosa basin was most likely to the east-southeast of the Big Hatchet Mountain region. This is consistent with Kottlowski (1965) who suggested that the Pedregosa basin should include Mississippian strata. This tectonism influenced relative sea level and adjusted accommodation space in the Pedregosa basin. Tectonism may have acted to control basin development during Paradise time in a manner similar to that proposed by Dickerson (1987) during the Pennsylvanian in the Pedregosa basin. Dickerson suggested that the Precambrian basement of the Pedregosa basin was splintered and acted as "piano keys" with each key behaving independently during pulses of deformation. Such movements could affect relative sea level in the basin by adjusting the depositional surface and accommodation space as basement moved up or down forcing facies to migrate either basinward or landward. The redistribution of facies disrupts the natural progression of facies in a cycle. Tectonism can also cause an increase or decrease in the rate of sedimentation by influencing the amount of detritus the basin receives, or by affecting the rate of carbonate production, resulting in carbonate or siliciclastic dominated cycles. This model for deformation of the basin during the Late Mississippian may also have controlled the development of 3<sup>rd</sup> order cycles, and as mentioned earlier, is the cause for the discrepancy between the number of 3<sup>rd</sup> order cycles reported by Ross and Ross (1987, 1988) and those reported from the Paradise (This study).

Changes in the length of glacioeustatic cycles due to changing Milankovitch periodicity could induce changes in cycles. These changes would be reflected in eustatic sea level causing abrupt migrations in facies belts and produce incomplete cycles. Using a combination of regional tectonics and varying magnitudes of glacioeustasy to control patterns in sedimentation provides a viable means to produce the variety of cycles observed in the Paradise Formation.

The incomplete cycles in the Paradise Formation could conceivably be the result of subaerial exposure between cycles. If the uppermost beds of a cycle were removed by dissolution, there should be some evidence of soil development and karst features, such as dissolution breccias, on the uppermost beds of the underlying cycle. The uppermost surfaces of cycles would be erosional and irregular. Paleogeography, however, suggests that the Pedregosa basin was most likely located in an arid climatic region. In arid regions carbonates undergo little, if any dissolution upon exposure. This suggests that even if exposure did occur in the cycles identified by this study it is unlikely that there would be any record of exposure.

### **Global Comparisons**

If eustasy is the primary driving mechanism of cyclic sedimentation in the Paradise Formation, time equivalent strata should reflect similar cyclicity on a global scale. Ross and Ross (1987, 1988) indicate, through a series of sea level charts, that the Late Mississippian is cyclic and that the cycles are correlative across North America and the Russian platform. Ramsbottom (1979) defined similar cycles in time equivalent strata to the Paradise in England that are of similar duration to those in the Paradise. Saunders et al. (1979) discuss cycles of similar durations in the Ozark shelf region of the

Ouachita Basin. Even though there are differences in the numbers of cycles that likely reflect local and regional tectonic effects on sedimentation, the presence of coeval cyclic strata worldwide indicates that during Late Mississippian time sedimentation was greatly influenced by eustasy.

### **Cyclicity in the Paradise Formation: Synthesis**

Several orders of cyclicity are present in the Paradise Formation. These orders of cycles form a hierarchy consistent with established geologic events and potential causes during Paradise time. The presence of cycles of similar duration in coeval rocks in the Black Warrior Basin, and in England, as well as evidence for significant continental glaciation during the Late Mississippian suggest that the primary control on cyclic sedimentation was glacioeustatic. Variations in the thickness and completeness of the high-frequency 4<sup>th</sup> and 5<sup>th</sup> order cycles suggest a combination of processes acted concurrently to control sedimentation and produce these variations. Variations in these cycles are likely related to changes in Milankovitch periodicity and local tectonism.



## **DIAGENESIS**

Diagenesis includes all of the processes that affect sediments following deposition and prior to metamorphism. The diagenetic process is complex and includes many steps. Diagenesis and the products of diagenesis are not necessarily indicators of depositional environments. The products of diagenesis are controlled by the chemistry of fluids and the diagenetic environment the sediments were subjected to following deposition. One important result of understanding diagenesis is the resulting enhancement, development, or destruction of porosity and permeability. These two properties directly impact the economic potential of the rocks with regard to hydrocarbon and ground water resources, as well as the ability of hazardous materials to move through the rocks.

Carbonates are particularly susceptible to diagenesis due to their mixed mineralogy. Diagenetic processes can be placed into four main categories: solution of unstable carbonate minerals, filling of pore spaces by cements, the alteration of minerals into new ones (neomorphism), and compaction (Folk, 1980). These processes are known to take place in several general diagenetic environments: marine phreatic, freshwater vadose, freshwater phreatic, mixing zone (Longman, 1980), burial diagenetic (Scholle and Halley, 1985), and telogenetic (Moore, 1989).

### **Diagenetic Features**

#### **Neomorphism**

Neomorphism is a useful catchall term introduced by Folk (1965) meaning “all transformations between one mineral and itself or a polymorph—whether inversion or

recrystallization, whether the new crystals are larger or smaller or simply differ in shape from the previous ones". Neomorphic textures can be divided into two groups: aggrading neomorphism and degrading neomorphism. In aggrading neomorphism there is an overall increase in grain size, whereas in degrading neomorphism there is an overall decrease in grain size.

Inversion applies to neomorphic change from aragonite to low-magnesium calcite, while recrystallization describes the change from high-magnesium calcite to stable, low-magnesium calcite (Folk, 1965). The recrystallization of high-magnesium calcite to low-magnesium calcite typically occurs by incongruent dissolution in which simultaneous dissolution of high-magnesium calcite and precipitation of low-magnesium calcite at the lattice level is accomplished by thin films of water, which acts to preserve the original fabric of the grain following neomorphism (Bathurst, 1980). This process typically takes place in the stagnant zone of the freshwater phreatic diagenetic environment (Longman, 1980).

### **Neomorphic Textures in the Paradise Formation**

Neomorphic textures are common in the Paradise Formation where recrystallization of calcite occurred in high-magnesium calcite skeletal grains. In the Paradise Formation, skeletal grains presumed to be composed originally of high-magnesium calcite are pelmatozoans. Through neomorphism, they are now composed of low-magnesium calcite.

An interesting issue is whether or not the radial fabric calcite ooids in the Paradise Formation were originally precipitated as high-magnesium calcite, as has been suggested for some radial fabric calcite ooids (Marshall and Davies, 1975; Land et al.,

1979), or as low-magnesium calcite. Under cathodoluminescence, the ooids from the Paradise have a dull to bright orange luminescence, similar to pelmatozoans that have undergone neomorphism from high-magnesium calcite to low-magnesium calcite. Although Barbin et al., (1991) showed that some recent biogenic marine carbonate is luminescent, there are no such studies of the luminescent characteristics of ooids. Therefore, it is conceivable that the ooids were originally luminescent. The dissolution of some nuclei and preservation of brachiopods, other low-magnesium calcite grains, and high-magnesium calcite nuclei suggest that the dissolved nuclei were originally aragonitic (Figure 40). These observations suggest that ooids from the Paradise were originally precipitated as calcite. Since the ooids are now luminescent, there is a possibility that either the ooids were originally high-magnesium calcite that was stabilized by freshwater to low-magnesium calcite during diagenesis, or that the ooids were originally composed of luminescent low-magnesium calcite. It may be impossible to determine which case is true, however one way to determine which interpretation is most likely is by evaluating the stable isotopic composition of the ooids. This is considered in the following section on stable isotope analysis.

Skeletal grains in the shapes of mollusks (i.e., gastropods and bivalves) were dissolved during diagenesis leaving only micritic rims or molds in the shape of the original grain. The presence of these dissolved grains with other surviving skeletal grains composed of low-magnesium calcite or high-magnesium calcite suggests that the dissolved grains were originally composed of aragonite. The dissolution of aragonitic skeletal grains also suggests that the aragonite never inverted to low-magnesium calcite.

### *Aggrading Neomorphic Textures and Matrix*

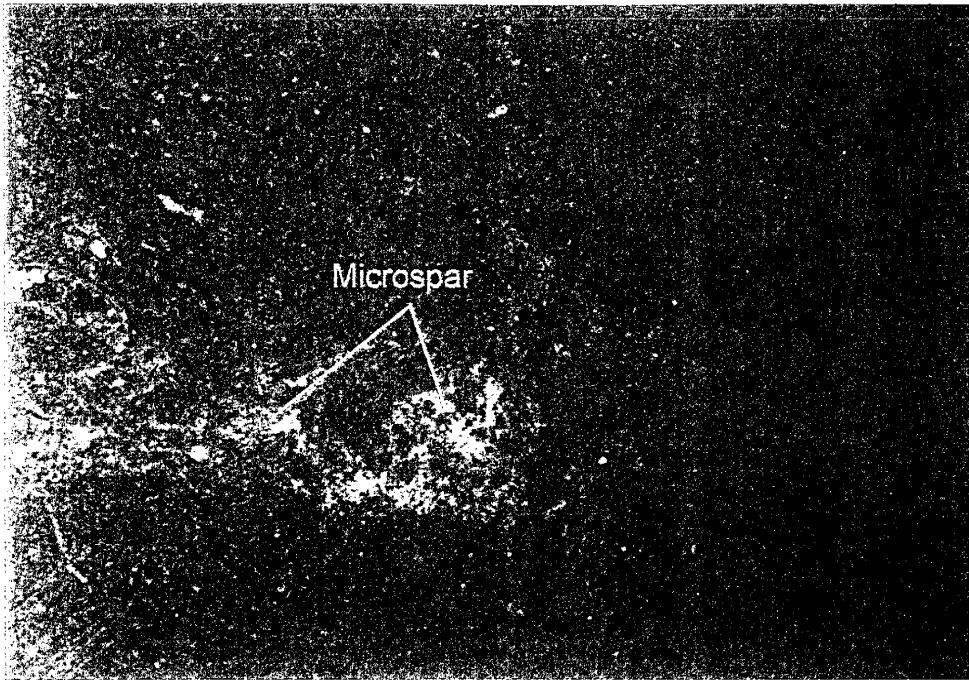
The process of aggrading neomorphism most likely occurs during early diagenesis. Aggrading neomorphism and the generation of microspar or pseudospar typically takes place in the marine stagnant zone where interstitial pores are fluid filled and aid in the process of forming micrite (Folk, 1965). Aggrading neomorphic textures in the most basic form constitute the change of lime mud to micrite. If the process of aggrading neomorphism continues, the calcite crystals will continue to grow in size forming microspar and pseudospar.

### *Aggrading Neomorphism in the Paradise Formation*

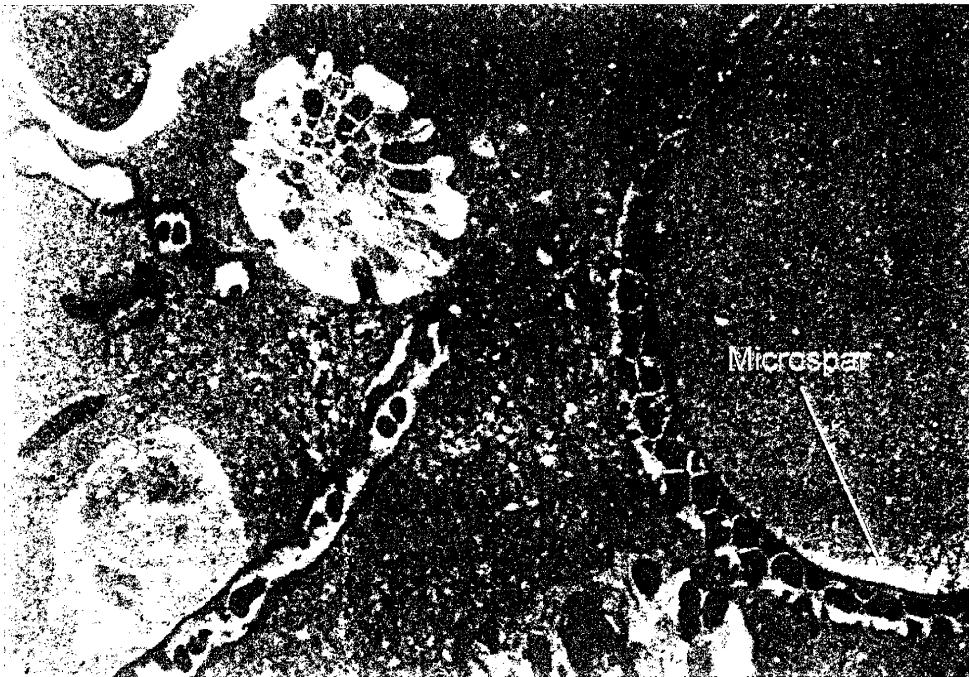
Examples of aggrading neomorphic textures are extremely common and found throughout the Paradise Formation. Growth of microspar occurs as patches in micritic matrix material, or along the boundaries between skeletal grains and micrite matrix (Figure 37 A and B). In other instances, the cement-like sparry calcite present in grain-rich rocks is actually pseudospar. Evidence supporting this interpretation is the cloudy nature of the spar, floating grains, and patches of micrite floating within the sparry material (Figure 38).

### **Micritization**

Micritization is the process of forming a durable, dark rind around carbonate grains. This is done by endolithic organisms whose borings are filled by cements (Bathurst, 1975). The durability of this rind results from the neomorphism of the original carbonate material to a more stable low-magnesium calcite and the inclusion of remnant organic material in the shell wall (Kendall et al., 1966; Bathurst, 1975). Typically



A



B

Figure 37. A and B. Examples of two types of microspar development in the Paradise Formation. Example A shows patches forming in a fine mudstone. Example B shows microspar developing along the boundaries between skeletal material and micrite matrix. (Fields of view approximately: 600  $\mu$ m)

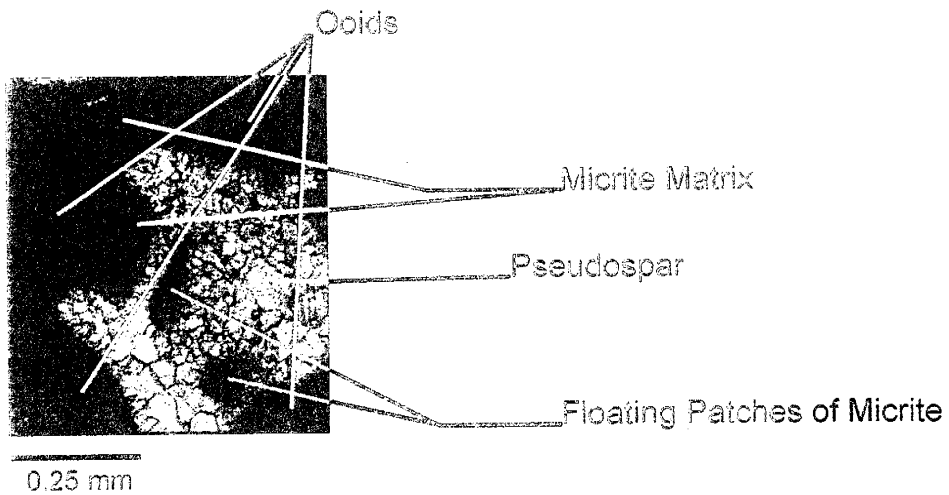
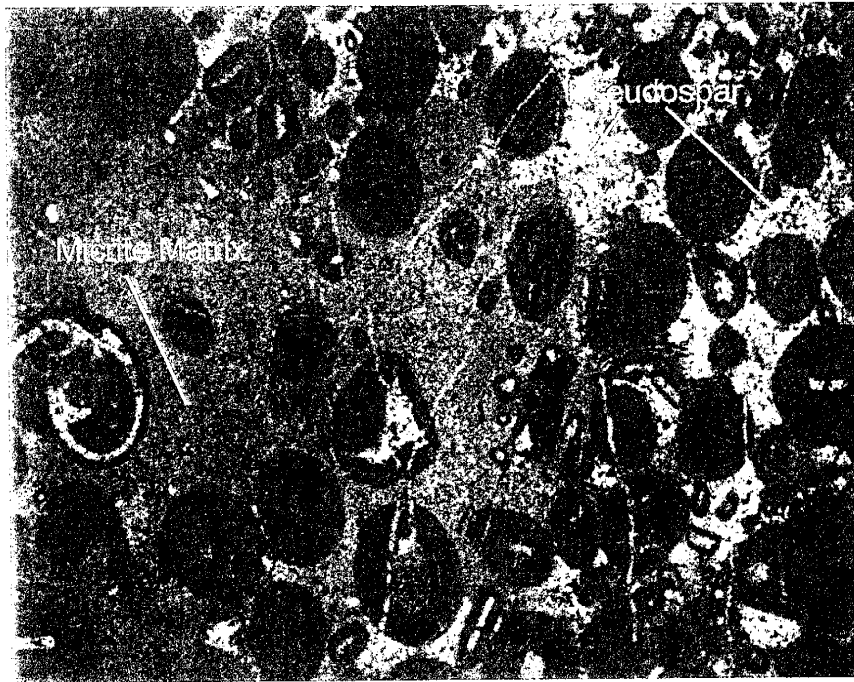


Figure 38 Photomicrograph showing development of pseudospar in a oolitic wackestone (upper image, field of view approximately 6.00 mm). Clearly visible in the lower image are patches of micrite floating in the pseudospar.

micritization occurs at or near the sediment-water interface during early diagenesis in both the active and stagnant marine phreatic zone (Longman, 1980; Heckle, 1983).

#### Micritization in the Paradise Formation

Micritized grains are common in the Paradise Formation, and they typically consist of mollusks, ooids, and pelmatozoan fragments. In some instances entire grains have been micritized and are only recognizable by their external morphology. If the micritized grains are extremely small, the nature of the original grain may not be identifiable. In this instance they are classified as peloids. Following the dissolution of the aragonitic shell material of mollusks in the Paradise, dark micritic rims are all that remain (Figure 39).

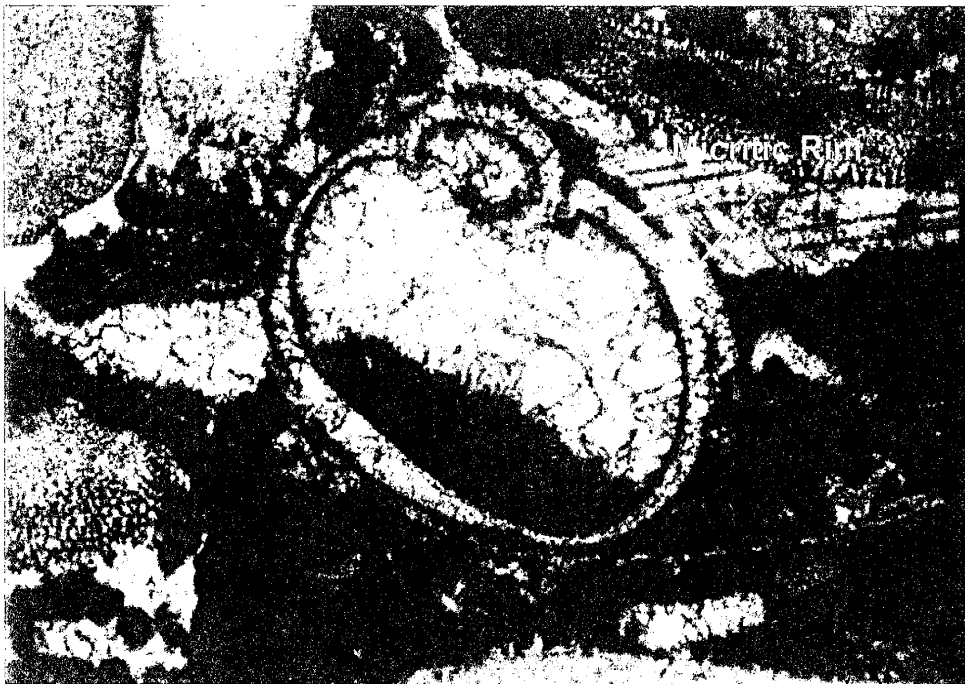


Figure 39. Photomicrograph of well developed micritic rim on a gastropod. Subsequent dissolution of the gastropod shell left an outer and inner micrite rim in the original shape of the mollusk. Fracturing of outer rim suggests early compaction following dissolution, but prior to cementation. (Field of view 1.3 mm.)

## **Dissolution**

The dissolution of carbonate grains occurs in waters undersaturated with respect to calcium carbonate. Dissolution of aragonite commonly takes place during early diagenesis in the freshwater or mixed fresh-marine waters that are undersaturated with respect to aragonite (Moore, 1989). The dissolution process can also take place in the zones of solution in the freshwater vadose environment, in the freshwater phreatic environment (Longman, 1980), or during burial diagenesis (Scholle and Halley, 1985).

### **Dissolution in the Paradise Formation**

Dissolution of aragonitic grains occurred throughout the Paradise Formation, and was not confined to any specific lithofacies. In the Paradise, skeletal grains originally composed of aragonite include mollusks. This is based on the remaining shapes of the dissolved grains, and their association with other skeletal grains composed of low-magnesium calcite. In both grainstones and packstones, aragonitic grains were dissolved leaving micritic rims that outline the shapes of the original grains. In mud-rich rocks the aragonitic grains were dissolved leaving molds in the shapes of the original grains. In all of these cases, the void space left by the dissolution process created secondary moldic porosity. Unusual cases of this are the dissolution of aragonitic nuclei of calcitic ooids (Figure 40). Subsequently, the secondary porosity created by dissolution was filled with pore-filling sparry calcite cements.

## **Compaction**

Compaction in limestones may be the result of chemical or mechanical processes. Compaction of grains, matrix, and significant reductions in porosity in carbonates begins



soon after deposition (typically within the first few centimeters of burial (Ginsberg, 1957). This early reduction in porosity results in the dewatering of the sediments. Crushing and breaking of grains indicates deeper burial and increased compaction. Meyers (1980) suggests that mechanical compaction resulting in the overpacking and crushing of



Figure 40. Ooid with original aragonitic nucleus dissolved and replaced pore-filling ferroan spar cement. This figure also shows the preservation of the ooid's internal fabric indicating the ooid was originally precipitated as calcite (Field of view approximately 1.3 mm)

carbonate grains begins within the first several 100's of meters of burial and may stop around 2000 m of burial.

Indications of mechanical compaction are present throughout the Paradise Formation and include: overpacking of grains, interpenetrating grains, collapsed micritic rims, soiled ooids, and crushed or fractured grains. The crushing and fracturing of grains in the Paradise Formation suggest that compaction occurred following burial of at least several hundreds of meters.

One approach to estimating the depth of burial in carbonates at the time of significant cementation is to determine the intergranular volume of the rock using the percent of remaining open porosity. In cases where all porosity is filled with cement (such as in the Paradise Formation) the percent of sparry calcite cement can be used to determine intergranular volume. This gives an approximation of intergranular volume in the rock prior to cementation of the grains significant enough to create a ridged framework arresting further compaction. Comparing the percentage of intergranular volume of a rock to compaction curves makes it possible to arrive at an approximate depth of burial (Meyers and Hill, 1983). This approach has an advantage in that it is compatible with thin section data gathered using the bulk grain method (Dunham, 1962). Applying Meyers' and Hill's (1983) approach data collected using the grain bulk method can be used for a quick means to assess the depth of burial prior to significant cementation without having to go back and point count samples for porosity. Another advantage in using this method is that it can be applied to older data sets where the original material may not be available for re-examination.

Figure 41 is a plot of the range of intergranular volume for the Paradise Formation based upon the volume of intergranular cements from grainstones. The highest intergranular volumes found in the grainstones (Figure 41) correspond to rocks from the lower Paradise with significant volumes of low-magnesium calcite cements. There are also some rocks from the lower Paradise that have low intergranular volumes. These rocks with lower intergranular volume from the bottom part of the section, either had only a minor amount of early cementation, or underwent a high degree of early

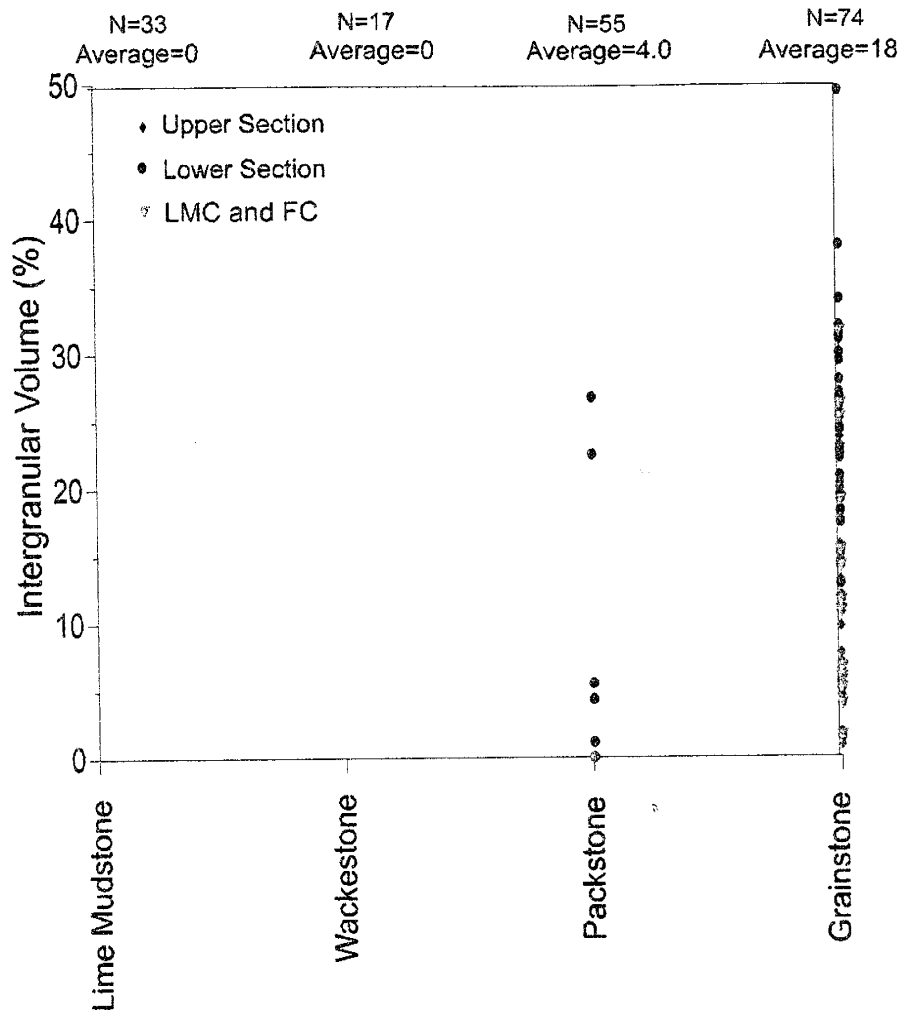


Figure 41. Plot of the range of intergranular volumes (porosity) from the main carbonate rock types in the Paradise Formation. Intergranular volume is calculated as the percent sparry calcite filling intergranular void space based on total volume of rock. Percents are listed above each column. (Data from point counting. LMC-Low-magnesium calcite, FC-Ferroan Calcite.)

compaction, which can occur in the first 200 m of burial (Meyers, 1980). In the case where there was a significant amount of early cements, the cements acted to arrest compaction as burial continued.

The intergranular volume for grainstones in the Paradise Formation ranges from 50% to 2% with an average intergranular porosity of 18% (Figure 41). Grainstones, similar to those in the Paradise, typically have original intergranular volumes of 42%

(Meyers and Hill, 1983). Using 42% as an initial value for intergranular volume for the Paradise grainstones and 18% for a post compaction intergranular volume indicates that there has been on average a reduction in intergranular volume of 24% due to compaction.

According to data from Meyers and Hill (1983) grainstones with intergranular porosities on the order of 18% suggest depths of burial on the order of 600 m prior to significant cementation of the carbonates. This number compares well with the estimated depth of burial for grainstones with 18% porosity from a porosity-depth curve plotted for grainstones from Moore (1989). Moore's plot takes into account both inter- and intragranular porosity. The close agreement between this plot and the depth of burial using only intergranular volume using Meyers and Hill's (1983) method suggests that only using the intergranular volume is a reliable means of estimating depths of burial. The amount of pre-cementation burial suggested for the Paradise Formation is less than the 1000 m of preserved Pennsylvanian rocks overlying the Paradise Formation in the Pedregosa basin, suggesting that compaction was arrested before the end of the Pennsylvanian.

### **Calcite Cements**

There are several types of calcite cements found in the Paradise Formation. These cements include: a clear, blocky, isopachous sparry cement; clear blocky pore-filling sparry cement; a clear poikilotopic sparry cement; and a clear, sparry syntaxial overgrowths. Most commonly, these cements are associated with grainstones and grain-rich rocks, but they are also found as pore-filling cements in mud-rich rocks. Of the morphologies observed in the Paradise, blocky spar cements are the most common. Syntaxial overgrowths are associated exclusively with pelmatozoan fragments.

Petrographic observations of potassium ferricyanide and Alizarin Red-S stained thin sections and cathodoluminescence petrography revealed two types of sparry calcite cements: a low-magnesium calcite and a ferroan calcite.

Using cathodoluminescence petrography and staining, it is possible to determine cement stratigraphies and establish a parageneses for the sparry calcite cements. The first cement precipitated was the low-magnesium calcite spar, and ferroan spar was precipitated second. There were no discernible paragenetic relationships between the cements using cathodoluminescence petrography, other than those determined by standard petrographic techniques and staining, which suggest that there were at least two episodes of diagenesis resulting in sparry calcite cementation.

#### **Low-Magnesium Sparry Calcite Cements**

The early low-magnesium calcite cements are confined to the lower 72 meters of the stratigraphic section (Figure 42). These cements typically form isopachous rims of bladed, clear sparry calcite and blocky, equant, clear sparry calcite that act to bind framework grains (Figures 43 and 44). These blocky spar cements fill all open pore spaces between framework grains and fill open intragranular pore spaces. Low-magnesium calcite cement can form under a variety of diagenetic environments, from shallow to burial. The morphologies (isopachous rims of bladed, clear sparry calcite and blocky, equant, clear sparry calcite) of these low-magnesium calcite cements are typical of those formed during shallow freshwater phreatic diagenesis (Longman, 1980; Moore, 1989). The morphologies of these cements combined with higher intergranular volumes

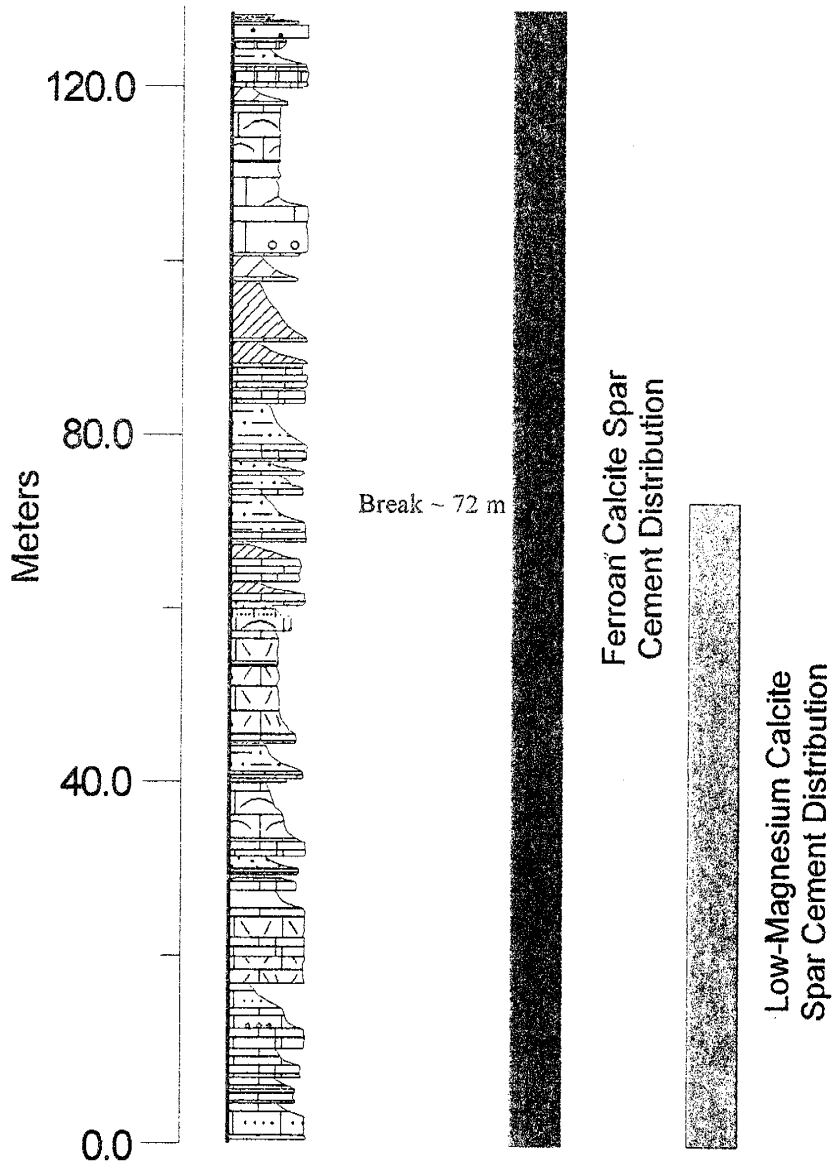


Figure 42. Plot showing the stratigraphic distribution of freshwater cements in the Paradise Formation. Break at 72 meters does not correspond to any recognizable stratigraphic division, or surface. (See Figure 10 for key to lithologic symbols.)

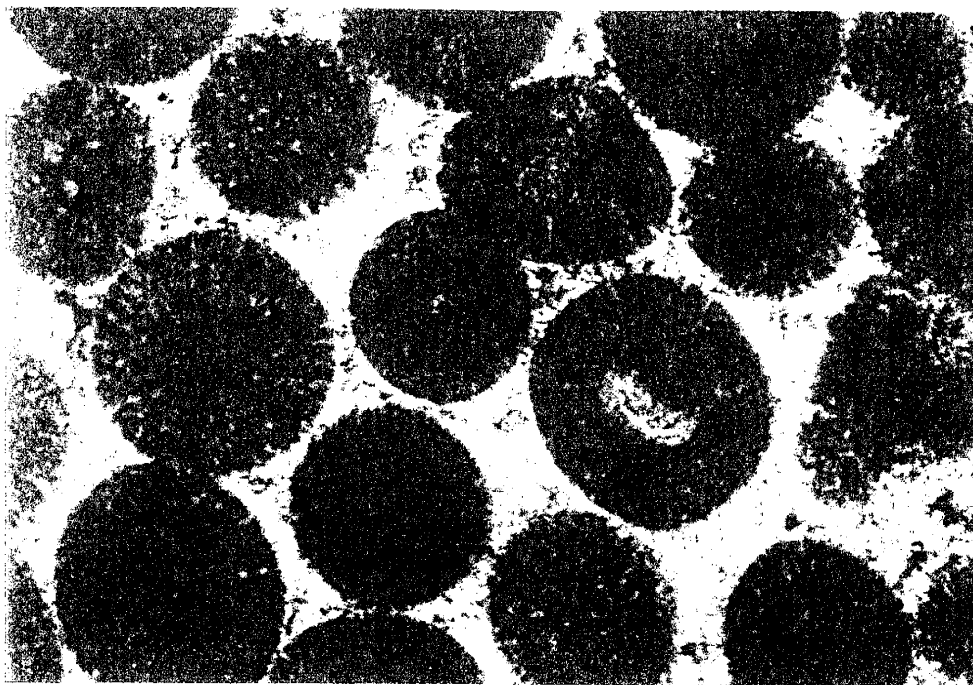


Figure 43. Photomicrograph of an oolitic grainstone showing freshwater, isopachous, sparry calcite cements on ooids with the pore spaces between the isopachous cements filled with ferroan calcite cement. (Field of view approximately 6.0 mm)



Figure 44. Photomicrograph of an abraded grainstone showing ferroan calcite, (stained blue) pore-filling cement with a poikilotopic texture. Also apparent in this image is evidence of early compaction, resulting in the crushing and interpenetrating of grains prior to cementation. (Field of view approximately 6.0 mm)

in the lower part of the stratigraphic section, where these cements dominate, suggest that these cements formed during early diagenesis and are most likely shallow, freshwater cements.

### **Ferroan Sparry Calcite Cements**

The ferroan spar cements are found throughout the entire stratigraphic section, but only make up a small percentage (< 5%) of cements in the lower 72 m (Figure 42). These cements are found in three morphologies: equant, blocky spar; poikilotopic cements; and syntaxial overgrowths on pelmatozoan fragments. These cements are found filling both inter- and intragranular pore spaces, occluding all remaining open pores (Figure 40).

The ferroan nature of these cements indicates that they were precipitated under low oxygen conditions allowing the  $\text{Fe}^{+2}$  to be incorporated into the calcite lattice (Morse and Mckenzie, 1990). Although  $\text{Fe}^{+2}$  can come from a variety of sources, the most likely source of the  $\text{Fe}^{+2}$  is from the clays in the shale units and argillaceous carbonates.

Low oxygen waters capable of precipitating ferroan calcite may exist at any burial depth, providing that there is a source of available iron. The morphologies of these cements are also common in both freshwater and burial cements. The overall coarse crystal sizes and the high volume of poikilotopic cements indicate slow rates of precipitation, at low concentrations of calcite in solution, and can be representative of either early, shallow diagenesis from freshwater, or later burial cementation (Scholle and Halley, 1985). The small intergranular volumes and the depth of burial to at least 600 m suggest that these ferroan calcite cements were precipitated in a burial diagenetic setting. Furthermore, it would appear likely from the depth of burial assumed from intergranular



volume data that the ferroan cements were precipitated and that all of the open pore spaces in the Paradise Formation were occluded by the end of the Pennsylvanian.

There are ferroan calcite cements that fill fractures that cut both matrix and grains. This suggests that the fractures occurred after lithification of the sediments. Fracturing could have been caused by deeper burial of the rock, or may have formed late in the diagenetic history of the Paradise Formation during unloading and uplift of the region. In either case, they were subsequently filled with ferroan calcite cements during late burial or telogenetic diagenesis.

Based on general cement relationships, cement morphologies, and intergranular volume data, it is suggested that the low-magnesium sparry calcite cements were formed relatively early, in a shallow freshwater diagenetic setting, and that the ferroan sparry calcite cements were most likely formed during late diagenesis, in the burial and telogenetic environments. Additional information from stable isotopic analysis will be used to further define these general conclusions concerning the sparry calcite cements.

### **Dolomitization**

Three distinctive types of dolomite were observed in the Paradise Formation. They include: aphanitic, microcrystalline, and skeletal replacement dolomite. Of these, the skeletal replacement dolomite is the rarest, with aphanitic dolomite being most abundant.

Aphanitic dolomite is found only in the lowermost part of the Horse Pasture Canyon section. These dolomites likely represent the original mineralogy of the units deposited (see interpretation on Page 59). It is not known whether these were originally

precipitated as non-stoichiometric or stoichiometric dolomite. As such, there is little to say concerning the subsequent diagenesis of these dolomites.

Microcrystalline dolomites occur only in lime mud-rich lithofacies. This dolomite is found as rhombs that likely replaced lime mud. This is based on the observation that in some instances, the distribution of dolomite is patchy where incomplete dolomitization of the lime mud has taken place. Typically, dolomite rhombs are uniform, euhedral, and less than 0.04 mm in size (Figure 45). In some instances, dolomite rhombs are intermittently scattered in the lime mud matrix of wackestones.

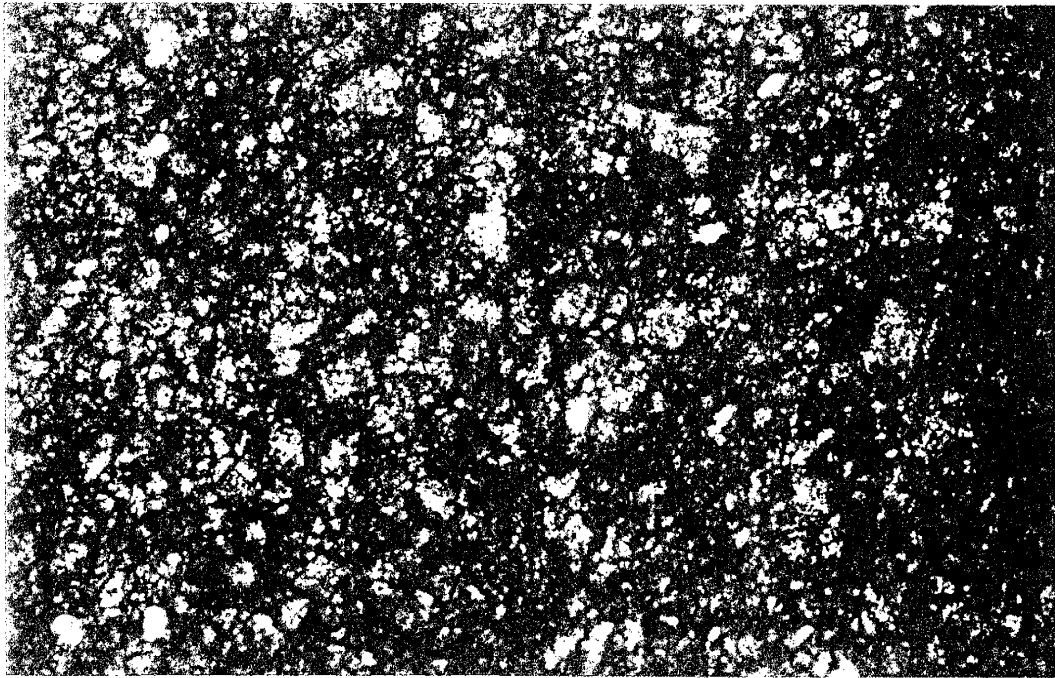


Figure 45. Photomicrograph of a replacement dolomite. Dolomite is replacing a lime mudstone. (Field of view 1.3 mm)

Skeletal replacement dolomites are rare in the Paradise Formation, are found intermittently throughout the stratigraphic interval and are confined to brachiopods and peimatozoan debris. Two types of skeletal replacement dolomite are present. The first

replaces the shell material up to the boundary between the shell and matrix. No dolomites of this type were observed in mud-poor lithologies. The second type of skeletal replacement dolomite was only observed in the uppermost Paradise in Chaney Canyon. These dolomites are ferroan and replace mollusk shells.

### **Dolomitization Models**

The process of dolomitization is one of the most controversial topics in geology. Detailed reviews of various models for dolomitization can be found in Morrow (1982a, 1982b) and in Hardie (1987). Morrow (1982b) suggested that the depositional setting, lithofacies relationships, and petrographic characteristics of the dolomite are important in narrowing the potential dolomitization models to a reasonable number. Of these properties, the petrographic nature of the dolomites observed in the Paradise Formation is most distinguishing. Euhedral microcrystalline dolomites, such as those in the Paradise, are commonly formed in the mixed-water diagenetic setting (Morrow, 1982b; Folk and Land, 1975). The skeletal replacement dolomites in the Paradise have somewhat larger, more anhedral crystals. Dolomites such as these are typical of late, freshwater phreatic, burial diagenetic environments (Morrow, 1982b). Typically, these late diagenetic dolomites replace skeletal material in a manner similar to that observed in the Paradise during burial diagenesis. An obvious difference between the ferroan and the anhedral skeletal replacement dolomites is that some source of  $\text{Fe}^{+2}$  was available, and that reducing conditions existed during precipitation of the ferroan dolomite. Although the source of iron for these dolomites is not known, a likely source would be from the same sources as those listed for the iron in the ferroan calcite cements.

## Silicification and Silica Cements

### Silicification

Silicification in the Paradise Formation is even rarer than dolomitization.

Silicification is distributed randomly throughout the stratigraphic interval in the form of chert, which is restricted to skeletal grains (mostly pelmatozoans). Where dolomitization and silicification have both occurred, the dolomite appears to replace the silica, suggesting that silicification occurred prior to dolomitization. This is based on the irregular margins between the silica and the dolomite, and isolated patches of euhedral dolomite within the silica. If the silica was replacing the dolomite the margins of the dolomite rhombs would be more irregular and ragged.

The above observations are consistent with those reported by Maliva and Siever (1988) for the silicification of fossils. They argue that the decaying organic matter in carbonate grains enhances the dissolution of carbonate and the precipitation of silica as either quartz or opal-CT. Once a nucleation of silica begins and silica precipitates, a concentration gradient is created toward zones of decaying organic matter. This gradient is maintained until either the silica is exhausted or chemical conditions change halting the process. Thin aqueous films and the force of crystallization also control silicification.

Maliva and Siever (1988) suggest that the silicification of fossils is a relatively early diagenetic process. This contention is based upon the need for organic matter to act as a catalyst for silicification by creating localized acidic conditions. Observations from material in the Paradise Formation do not confirm or contradict this contention, but merely indicates that silicification took place prior to dolomitization.

### Silica Cements

Silica cements were observed in only a single unit within the entire Paradise Formation in the Big Hatchets. This occurrence is in unit 58, a sandstone bed near the top of the Horse Pasture section. There the silica cement occurs as quartz overgrowths precipitated on detrital quartz (Figure 46). The presence of this cement indicates a change in the composition of pore-water or temperature from those that precipitated the carbonate cements. Lower temperature waters capable of carrying significant amounts of silica in solution need to be significantly alkaline ( $\text{pH} > 9$ ). Increased temperatures also play a significant role in the ability of diagenetic fluids to carry silica in solution by increasing the solubility of detrital (non-biogenic) silica and allowing more silica to be held in solution. Silica can be put into solution by the alteration of detrital clays and feldspars, pressure solution and dissolution of detrital quartz, volcanic glass, and biogenic silica (Pettijohn et al., 1987; Fuchtbauer, 1983). Crystalline quartz and biogenic silica (opal-A) are the most common sources for silica (Pettijohn et al., 1987). Of these, biogenic silica is more soluble at shallower depths and/or at lower temperatures and can be precipitated as silica cement relatively early during diagenesis. In order for significant amounts of quartz cementation to occur, temperatures must be at least  $80^{\circ}\text{C}$  (Oelkers et al., 1996).

The sandstone in unit 58 (Horse Pasture Canyon Section) shows little indication of significant compaction and pressure solution. This may indicate that silica cementation occurred relatively early during diagenesis. If this was the case then the source for the silica was either from biotic grains supplying opal-A, or from groundwater

carrying silica in solution. Increasing the solubility of silica in groundwater is possible without significantly increasing the water temperature if the pH is above nine.

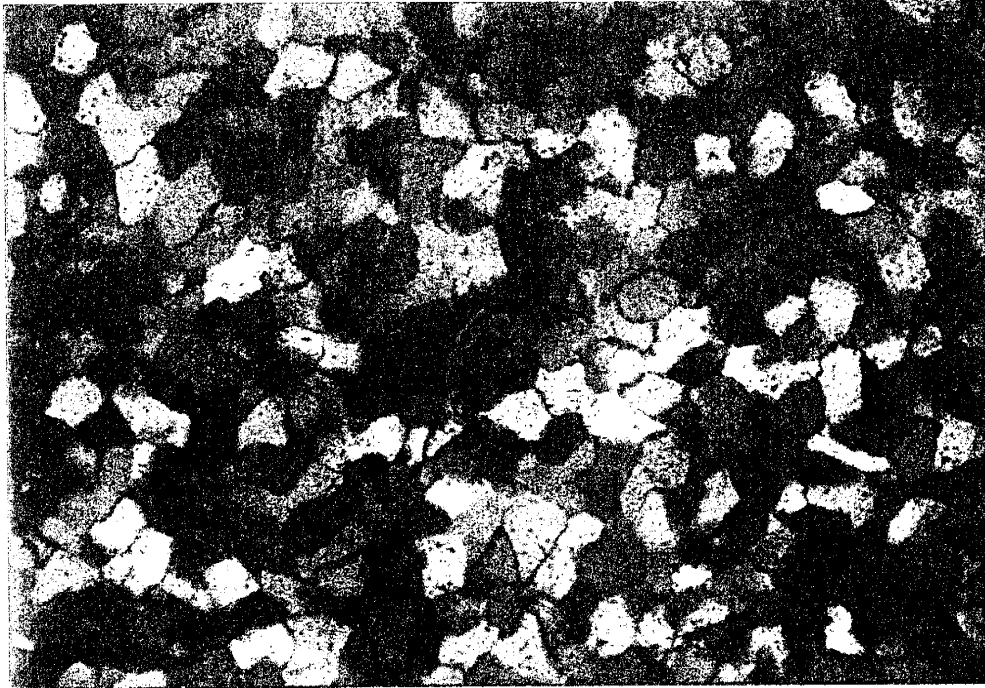


Figure 46. Silica cemented quartz sandstone from the Paradise Formation. Faint dust rings are present on some of the grains indicating the boundary between the grain and the quartz overgrowth. (Field of view approximately 6.00 mm)

Alkaline waters with elevated pHs are commonly associated with arid regions (Pettijohn et al., 1987). Although there can be quartz cementation in the shallow burial diagenetic environment, it is not volumetrically important (Surdam et al., 1989) and these cements typically only partially occlude open pore spaces. The precipitation of quartz cements on sand grains would begin as the diagenetic fluids become super saturated with respect to silica. This is likely to occur as more silica was placed into solution with increasing temperatures relative to increasing depth of burial Oelkers et al. (1996) suggest that sufficient volumes of silica may be in solution at or above a temperature of 80°C. It would take an inferred depth of burial of at least 2 km of the Paradise Formation to provide a sufficient increase in temperature (80°C) to initiate the formation of quartz

overgrowths as diagenetic fluids became super saturated with respect to silica. The detrital quartz grains composing the sand units would then act as nucleation sites for silica precipitation. This model suggests that these silica cements formed during burial diagenesis at a depth of burial significantly greater than 600 m as indicated by the intergranular volume data and the timing of significant calcite cementation.

This discrepancy suggests one of two possibilities. First that the amount of burial indicated by the intergranular volume data is grossly underestimating maximum burial depth for the Paradise Formation. Second that the calcite cementation occurred early during burial diagenesis, halting further any further compaction, and the silica cementation took place during deeper burial of the Paradise.

There are no observable relationships between the quartz overgrowths and the sparry calcite cements to aid in establishing their paragenetic relationships. The increased depth of burial required to produce high enough temperatures for quartz overgrowth formation strongly suggest that the silica cements formed after the calcite cementation making the second scenario the most likely.

The source of the silica that was precipitated in these sandstones is somewhat problematic. There are no indications that there was significant pressure solution of detrital quartz to act as supply of silica. Other sources for silica can include opal-A available from biotic sources in the surrounding carbonates, clays and feldspars. There is little evidence that there was any feldspar in the detrital material in the Paradise Formation, or other Paleozoic formations. The clays in the shales may have been a source for the silica, or it may have been carried in solution by basinal fluids from another location.

## General Paragenesis

Diagenetic features can be placed into a relative time frame with one another to form a paragenetic sequence (Figure 47). Timing is based upon petrographic relationships observed between the diagenetic features, as described in each of the previous sections.

### Integration of Diagenesis and Lithofacies

For the most part, all of the diagenetic features described from the Paradise Formation are found throughout the entire stratigraphic interval. The overall timing of events is similar for each lithofacies. This allows the construction of a single paragenetic diagram based on cross cutting relations of diagenetic features keyed to individual lithofacies (Figures 47). It is apparent from Figure 47 that there are few differences in the diagenetic features present in the different lithofacies. The biggest difference is in the amount of sparry calcite cement present and in the number of carbonate grains that underwent dissolution. These features are more common in the grain-rich lithofacies than in the mud-rich lithofacies. In mud-rich lithofacies the process of neomorphic conversion of lime mud to micrite took place, yet did not occur in grainstones, due to the complete lack of lime mud in these lithofacies.

Diagenetic features common to the Paradise Formation are not so much indicative of a given environment as they are of a process, or sediment type. For instance, products of diagenesis such as aggrading neomorphic textures are limited to mud-rich lithofacies. Replacement dolomitization is not common in the Paradise and is found without regard to any individual lithofacies or depositional setting. Silicification is rarer than dolomitization and also appears not to be related to depositional setting. Silica cements



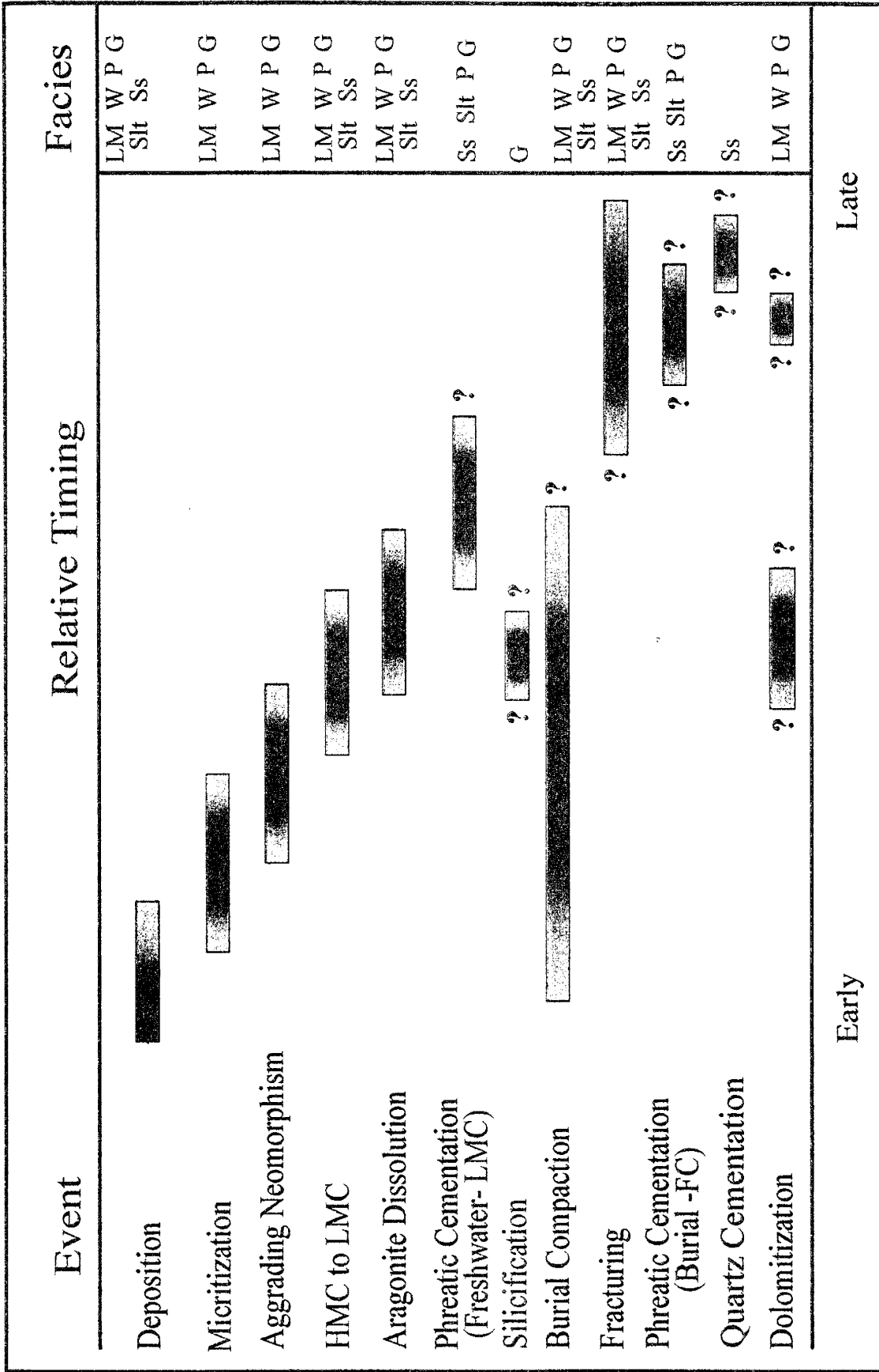


Figure 47. Overall paragenetic sequence for the Paradise Formation Note Lighter shading indicates some uncertainty of timing and overlap of features. (HMC-High-magnesium calcite, LMC-Low-magnesium calcite, FC-Ferrous Calcite; Facies Codes-LM-Lime mudstone; W-Wackestone; P-Packstone; G-Grainstone (Abraded and Oolitic); Slt-Siltstone; Ss-Sandstone)

are so rare that little can be said except that the single occurrence is restricted to the sandstone lithofacies, and represent silica precipitation during late diagenesis in a burial setting.

### **Porosity and Permeability**

The evaluation of porosity and permeability was not a primary focus of this study, yet they are directly impacted by diagenetic processes. Although no direct measurements of porosity and permeability were made, petrographic observations of diagenetic features in thin section permits a first approximation of porosity and permeability.

Two types of porosity were identified in the Paradise Formation, primary porosity and secondary porosity. Primary porosity refers to pore spaces that remained open following deposition, and secondary porosity developed following the dissolution of carbonate grains by freshwater diagenesis and through the development of fractures. Compaction of sediments acted to reduce both primary and secondary porosity through the collapse of pore space. Subsequent cementation by calcite and silica resulted in significant occlusion of primary and secondary porosity. There may have been minor development of secondary porosity related to dolomitization of lime mudstones, but it is not known whether or not any of this is preserved.

Permeability has been affected by diagenesis in the same manner as porosity. It is likely that the pervasive cementation greatly reduced permeability. Petrographic evidence for this is the visible blocking of pore throats between grains and in fractures by cement.

Taking these factors in account clearly indicates that the reservoir quality (porosity and permeability) of the Paradise Formation is extremely poor.

## **STABLE ISOTOPE GEOCHEMISTRY**

Stable isotopes are commonly used in carbonates to answer questions concerning the composition of paleoseawaters, paleoecology, and the effects of diagenetic fluids on carbonates (Flügel, 1982). Stable isotopic compositions of carbonates from the Paradise Formation were used in evaluating patterns of cyclic sedimentation. Due to their stable mineralogy, brachiopods were considered as a potential candidate for possibly retaining original isotopic compositions. Because of this, they may also be used as base compositions, to which other altered material could be compared and they may be used to assess paleoseawater isotopic compositions of the Pedregosa basin.

### **Approach**

Samples for isotopic analysis were from the Horse Pasture Canyon and Chaney Canyon sections. From these sections, 90 samples were analyzed for carbon and oxygen isotopes. The majority of the analyses from these sections are from whole-rock samples. The whole-rock isotopic data were evaluated and used as a means to assess overall patterns in isotopic alteration. Specific carbonate components were also analyzed from selected samples. Components were selected for isotopic analysis using standard optical and cathodoluminescence petrography. These individual carbonate components consisted of brachiopods, pelmatozoans, ooids, and carbonate cements. The isotopic data from selected carbonate components were used to evaluate the possible retention of original isotopic compositions. Both the whole rock and component data were also used to determine the possibility of using isotopic patterns to further define cyclicity in the Paradise.

**DATA**

Whole-rock isotopic data from the Horse Pasture and Chaney Canyon stratigraphic sections are presented in a cross-plot of  $\delta^{13}\text{C}$  vs.  $\delta^{18}\text{O}$  (Figure 48). The majority of the data points cluster together to the left of the range of carbonate precipitated in equilibrium with Mississippian seawater, with the exception of two data points that have markedly separated by heavier  $\delta^{18}\text{O}$  values (Figure 48). These two points are from dolomites. Commonly, dolomites are slightly heavier by several permil in  $\delta^{18}\text{O}$  than coexisting calcites (Land, 1980). As these are the only two dolomite samples in the data set, and their isotopic composition is primarily a function of original mineralogy, they are not considered further. The remaining samples have a moderately wide range in  $\delta^{13}\text{C}$ , from -5‰ to +2‰ PDB, and a relatively narrower  $\delta^{18}\text{O}$  range, from -5‰ to -9‰ PDB. These samples are all depleted, in both  $\delta^{13}\text{C}$  and  $\delta^{18}\text{O}$ , relative to the estimated values for marine carbonates precipitated in equilibrium with Mississippian seawater (Figure 48; Popp et al., 1986; Veizer et al., 1986).

The majority of isotopic values from the Paradise Formation fall within the field of other published Mississippian rocks (Figure 49). This shows that the majority of Mississippian materials sampled are depleted with respect to carbon and oxygen, suggesting widespread diagenesis. Some of the samples plot to the right of the Mississippian carbonate box indicating they are isotopically enriched with respect to carbonate in equilibrium with Mississippian seawater. With the exception of one of these data points, the isotopically enriched data that group together are from dolomites. The other data point is from a luminescent brachiopod and, without further information regarding the diagenetic

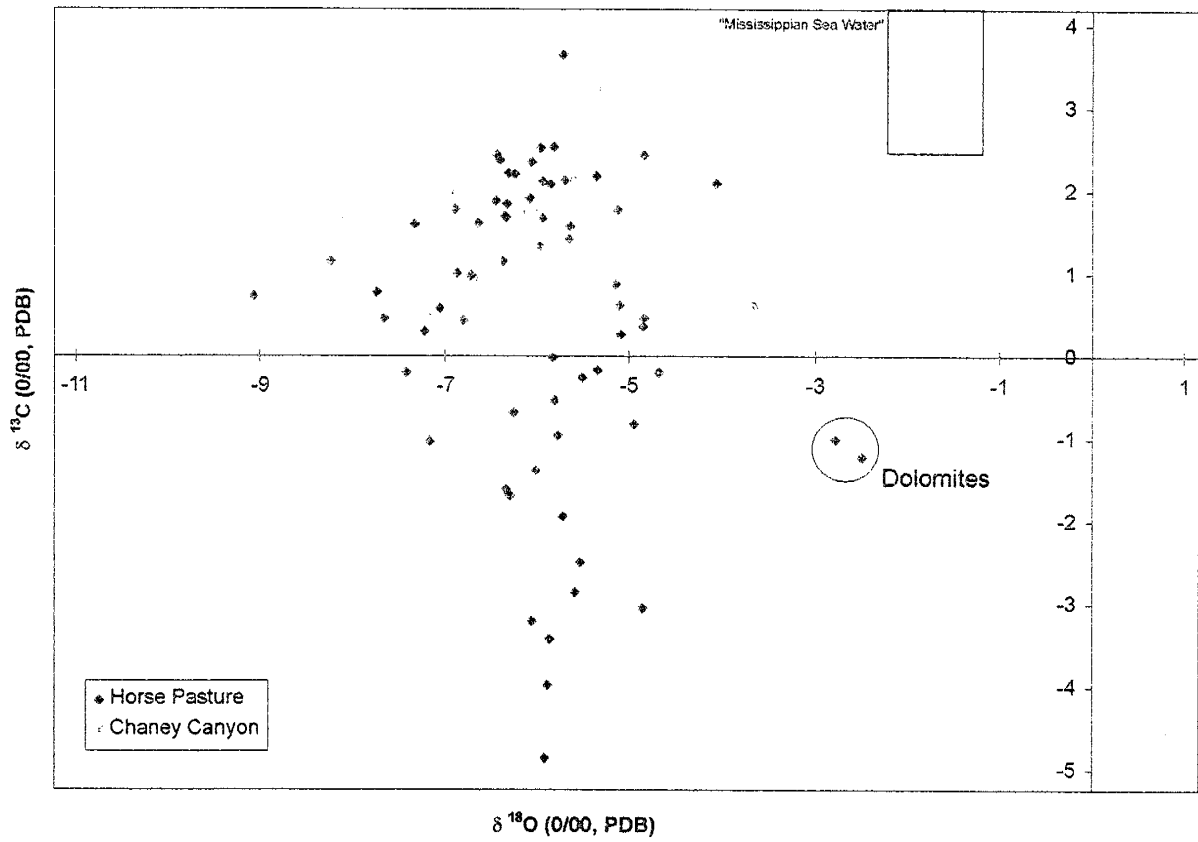


Figure 48. Isotopic distribution of whole rock samples from the Paradise Formation.

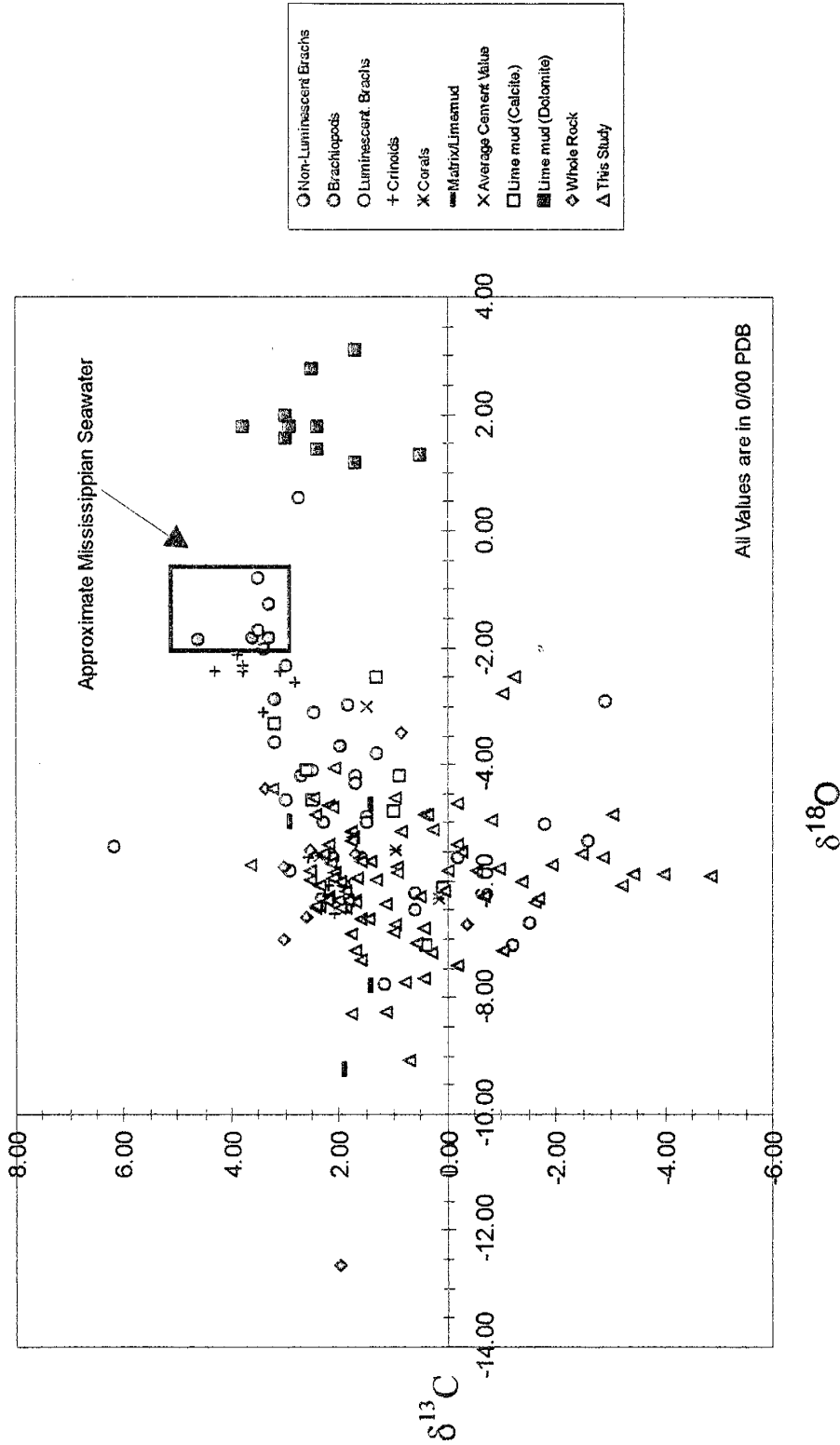


Figure 49. Distribution of whole rock isotopic values from this study compared to published Mississippiian isotopic data. (Data from Veizer et al., 1986; Popp et al., 1976; Veizer and Hoefs, 1986; Brand, 1981; Meyers and James, 1976; Choquette, 1968; Keith and Weber, 1964; Brand, 1961)

history of that sample, all that can be said is that it was enriched with respect to normal Mississippian marine calcite isotopic values.

### **Data Distribution, Interpretation, and Models**

Whole-rock isotopic data from the Paradise Formation are consistent, in terms of carbon and oxygen values, with other isotopic data from the Phanerozoic (Keith and Weber, 1964; Veizer and Hoefs, 1876; Allen and Matthews, 1977, 1982; Adlis et al., 1988). It is apparent from Figure 48 that all of the rocks from the Paradise must have been isotopically altered subsequent to deposition. A popular interpretation of isotopic data patterns similar to that of the Paradise was put forward by Lohmann (1988). He described data with a similar appearance as an inverted "J" curve. Data plotting in this manner is suggested to reflect increasing isotopic alteration with respect to the original isotopic composition as a function of increasing water/rock ratios (Lohmann, 1988). This means the more altered a sample the greater the exposure to isotopically altering fluids, and thus the greater the water/rock ratio.

If the data from the Paradise Formation reflect alteration similar to those data reflected in an inverted "J" curve, there should be increasing isotopic alteration away from the postulated field representing precipitation of carbonate in equilibrium with Mississippian seawater indicating increasing rock/water ratios (Figure 50). If the data distribution represents alteration from a single diagenetic event, the data points should show increasing isotopic alteration from samples closer to the source of the freshwater mirroring the changing water/rock ratios. One way to test this would be to use the unconformity between the Paradise Formation and the Horquilla Limestone as the surface for introducing fresh waters, into the Paradise. These fluids could be the same ones that

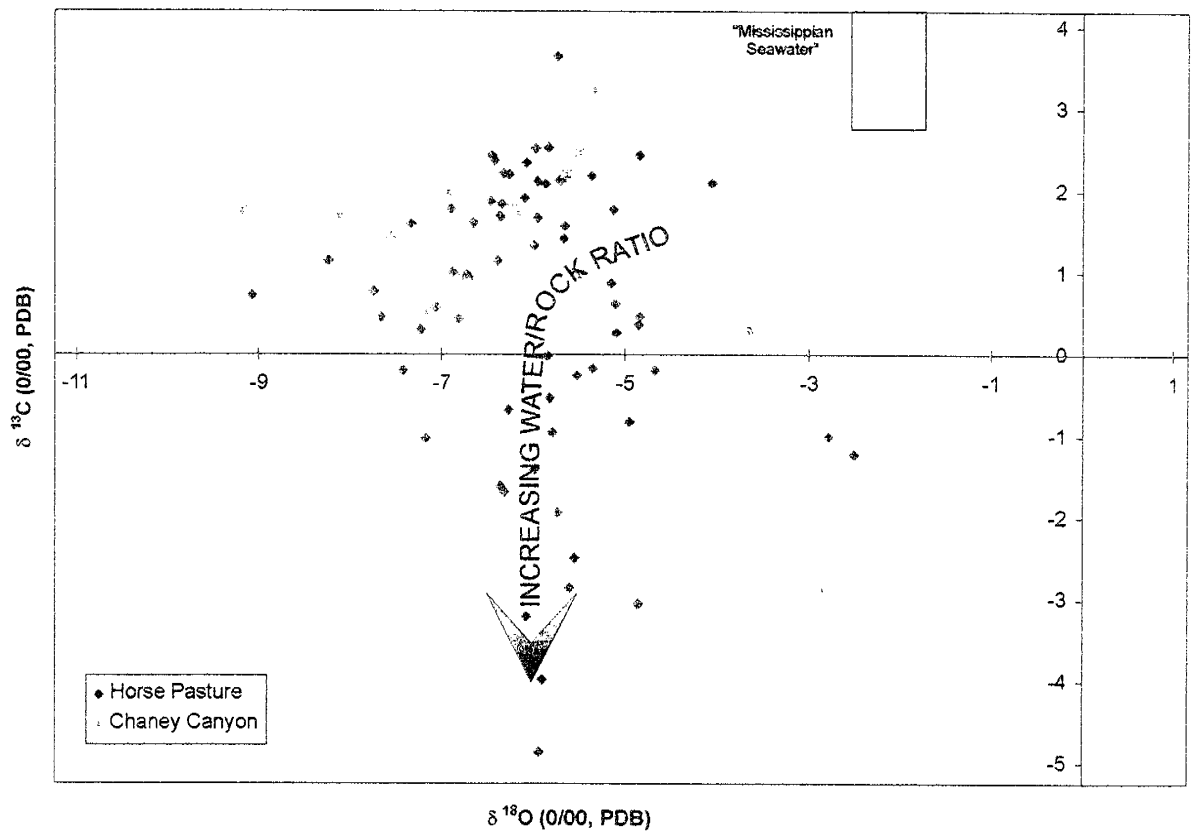


Figure 50. Isotopic distribution showing possible alteration trend assuming a single diagenetic event.



precipitated the ferroan calcite cements. If this were the case the data should show that the most altered sample should be at the top of the section with progressively older strata showing less alteration and, the least altered samples being at the base of the section. This alteration pattern is also similar to those observed by Allen and Matthews (1977, 1982) in carbonates subjected to subaerial exposure and freshwater diagenesis in Barbados, where they observed increased isotopic alteration near the exposure surface.

To test this possibility samples were plotted corresponding to stratigraphic position in order to establish trends within the data related to stratigraphic position. This exercise did not show any systematic pattern suggesting alteration similar to that observed by Allen and Matthews (1977, 1982), or to that of Lohman's (1982) inverted "J" curve.

The stratigraphic ordering of the data did reveal that these data fall into two distinctive fields with only minor overlap (Figure 51). Data grouped into field 1 are from the lower 72 m of the Paradise Formation. The data grouped in field 2 are, with a few exceptions, from the remaining stratigraphic section. All of the data points from the Chaney Canyon section fall within field 2. This break in the stratigraphic section, between fields 1 and 2, also coincides with a fundamental change in the stratigraphic distribution of sparry calcite cements (Figure 42, Page 107). Data plotting in field 1 correspond to samples dominated by low-magnesium calcite cements, whereas data falling into field 2 correspond to sample with ferroan calcite cements.

The early diagenetic event affecting the data grouped in field 1 coincides with the break in sparry calcite cementation found up to 72 m above the base of the Paradise Formation. Using samples labeled in stratigraphic order as a means of assessing

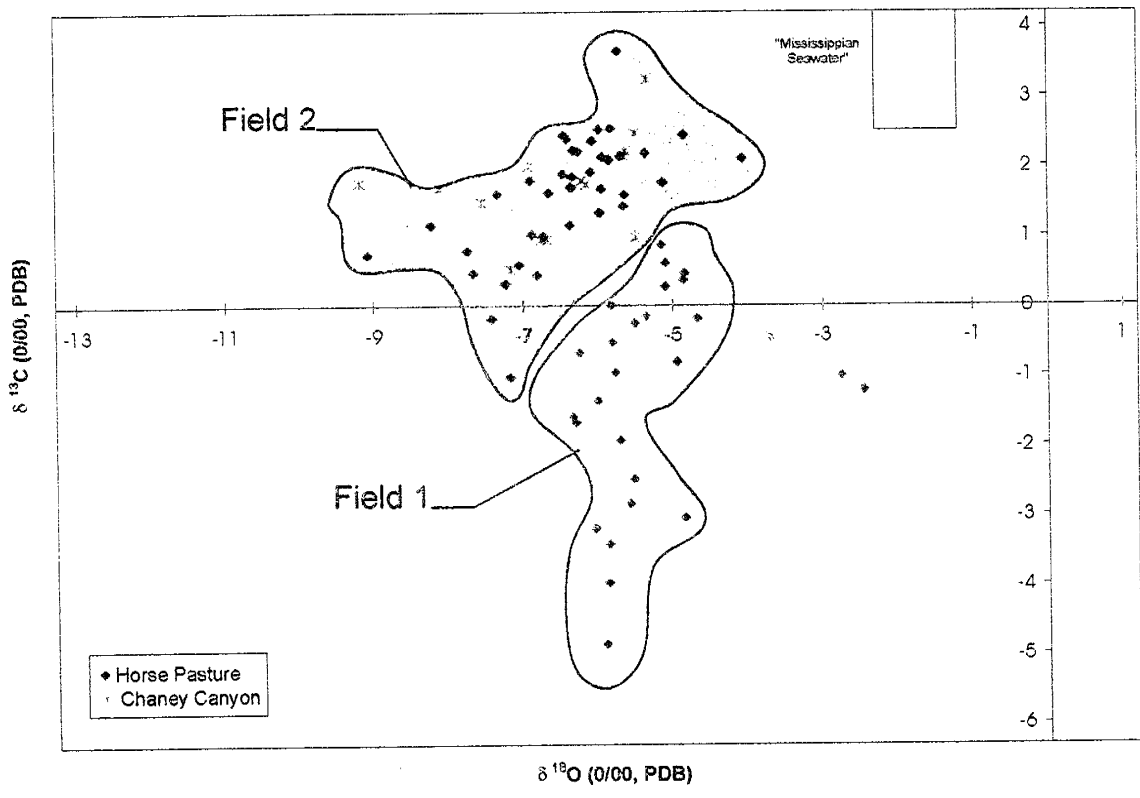


Figure 51. Plot showing the separation of data into two fields based on the stratigraphic order of the data.

systematic isotopic alteration revealed a subtle, but poorly developed, repetitive pattern of stratigraphically older to younger samples in field 1, but no identifiable pattern in field 2. The subtle hint of stratigraphically ordered alteration in field 1 is similar to isotopic alteration patterns associated with exposure and freshwater diagenesis observed in modern carbonates (Allen and Matthews, 1977, 1982). Even though the alteration patterns observed show no good evidence of large-scale systematic spatial isotopic alteration resulting from changing water/rock ratios related to exposure and subsequent diagenesis, the separation of the data into two fields does suggest that two pervasive diagenetic events affected the Paradise.

An alternative explanation for the observed isotopic alteration in the samples from the Paradise Formation is that the isotopic composition of the rocks is dependent on lithology. Variations in rock type could effect porosity and permeability, which in turn would impact diagenesis and isotopic exchange. The degree of isotopic alteration may be controlled not only by the volume of water but also by the nature of the carbonate grains. This would include the type of carbonate mineralogy (i.e., aragonite, high-magnesium calcite, or low-magnesium calcite) and grain size, which determines the surface area available for diagenesis and isotopic exchange. Variations in the primary porosity of individual lithotypes would act as a control on the volume of water passing through the sediments and subsequent volumes of pore-filling cements in individual lithotypes. Such variations in porosity, rock/water ratios, and carbonate mineralogy may all influence the degree of isotopic alteration.

Labeling rock types on a plot of  $\delta^{13}\text{C}$ - $\delta^{18}\text{O}$  permits the evaluation of isotopic alteration with respect to rock type (Figure 52). This plot shows that the majority of

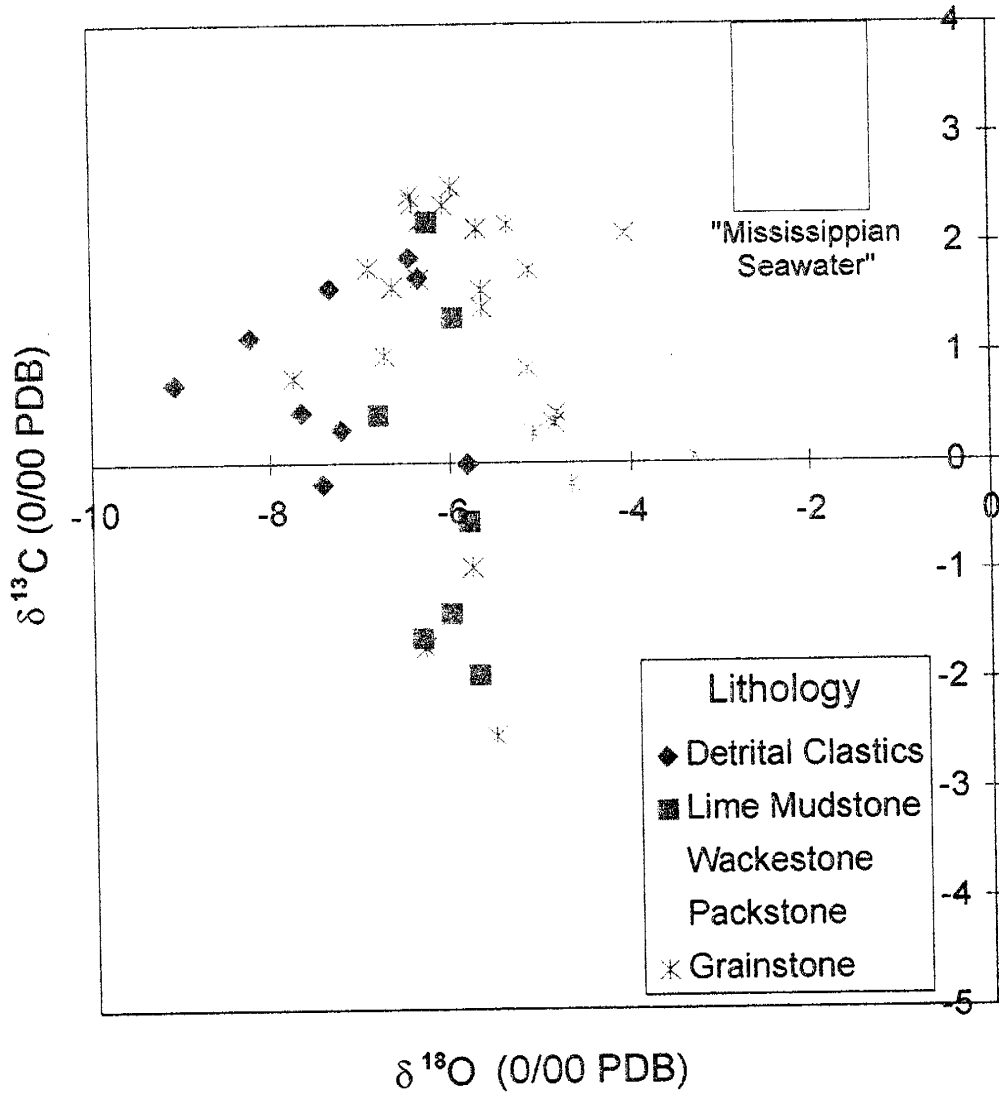


Figure 57. Plot showing the relationship between rock type and isotopic composition.

grainstones and detrital clastics plot in field 2. This is an expected outcome since there is an increase in these lithologies in the upper part of the Paradise Formation. Other than that there does not appear to be any correlation between rock type and the degree of isotopic alteration. Plotting the isotope data with respect to stratigraphic position illustrates how the data from fields 1 and 2 vary with stratigraphic position (Figure 53). Perhaps the most striking feature about this plot is the limited variation of  $\delta^{18}\text{O}$  with respect to stratigraphic position. Oxygen values tend to become lighter up section, averaging -6‰ PDB, relative to an average value of -5‰ PDB for the lower part of the section. The lack of high degree of variation in  $\delta^{18}\text{O}$  suggests that the waters had reached isotopic equilibrium with the rock. The  $\delta^{13}\text{C}$  data show more variation with respect to stratigraphic position. The variation is greatest in the lower 72 m of the section, which corresponds to data grouped into field 1 on Figure 51. Carbon 13 values range from -5‰ PDB to +2‰ PDB and average +0.64‰ PDB over the entire stratigraphic interval. Carbon variation in the lower part of the section ranges from -5‰ to near 0‰ PDB over several intervals ranging from 5 to 15 m in thickness. These patterns are similar to those observed in recent carbonate sequences that have undergone episodes of subaerial exposure and subsequent freshwater diagenesis, with the lighter carbon values at the top of each interval reflecting the input of lighter atmospheric carbon into the system (Allen and Matthews, 1977, 1982). Paleogeographic evidence indicating that the region was relatively arid suggests that even if exposure did occur, there would be limited amounts of freshwater available for diagenetic alteration and input of light carbon. The lack of any stratigraphic or thin-section data indicating exposure surfaces suggests it is unlikely that freshwater was introduced on exposed cycles, at least in the Big Hatchet region.

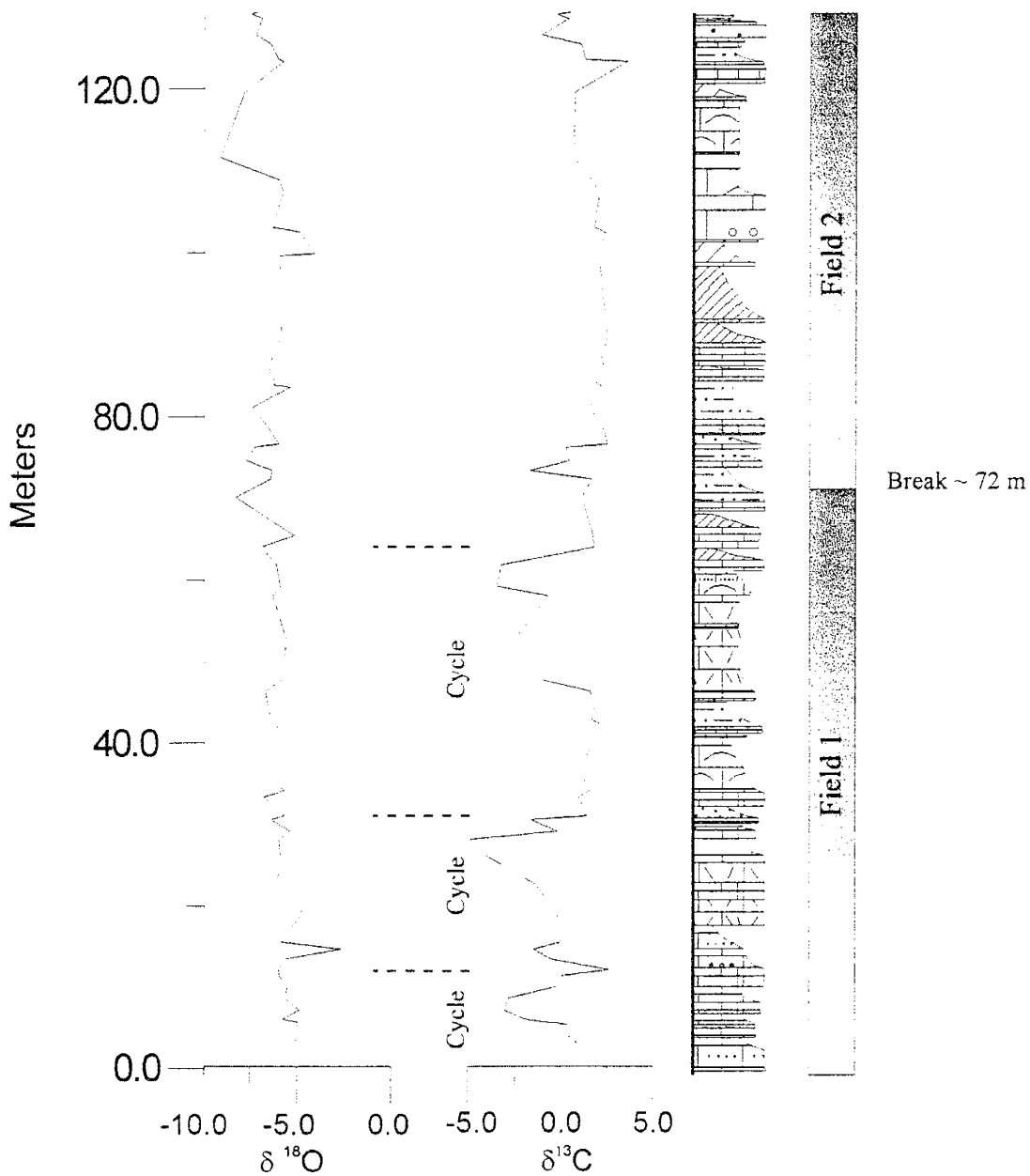


Figure 53. Plot showing the stratigraphic distribution of stable isotopes from the Horse Pasture Canyon measured section. Noted on the plot is the division between fields 1 and 2 on Figure 51. (Note shading in bars has no meaning, and is just a for visual separation of the fields.)

Alternatively, there is the possibility that the diagenetic waters with light carbon were introduced from exposed regions during relative lowstands in sea level. These waters, traveling as fresh-water lenses originating from the exposed areas, could produce similar isotopic alteration patterns to those produced by subaerial exposure and the downward percolation of diagenetic waters. In this case, the lighter carbon values at the tops of cycles reflect a greater volume of calcite cement than cements precipitated in the mud-rich rocks in the lower part of the cycle. This mechanism for delivering waters also accounts for the poorly developed cyclic-like patterns observed in field 1 of Figure 51. The differences between the thickness of the isotopic patterns and sedimentary cycles could be governed by the thickness of developing aquifers (Read and Horbury, 1993).

As previously discussed the ferroan calcite cements were most likely precipitated under burial conditions (~600 m) at elevated temperatures. Increasing temperatures, and changing water compositions in the burial environment were the most likely control of the isotopic variation observed in the upper part of the stratigraphic section. The light oxygen values may have been controlled by either the increase in temperature resulting in greater isotopic fractionation of heavier basinal waters during isotopic alteration, or by the input of isotopically lighter freshwater input in to the diagenetic system by groundwater. Carbon values in this part of the section remain close to those of marine carbonate. This suggests that in the burial environment there was not a readily available source for light carbon, either organic or atmospheric, and that the carbon values were buffered by the marine carbonates.

### Water Composition

Using the diagenetic interpretations of calcite cements and the discussion concerning possible interpretations of the isotopic patterns, it can be assumed that the waters responsible for the isotopic alteration reflect both freshwater and burial origins. Figure 48 can be used to estimate an isotopic value for calcite that can be used to calculate an isotopic value for water. The key to arriving at a reasonable calcite isotopic value is related to the high variability in  $\delta^{13}\text{C}$ , but a small degree of variability in  $\delta^{18}\text{O}$ . This indicates that the diagenetic system had reached isotopic equilibrium with respect to oxygen between the water and rock. Drawing a vertical best-fit line through the oxygen data gives us an equilibrium value for the rock, referred to as a meteoric calcite line (Lohmann, 1988). The oxygen value of the meteoric calcite line can be used as a proxy for estimating the oxygen composition of the water responsible for the isotopic alteration. For the Paradise Formation the meteoric calcite line has a value of  $-6\%$  PDB (Figure 54). This number actually refers to the carbonate material in equilibrium with the water and not the true oxygen value of the water. This value can be converted to an  $\delta^{18}\text{O}$  value that corresponds to the diagenetic water at a given temperature by using a fractionation equation. Using the fractionation equation of Freidman and O'Neil (1977; Equation 1) for calcite-water, a plot of water compositions at varying temperatures can be constructed (Figure 55).

$$1000\ln\alpha \text{ (calcite-water)} = 2.78 \text{ H } 10^6 \text{ T}^{-2} - 2.89 \text{ (For: 0-500}^\circ\text{C)} \quad \text{(Equation 1)}$$

Based on petrographic analysis, the low-magnesium calcite cements probably represent early diagenesis by freshwater. These data correspond to the isotopic data in field 1 of Figure 52. A temperature of  $25^\circ\text{C}$  is appropriate for reflecting shallow burial



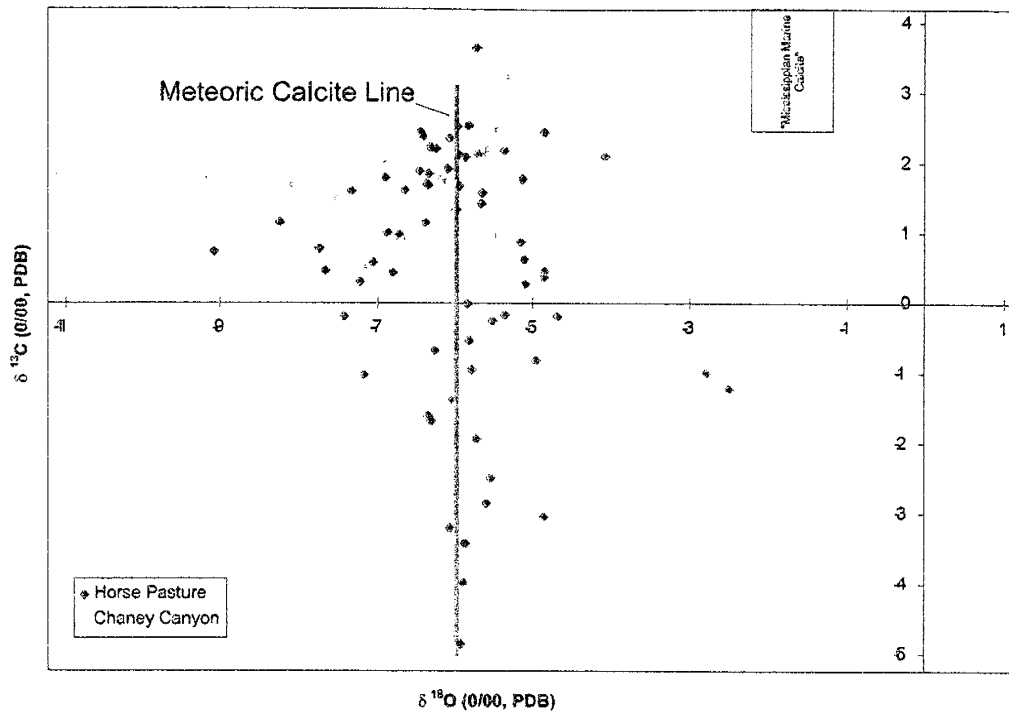


Figure 54. Isotopic distribution from the Paradise Formation with a meteoric calcite line. This line indicates the equilibrium oxygen value between calcite and water ( $\sim -6$ ‰).

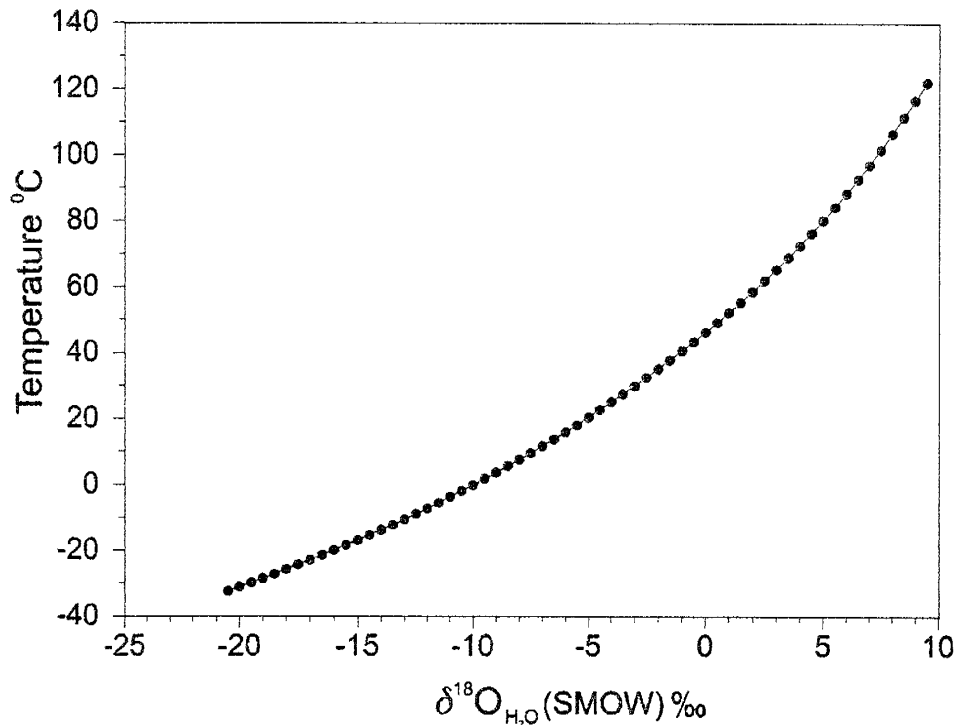


Figure 55. Temperature and  $\delta^{18}\text{O}(\text{H}_2\text{O})$  SMOW relationship for the Paradise Formation calculated using an equilibrium calcite value of  $-6$ ‰PDB and the fractionation equation for calcite-water of Friedman and O'Neil, 1977.

conditions, and returns a water value of  $-4\text{‰}\delta^{18}\text{O}(\text{H}_2\text{O})$  SMOW. This isotopic composition is consistent with waters found in low latitudes (Welhan, 1989) and is compatible with paleogeographic reconstructions placing the Pedregosa basin at low latitudes during Paradise time (Figure 30, Page 73). Using a temperature of  $40^\circ\text{C}$  as a minimum temperature during the precipitation of the ferroan calcite cements during burial diagenesis, results in a water composition of  $-1\text{‰}\delta^{18}\text{O}(\text{H}_2\text{O})$  SMOW. A value of  $-1\text{‰}\delta^{18}\text{O}(\text{H}_2\text{O})$  SMOW is compatible with a burial diagenetic setting. Waters of this composition may reflect seawater that has been modified with small amounts of meteoric water, or basinal waters that have evolved from a dominantly meteoric source, having become enriched in a burial setting. Waters produced in either manner are compatible with alteration in a burial diagenetic setting (Scholle and Halley, 1985; Longstaffe, 1989).

These water values may actually represent minimums, because the data are from whole-rock analysis and there is the possibility that not all of the carbonate components had equilibrated with the water. However, they may be very close to approaching actual oxygen value for the waters. This is because there are isotopic data plotted in Fields 1 and 2 (Figure 51) from calcite cemented siltstones and sandstones, and in these samples the carbonate material is from both the ferroan spar and low-magnesium spar cements precipitated in isotopic equilibrium with the diagenetic waters. This precludes any potential contamination by carbonate grains that may not have reach isotopic equilibrium with the altering water.

### Carbonate Component Isotopic Data

Several workers have suggested that certain individual skeletal grains (i.e., brachiopods) are more likely to retain their original isotopic compositions over time due to their original low-magnesium calcite mineralogy (Lowenstam, 1961; Brand and Veizer, 1981; Popp et al., 1988; Adlis et al., 1988). The initial reasoning behind evaluating whole-rock data from the Paradise Formation was to establish a framework for evaluating the degree of isotopic alteration relative to rock type and stratigraphic position in order to determine regions of interest for further sampling using individual carbonate components. The component samples might also be useful for examining cyclicity in the Paradise, as isotopic compositions change with respect to position within a cycle reflecting subsequent episodes of diagenesis and isotopic alteration related to changes in relative sea level. Test samples were selected based upon the degree of alteration indicated by the whole rock data, and on minimal alteration as demonstrated by optical and cathodoluminescent petrography. Typically, carbonate grains that are non-luminescent reflect no, or minimal diagenetic alteration, whereas the greater the luminescence, the greater degree of diagenetic alteration (Popp et al., 1986). There are, however, instances of recent biotic calcite being luminescent (Barbin et al., 1991). This could result in erroneous results when using the luminescent properties of fossils as an indication to the degree of their diagenetic alteration. The biota examined by Barbin et al. (1991) includes foraminifera, mollusks, and algae, and as indicated by Barbin et al. little is known about the trace element composition of fossil examples of these groups. The biotic groups studied by Barbin et al. (1991) do not include fossils typically used in isotopic studies of ancient rocks, such as fabric-retentive brachiopods (Popp et al., 1986)

which do appear to be originally composed of non-luminescent carbonate. Although Rush and Chafetz (1990) suggest that not all non-luminescent brachiopods represent pristine carbonate material, of the components selected, the fabric-retentive non-luminescent brachiopods are the most likely candidates for retaining their original isotopic composition (Popp et. al., 1986).

Based upon their petrographic and luminescent characteristics brachiopods and ooids were plotted with the whole-rock data (Figure 56). The distribution of these data with respect to carbonate in equilibrium with Mississippian seawater suggests that these components were altered in a similar manner as matrix materials. The distribution of individual grain data with respect to their parent sample supports this contention (Figure 57). This indicates that isotopic alteration was pervasive, and little information can be gained from the sampling of individual carbonate components in the Paradise Formation. Since the non-luminescent brachiopods should have been the best candidates for retaining original isotopic composition (Popp et al., 1986) they should plot very near or within the field representing carbonates precipitated in isotopic equilibrium with Mississippian sea water. Data from these brachiopods should also plot within the range of other pristine Mississippian brachiopods. The distribution of brachiopod data compiled from the literature is compared with brachiopod data from this study and is presented in Figure 58. Isotopic samples from brachiopods in this study plot within the range of the published brachiopod isotopic data. None of the brachiopods from this study appear to represent presumed original Mississippian isotopic values, yet petrographically they appear reasonably pristine, supporting the contention of Rush and Chavetz (1990) that not all fabric retentive, non-luminescent brachiopods are pristine. The likely cause

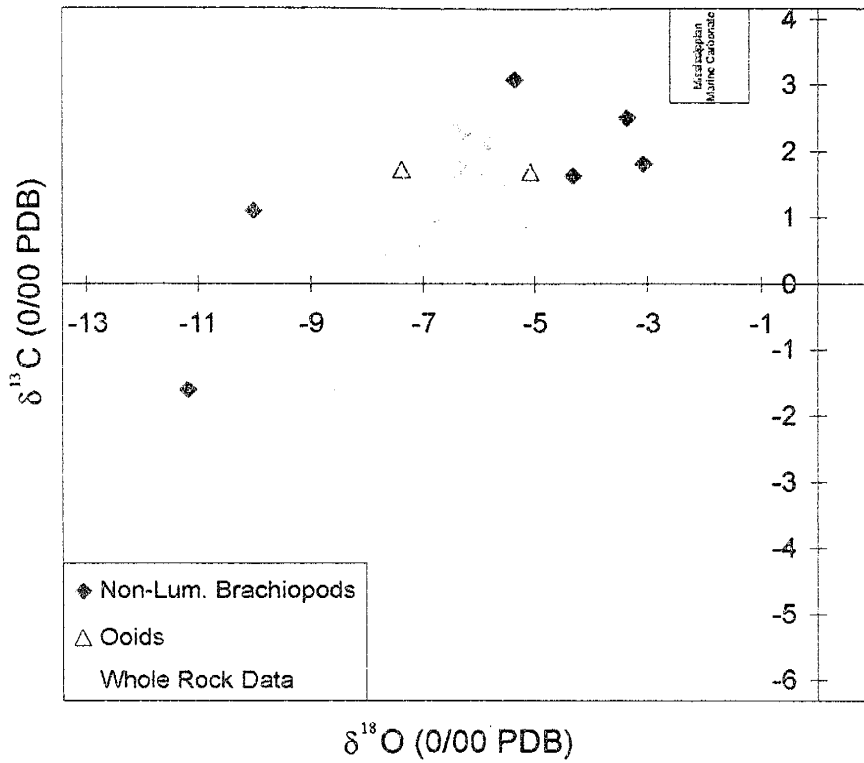


Figure 56. Distribution of carbonate components with respect to whole rock data.

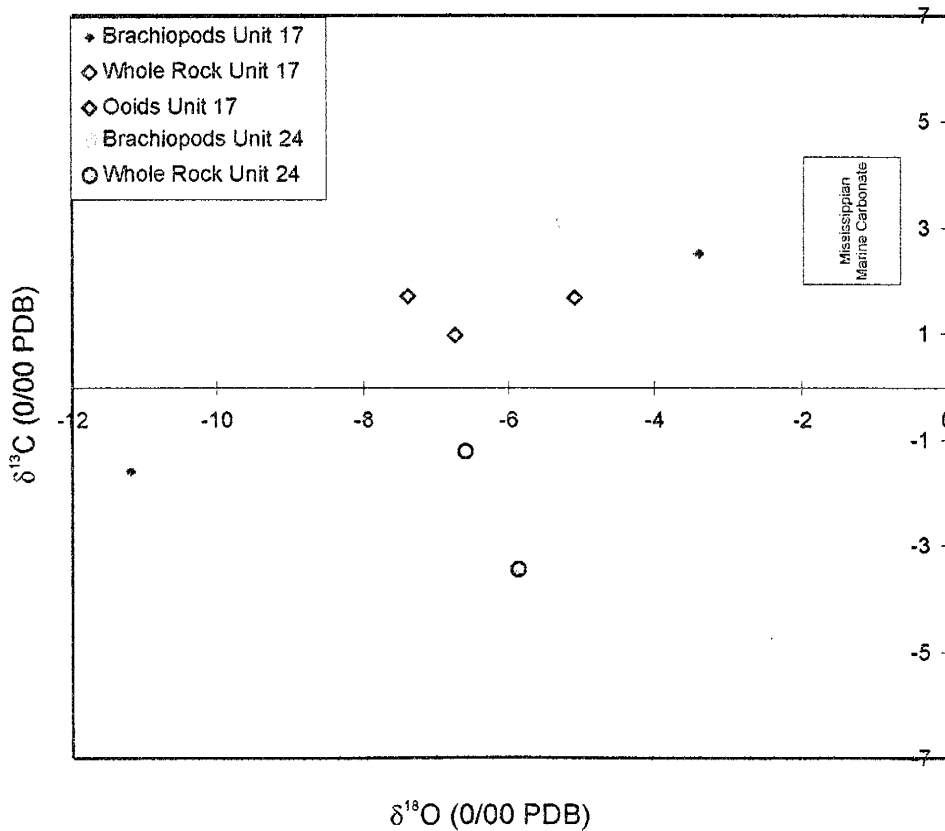


Figure 57. Distribution of carbonate components and their respective host sample. In all instances the components are altered to some degree from the host material.

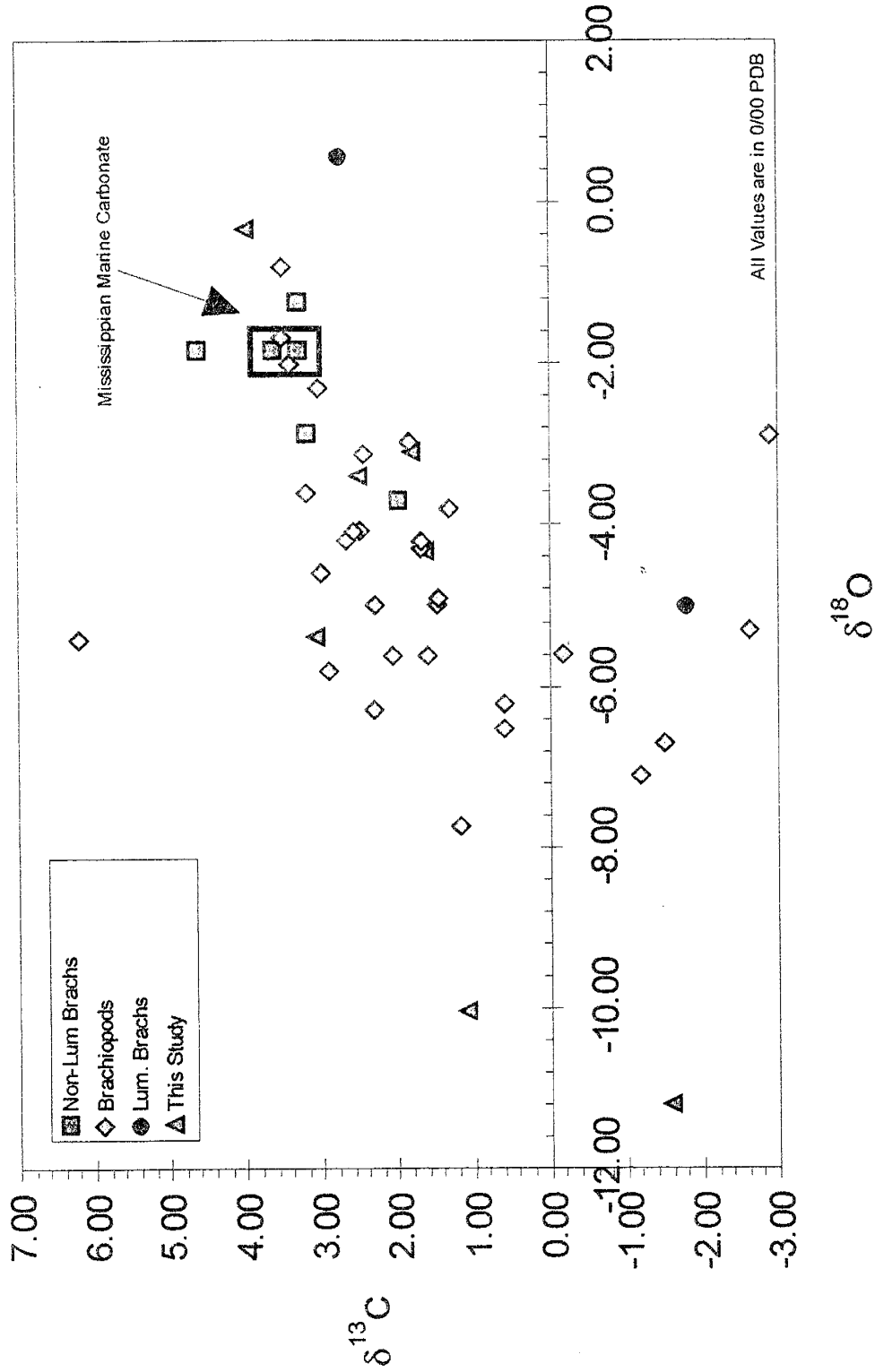


Figure 58. Plot showing the distribution of Mississippian brachiopods from published sources as compared to those analyzed from the Paradise Formation. (Published data from: Popp et al., 1986; Veizer et al., 1986; Dickinson and Coleman, 1980)

of this is degradation of shell margins and abundant microfractures present in the brachiopods (Figure 59). These fracture systems may have allowed diagenetic waters traveling through the brachiopod shell to isotopically alter the surrounding shell material and fill the fractures with isotopically lighter sparry calcite cement.

Low-magnesium calcite radial-fabric ooids are believed to be precipitated from seawater and be in isotopic equilibrium with that water (Sandberg, 1983; Wilkinson, 1985). Under standard petrography, the ooids from the Paradise Formation have what appear to be pristine internal structures. As described in the diagenesis section, under cathodoluminescence ooids from the Paradise Formation are brightly to dully-

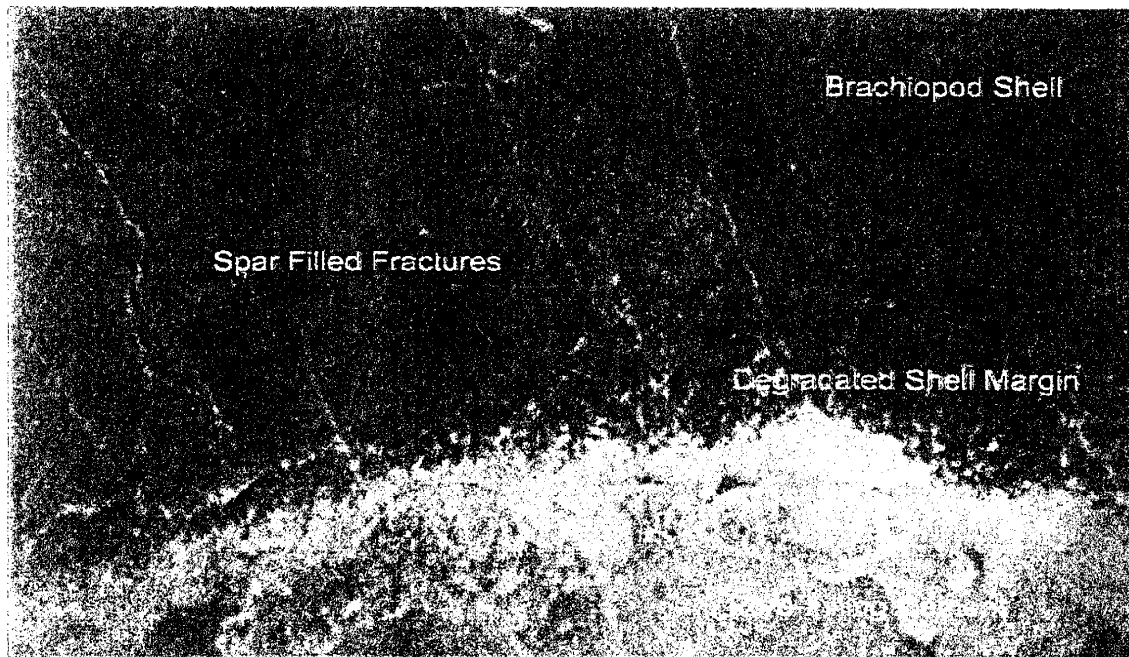


Figure 59. Photomicrograph taken under cathodoluminescence of a brachiopod shell showing the degree of fracturing and shell degradation assumed as the cause of isotope exchange between diagenetic fluids and brachiopods. (View in photo approximately 1 mm.)

luminescent suggesting possible diagenetic alteration. By evaluating the isotopic composition of the most pristine looking ooids, it may be possible to assess original isotopic values for Mississippian seawater. The isotopic values from the ooids plot away from postulated Mississippian equilibrium carbonate values, and fall within the rest of the data set indicating isotopic alteration. This adds support to the idea that the ooids in the Paradise were originally precipitated as high-magnesium calcite. If the ooids were originally low-magnesium calcite they would be less luminescent, similar to the brachiopods (See Page 96). Preservation of the ooid's internal fabric could be maintained in a similar manner as it is in echinoderms through calcitization slow enough to preserve the structural fabric (Bathurst, 1975). This process would allow the ooids to maintain their structural integrity, yet alter isotopically.

Isotopic data obtained from calcite cements is also useful in evaluating diagenetic fluids (Meyers, 1978; Lohmann, 1988). As a result of post-depositional compaction intergranular pore spaces in the Paradise Formation are extremely small. Typically, the maximum dimension is on the order of 0.06 mm, and average 18% of the total bulk volume in grainstones. Subsequent filling of these pores by sparry calcite resulted in relatively small volumes of cement. This combination of small pores and volumes of cement make it difficult to sample the cements without inadvertently sampling the surrounding material. Sampling one of the two recognizable pore-filling cements in order to make a comparison between different layers of cements is impossible. Nonetheless, an attempt was made to sample some cement material. Due to the small sample size, the standard deviation of these data are significantly greater (2.0 and greater permil), than the acceptable standard deviation of 0.05‰, making it difficult to interpret



these data due to the high degree of uncertainty associated with these data. Isotopically, these cements are extremely light ( $-15\text{‰}$   $\delta^{18}\text{O}$  and  $-5\text{‰}$   $\delta^{13}\text{C}$  PDB) compared to all the other isotope data from this study. They are also isotopically light when compared with what can be considered isotopic composition of calcite cements from detrital clastics, that average  $-6\text{‰}$   $\delta^{18}\text{O}$  PDB.

### **Stable Isotopes and Diagenesis: Synthesis**

It is clear from the petrographic data that the Paradise Formation has undergone a minimum of two pervasive diagenetic events. The first of these is related to the precipitation of low-magnesium calcite cements, while the second is related to the precipitation of ferroan calcite cements. Petrographic evidence suggests that the low-magnesium calcite cements are likely early diagenetic and the ferroan calcite cements are later burial cements. Isotopic data is consistent with both of these interpretations. Evidence supporting the pervasive nature of diagenesis and isotopic alteration includes the alteration not only of matrix material, but also of all carbonate components, including brachiopods. The exact timing and nature of these events is still unclear. What can be said is that isotopic data from the lower part of the Paradise not only is compatible with the early, shallow burial freshwater diagenetic interpretation of the low-magnesium calcite cements, but also with cyclicity. The repeating, stacked pattern of lighter to heavier carbon in the lower section is what would be predicted by the successive changes in relative sea level and subsequent diagenesis by freshwater lenses. Each lens may not directly correspond to an individual cycle, but instead may reflect the magnitude of sea-level change and the distribution of aquitards in the sediments (Read and Horbury, 1993).

Lenses traveling through the sediments could be as much as 200 m thick or as thin as several meters (Read and Horbury, 1993).

The ferroan calcite cements and isotopic data match well with the diagenesis in a burial setting. The inferred depth of burial, approximately 600 m of the Paradise Formation, suggests that both the diagenetic and isotopic alteration of the Paradise was completed by the end of Pennsylvanian. By this time all of the available pore spaces were filled by cements effectively arresting further significant compaction hindering the flow of diagenetic waters through the rocks. This would stop any further diagenetic and isotopic alteration of the Paradise. The calculated isotopic composition of the waters derived from calcite in the upper part of the Paradise is compatible with basinal waters that could have evolved from either meteoric or marine sources.

Finally, since the isotopic data is compatible with isotopic alteration during either freshwater diagenesis or during burial diagenesis, they cannot be used to conclusively determine the diagenetic settings that the rocks in the Paradise Formation were subjected to.

## CONCLUSIONS AND SUMMARY

A variety of conclusions can be made which are directly related to the Paradise Formation in the Big Hatchet Mountains, and the overall Paradise. In addition to these more focused conclusions there are two findings from this study that have implications for the geologic community as a whole. The first of which is that cyclic sedimentation in the Paradise is dominantly driven by eustasy, and can be correlated on a global basis. This contributes to the geological knowledge base of what was controlling sedimentation worldwide during the Late Mississippian and provides a control point during a period of geologic time when there is a paucity of preserved rocks. The second is the contention that fabric retentive, non-luminescent brachiopods are a source for pristine carbonate material for isotopic analysis. Findings from this work indicate that pervasive diagenesis and microfractures in the brachiopod shells resulted in isotopic alteration of the brachiopods. These fractures are difficult to observe under routine inspection of the shells and could be easily missed. This has an impact on the reliability of currently published brachiopod data and supports claims of other workers who have questioned the reliability of such brachiopods.

Conclusions related directly to the Paradise Formation are:

1. The Paradise Formation reaches its maximum preserved thickness of 130 m in the Big Hatchet Mountains. The stratigraphic interval is divisible into three distinctive members based upon the changing volumes of shale and fine-grained detrital clastics. Each member of the Paradise is composed of nine distinctive lithofacies; lime mudstones, brachiopods-bryozoan wackestones, brachiopods-pelmatozoan

packstones, abraded grainstones, oolitic grainstones, dolomitic mudstones, shales, sandstones and siltstones. These lithofacies are arranged in 2 to 12 meter coarsening-upward cycles.

2. Environmental interpretations suggest that deposition of the Paradise Formation occurred on an easterly dipping carbonate ramp. Successive changes relative in sea level controlled carbonate sedimentation on the ramp. Carbonate sedimentation was mainly aggradational with minor amounts of basinward progradation. Changes in relative sea level controlled not only carbonate sedimentation, but also controlled the distribution of coarse-grained detrital clastics through the process of cyclic and reciprocal sedimentation. This resulted in the capping of carbonate cycles by siltstones or sandstones.
3. Using the lateral and vertical distribution of facies the best fitting modern analog for the Paradise Formation is the Persian Gulf carbonate depositional system. Paleogeographic interpretations of the Paradise are also similar to the modern Persian Gulf adding support for using it as an analog for the Paradise.
4. Several orders of cyclicity are present in the Paradise Formation and are arranged in a reasonable hierarchy; the entire formation represents a 2<sup>nd</sup> order cycle, each member is a 3<sup>rd</sup> order cycle, and is comparable to similar scale cycles described in the Black Warrior basin and in England. The smallest scale cycles are 4<sup>th</sup>/5<sup>th</sup> order. Mechanisms responsible for these various orders of cyclicity are large-scale tectonics, regional and local tectonism related to the Ouachita Orogeny, and glacial eustasy.

5. The calculated average duration of 500 k.y. for the 4<sup>th</sup>/5<sup>th</sup> order cycles is comparable to the estimated duration of coeval cycles described elsewhere in North America and in England.
6. Two distinctive episodes of sparry calcite cementation are recognized in the Paradise Formation: a low-magnesium calcite spar cementation, and a ferroan calcite spar cementation. These cements form isopachous rims, equant blocky spar, poikilotopic spar, and syntaxial overgrowths. Cross cutting relationships between cements indicate that the low-magnesium sparry calcite cement was precipitated first, followed by the ferroan sparry calcite cements. There is a unique stratigraphic relationship between these cements. The low-magnesium calcite spar cements are restricted to the lower part of the Paradise, while the ferroan spar cements are found throughout the entire stratigraphic section. Intergranular volume data suggest that there was at least a 24% reduction in intergranular volume due to compaction. Using these data a depth of burial on the order of 600 m is estimated before compaction was arrested by cementation.
7. The luminescent nature of radial fibrous ooids suggests they may have been precipitated as high-magnesium calcite rather than low-magnesium calcite. This interpretation is supported by the limited stable isotope data from the ooids.
8. Dolomitization and silicification were extremely rare diagenetic processes in the Paradise Formation.
9. The extensive nature of sparry calcite cementation combined with compaction effectively reduced all porosity and permeability to near zero.

10. Stable isotope geochemistry of the Paradise Formation corroborates the pervasive nature of diagenesis, affecting isotopic compositions not only of matrix material, but also to a lesser degree the carbonate components, effectively altering all original isotopic values.
11. The repetitive isotopic patterns suggest that the low-magnesium calcite spar cements were precipitated as several separate diagenetic episodes rather than a single diagenetic episode. These episodes were likely related to relative lowstands in sea level and the creation of freshwater lenses from exposed highlands. This interpretation is consistent with isotopic data suggesting that waters with compositions of  $-4 \delta^{18}\text{O}\text{‰}(\text{H}_2\text{O})$  (SMOW) isotopically altered the rocks and precipitated these cements. The  $\delta^{18}\text{O}$  values from isotopic analysis and the petrographic character of the ferroan calcite spar cements suggest that they are burial cements. Burial was on the order of 600 m with temperatures at least as high as  $40^\circ\text{C}$ . Based on these data the isotopic composition of water during late diagenesis is  $-1 \delta^{18}\text{O}\text{‰}(\text{H}_2\text{O})$  (SMOW). Because isotopic data supports both interpretations it can not be used as definitive tool in this study in refining diagenetic settings.
12. Quartz cementation requires a minimum temperature of  $80^\circ\text{C}$ , suggesting burial to a depth of 2 km. A depth of 2 km corresponds to the thickness of the preserved Late Paleozoic strata in the Pedregosa basin suggesting that all cementation was completed by the end of the Permian.

In summary the Paradise Formation represents a shallow water carbonate dominated depositional system that developed on a gently dipping ramp in the incipient Pedregosa basin. Carbonate and detrital clastic sedimentation on this ramp was driven by

changes in relative sea level, which created a series of stacked, genetically related depositional packages. Changes in relative sea level were controlled by a combination of local and regional tectonism related to the early Ouachita Orogeny, and eustatic changes governed by glaciation. These changes in relative sea level resulted in the development of 30 meter-scale cycles in the Paradise. This number of cycles closely matches the number of cycles reported from other locations in North America and in Britain. The coincidence in the numbers of cycles supports a largely eustatic component for changes in relative sea level during the Late Mississippian.

Following the deposition of the Paradise Formation pervasive freshwater and burial diagenesis acted on the sediments and essentially occluded all porosity and permeability in the Paradise rendering the formation unusable as a reservoir for any type of fluid. This pervasive diagenesis also resulted in the isotopic alteration of not only carbonate matrix material, but also all carbonate grains including stable, low-magnesium calcite grains such as brachiopods.

## REFERENCES CITED

- Adlis, D.S, Grossman, E.L., Yancey, T.E., and McLerran, R.D., 1988, Isotope stratigraphy and paleodepth changes of Pennsylvanian cyclic sedimentary deposits: *Paleos*, v. 3, p. 487-506.
- Ahr, W.M., 1973, The carbonate ramp: an alternative to the shelf model: *Gulf Coast Association Geological Society Transactions.*, v. 23, p. 221-225.
- Alderman, R.A., 1959, Aspects of carbonate sedimentation: *Geological Society of Australia Journal*, v. 6, p.1-10.
- Algeo, T.J., Wilson, J.L., and Lohmann, K.C., 1991, Eustatic and tectonic controls on cyclic sediment accumulation patterns in lower-middle Pennsylvanian strata of the Orogrande basin, New Mexico, *in* Barker, J.M., Kues, B.S., Austin, G.A., and Lucas, S.J., eds., *New Mexico Geological Society Guide Book, 42<sup>nd</sup> Field Conference, Sierra Blanca, Sacramento, Capitan Ranges: New Mexico Geological Society*, p. 203-212.
- Allen, J.R.L., 1984, *Developments in sedimentology 30, sedimentary structures their character and physical basis volume 1: Amsterdam, Elsevier*, 593 p.
- Allan, J. R.; Matthews, R. K., 1977, Carbon and oxygen isotopes as diagenetic and stratigraphic tools; surface and subsurface data, Barbados, West Indies: *Geology*, v.5, p.16-20.
- \_\_\_\_\_, 1982, Isotopic signatures associated with early meteoric diagenesis: *Sedimentology*, v. 29, p. 797-817.
- Armstrong, A.K., 1962, Stratigraphy and paleontology of the Mississippian System in southwestern New Mexico and adjacent southeastern Arizona: *New Mexico Bureau of Mines and Mineral Resources Memoir 8: New Mexico Bureau of Mines and Mineral Resources*, 85 p.
- Armstrong, A.K. and Mamet, B.L., 1978, The Mississippian System of southwestern New Mexico and southeastern Arizona, *in* Callendera, F.J., J.F. Wilt, and Clemons, R.E. eds, *Land of Cochise: Southeastern Arizona: New Mexico Geological Society Field Conference, 29th, Guidebook: New Mexico Geological Society*, p. 183-192.
- \_\_\_\_\_, and Mamet, B.L., 1988, Mississippian (Lower Carboniferous) biostratigraphy, facies, and microfossils, Pedregosa basin, southeastern Arizona and southwestern New Mexico: *U.S. Geological Survey Bulletin 1826*, 40 p.



- Armstrong, A.K., Mamet B.L., and Repenski, J.E., 1980, Mississippian System of New Mexico and southern Arizona, *in* Fouch, T.D., and Magathan, E.R., eds., Paleozoic Paleogeography of the west-central United States: Rocky Mountain Paleogeography Symposium 1: Denver, Society of Economic Paleontologists and Mineralogists, Rocky Mountain Section, p. 82-99.
- Armstrong, A.K., Kottowski, F.E., Stewart, W.J., Mamet, B.L., Blatz, E.H. Jr., Siemers, W.T., and Thompson, Sam, III, 1979, The Mississippian and Pennsylvanian Systems (Carboniferous) in the United States-New Mexico, U.S. Geological Survey Professional Paper 1110-W, p. W1-W27.
- Bahlburg, W.C., 1977, Depositional environments of the Tamaroa Sequence (Mississippian) of southeastern Arizona, southwestern New Mexico and northern Mexico: Unpublished master's thesis, Arizona State University, 214 p.
- Bates, N.R. and Brand, U., 1991, Environmental and physiological influences on isotopic and elemental compositions of brachiopod shell calcite; implications for the isotopic evolution of Paleozoic oceans: *Chemical Geology; Isotope Geoscience Section*, v.94, p.67-78.
- Bathurst, R.G.C., 1975, Carbonate sediments and their diagenesis, 2nd edition: Amsterdam, Elsevier, 658 p.
- \_\_\_\_\_, 1980, Lithification of carbonate sediments: *Science Progree*, v. 66, p. 451-471.
- Barbin, V., Ramseyer, K., Debenay, J.P., Schein, E., Roux, M., and Decrouez, D., 1991, Cathodoluminescence of Recent biogenic carbonates: An environmental and ontogenetic fingerprint: *Geological Magazine*, v. 128, p. 19-26.
- Bayless, G.S. and Schwarz, R.R., 1979, Organic geochemical analysis, outcrop samples, Cambrian-Mississippian rocks Mescal Canyon section, Big Hatchet Mountains, Sec. 28 & 29, T30S, R15W, Hidalgo County, New Mexico: New Mexico Bureau of Mines and Mineral Resources Open-File Report 312, 21 p.
- Berger, A., and Loutre, M.F., 1989, Pre-Quaternary Milankovitch frequencies: *Nature*, v. 342, p. 133
- Brand, U., 1982, The oxygen and carbon isotopic composition of Carboniferous fossil components: sea-water effects: *Sedimentology*, v. 29, p. 139-147.
- Brand, U. and Veizer, J., 1981, Chemical diagenesis of a multicomponent carbonate system; 2, Stable isotopes: *Journal of Sedimentary Petrology*, v.51, p.987-997
- Brown, M.L. 1985, Geology of Sierra de los Chinos-Cerro La Cueva area northwestern Chihuahua, Mexico: Unpublished master's thesis, University of Texas at El Paso, 163 p.

- Burchette, T.P. and Wright, V.P., 1992, Carbonate ramp depositional systems: *Sedimentary Geology*, v. 79, p. 3-57.
- Butler, W.C., 1988, The rationale for assessment of undiscovered, economically recoverable oil and gas in south-central New Mexico: A geologic overview and play analysis of two favorable areas: U.S. Geological Survey, Open-file Report 88-450-B, 134 p.
- \_\_\_\_\_, 1989, The geologic setting of southern Arizona and southwestern New Mexico, with rationale for assessment of undiscovered, economically recoverable oil and gas: A summary of four potential plays: U.S. Geological Survey, Open-file Report 88-450-M, 150 p.
- \_\_\_\_\_, 1993, Southern Arizona-southwestern New Mexico Province, *in* Powers, R.B., ed., Petroleum exploration plays and resource estimates, 1989, onshore United States — Region 3, Colorado Plateau and Basin and Range: U.S. Geological Survey Open-file Report 93-248, p 103-108.
- Calvet, F., Tucker, M.E., and Henton, J.M., 1990, Middle Triassic carbonate ramp systems in the Catalan Basin, northeast Spain: facies, systems tracts, sequences, and controls, *in* Tucker, M.E., Wilson, J.L., Crevello, P.D., Sarg, J.R., and Read, J.F., eds., Carbonate Platforms: London, International Association of Sedimentologists and Blackwell Scientific Publication, p. 79-108
- Capto, M.V. and Crowell, J.C., 1985, Migration of glacial centers across Gondwana during Paleozoic era: *Geological Society of America Bulletin*, v. 96, p.1020-1036.
- Carrol, D., 1958, Role of clay minerals in the transport of iron: *Geochemica et Cosmochemica Acta*, v. 14, p. 1-28.
- Carozzi, A.V., 1989, Carbonate Rock Depositional Models: A microfacies approach: New Jersey, Prentice Hall, 604 p.
- Cook, T. D.; Bally, A. W.; Milner, S.; Buffler, R. T.; Farmer, R. E.; and Clark, D. K., 1975, Stratigraphic atlas of North and Central America: New Jersey, Princeton University Press, 272 p.
- Craig, H., 1957, Isotopic standards for carbon and oxygen and correction factors for mass spectrometric analysis of carbon dioxide: *Geochimica Cosmochimica Acta*, v. 12, p. 133-149.
- Crowell, J.C., 1978, Gondwanan glaciation, cyclothems, continental positioning, and climate change: *American Journal of Science*, v. 278, p. 1345-1372.
- Devery, J.V., 1979, Sedimentary petrology of the upper Paleozoic carbonate near Bavispe, Sonora, Mexico: Unpublished master's thesis, TCU, 79 p.

- Dickerson, P.W., 1987, Structural and depositional setting of southwestern U.S. and northern Mexico and a Paleozoic transform plate margin: Paleozoico de Chihuahua: Universidad Autonoma de Chihuahua, Sociedad Geologica Mexicana A.C., v. 1, p. 129-159.
- Dickson, J.A.D., 1966, Carbonate identification and genesis as revealed by staining, *Journal of Sedimentary Petrology*, v. 36, n. 2, p. 491-505.
- Dickson, J. A. D.; Smalley, P. C.; Kirkland, B. L., 1991, Carbon and oxygen isotopes in Pennsylvanian biogenic and abiogenic aragonite (Otero County, New Mexico); a laser microprobe study: *Geochimica et Cosmochimica Acta*, v.55, n.9, p.2607-2613.
- Drewes, H., 1991, Geologic map of the Big Hatchet Mountains, Hidalgo County, New Mexico: U.S. Geological Survey Map I-2144, 1:24,000.
- Dunham, R.J., 1962, Classification of carbonate rocks according to depositional texture, *in* Ham W.E., ed., *Classification of carbonate rocks: AAPG Memoir 1*, p. 108-121.
- Ekdale, A.A., 1985, Paleoecology of the marine endobenthos: *Paleogeography, Paleoclimatology, Paleoecology*, v. 23, p. 63-81.
- Ekdale, A.A., 1988, Pitfalls of paleobathymetric interpretations based on trace fossil assemblages: *Palaios*, v. 3, p. 464-472.
- Enos, P., 1983, Shelf environment, *in* P.A. Scholle, Bebout, D.G., and C.H. Moore, eds., *Carbonate depositional environments: AAPG Memoir 33*, p. 268-295.
- Fischer, A.G and Sarnthein, 1988, Airborne silts and dune-derived sands in the Permian of the Delaware Basin: *Journal of Sedimentary Petrology*, v. 58 no. 4, p 637-643.
- Flügel, E., 1982, *Microfacies analysis of limestones*: Berlin, Springer-Verlag, 633 p.
- Folk, R.L., 1962, Spectral subdivision of limestone types, *in* Ham W.E., ed., *Classification of carbonate rocks: AAPG Memoir 1*, p. 62-84.
- Folk, R.L., 1965, Some aspects of recrystallization in ancient limestones, *in* Pray, L..C., and Murry R.C., eds., *Dolomitization and limestone diagenesis: SEPM Special Publication 13*, p.13-48.
- \_\_\_\_\_, 1980, *Petrology of sedimentary rocks*: Austin, Hemphill, 182 p.
- Folk, R.L. and Land, L.S., 1975, Mg/Ca ratio and salinity: Two controls over crystallization of dolomite: *AAPG Bulletin*, v. 59, p. 60-68.

- Friedmann, I., and O'Neil, J.R., 1977, Compilation of stable isotope fractionation factors of geochemical interest, *in* Fleischer, M., ed., *Data of Geochemistry*, 6<sup>th</sup> ed.: USGS Professional Paper 440-KK, 12 p.
- Frenzel, H.N., Bloomer, R.R., Cline, R.B., Cys, J.M., Galley, J.E., Gibson, W.R., Hills, J.M., King, W.E., Seager, W.R., Kottowski, F.E., Thompson, Sam, III, Luff, G.C., Pearson, B.T., and Van Siclen, D.C., 1988, *in* Sloss, L.L., ed., *The Permian Basin region; Sedimentary Cover-North American Craton*; U.S.: Geological Society of America, Boulder, Colorado, p. 261-306.
- Fuchtbauer, F., 1983, Facies controls on sandstone diagenesis, *in* Parker, A., and Sellwood, B.W., eds., *Sediment diagenesis: NATO Advanced Study Institute Series C115*, Dordrecht, Reidel, p. 269-288.
- Gall, J. -C., 1983, Ancient sedimentary environments and the habitats of living organisms: Berlin, Springer-Verlag, 219 p.
- Ginsberg, 1957, Early diagenesis and lithification of shallow-water carbonate sediments in south Florida, *in* Leblanc, R.J. and Breeding, J.R. eds., *Regional aspects of carbonate deposition: Society of Economic Paleontologists and Mineralogists Special Publication No. 5*, p. 80-100.
- Goodwin, P.W. and Anderson, E.J., Punctuated aggradational cycles: A general hypothesis of episodic stratigraphic accumulation: *The Journal of Geology*, v. 93, p. 515-533.
- Greenwood, E.; Kottowski, F. E.; Thompson, S., III, 1977, Petroleum potential and stratigraphy of Pedregosa basin; comparison with Permian and Orogrande basins: *AAPG Bulletin*, v.61, p.1448-1469.
- Handschy, J.W, Keller, G.R, and Smith, K.J., 1987, The Ouachita system in Northern Mexico: *Tectonics*, v. 6, p. 323-330.
- Hardie, L.A., 1987, Perspectives dolomitization: A critical view of some current views: *Journal of Sedimentary Petrology*, v. 57, p. 166-183.
- Harris, P.M., Kendall, C.G.St. C., and Lerche, I., 1985, Carbonate cementation-a brief review, *in* Scheidemann, N and Harris, P.M. eds., *Carbonate cements: SEPM Special Publication No. 36*, p. 79-95.
- Harris, P.M, 1995, Heterogeneity within carbonate reservoirs guidelines from modern analogs, *in* Pause, P.H. and M.P. Candelaria, eds., *Carbonate facies and sequence stratigraphy: Practical applications of carbonate models*, PBS-SEPM Publication 95-36, p. 103-119.

- Heckle, P.H., 1972, Recognition of ancient shallow marine environments *in* Recognition of ancient sedimentary environments: Rigby, J.K. and W.M. Hamblin eds., Society of Economic Paleontologists and Mineralogists Special Publication No. 16, p. 226-286.
- \_\_\_\_\_, 1983, Diagenetic model for carbonate rocks in midcontinent Pennsylvanian ecstatic cyclothems: *Journal of Sedimentary Petrology*, v. 53, p. 733-759.
- Holcomb, R.A., 1979, Conodont biostratigraphy of Paleozoic carbonates near Bavispe, Sonora, Mexico: Unpublished master's thesis, TCU, 99 p.
- Imbrie, J., and Imbrie, K.P., 1979, *Ice ages: Solving the mystery*: New York, McMillian, 224 p.
- Imlay, R., 1939, Paleogeographic studies in northeastern Sonora: *Geological Society of America Bulletin*, v. 50, p. 1722-1744.
- Irwin, M.L., 1965, General theory of epeiric clear water sedimentation: *AAPG Bulletin*, v. 49, no. 4, p. 445-459.
- Keith, M. L.; Weber, J. N., 1964, Carbon and oxygen isotopic composition of selected limestones and fossils: *Geochemica et Cosmochemica Acta*, v. 28, p. 1787-1816.
- Kendall, G.G.St.C., Rees, G., Shearman, D.J., Skipworth, P.A. D'E., Twyman, J., and Karimi, M.Z., 1966, On the mechanical role of organic matter in the diagenesis of limestones: *Geologist's Association of England, Circular 681*, p. 1-2.
- Kluth, C.F. and Coney, P.J., 1981, Plate tectonics of the Ancestral Rocky Mountains: *Geology*, v. 9, p. 10-15
- Kottlowski, F.E., 1958, Pennsylvanian and Permian rocks near the Late Paleozoic Florida Islands, in the Hatchet Mountains and the Cooks Range-Florida Mountains area: *Roswell Geological Society, 11th Field Conf. Guidebook*, p. 79-87.
- \_\_\_\_\_, 1959, Real wildcat country-Pennsylvanian of SW New Mexico: *Oil and Gas Journal*, v. 57, p. 148-151.
- \_\_\_\_\_, 1963, Paleozoic and Mesozoic strata of southwestern and south-central New Mexico: *New Mexico Bureau of Mines and Mineral Resources Bulletin 79*: New Mexico Bureaus of Mines and Mineral Resources, 100 p.
- \_\_\_\_\_, 1965, Sedimentary basins of south-central and southwestern New Mexico: *AAPG Bulletin*, v. 49, p. 2120-2139.
- \_\_\_\_\_, 1969, Summary of Late Paleozoic in El Paso Border Region, *in* Kottlowski F.E and LeMone, D.V., eds., *Border stratigraphy symposium*, New Mexico Bureau of Mines and Mineral Resources Circular 104, p. 38-51.

- Krinsley, D, and Trusty, P., 1985, Environmental interpretation of quartz grain surface textures, *in* Zuffa, G.G. ed., Provenance of arenites: Amsterdam, Reidel, p-213-229.
- Land, L.S., 1980, The isotopic and trace element geochemistry of dolomite: The state of the art, *in* Zenger, D.H, Dunham, J.B., and Ethington R.L. eds., Concepts and models of dolomitization: SEPM Special Publication No. 28, p. 87-110.
- Land, L.S., Behrens, E.W., and Frishman, S.A., 1979, The ooids of Baffin Bay, Texas: *Journal of Sedimentary Petrology*, v. 49, p. 1269-1278.
- Laporte, L., 1968, Recent carbonate environments and their paleoecologic implications, *in* Drake, T.E., ed., Evolution and environment, p. 229-258.
- Lees, A., 1975, Possible influence of salinity and temperature on modern shelf carbonate sedimentation: *Marine Geology*, v. 19, p. 159-198.
- Lisbee, A.L., Woodward, L.A., and Connolly, J.R., 1979, Tijeras-Canoncito fault system-A major zone of recurrent movement in north-central New Mexico, *in* New Mexico Geological Society Guidebook, 30<sup>th</sup> Conference, Santa Fe County: New Mexico Geological Society, p. 89-99.
- Lohmann, K.C., 1988, Geochemical patterns of meteoric diagenetic systems and their application to studies of paleokarst, *in* James, N.P. and Choquette, P.W. eds., Paleokarst: Berlin, Springer-Verlag, p. 58-80.
- Longman, M.W., 1980, Carbonate diagenetic textures from near surface diagenetic environments: *AAPG Bulletin*, v. 64, p. 461-487.
- Longstaffe, F.J., 1989, Stable isotopes as traces in clastic diagenesis, *in* Hutcheon, I.E. ed., Short course in burial diagenesis: Mineralogical Association of Canada, p. 201-277.
- Lowenstam, H.A., 1961, Mineralogy, O<sup>18/16</sup> ratios, and strontium and magnesium contents of Recent and fossil brachiopods and their bearing on the history of the oceans: *Journal of Geology*, v. 69, p. 241-260.
- Madden, H. D., 1984, Stratigraphy and microfacies analysis of the Mississippian System North Franklin Mountains, Dona Anna County, south-central New Mexico: Unpublished master's thesis, University of Texas at El Paso, 266 p.
- Magaritz, M.; Turner, P., 1982, Carbon cycle changes of the Zechstein Sea; isotopic transition zone in the Marl Slate: *Nature*, v. 297, p. 389-390.
- Maliva, R.G. Siever, R., 1988, Mechanism and controls of silicification of fossils in limestones: *Journal of Geology*, v. 96, p. 387-398.

- Marhsall, J.F. and Davies, P.J., 1975, High-magnesium calcite ooids from the great barrier reef: *Journal of Sedimentary Petrology*, v. 45, p. 285-291.
- McCrea, J.M., 1950, The isotopic composition of carbonates and a paleotemperature scale: *Journal of Chemistry and Physics of Minerals*, v. 18, p. 849-857.
- Meyers, W.J., 1978, Stable isotopes of cherts and carbonate cements in the Lake Valley Formation (Mississippian), Sacramento Mts., New Mexico: *Sedimentology*, v. 25, p. 105-124.
- \_\_\_\_\_, 1980, Compaction in Mississippian skeletal limestones southwestern New Mexico: *Journal of Sedimentary Petrology*, v. 50, p. 457-474.
- Meyers W.J., and Hill, B.E., 1983, Quantitative studies of compaction in Mississippian skeletal limestones, New Mexico: *Journal of Sedimentary Petrology*, v. 53, p. 231-242.
- Meyers, W.J. and Lohmann, K.C., 1985, Isotope geochemistry of regionally extensive calcite cement zones and marine components in Mississippian limestones, New Mexico, *in* Schneidermann, N. and Harris, P.M., eds., *Carbonate cements: SEPM Special Publication 36*, p. 233-240.
- Miall, A.D., 1990, *Principles of sedimentary basin analysis*: Berlin, Springer-Verlag, 668 p.
- Moore, C.M., 1989, *Carbonate diagenesis and porosity*: Amsterdam, Elsevier, 338 p.
- Morrow, D.W., 1982a, Diagenesis 1 Dolomite-part 1: The chemistry of dolomitization and dolomite precipitation: *Geoscience Canada*, v. 9, p. 5-13.
- Morrow, D.W., 1982b, Diagenesis 2. Dolomite-part 2: Dolomitization models and ancient dolostones: *Geoscience Canada*, v. 9, p. 95-107.
- Morse, J.W. and Mackenzie, 1990, *Geochemistry of sedimentary carbonates*: Amsterdam, Elsevier, 707 p.
- Norby, R.D., 1971, Conodont biostratigraphy of the Mississippian rocks of southeastern Arizona: Unpublished master's thesis, Arizona State University, 195 p.
- Oelkers, E.H., Bjørum, P.A., and Murphy W.M., 1996, A petrographic and computational investigation of quartz cementation and porosity reduction in North Sea sandstones: *American Journal of Science*, v. 296, p.1-28.
- Packard, F.A., 1955, The stratigraphy of the Upper Mississippian Paradise Formation of southeastern Arizona and southwestern New Mexico: Unpublished master's thesis, University of Wisconsin, Madison, 103 p.

- Palmer, A.R., 1983, The decade of North American Geology 1983 geologic time scale: *Geology*, v. 11, p. 503-504.
- Pettyjohn, F.J., Potter, P.E., and Seiver, R., 1987, *Sand and sandstone*: New York, Springer-Verlag, 618 p.
- Popp, B.N., Anderson, T.F., and Sandberg, P.A., 1986, brachiopods as indicators of original isotopic compositions in some Paleozoic limestones: *Geological Society of America Bulletin*, v. 97, p. 1262-1269.
- Prezbindowski, D., 1980, Microsampling technique for stable isotopes in carbonates: *Journal of Sedimentary Petrology*, v. 50 p. 643-644.
- Prudy, E.G., 1962, Recent calcium carbonate facies of the great Bahama bank. 2. *Sedimentary facies: Journal of Geology*, v. 71 p. 472-497.
- Ransome, F.L., 1904, *The geology and ore deposits of the Bisbee quadrangle, Arizona*: U.S. Geological Survey Professional Paper 21
- Ramsbottom, W.H.C., 1979, Rates of transgression and regression in the Carboniferous of NW Europe: *Journal of Geological Society of London*, v. 136, p. 147-153.
- Reid, S.K. and Dorobek, S.L., 1993, Sequence stratigraphy and evolution of a progradational, foreland carbonate ramp, Lower Mississippian Mission Canyon Formation and stratigraphic equivalents, Montana and Idaho, *in* R.G. Loucks and J.F. Sarg eds., *Carbonate sequence stratigraphy recent developments and applications*, AAPG Memoir 57, p. 327-352.
- Ross, C.A., 1979, Late Paleozoic collision of North and South America: *Geology*, v. 7, p. 41-44.
- Ross, C.A. and Ross, J.P., 1987a, Late Paleozoic sea levels and depositional sequences, *in* Ross, C.A., and Haman, D., eds., *Timing and depositional history of eustatic sequences: Constraints on seismic stratigraphy*: Cushman Foundation for Foraminiferal Research, Special Publication 24, p. 137-149.
- Ross, C.A. and Ross, J.P., 1987b, Biostratigraphic zonation of Late Paleozoic depositional sequences *in* Ross, C.A., and Haman, D., eds., *Timing and depositional history of eustatic sequences: Constraints on seismic stratigraphy*: Cushman Foundation for Foraminiferal Research, Special Publication 24, p. 151-168.
- \_\_\_\_\_, 1988, Late Paleozoic transgressive-regressive deposition, *in* Wilgus, C.K., Hastings, B.S., Kendall, C.G.St.C., Posamentier, H.W., Ross, C.A., and Van Wagoner, J.C., eds., *Sea-level changes an integrated approach*, SEPM Special Publication No. 42, p. 227-247.



- Rush, P.F. and H.S. Chafetz, 1990, Fabric-retentive, non-luminescent brachiopods as indicators of original  $\delta^{13}\text{C}$  and  $\delta^{18}\text{O}$  composition: a test: *Journal of Sedimentary Petrology*, v. 60, p. 968-981.
- Sandberg, P.A., 1983, An oscillating trend in Phanerozoic non-skeletal carbonate mineralogy: *Nature*, v. 305, p. 19-22.
- Saunders, W.B., Ramsbottom, W.H.C. and W.L. Manger, 1979, Mesothemic cyclicity in the mid-Carboniferous of the Ozark shelf region: *Geology*, v. 7, p. 293-296.
- Scholle, P.A., and Halley, Robert, B, 1985, Burial Diagenesis: Out of sight, out of mind!, *in* Scheidemann, N and Harris, P.M. eds., *Carbonate cements: SEPM Special Publication No. 36*, p.309-334.
- Schwarzacher, W., 1991, Milankovitch cycles and the measurement of time, *in* Einsele, G., Ricken, W., and Seilacher, A. eds., *Cycles and events in stratigraphy*: Berlin, Springer-Verlag, p.855-863.
- Seager, W.R. and Mack, G.H., 1986, Laramide Paleotectonics of southern New Mexico, *in* J.A. Peterson ed., *Paleotectonics and sedimentation: AAPG Memoir 41*, p.669-685.
- Seilacher, A., 1967, Bathymetry of trace fossils: *Marine Geology*, v. 5, p.413-428.
- Shaw, A.B., 1964, *Time and stratigraphy*: New York, McGraw-Hill, 365 p.
- Shinn, G., 1983, Tidal flat environment, *in* Scholle, P.A., Bebout, D.G., and Moore, C.H., eds., *Carbonate depositional environments: AAPG Memoir 33*, p. 172-210.
- Sivils, D.J. and Johnson, D.B., 1993, The Late Mississippian Paradise Formation and it's Tectono-Stratigraphic Implication [abst]: *CSPG-GSGP International Symposium on Mississippian to Jurassic Pangea Basins*, p. 283.
- Soreghan, G.S., 1994, Upper Pennsylvanian facies and cyclostratigraphy in Rodes and Hembrillo canyons, San Andres Mountains, *in* Garber, R.A. and Keller, D.R., eds., *Field Guide to the Paleozoic section of the San Andres Mountains: PBS-SEPM Publication No. 94-35*, p. 71-85.
- Stoyanow, A.A., 1926, Recent stratigraphic work in Arizona, especially Upper Mississippian in southeastern Arizona: *American Journal of Science*, v. 12, p. 316-318.
- Surdam, R.C., Dunn, T.L., Heasler, H.P., and MacGowan, D.B, 1989, Porosity evolution in sandstone/shale systems *in* Hutcheon, I.E. ed., *Short Course in Burial Diagenesis: Mineralogical Association of Canada*, p. 61-134.

- Thomas, W. A., 1977, Evolution of Appalachian-Ouachita salients and recesses from reentrants and promontories in the continental margin: *American Journal of Science*, v. 277, p. 1233-1278.
- Thomas, W. A., 1983, Continental margins, orogenic belts, intracratonic structures: *Geology*, v. 11, p. 270-272.
- Thompson, S., III, and Jacka, A. D., 1981, Pennsylvanian stratigraphy, petrography, and petroleum geology of Big Hatchet Peak section, Hidalgo County, New Mexico: *New Mexico Bureau of Mines and Mineral Resources Circular 176*, 125 p.
- Veizer, J., Fritz, P., and Jones, B., 1986, Geochemistry of brachiopods: Oxygen and carbon isotopic records of Paleozoic oceans: *Geochimica et Cosmochimica Acta*, v. 50, p. 1679-1696.
- Weedon, G.P., 1991, The spectral analysis of stratigraphic time series, *in* Einsele, G., Ricken, W., and Seilacher, A. eds., *Cycles and events in stratigraphy*: Berlin, Springer-Verlag, p. 840-854.
- Welhan, J.A., 1989, Stable isotope hydrology, *in* Hutcheon, I.E. ed., *Short course in burial diagenesis*: Mineralogical Association of Canada, p. 129-161.
- Wilkening, Lee, 1984, Conodont biostratigraphy near the Mississippian\Pennsylvanian boundary in the New Well Peak section, Big Hatchet Mountains, Hidalgo County, New Mexico: Unpublished master's thesis, New Mexico Institute of Mining and Technology, 214 p.
- Wilkinson, B.W, R.M Owen, and A.R. Carroll, 1985, Submarine hydrothermal weathering, global eustasy, and carbonate polymorphism in Phanerozoic marine oolites: *Journal of Sedimentary Petrology*, v. 55, p. 171-183.
- Wilson, J.L., 1967, Cyclic and reciprocal sedimentation in Virgilian strata of southern New Mexico: *Geological Society of America Bulletin*, v.78, p. 805-818.
- \_\_\_\_\_, 1969, Microfacies and sedimentary structures in "deep water" limestone mudstones, *in* Freidman, G.F., ed., *Depositional environments in carbonate rocks*: SEPM Special Publication No. 14, p. 4-19.
- \_\_\_\_\_, 1974, Characteristics of carbonate platform margins: *AAPG Bulletin*, v.58, p. 810-824.
- \_\_\_\_\_, 1975 *Carbonate Facies in Geologic History*: New York, Spring-Verlag, 471 p.
- Wilson, J.L. and C. Jordan, 1983, Middle shelf environment, *in* Scholle, P.A., Bebout, D.G., and Moore, C.H., eds., *Carbonate depositional environments*: AAPG Memoir 33, p. 298-343.

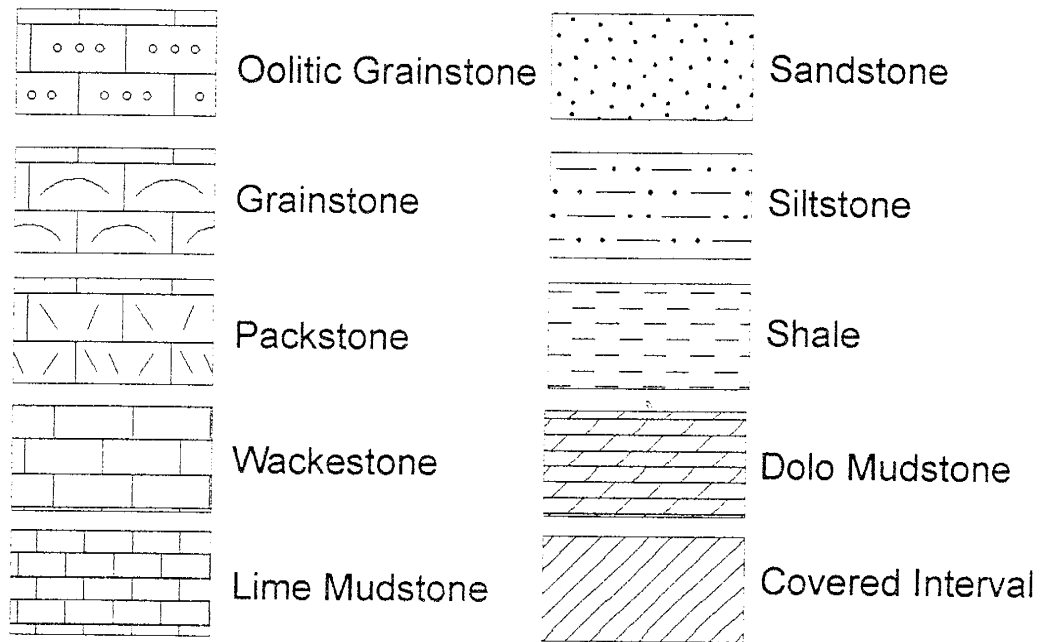
- Ye, H., Royden, L., Burchfiel, C., and Schuepbach, M., 1996, Late Paleozoic deformation of interior North America: the greater Ancestral Rocky Mountains: AAPG Bulletin, v. 80, p. 1397-1432.
- Yurewicz, D.A., 1977, Sedimentology of Mississippian basin-facies carbonates, New Mexico and west Texas-The Rancheria Formation, *in* Cook, H.E. and P. Enos eds., Deep water carbonate environments: SEPM Special Publication 25, p. 203-219.
- Zeller, R.A., Jr., 1958, The geology of the Big Hatchet Peak quadrangle, Hidalgo County, New Mexico: unpublished Ph.D. dissertation, University of California., Los Angeles, 260 p.
- Zeller, R.A., Jr., 1965, Stratigraphy of the Big Hatchet Mountains area, New Mexico, New Mexico Bureau of Mines and Mineral Resources Memoir 16: New Mexico Bureau of Mines and Mineral Resources, 128 p.
- Zeller, R.A., 1975, Structural geology of Big Hatchet Peak Quadrangle, Hidalgo County, New Mexico: New Mexico Bureau of Mines and Mineral Resources Circular 146, 23 p.

**APPENDIX A**

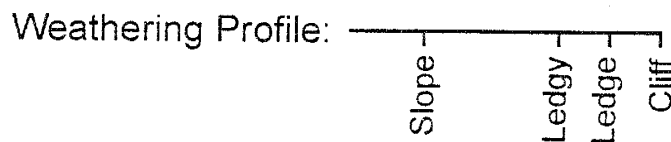
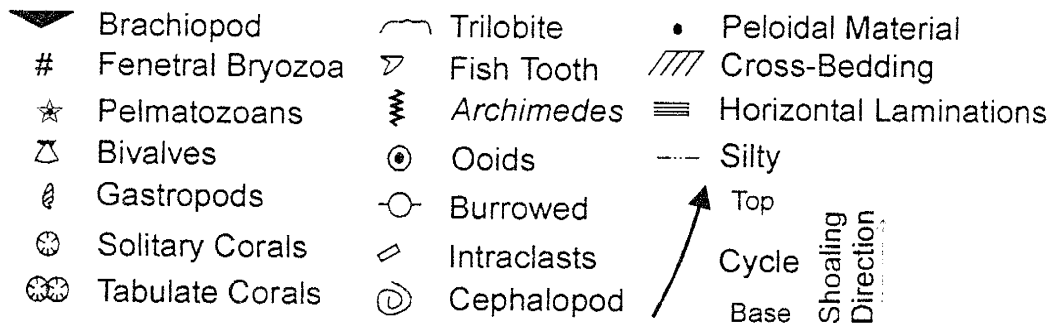
Detailed Graphic Stratigraphic Sections

# Measured Sections Legend

## Lithotypes

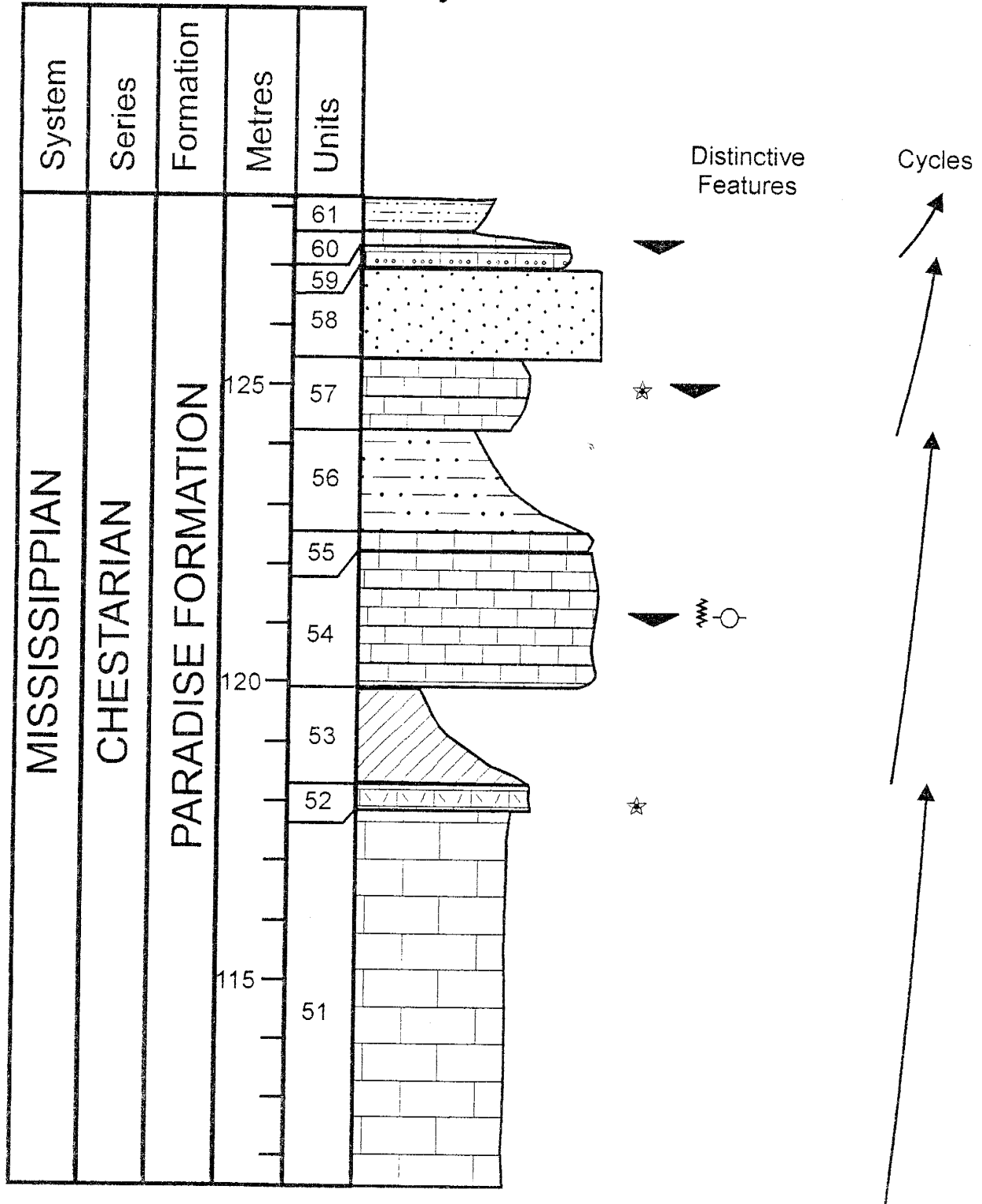


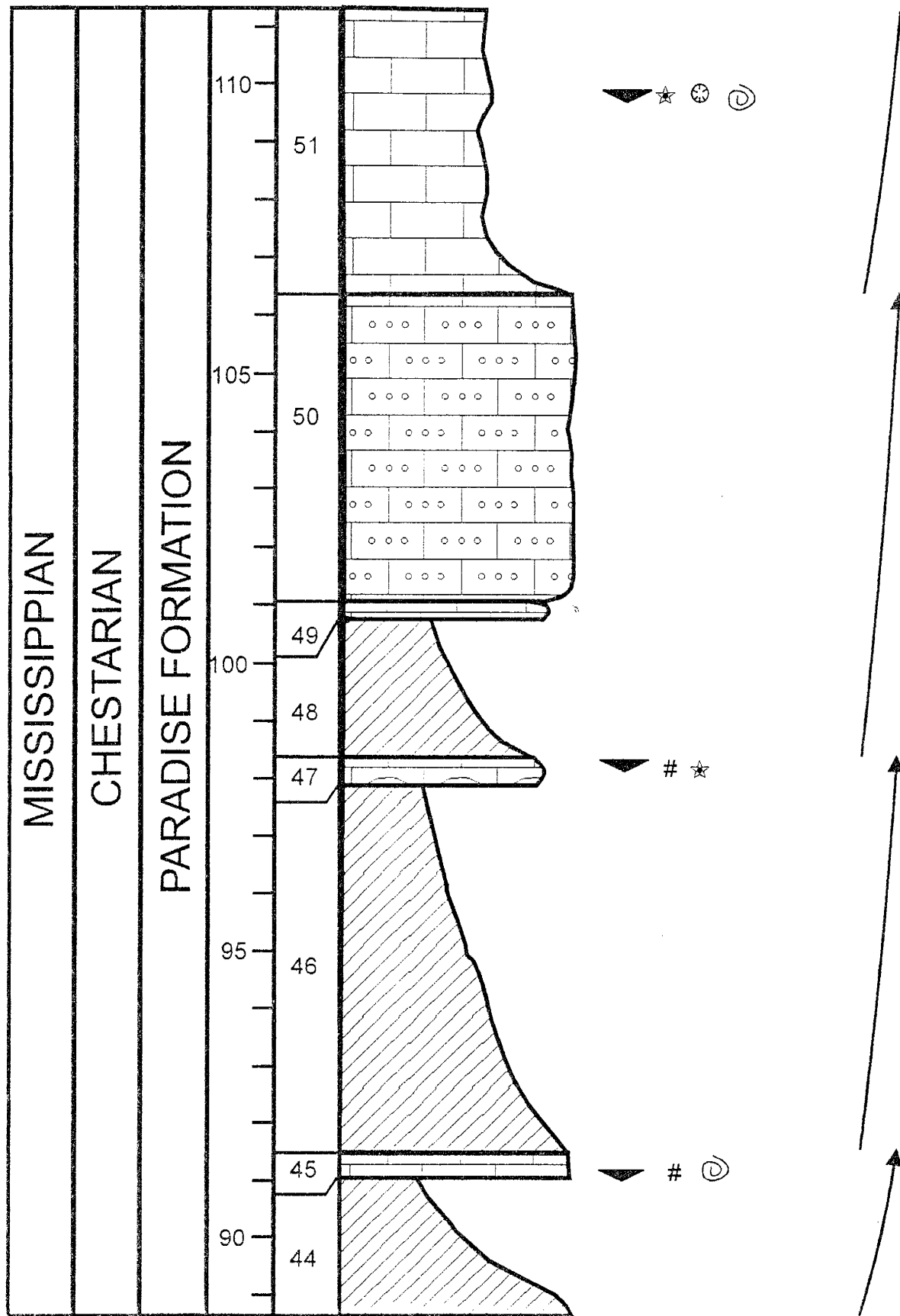
## Symbols

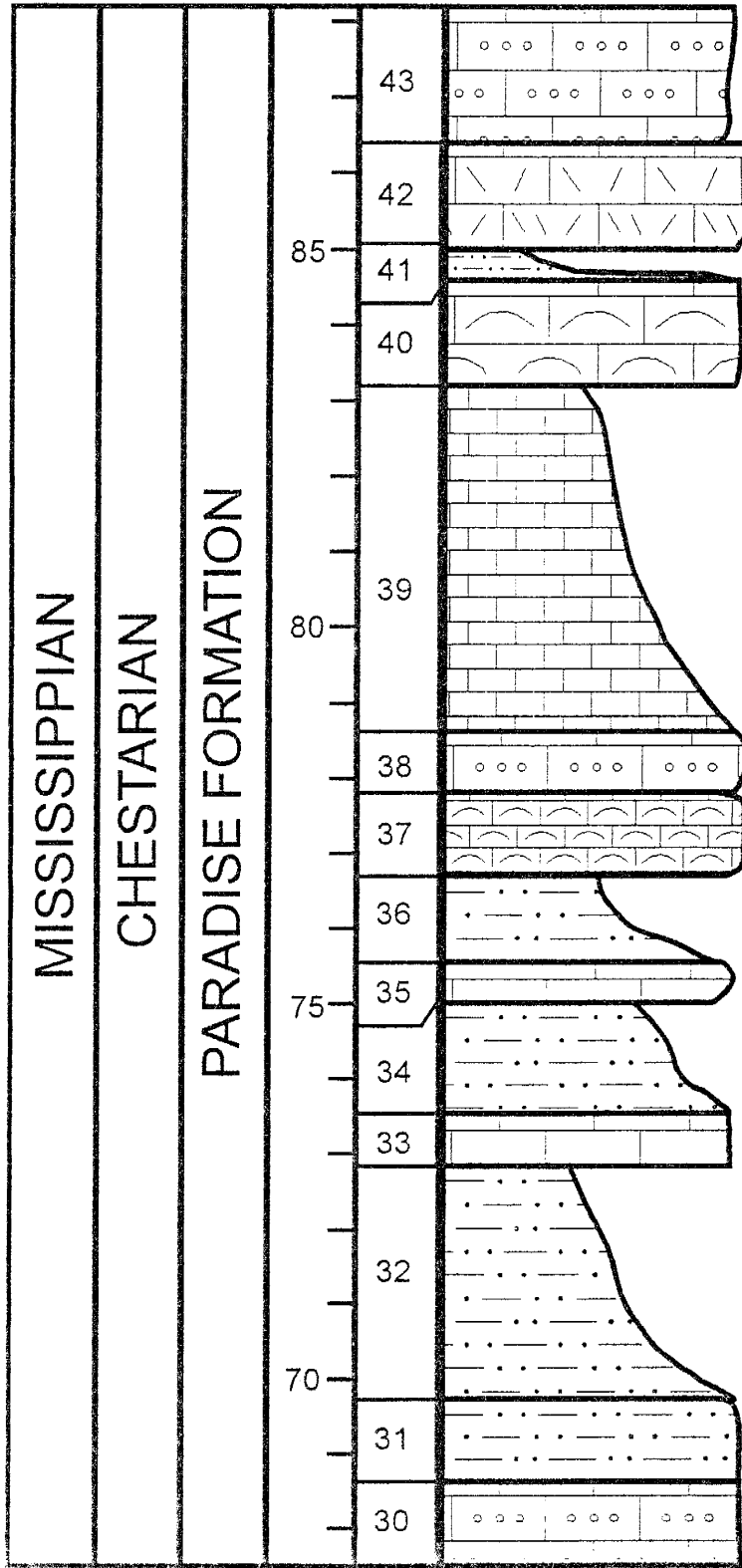


Vertical Scale: 1cm = 1m

# Horse Pasture Canyon Measured Section Big Hatchet Mountains, Hidalgo County, New Mexico



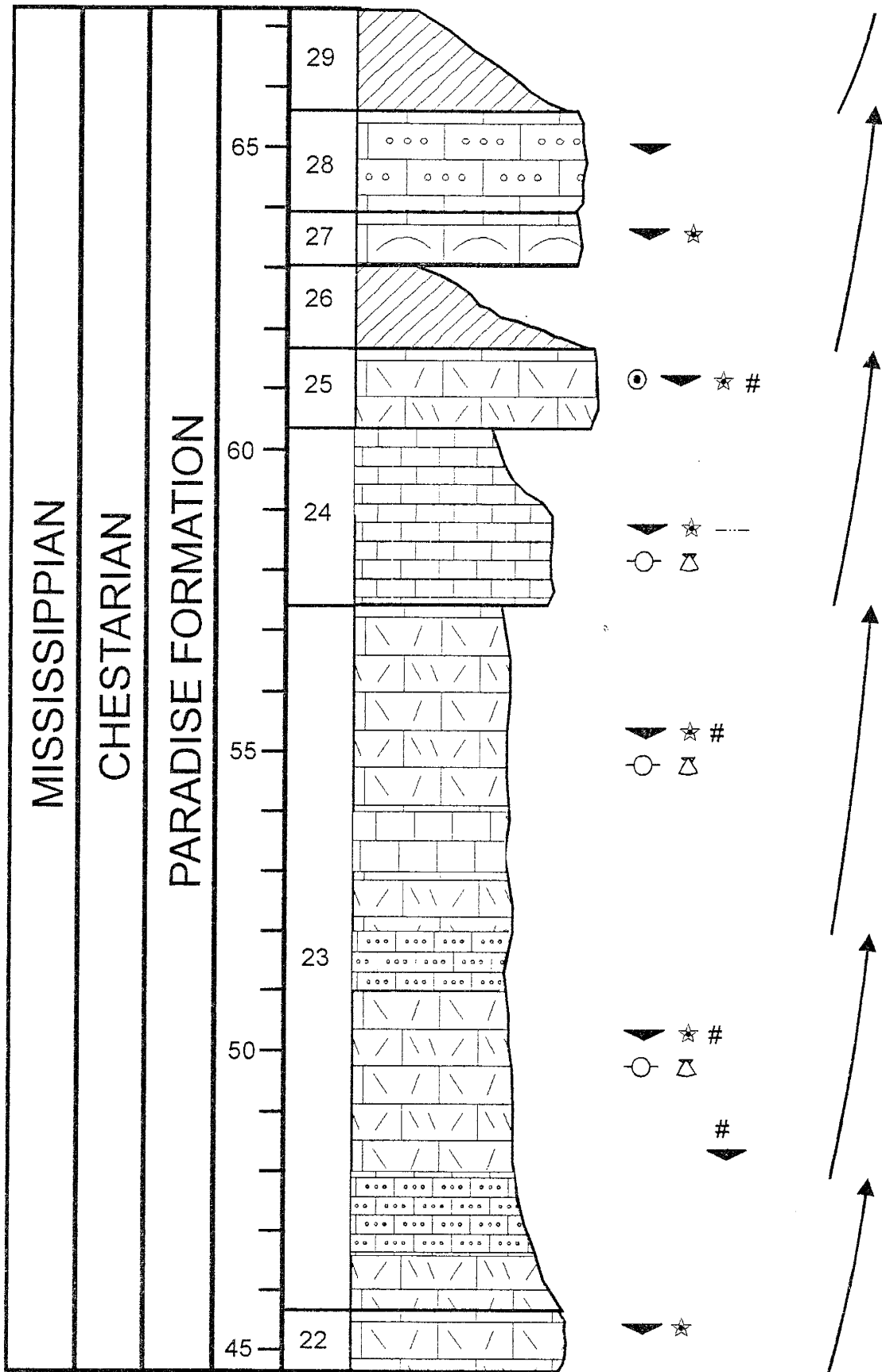


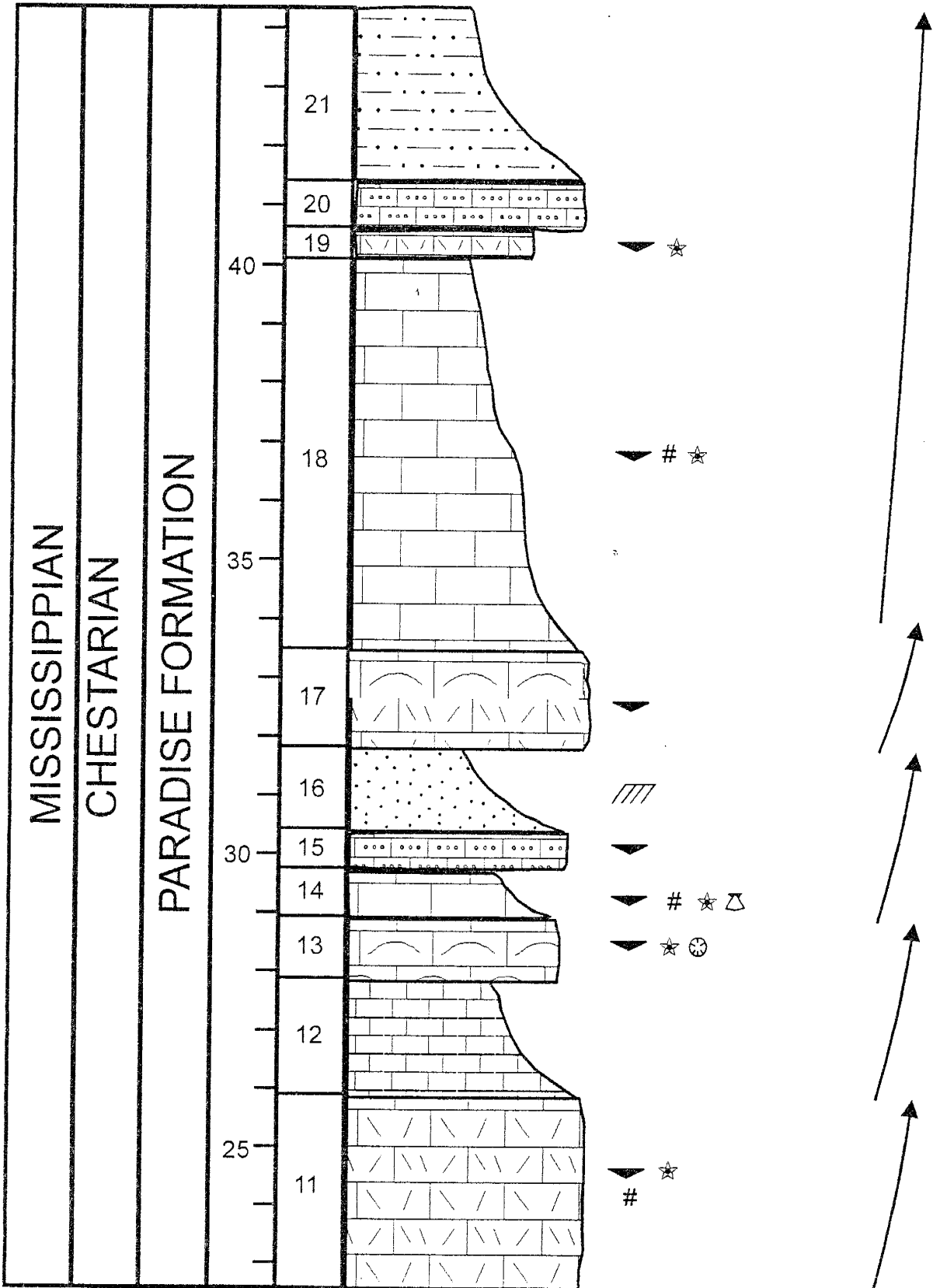


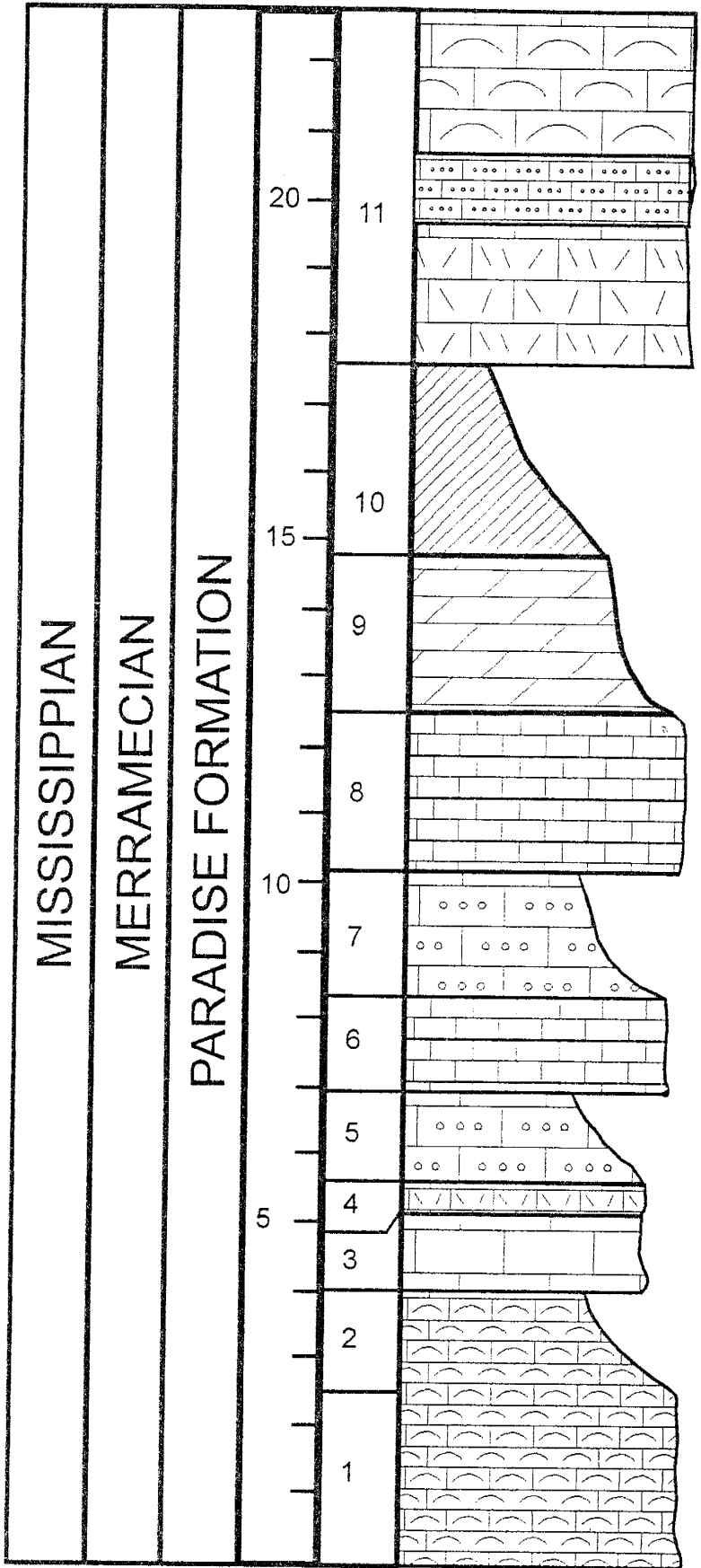
- ▼ # ☆ ◊
- ▼ # ☆ ◊
- ▼ # ☆ ◊
- ▼ # ☆ ◊
- ▼ ☆ #
- ▼ ☆ #
- ☆ ◊ ◊ //
- ▼ ☆







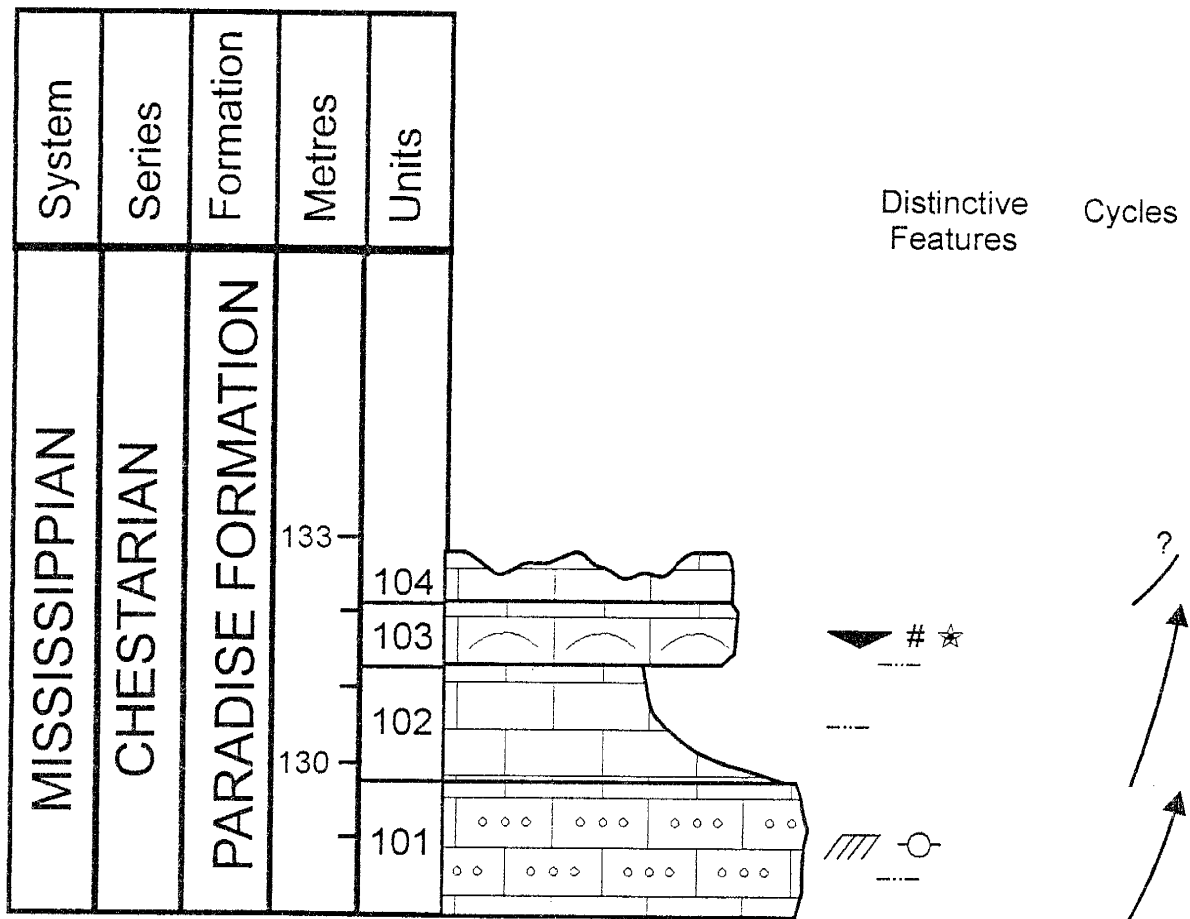


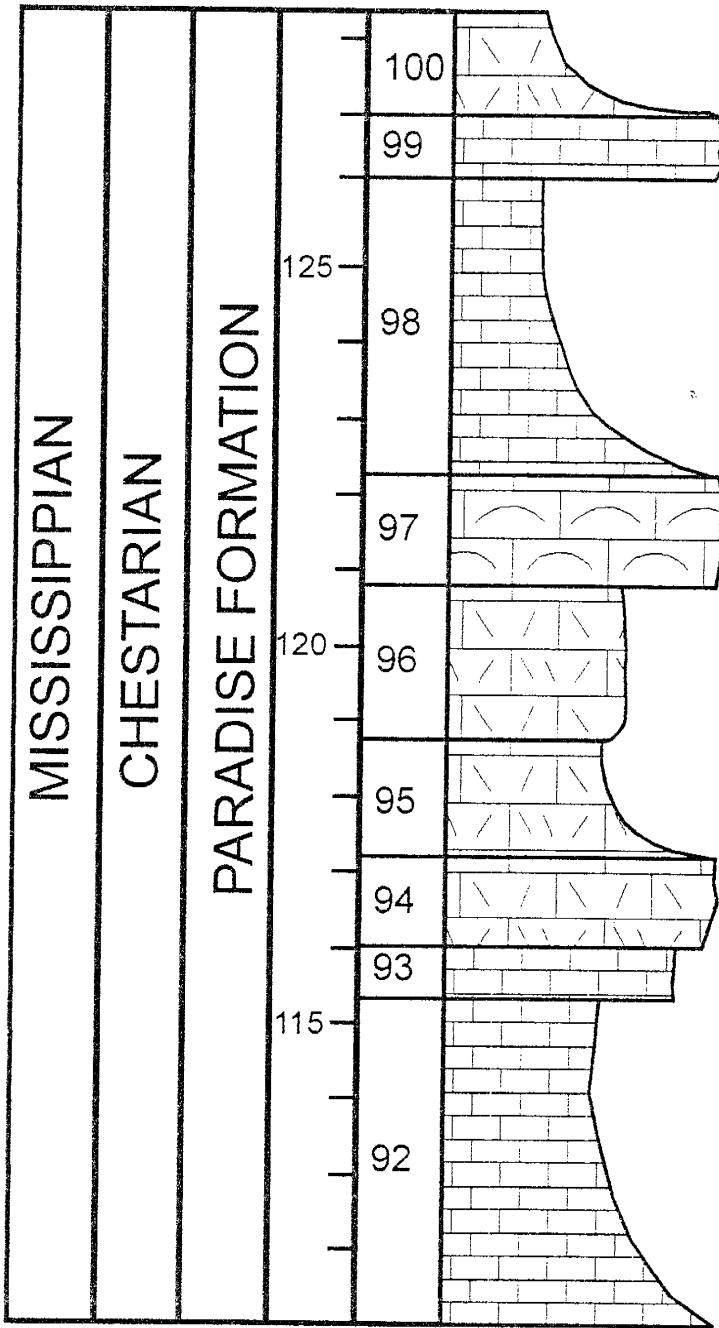


- ▼ ★
- △ ⊙
- # ▼ ★
- ⊙
- ▼ #
- 
- ▼ #
- /// ▼ ★ ⊙
- # ⊙
- ★ ---
- ▼ ---
- ★ ---



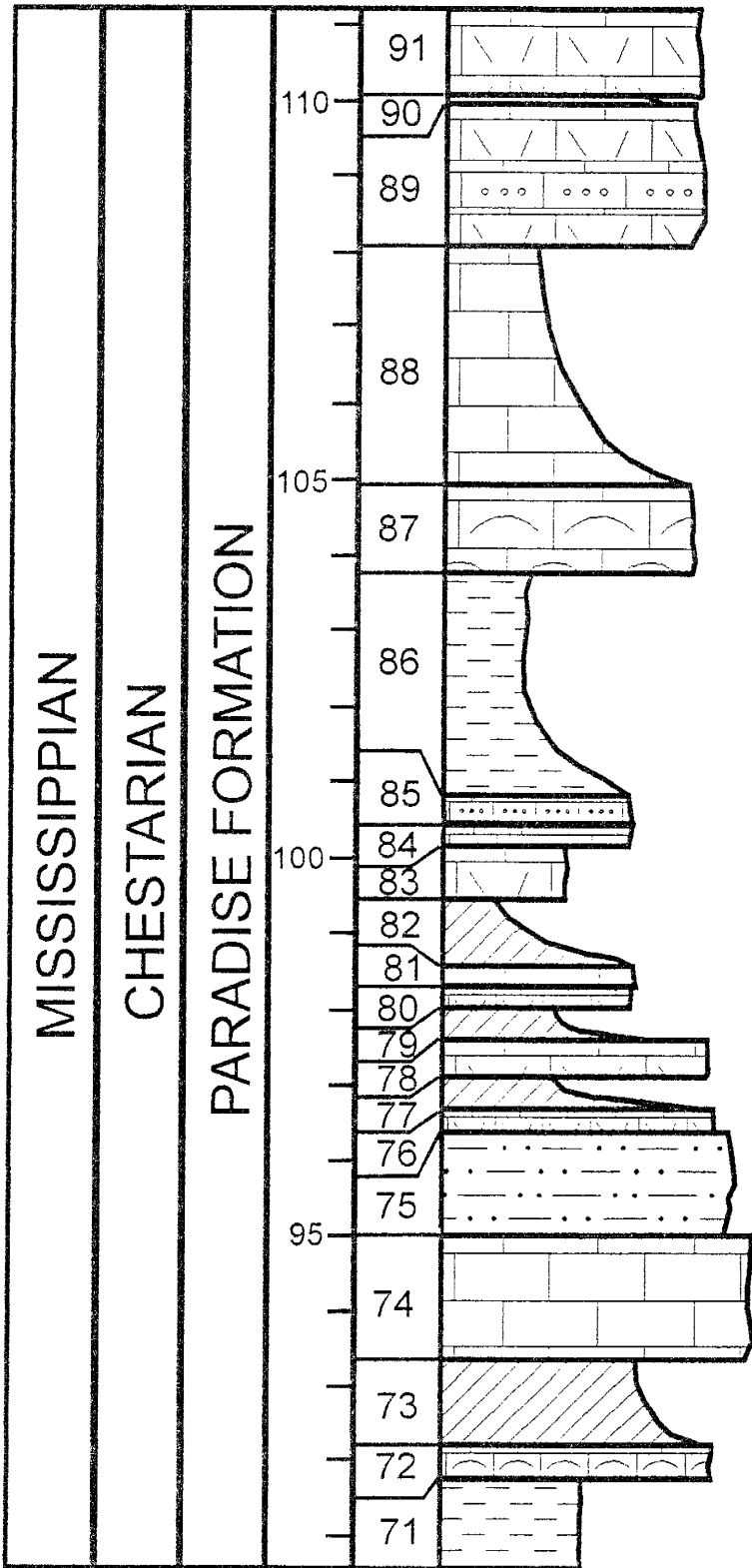
# New Well draw Measured Section Big Hatchet Mountains, Hidalgo County, New Mexico





- ☆
- ---
- ▲ ☆ ⊗ ---
- ▲ ☆
- ▲ ☆ # ⊙
- ▲ ☆ # ⚡
- ▲ # ⊗ ○
- ▲ ☆





▲ ☆ ⊙ ⚡

▲ # ☆  
 // ⚡

▲ # ☆  
 // ---

○

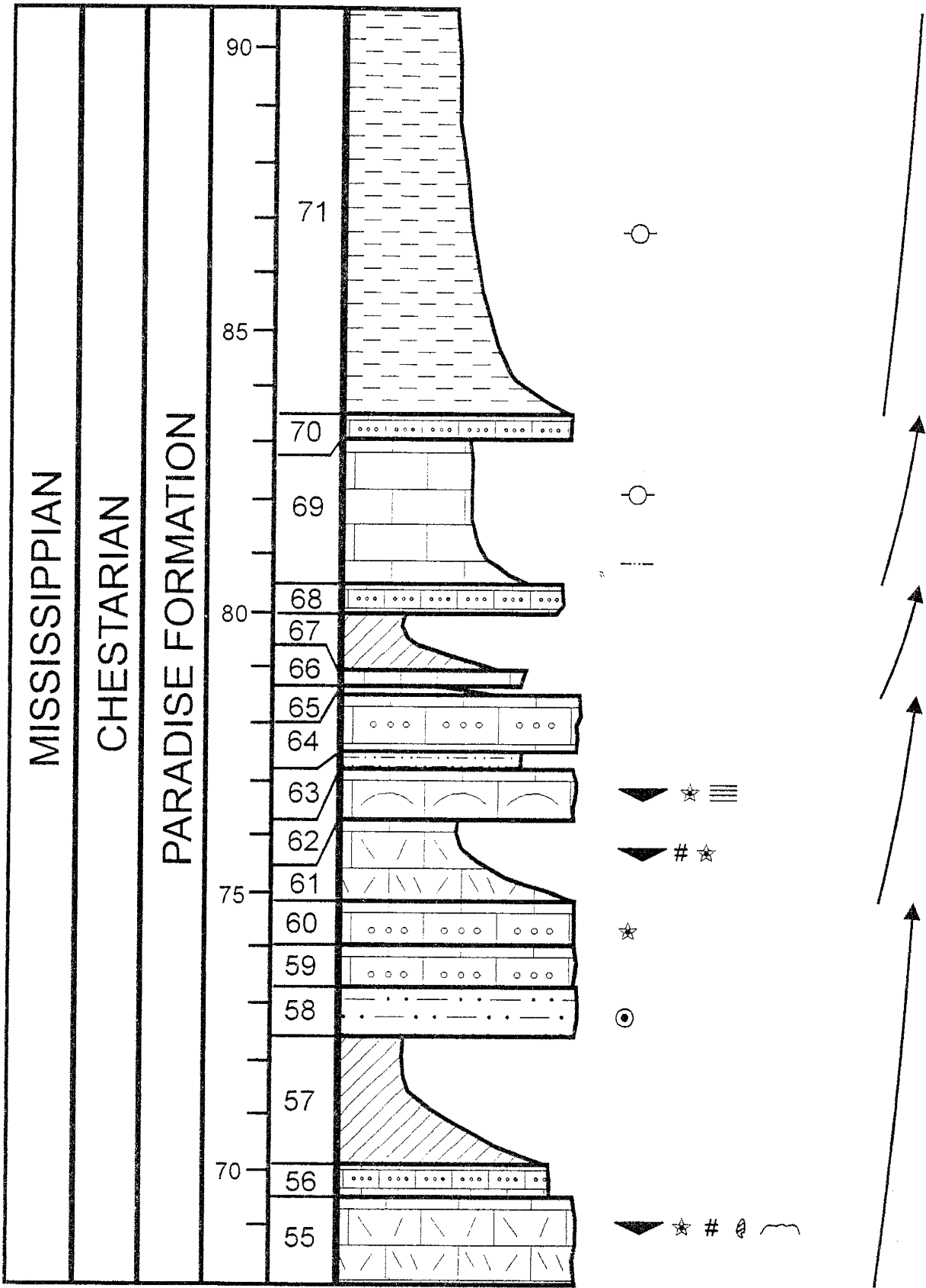
▲ # ☆

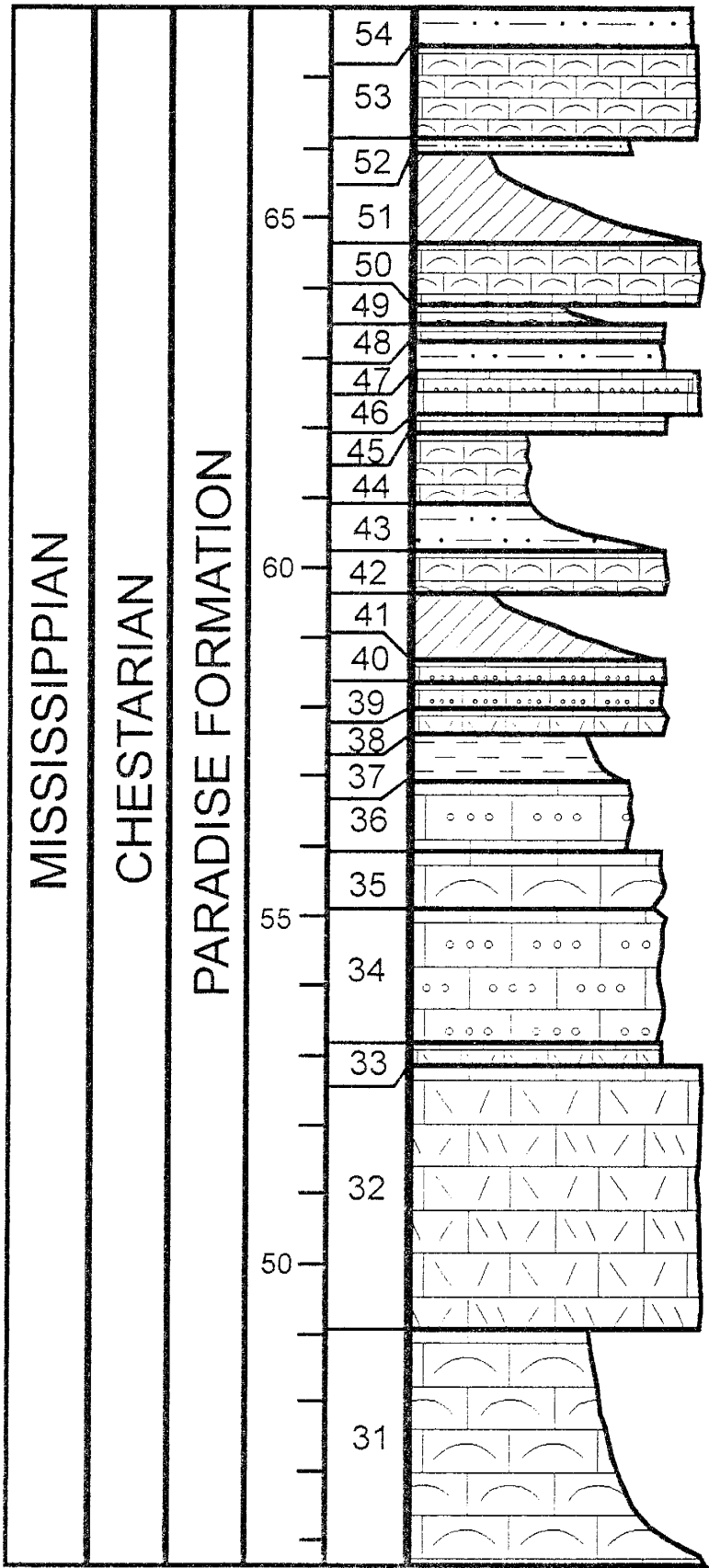
◻  
 // •

▲ # ☆  
 ⚡ ⊙

▲ ☆ # ◻



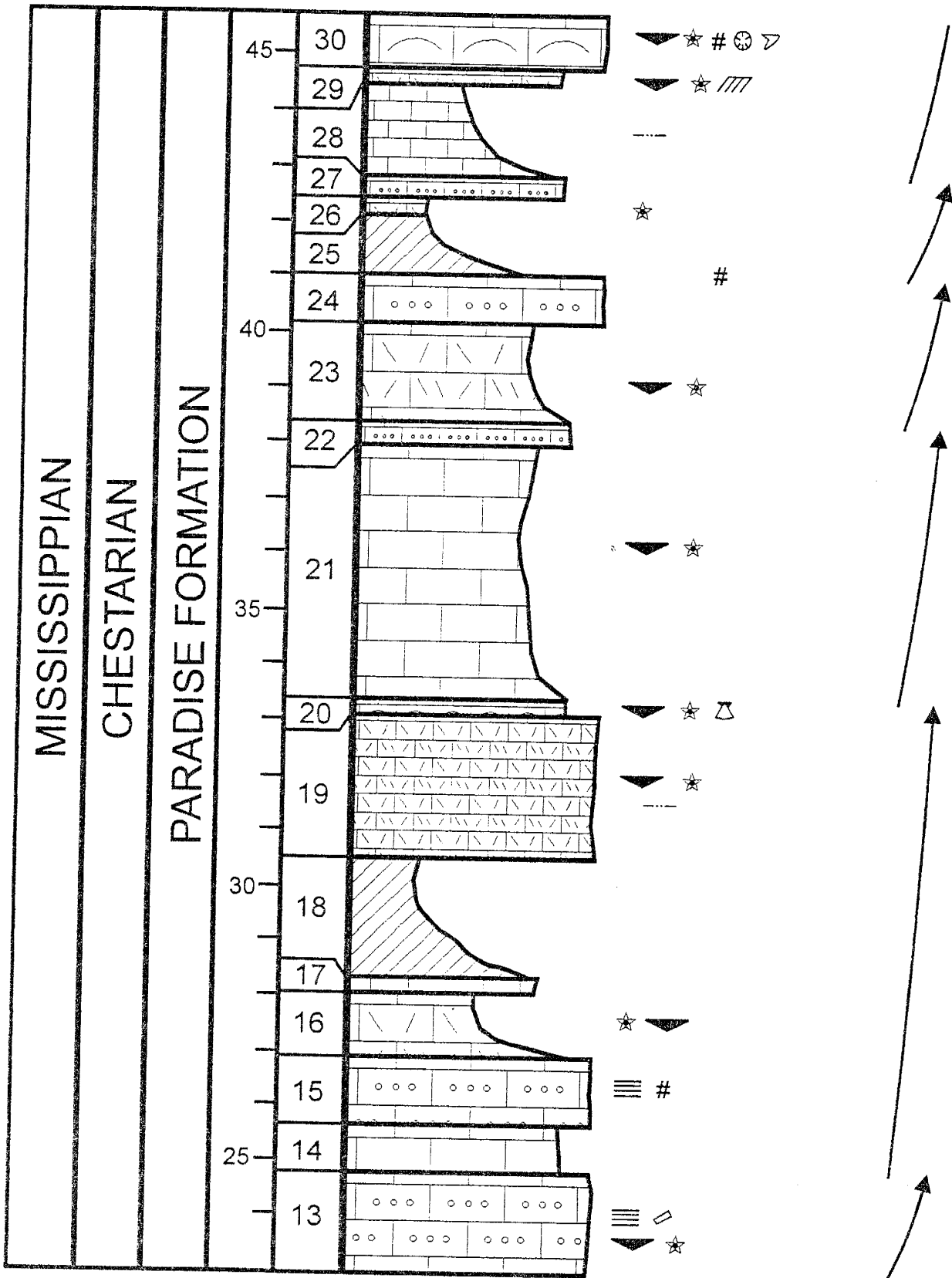




- ▼ # //
- ▼ # //
- ▼ # ☆ ◻ ⊙
- ☆
- ⊙ ◻
- ⊙ ▼ ☆
- // • ☆ - - -
- ▼ ☆ # ⊙ ≡
- // ◻ ☆ ▼
- ▼ # ☆ - - -
- ◻
- ▼ ☆ # ◻
- ▼ # ☆ ◻ - - -
- ▼ # ☆ //
- ▼ # ☆ //
- ▼ # ☆ //



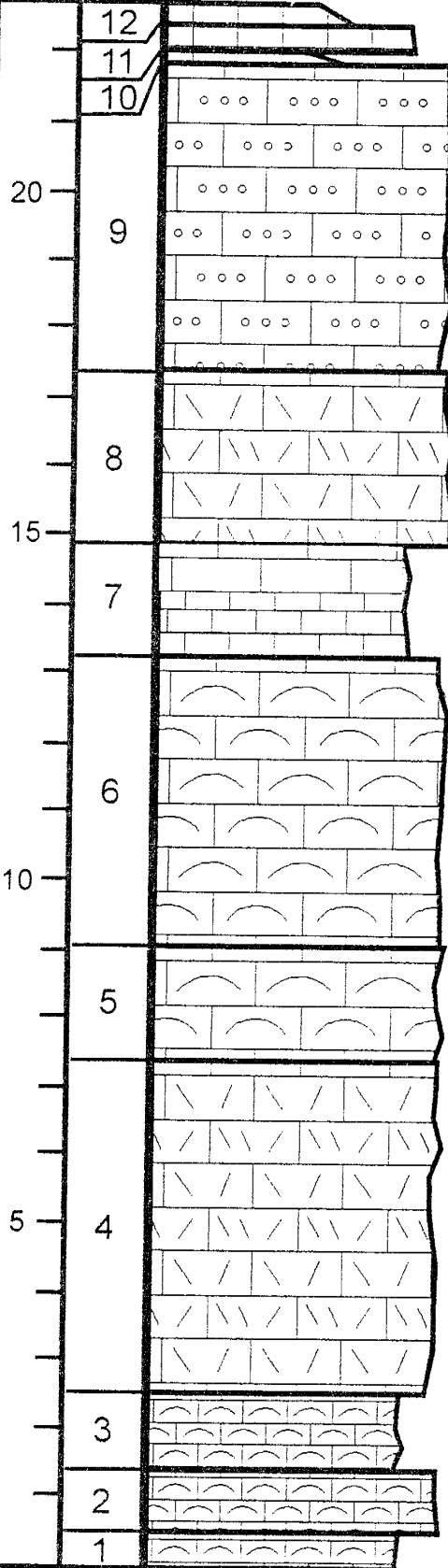




MISSISSIPPIAN

CHESTARIAN

PARADISE FORMATION



# ☆

▲ ☆

▲ ☆  
○

▲ # ☆

▲ ☆ ⊙

▲ # ☆  
---

▲ ☆ #  
⊕ ⊙

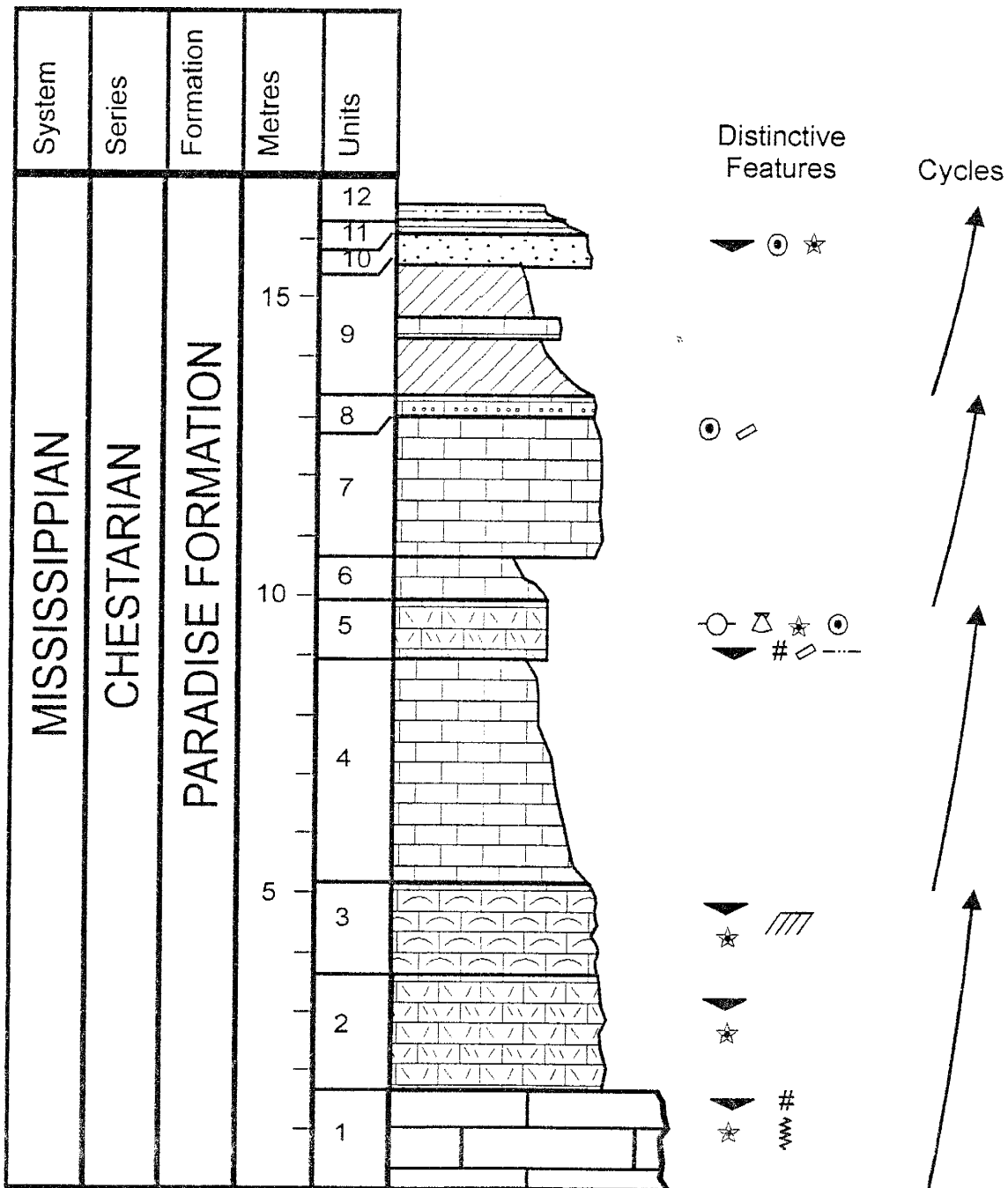
▲ ☆ ---

▲ ☆ ---

☆ ---



# Chaney Canyon Measured Section Big Hatchet Mountains, Hidalgo County, New Mexico



**APPENDIX B**

Written Descriptions of Measured Sections

## Horse Pasture Section, Big Hatchet Mountains

(Sec. 33, T30S, R15W) Hidalgo County, New Mexico

This section is located along a ridge just to the south of Horse Pasture Canyon on the northeastern flank of the Big Hatchet Mountains. Strata strike N-80-W and dip 29° to the west. Section was measured using a 1.5 m Jacob's staff and compass.

### *Top of section*

Horquilla Limestone not measured.

*Top of Paradise Formation.* Contact with overlying Horquilla Limestone is disconformable.

Unit	Description	Thickness (m)
Unit 61	Partially covered, poorly indurated, friable very fine-grained yellowish-gray (5 Y 7/2) weathering siltstone. No visible sedimentary structures or macrofossils. Fresh surface is pale olive (10 Y 6/2).	0.55
Unit 60	Slope forming, dark yellowish-orange (10 YR 6/6) weathering brachiopod bearing limestone. Fresh surface is dusky yellowish brown (10 YR 2/2).	0.25
Unit 59	Ledgy, yellowish gray (5 Y 8/1) weathering, iron stained oolitic grainstone. Fresh surface is pale yellowish brown (10 YR 6/2)	0.4
Unit 58	Massive ledge forming, pale yellowish brown (10 YR 6/2) weathering, silica-cemented quartz sandstone. No visible macrofossils, or sedimentary structures. Fresh surface is a pale brown (5 YR 5/2).	1.5
Unit 57	Partially covered, slope forming, light olive gray (5 Y 5/2) weathering Lime mudstone. Fossils are dominated by pelmatozoan fragments with minor brachiopods and fossil debris. Fresh surface is olive gray (5 Y 4/1).	1.1
Unit 56	Mostly covered, slope forming, light olive (5 Y 6/1) gray weathering, siltstone. No visible macrofossils. Fresh surface is olive gray (5 Y 3/2).	1.7
Unit 55	Ledgy, light olive gray (5 Y 5/2) weathering lime mudstone. No visible macrofossils. Unit is mottled with yellow-brown weathering patches. These may represent a bioturbated fabric. Fresh surface is medium dark gray (N4).	0.3
Unit 54	Ledgy, yellowish gray (5 Y 3/2) weathering bioturbated lime mudstone. Fossils include brachiopods, and <i>Archimedes</i> . The upper surface is irregular with Unit 55, and may represent an exposure surface with a micro-karst breccia. Fresh surface is yellowish gray (5 Y 8/1).	2.3
Unit 53	Slope forming, 100% covered interval. Probable siltstone.	1.6
Unit 52	Partially covered, slope forming light olive gray (5 Y 5/2) weathering pelmatozoan packstone. Other fossil debris is present, but is unidentifiable in handsample. Fresh surface is olive gray (5 Y 3/2).	0.55

Unit	Description	Thickness (m)
Unit 51	Slope forming, pale brown (5 YR 5/2) weathering, silty, wackestone to packstone. Fossils present include brachiopods, pelmatozoan fragments, gastropods, cephalopods, and other fine-grained debris. Upper stage plane beds are present in the lower half of the unit. Dewatering features are also present in the lower part of the unit. Fresh surface is very dusky red (10 R 2/2).	11.4
Unit 50	Ledge forming, light olive gray (5 Y 6/1) weathering oolitic grainstone. Interbedded with the oolitic grainstones are fossiliferous grainstones containing brachiopod, pelmatozoan, bryozoan debris, and lime mudstone intraclasts. No distinctive sedimentary structures in either rock type. Fresh surface is grayish black (N2).	5.3
Unit 49	Ledgy, light gray (N7) weathering, lime mudstone. No visible macrofossils. Fresh surface is light olive gray (5 Y 6/1).	0.3
Unit 48	Slope forming 100% covered interval. Probable shale.	2.4
Unit 47	Ledgy, pale yellowish brown (10 YR 6/2), weathering, interbedded wackestones and oolitic grainstone. Fossils present include pelmatozoans, brachiopods, bryozoans and mollusks. Fresh surface is olive gray (5 Y 3/2), and has a slight fetid odor.	0.5
Unit 46	Slope forming, 100% covered interval. Wackestone-Packstone(?).	6.3
Unit 45	Ledgy, medium gray (N5) weathering, lime mudstone capped grainstone. Fossils present include pelmatozoans, brachiopods, bryozoans, and gastropods. Fresh surface is brownish gray (5 YR 4/1).	0.5
Unit 44	Slope forming 100% covered interval. Probable light gray lime mudstone.	2.4
Unit 43	Ledgy, light olive gray (5 Y 6/1) weathering, oolitic grainstone. Unit also contains bryozoan, brachiopod and pelmatozoan fragments, and intraclasts. Fresh surface is olive gray (5 Y 3/2).	1.7
Unit 42	Ledge forming, light brownish gray (5 YR 6/1) weathering, bioturbated packstone. Fossils present include brachiopods, pelmatozoans, solitary corals, fenestral bryozoans, and <i>Archimedes</i> . Fresh surface is grayish black (N4).	1.4
Unit 41	Slope forming 100% covered interval. Probably lime mudstones.	0.4
Unit 40	Ledgy, Olive gray (5 Y 4/1) weathering horizontally laminated grainstone. Fossils present include pelmatozoans, bryozoans, brachiopods and gastropods. Fresh surface is olive black (5 Y 2/1).	0.9
Unit 39	Mostly covered, slope forming interval with small outcrops of moderate yellowish brown (10 YR 5/4) weathering siltstones. Fresh surface is an olive black (5 Y 2/1).	4.5
Unit 38	Ledge forming, light olive gray (5 Y 6/1) weathering oolitic grainstone. Upper surface is irregular, but shows no indication of subaerial exposure. Fossils present include pelmatozoans, brachiopods, fenestral bryozoans and <i>Archimedes</i> . Fresh surface is an olive gray (5 Y 4/1).	0.8
Unit 37	Ledgy, yellowish gray weathering (5 Y 7/2) medium bedded, grainstone. Upper surface has a slight reddish stain, but with no other evidence for subaerial exposure. Grains present include ooids, pelmatozoans, brachiopods, and the bryozoan <i>Archimedes</i> . Weathered surface is black (N1) and has a slight fetid odor.	1.0
Unit 36	Mostly covered, slope former. Unit contains small exposures of poorly weathering Grayish orange (10 YR 7/4) siltstone, with no observable fossils in this unit. Fresh surface is a dusky yellowish brown (10 YR 2/2).	1.1
Unit 35	Ledgy, light brown weathering (5 YR 6/4) cross-laminated wackestone. Fossils include brachiopods, pelmatozoans, and solitary corals. Fresh surface is dark yellowish brown (10 YR 4/2).	0.5

Unit	Description	Thickness (m)
Unit 34	Partially covered, slope forming, dark yellowish orange (10 YR 6/6) weathering, siltstone. There are no observable fossils in this unit. Fresh surface is dark yellowish brown (10 YR 4/2).	1.4
Unit 33	Ledgy, pale yellowish brown (10 YR 6/2) weathering grainstone. Fossils include pelmatozoans and brachiopods. Fresh surface is brownish black (5 YR 2/1).	0.7
Unit 32	Mostly covered, slope forming, light brown (5 YR 5/6) weathering siltstone. Beds are mildly cross-laminated. Fossils include brachiopods, pelmatozoans, and abundant gastropods. There are small pockets, which contain ooids. Fresh surface is dark gray (N3).	3.1
Unit 31	Ledgy, horizontally laminated Moderate brown (5 YR 4/4) weathering calcite cemented siltstone. Unit is bioturbated and contains no observable fossils. Fresh surface is grayish red (10 R 4/2).	1.1
Unit 30	Ledge forming, light olive gray (5 Y 6/1) weathering, oolitic grainstone. Observable fossils include brachiopods and pelmatozoan fragments. Fresh surface is Olive black (5 Y 2/1).	1.1
Unit 29	Slope forming 100% covered interval.	1.7
Unit 28	Ledge forming, light olive gray (5 Y 6/1) weathering oolitic grainstone. Unit is rich in brachiopod fragments. Other observable fossils include pelmatozoan fragments and solitary.	1.6
Unit 27	Ledge forming, light olive gray (5 Y 6/1) weathering, grainstone. Unit contains ooids, and large brachiopods. Other observable fossils include pelmatozoan fragments, and "bioclastic hash". This "hash" zone is located in the upper 30 cm of the unit. Fresh surface is a grayish red (10 R 4/2).	0.85
Unit 26	Slope forming 100 % covered interval.	1.4
Unit 25	Ledgy, pinkish gray (5 YR 8/1) weathering, ooid rich packstone. Other observable fossils include pelmatozoan fragments and small brachiopod fragments. Fresh surface is light brownish gray (5 YR 6/1).	1.3
Unit 24	Rubbly, slope forming, interbedded wackestones and siltstones. The upper 1.9 meters of this unit are partially covered. Wackestones weather to a yellowish gray (5 Y 8/1). Siltstones weather to a medium light gray (N6). Unit is mildly bioturbated. Observable grains include brachiopods, pelmatozoan fragments, mollusk fragments, and ooids. There are no fossils in the siltstone. Fresh surfaces are olive gray (5 Y 4/1) (wackestone) and medium gray (N5) (siltstone).	2.9
Unit 23	Partially covered, slope forming, series of grainstones and packstones. Grainstones weather to a light olive gray (5 Y 6/1). Packstones weather to a pale yellowish brown (10 YR 6/1). Fossils observed are the same in both the packstone and grainstones. They are pelmatozoan fragments, brachiopods, fenestral bryozoans, and mollusk fragments. Minor amounts of ooids are found in the grainstone beds. Packstone are bioturbated, and contain thin stringers of silt. Fresh surfaces are olive gray (5 Y 4/1) (grainstones) and dark yellowish brown (10 YR 4/2) (packstone).	11.7
Unit 22	Ledgy, grayish orange (10 YR 7/4) weathering, packstone. Dominant grains include pelmatozoan fragments, brachiopods, and ooids. Brachiopods are most abundant 30 cm from the base of the unit and the top of the unit. These may represent large thanatocoenocis. Fresh surfaces are a dusky yellowish brown (10 YR 2/2) and have a slight fetid odor.	1.0
Unit 21	Mostly covered, slope forming, pale yellowish brown (10 YR 6/2) weathering siltstone. No noticeable sedimentary structures or fossils. Fresh surface is an olive black (5 Y 2/1).	2.9

Unit	Description	Thickness (m)
Unit 20	Ledgy, medium bedded, grayish orange (10 YR 7/4) weathering oolitic grainstone. Minor pelmatozoan and brachiopod fragments are found throughout the unit. Fresh surface is a brownish black (5 YR 2/1).	0.8
Unit 19	Partially covered, ledgy, light olive gray (5 Y 6/1) weathering packstone. Abundant large brachiopods and pelmatozoan fragments. Rare ooids occur towards the top of the unit. Fresh surface is a grayish black (N2) and has a very strong fetid odor.	0.5
Unit 18	Mostly covered, slope forming, moderate yellowish brown (10 YR 5/4) weathering silty wackestone. Fossils fragments include pelmatozoans, brachiopods and fenestrate bryozoans. Fresh surface is a dark yellowish brown (10 YR 4/2), and has a strong fetid odor.	6.6
Unit 17	Ledge forming, pale yellowish brown (10 YR 6/2) weathering brachiopod, oolitic packstones. Brachiopods are most abundant along the upper bedding planes of the beds. Unit is capped by a brachiopod grainstone. No physical sedimentary structures in the unit. Fresh surface is an olive gray (5 Y 4/1) and has a fetid odor.	1.7
Unit 16	Mostly covered, slope forming, pale brown (5 YR 5/21) weathering, trough cross-bedded sandstone. No fossil debris in the unit. Cross beds are very low angle and trend 152°. Fresh surfaces are a dark yellowish brown (10 YR 4/2).	1.4
Unit 15	Ledgy, horizontally laminated, olive gray (5 Y 4/1) weathering brachiopod, ooid grainstone. Fresh surface is an olive black (5 Y 2/1) and has a slight fetid odor.	0.65
Unit 14	Partially covered, slope forming, light gray (N7) weathering wackestone. Fossils include fenestrate bryozoans, brachiopods, mollusk fragments and pelmatozoan debris. Fresh surface is a grayish brownish (5 YR 3/2).	0.8
Unit 13	Ledge forming, olive gray (5 Y 4/1), brachiopod grainstone. Other grains include pelmatozoan debris, mollusk fragments, solitary corals, ooids and lime mud intraclasts. Some of the brachiopods are silicified. Fresh surface is an olive black (5 Y 2/1).	1.1
Unit 12	Mostly covered, slope forming, thinly bedded, yellowish gray (5 Y 7/2) weathering lime mudstone. No macrofossils. Fresh surface is a light olive gray (5 Y 5/2).	2.0
Unit 11	Ledge forming, medium- to thin-bedded, medium light gray (N6) to pale yellowish brown (10 YR 6/2) weathering packstones and grainstones. Grains include abundant ooids, pelmatozoan fragments, brachiopods, echinoderm spines, mollusks, limestone nodules. Minor silicification of fossil grains common throughout the section. Fresh surfaces weather to a brownish gray (5 YR 4/1).	8.3
Unit 10	100% covered interval. Probable shale.	2.8
Unit 09	Partially covered, slope forming, pale yellowish orange (10 YR 8/6) weathering dolomitic lime mudstone. Rare diminutive gastropods, and bivalves. Unit is mildly burrowed and brecciated. Possible fenestral fabric in places. Fresh surface weathers to a pale yellowish brown (10 YR 6/2)	2.3
Unit 08	Ledgy, thinly bedded, cross-bedded, light olive gray (5 Y 6/1) weathering, silty lime mudstone. Fossils present include brachiopods and rare fenestral bryozoans. Cross-bedding trends 122°. Fresh surface is a grayish black (N2)	2.3
Unit 07	Mostly covered, slope forming, light olive gray (5 Y 6/1) weathering, ooid grainstone. Fossils include gastropods, brachiopods and pelmatozoan fragments. Fresh surface is olive gray (5 Y 4/1).	1.85
Unit 06	Ledgy, medium-bedded, medium gray (N5) weathering, chert-bearing lime mudstone. Fresh surface is olive gray (5 Y 4/1).	1.35



Unit	Description	Thickness (m)
Unit 05	Mostly covered, slope forming, thin bedded light brownish gray (5 YR 6/1) weathering ooid grainstone. Fresh surface is an olive gray (5 Y 4/1).	1.3
Unit 04	Ledgy, light gray (N7) weathering wackestone. Fossils are poorly preserved and are primarily bryozoans and brachiopod fragments. Fresh surface is a medium dark gray (N4).	0.45
Unit 03	Ledge forming, medium gray (N5) weathering, cross-bedded packstones. Abundant brachiopods and pelmatozoan debris are present as well as rare ooids. The upper 10 cm of the unit is trough cross-bedded and contains gastropods. Cross bedding trends 119°. Fresh surface is a brownish gray (5 YR 4/1).	1.1
Unit 02	Mostly covered, thin-bedded, light olive gray (5 Y 6/1) weathering, silty grainstone. The unit is distinctly horizontally laminated, but does not contain any readily identifiable fossils. Fresh surface is a dark gray (N3).	1.5
Unit 01	Partially covered, ledgy, medium light gray (N6) weathering, silty, grainstone. Fossils are dominantly composed of pelmatozoan debris. Brachiopods are also present. Fresh surface is a medium dark gray (N4).	2.5
Total measured Paradise Formation:		126.7 m

#### *Base of Section*

The Paradise Formation rests conformably on the Hachita Formation of the Escabrosa Group. The contact is sharp and is placed where the thick-bedded, cherty, crinoidal grainstones of the Hachita change to thinly bedded, quartz-bearing grainstones and packstones of the lowermost Paradise Formation.

## New Well draw Measured Section, Big Hatchet Mountains

(Sec. 29, T31S, R14W) Hidalgo County, New Mexico

This section is located on the south facing slope of the first small draw on the north side of New Well Canyon at the southern end of the Big Hatchet Mountains. Strata strike N-57-W and dip 11° to the southwest. Dip increases to 32° up section with the strike remaining constant. Section was measured using 1.5m Jacob's staff and compass.

### *Top of Section*

Horquilla Limestone not measured

*Top of Paradise Formation.* Contact with overlying Horquilla Limestone is irregular and disconformable.

Unit	Description	Thickness (m)
Unit 104	Ledgy, medium gray (N5) weathering, slightly mottled silty, lime mudstone. Upper surface is somewhat conglomeratic. No macrofossils. Fresh surface is a medium dark gray (N4).	1.0
Unit 103	Ledge forming, medium dark gray (N4) weathering, silty grainstone. Upper surface is highly irregular and karsted. Fossils include pelmatozoans, brachiopods, and fenestral bryozoans. Fresh surface is a brownish gray (5 YR 4/1).	0.9
Unit 102	Mostly covered slope forming medium dark gray (N4) weathering silty lime mudstone. Not macrofossils. Fresh surface is a brownish black (5 YR 2/1).	1.6
Unit 101	Cliffy, stripped, olive gray (5 Y 4/1) weathering oolitic grainstone. Unit is very distinctive. Lower 2/3 is trough cross-bedded and contains abundant brachiopod and gastropod fossil fragments. Upper 1/3 is bioturbated with horizontal and vertical burrows. There is some silt in the unit as well as some mud in the burrows. Fresh surface is a dark gray (N5).	2.7
Unit 100	Mostly covered, light brown (5 YR 6/4) weathering, thinly bedded oolitic grainstones. Unit also contains abundant pelmatozoan fragments and brachiopods. Fresh color is a moderate brown (5 YR 4/4).	2.4
Unit 99	Ledge forming, dark gray (N3) weathering, silty, bioturbated lime mudstone. No macrofossils. Fresh surface is a medium gray (N5).	0.8
Unit 98	Mostly covered, slope forming, dark gray (N3) weathering, lime mudstone. Slight hint of horizontal laminates in the exposed beds. No macrofossils. Fresh surface is a medium dark gray (N4).	3.9
Unit 97	Ledge forming, medium light gray (N6) weathering grainstones. Unit is fossiliferous with abundant pelmatozoan debris, brachiopods, and rare tabulate corals. The upper 1/3 of the unit is distinctly striped with light brownish gray (5 YR 6/1) weathering hearing bone, cross-bedded siltstones indicative of tidal deposition. Fresh surfaces are medium gray	1.4

Unit	Description	Thickness (m)
Unit 96	(N4). Somewhat covered, ledgy, light brown (5 YR 6/4) weathering pelmatozoan packstones. Fossils are dominated by pelmatozoan debris with rare brachiopod fragments. No distinctive sedimentary structures. Fresh surface is a moderate brown (5 YR 4/4).	2.0
Unit 95	Mostly covered, slope forming, grayish orange pink (5 YR 7/2) weathering, wackestones and packstones. Fossils include pelmatozoan debris, brachiopods, and fenestrate bryozoans. Unit also contains ooids probably washed in from an adjacent ooid shoal. Fresh surface is a pale brown (5 YR 5/2).	1.6
Unit 94	Ledge forming, light brownish gray (5 YR 6/1) weathering, packstones. Unit is fossiliferous containing abundant pelmatozoan debris, brachiopods, fenestral bryozoans, <i>Archimedes</i> , solitary rugosan corals and tabulate corals. Minor intraclasts are present at the top of the unit indicating a possible storm event. Fresh surface is a medium gray (N4).	1.2
Unit 93	Ledge forming, dark gray (N3) weathering, burrowed lime mud stone. Fossils include pelmatozoan debris, brachiopods, fenestral bryozoans, and gastropods. Fresh surface is a medium, dark gray (N4) color.	0.7
Unit 92	Slope forming, thinly-bedded, olive black (5 Y 2/1) weathering lime mudstones. Rare brachiopod and pelmatozoan fragments are present in the lower .5 m. Fresh surface is medium dark gray (N4).	4.3
Unit 91	Ledge forming, pale brown (r YR 5/2) weathering, wackestones--packstones. Fossils present include pelmatozoan debris, brachiopods, abundant blastoids, <i>Archimedes</i> , and solitary rugosan corals. Rare intraclasts are found near the top of the unit. Fresh surface is a brownish gray (5 YR 4/1).	1.1
Unit 90	Very thin, grayish red (5 R 4/2) weathering, gastropod packstone. Lower contact with unit 89 is irregular and scoured. Fossils in unit include abundant gastropods, pelmatozoan debris and brachiopods. Fresh surface is a dusky red (5 R 3/4).	0.03
Unit 89	Ledge forming, light olive-gray (5 Y 5/2) weathering, packstones and oolitic grainstone. The oolitic grainstone sandwiched between two packstones. Packstones are faintly cross-laminated, and contain abundant current-aligned <i>Archimedes</i> . Paleocurrent trend from <i>Archimedes</i> is N-40-W. Fresh surface is an olive gray (5 Y 4/1).	2.1
Unit 88	Mostly covered, slope forming, interbedded shales and grayish red (5 R 4/2) weathering lime mudstones. No significant sedimentary structures or macrofossils. Fresh surface is a dusky red (5 R 3/4).	3.1
Unit 87	Ledgy, light olive gray (5 Y 5/2) weathering, cross-bedded grainstones. Cross-bedding laminations are silty. Fossils include brachiopods, pelmatozoan debris, and rare bryozoans. Ooids are found throughout the unit, but increase significantly upwards. Fresh surface is a grayish olive (10 Y 4/2).	1.1
Unit 86	Mostly covered, slope forming interval composed of yellowish gray (5 y 8/1) weathering interbedded shales lime mudstones. No macrofossils or sedimentary structures. Fresh surface is a grayish black (N 2).	3.1
Unit 85	Ledgy, grayish orange (10 YR 7/4) weathering, oolitic grainstone. No sedimentary structures. Unit contains rare brachiopods and intraclasts. Upper contact is gradational with unit 86. Fresh surface is a brownish gray (5 YR 4/1).	0.25
Unit 84	Ledge forming, olive gray (5 Y 4/1) weathering, grainstone. Unit fines upward without any observable sedimentary structures. Unit contains	0.3

Unit	Description	Thickness (m)
	pelmatozoan debris (columnals and plates) and brachiopod fragments. Fresh surface is a brownish black (5 YR 2/1).	
Unit 83	Slope forming, light brown (5 YR 5/6) weathering, packstones. Fossils include pelmatozoan debris, brachiopods, bryozoans, fenestral and branching and trilobites. Small pockets of yellowish material in unit may be silt and clay filling burrows. Fresh surface is a moderate reddish brown (10 R 4/6).	0.7
Unit 82	100% Covered slope forming interval. Probable shale?	0.8
Unit 81	Ledgy, light olive gray (5 Y 6/1) weathering grainstone. Upper surface has a distinctive light pinkish coloration, possibly indicating an exposure surface. Fossils found include pelmatozoan debris, brachiopod fragments and abundant unrecognizable fragments. Fresh surface is a dusky brown (5 YR 2/2).	0.3
Unit 80	Ledgy, grayish orange (10 YR 7/4) weathering, trough cross-bedded, silty peloidal packstone. No macrofossils. Fresh surface is a dusky yellowish brown (10 YR 2/2).	0.2
Unit 79	Mostly covered, slope forming, whitish-gray shale. No fossils.	0.5
Unit 78	Ledge forming, light olive gray (5 Y 6/1) weathering packstone. Fossils include pelmatozoan debris, brachiopods, fenestral bryozoans, and unrecognizable fragments. Amount of lime mud matrix decrease upward through the unit. Fresh surface is an olive black (5 Y 2/1).	0.5
Unit 77	Mostly covered, slope forming, light gray weathering shale. No fossils.	0.4
Unit 76	Ledge forming, pale red (5 R 6/2) weathering, intraclastic wackestone to packstone. Unit has a slight hint of tabular cross-bedding. Silt drapes over many of these cross-bed sets. Intraclasts are composed of oolitic grainstones, lime mudstones, wackestones and packstones. Fresh surface is a dark reddish brown (10 R 3/4).	0.3
Unit 75	Ledge forming, light brown (5 YR 6/4) weathering, cross-bedded, silty grainstones. Lower 2/3s of unit is tabular cross-bedded, while the upper 1/3 is trough cross-bedded and contains highly convoluted bedding indicative of extremely high rates of sedimentation. Rare fossils include brachiopod fragments, pelmatozoan debris and <i>Archimedes</i> . Paleocurrent direction from tabular bed sets is N-45-W. Fresh surface is a grayish brown (5 YR 3/2)).	1.4
Unit 74	Cliffy, medium gray (N 5) and moderate reddish orange (10 R 6/6) weathering, bryozoan wackestones. Unit appears to be channeled with silt-rich channels cut into wackestones. "Channels" are actually wackestones that have been pervasively replaced by iron-rich dolomite. Fossils include <i>Archimedes</i> , brachiopods, and pelmatozoan debris and rare coiled ammonoids. Fresh surface is a grayish red (10 R 4/2).	1.6
Unit 73	Mostly covered slope forming, light gray (N 7) weathering shale. No macrofossils.	1.1
Unit 72	Ledgy, olive gray (5 Y 4/1) weathering, grainstones. Fossils include pelmatozoan debris, brachiopods and fenestrate bryozoans. Middle of unit contains lime mudstone intraclasts, suggesting a storm event. Fresh surface is an olive gray (5 Y3/4).	0.45
Unit 71	Slope forming, light olive gray (5 Y 6/1) interbedded shales and light gray lime mudstones. Both the shales and lime mudstones are fossil-poor. However, the lime mudstones contain two species of trace fossils. Both <i>Planolites</i> and <i>Chondrites</i> are present in all the lime mudstone units. The upper contact is gradational with unit 72. Fresh surface is an olive gray (5 Y 4/1).	8.2

Unit	Description	Thickness (m)
Unit 70	Ledge forming, light olive gray (5 Y 5/2) weathering, oolitic grainstone. Fossils include abundant pelmatozoan debris and brachiopods. Upper surface has a distinctive reddish coloration as some silt filled burrows. This may indicate an exposure surface. Fresh surface is an olive black (5 Y 2/1).	0.4
Unit 69	Partially covered, slope forming, light brown gray (5 YR 6/1), interbedded shale, siltstone and lime mudstone interval. Shales contain no macrofossils. Lime mudstone beds also do not contain any macrofossils, but are burrowed with <i>Planolites</i> . Siltstones are slightly trough cross-laminated and contain no fossils. Fresh surface is a dark yellowish brown (10 YR 4/2) for the lime mudstones and siltstones.	2.5
Unit 68	Ledge forming, grayish orange (10 YR 7/4) weathering, oolitic grainstone. Fossils include brachiopods and pelmatozoan debris. Shallow scours have silt bases and are filled by ooids. Fresh surface is a dark yellowish brown (10 YR 4/2).	0.4
Unit 67	100% Covered slope forming interval.	1.0
Unit 66	Ledgy, olive gray (5 Y 4/1) weathering grainstones. Fossils include pelmatozoan debris and brachiopods. Other carbonate grains found in unit are ooids and intraclasts. Intraclasts are only found at the top of the unit and may indicate submarine or subaerial exposure of unit. Fresh surface is an olive black (5 Y 2/1).	0.25
Unit 65	Mostly covered, slope forming, pale red (5 R 6/2) weathering, lime mudstone. Unit is shale-like and contains grainstone (?) clasts. This may represent a paleosol developed on an exposure surface. Fresh color is a grayish red (10 R 4/2).	0.15
Unit 64	Ledge forming, light olive gray (5 Y 5/2) weathering, burrowed, oolitic grainstone. Common fossils include brachiopods and pelmatozoan debris. Upper surface is irregular and has a reddish tint. The middle of this unit also has thin, 10cm, reddish, conglomeratic layer. This may also be an exposure surface. Fresh surface is an olive gray (5 Y 3/2).	1.0
Unit 63	Ledgy, dark yellowish brown (10 YR 4/2) weathering, trough cross-bedded, siltstone. The lower surface is erosional and irregular with unit 62. The upper surface is slightly hummocky. Unit is identical to unit 59. Fresh surface is a moderate brown (5 YR 3/4).	0.3
Unit 62	Ledge forming, mottled olive gray (5 Y 3/2) weathering, horizontally laminated grainstone. Common fossils are brachiopods, pelmatozoan debris and unidentifiable fragments. Upper surface is erosional with overlying unit 63. Fresh surface is an olive black (5 Y 2/1).	0.8
Unit 61	Slope forming, pale yellowish brown (10 YR 6/2) weathering, interbedded silty packstones and siltstones. Both carbonates and siliciclastics are trough cross-bedded. Fresh surface is a moderate yellowish brown (10 YR 5/4).	1.4
Unit 60	Ledge forming, medium light gray (N 6) weathering, grainstone with silt filled burrows. Common fossils include pelmatozoan debris and brachiopods. Ooids are fairly abundant. Fresh surface is a dusky yellowish brown (10 YR 2/2).	0.79
Unit 59	Ledge forming, moderate yellowish brown (10 YR 5/4) weathering, horizontally laminated oolitic grainstone. Common fossils include brachiopods, pelmatozoan debris, rare fenestral bryozoans and a variety of unidentifiably fragments. Ooids are very abundant in this unit. Fresh surface is a grayish red (10 R 4/2).	0.7
Unit 58	Ledge forming, dark yellowish brown (10 YR 4/2) weathering, cross-	0.9

Unit	Description	Thickness (m)
	bedded siltstone. Thin oolitic bed is present in the center of this unit. Ooids rest on a slightly irregular surface. Fresh surface is an olive black (5 Y 2/1).	
Unit 57	100% covered slope forming interval.	2.2
Unit 56	Ledge forming, olive gray (5 Y 4/1) weathering, oolitic grainstone. Common fossils include brachiopods, fenestral bryozoans, and pelmatozoan debris. Fresh surface is a brownish black (5 YR 2/1).	0.5
Unit 55	Ledge forming, pale olive (10 Y 6/2) weathering, packstone. Common fossils include brachiopods, pelmatozoan debris, fenestrate bryozoans, gastropods and trilobites. Ooids are also distributed throughout the unit. Small vertical burrows filled with silt occur throughout the unit. Fresh surfaces is an olive gray (5 Y 3/2).	1.5
Unit 54	Ledgy, light brown (5 YR 6/4) weathering, fossil bearing, cross-bedded siltstone. Rare fossils include fenestrate bryozoans and brachiopods. Cross-bedding is very low angle and trough shaped. Lower surface is slightly irregular indicating some degree of erosion. In places the unit has down cut over 1/2m into the underlying limestones of unit 53. Fresh surfaces is a pale yellowish brown (10 YR 6/2)	0.5
Unit 53	Ledge forming, yellowish gray (5 YR 7/2) weathering, grainstones. Lower 1/3 is cross-bedded and contains <i>Archimedes</i> . The upper 2/3s of the unit becomes increasingly more ooid rich and horizontally laminated. Common fossils include pelmatozoan debris, brachiopods and fenestrate bryozoans. Rare intraclasts occur in the lower cross-bedded portion. The lower contact is irregular with unit 52. Fresh surface is an olive gray (5 Y 3/2).	1.3
Unit 52	Ledgy, pale yellowish brown (10 YR 6/2) weathering, horizontally laminated, siltstones. No macrofossils. Fresh surface is a grayish brown (5 YR 3/2).	0.16
Unit 51	100% Covered, slope forming unit.	1.3
Unit 50	Ledgy, greenish gray (5 GY 6/1) weathering, grainstone. Common fossils include pelmatozoan debris, brachiopods and fenestrate bryozoans. Common abiotic grains include intraclasts and ooids. The intraclasts and brachiopods tend to be concentrated in the upper 10 cm of the unit. Fresh surface is an olive gray (5 Y 4/1).	0.9
Unit 49	Partially covers, slope forming, light olive gray (5 Y 5/2) weathering grainstone. Common fossils include pelmatozoan debris and brachiopods. Abiotic grains consist of ooids and dark gray intraclasts. Fresh surface is an olive gray (5 Y 4/1).	0.3
Unit 48	Ledgy, grayish orange (10 YR 7/4) weathering packstone. Common fossils include brachiopods, pelmatozoan debris and gastropods. Rare ooids are also found distributed throughout the unit. Fresh surface is a light olive gray (5 Y 5/2).	0.25
Unit 47	Ledgy, light olive brown (5 Y 5/6) weathering, thinly-bedded, trough cross-bedded siltstone. Upper surface with unit 48 is irregular. Fresh surface is a light olive gray (5 Y 5/2).	0.3
Unit 46	Ledge forming, dusky yellow (5 Y 6/4) weathering, silty, cross-bedded lime mudstone which is capped by a 5 cm thick oolitic grainstones. Unit is burrowed by <i>Chondities</i> . The upper oolitic bed also contains brachiopods and pelmatozoan debris. Fresh surface is an olive black (5 Y 2/1).	0.6
Unit 45	Ledge forming, olive gray (5 Y 4/1) weathering, oolitic grainstones. Common fossils include brachiopod fragments and pelmatozoan debris.	0.5

Unit	Description	Thickness (m)
	The lower half of the unit is burrowed. Burrows are filled with lime mud. Fresh surfaces have a potent fetid odor. Fresh surface is an olive black (5 Y 2/1).	
Unit 44	Mostly covered, ledgy, moderate yellowish brown (10 YR 5/4) weathering, trough cross-bedded, silty peloidal grainstone. Upper 1/3 of unit trough cross-bedding becomes more tabular. No macrofossils. Fresh color is an olive black (5 Y 2/1).	0.9
Unit 43	Mostly covered, slope forming, pale olive (10 YR 6/2) weathering, interbedded shales (?) capped by an oolitic grainstone. Ooids are limonite stained and have a yellowish tint. Common fossils in the oolitic grainstones are pelmatozoan debris, brachiopods and fenestral bryozoans. Fresh surfaces is a moderate olive brown (5 Y 4/4).	0.7
Unit 42	Ledge forming, pale yellowish brown (10 YR 4/2) weathering, grainstone. Common fossils include abundant brachiopods, pelmatozoan debris and fenestrate bryozoans. Small ooids are fairly common throughout the unit. Crude horizontal laminations are also present. Fresh surface is a dark yellowish brown (10 YR 4/2).	0.7
Unit 41	100% covered slope forming interval.	1.0
Unit 40	Ledge forming, pale yellowish brown (10 YR 4/2) weathering, burrowed, oolitic grainstones. Herring bone cross-bedding in unit indicates tidal currents. Burrows are vertical and are filled with lime mud. Burrows may be a variety of <i>Skolithos</i> . Fresh surface is a dusky yellowish brown (10 YR 2/2).	0.3
Unit 39	Ledge forming, dark yellowish brown (10 YR 4/2) weathering, grainstone. Ooids are common throughout the unit. Common fossils include brachiopods, pelmatozoan debris, fenestrate bryozoans and unidentifiable fossil fragments. Upper surface of unit is heavily burrowed. Burrows are indistinct. Fresh surface is a dusky brown (5 YR 2/2).	0.4
Unit 38	Ledge forming, pale yellowish brown (10 YR 6/2) weathering, silty, packstones and grainstones. Common fossils are brachiopods, pelmatozoan debris and fenestrate byozoans. Ooids are distributed throughout the unit, but are most common in the upper 15 cm. Fresh surface is a pale yellowish orange (10 YR 8/6).	0.4
Unit 37	Partially covered, slope forming, reddish-brown weathering shale. No macrofossils.	0.7
Unit 36	Ledgy, light olive gray (5 Y 6/1) weathering, oolitic grainstones. Common fossils include brachiopods and pelmatozoan debris. Surface is slightly mottled similar to an exposure surface. Fresh surface is a light gray (N 7).	1.0
Unit 35	Ledge forming, brownish gray (5 YR 4/1) weathering, burrowed grainstone. Common fossils are pelmatozoan debris, brachiopods and fenestrate bryozoans. Burrows are sub-horizontal and vertical. They are filled with lime mud. Fresh surface is a light gray (N 7).	0.9
Unit 34	Ledge forming, pinkish gray (5 YR 8/1) weathering oolitic grainstones. Only fossils in unit are rare brachiopods. Fresh surface is a brownish gray (5 YR 4/1).	1.6
Unit 33	Ledge forming, olive gray (5 Y 5/2) weathering, silty packstone. Common fossils are brachiopods, pelmatozoan debris, fenestral bryozoans and gastropods. Fresh surface is a medium dark gray (N 4).	0.4
Unit 32	Cliff forming, light olive gray (5 Y 5/2) weathering packstones and grainstones. Lower 30 cm of unit contains tabular cross-bed sets.	3.8

Unit	Description	Thickness (m)
Unit 31	Common fossils are brachiopods, pelmatozoan debris and fenestrate bryozoans. Ooids become more common in the upper .7 m. Fresh surface is a dark gray (N 3). Partially covered, Light brownish gray (5 YR 6/1) weathering grainstones. Common fossils are brachiopods, pelmatozoan debris, <i>Archimedes</i> , fenestrate bryozoans and branching bryozoans. Fresh surface is a light gray (N 7).	3.4
Unit 30	Ledge forming, pale yellowish brown (10 YR 6/2) weathering, grainstones. Common fossils are brachiopods, pelmatozoan debris, fenestrate bryozoans and gastropods. Single fish tooth exposed on upper surface. Ooids are present but not common. Fresh surface is a dusky yellowish brown (10 YR 2/2).	0.9
Unit 29	Ledgy, pale yellowish brown (10 YR 6/2) weathering, pelmatozoan packstones to grainstones. Faint trough cross-bedding is visible throughout the unit. Common fossils are pelmatozoan debris and rare brachiopods. Fresh surface is a light olive gray (5 Y 6/1).	0.3
Unit 28	Mostly covered, ledgy, pale yellowish brown (10 YR 6/2) weathering, nodular, silty lime mudstones. Rare horizontal burrows on some bedding planes. Rare pelmatozoan debris is present throughout the unit. Fresh surface is a dark yellowish brown (10 YR 4/2).	1.6
Unit 27	Ledge forming, light brownish gray (5 YR 6/1) weathering, oograinsone. Minor horizontal laminations are present. Common fossils are brachiopods and pelmatozoan debris. Ooids are abundant throughout the unit. Fresh surface is a medium light gray (N 6).	1.0
Unit 26	Ledgy, pale yellowish brown (10 YR 6/2) weathering, nodular packstones. Common fossils are small pelmatozoan debris, brachiopods and gastropods. Rare small ooids are found throughout the unit. Fresh surface is a dusky yellowish brown (10 YR 2/2).	0.4
Unit 25	100 % covered, slope forming interval.	1.3
Unit 24	Ledge forming, very pale orange (10 YR 8/2) weathering oograinsone. Common fossils are pelmatozoan debris, brachiopods and fenestrate bryozoans. Ooids are common throughout the unit. Horizontal burrows are present in the lower 1/3 of the unit. Fresh surface is a dark yellowish brown (10 YR 4/2).	0.8
Unit 23	Slope forming, grayish orange (10 YR 7/4) weathering, packstone. Common fossils are pelmatozoan debris and abundant unidentifiable fossils fragments. Fresh surface is a dusky yellowish brown (10 YR 2/2).	1.7
Unit 22	Ledgy, dark yellowish orange (10 YR 6/6) weathering oograinsone. Common fossils are brachiopods, pelmatozoan debris, straight nautiloids and fenestrate bryozoan fragments. Ooids are very common throughout the unit. Fresh surface is a moderate yellowish brown (10 YR 5/4).	0.4
Unit 21	Partially covered, pale yellowish orange (10 YR 8/6) weathering interbedded shales, siltstones and wackestones. Siltstones are not fossiliferous. Common fossils in the wackestones are brachiopods, and pelmatozoan debris. Fresh surface is a moderate yellowish brown (10 YR 5/4).	4.3
Unit 20	Ledgy, dark medium gray (N 4) weathering grainstone. Common fossils are brachiopods, pelmatozoan debris, fenestrate bryozoans and mollusks. Fresh surface is a dark gray (N 3).	0.3
Unit 19	Cliffy, olive gray (5 Y 4/1) weathering silty packstones. Ooids are common and distributed throughout the unit. Common fossils are brachiopods with rare pelmatozoan fragments. Fresh surface is a	2.4



Unit	Description	Thickness (m)
Unit 18	brownish gray (5 YR 4/1). 100% covered, slope forming interval, lime mudstone?	2.0
Unit 17	Ledge forming, grayish orange (10 YR 7/4) weathering, silty grainstone. Common fossils include brachiopods, mollusks and pelmatozoan debris. Fresh surface is a dark gray (N 3).	0.3
Unit 16	Mostly covered, dark yellowish brown (10 YR 4/2) weathering interbedded shales and packstones. Common fossils in the packstones are brachiopods and pelmatozoan debris. Fresh surface has a strong fetid odor, and is a light brownish gray (5 YR 6/1).	1.1
Unit 15	Ledge forming, light olive gray (5 Y 6/1) weathering, horizontally laminated oograins. Ooids are very common and are distributed throughout. Common fossils are brachiopods, pelmatozoan debris, mollusks, fenestrate bryozoans and <i>Archimedes</i> . A single shark tooth was exposed on the upper surface of the unit. Fresh surface is a medium gray (N 5).	1.2
Unit 14	Ledgy, partially covered, light brownish gray (5 YR 6/1) weathering lime mudstone. No visible macrofossils. Fresh surface is a very dusky red (10 R 2/2).	0.8
Unit 13	Ledge forming, brownish gray (5 YR 4/1) weathering grainstone. Lower part of unit is conglomeratic. Clasts are rounded and are internally stratified. Upper part of unit is horizontally laminated. Common fossils are pelmatozoan debris, brachiopods, gastropods and unidentifiable fragments. Ooids are common and distributed throughout the unit. Fresh surface is a Medium dark gray (N4).	1.7
Unit 12	Slope forming, mostly covered, light gray (N7) weathering lime mudstone. No macrofossils. Fresh surface is a dark gray (N4).	0.3
Unit 11	Ledgy, pinkish gray (5 YR 8/1) weathering packstone to grainstone. Lower contact with unit 10 is irregular, but sharp. Common fossils are brachiopods, pelmatozoan debris and rare fenestrate bryozoans. Fresh surface is a light brownish gray (5 YR 6/1).	0.4
Unit 10	Mostly covered, pinkish gray (5 YR 8/1) weathering, packstone. Common fossils are fenestrate bryozoans, brachiopods and pelmatozoan debris. Fresh surface is an olive gray (5 Y 4/1).	0.06
Unit 09	Ledge forming, light brownish gray (5 YR 6/1) weathering oograins. Ooid rich grainstones which have a slight hint of horizontal stratification to them. Rare brachiopods and pelmatozoan fragments are distributed throughout the unit. Fresh surface is a medium gray (N5).	4.3
Unit 08	Cliffy, banded, grayish orange pink (5 YR 7/2) weathering interbedded siltstones and packstones. There minor chertification of some of the tan siltstones. Common fossils are pelmatozoan debris and brachiopods. Minor subhorizontal burrowing is present throughout the unit. Fresh surface is a brownish gray (5 YR 4/1).	2.2
Unit 07	Ledgy, light gray (N7) weathering lime mudstones and wackestones. Common fossils are brachiopods, pelmatozoan debris and fenestrate bryozoans. Fresh surface is an olive gray (5 Y 4/1).	1.6
Unit 06	Ledge forming, medium gray (N5) weathering, grainstones. Minor horizontal stratification is present throughout the unit. Common fossils are pelmatozoan debris and brachiopods mixed in with abundant unidentifiable fragments. Ooids are common and distributed throughout the unit. Fresh surface is a brownish gray (5 YR 4/1).	4.1
Unit 05	Ledge forming, grayish pink (5 R 8/2) weathering, silty grainstones with	1.6

Unit	Description	Thickness (m)
Unit 04	minor horizontal stratification. Common fossils are pelmatozoans, brachiopods and fenestrate bryozoans. Ooids are present, but not in any significant volume. Fresh surface is a moderate olive brown (5 Y 4/4). Ledge forming, grayish orange (10 YR 7/4) weathering packstones and grainstones. Common fossils are brachiopods, pelmatozoan debris, fenestrate bryozoans and rare solitary rugosan corals. Ooids are very common and are distributed throughout the unit. Fresh surfaces is a pale brown (5 YR 5/2).	4.7
Unit 03	Ledgy, grayish orange (10 YR 7/4) weathering, silty grainstones. Current ripple laminates are found throughout the unit. Common fossils are brachiopods and pelmatozoan debris. Fresh surface is an olive gray (5 Y 4/1).	1.1
Unit02	Ledge forming, pale yellowish brown (10 YR 6/2), grainstone. Horizontal stratification present throughout. Very coarse fossil grains include brachiopods and pelmatozoan debris. Lower contact with unit 01 is irregular and may be a submarine erosional surface. Fresh surface is a moderate brown (5 YR 3/4).	0.9
Unit 01	Ledgy, light brownish gray (5 YR 6/1) weathering, silty grainstone. Small scale ripple laminates are present throughout the unit. Common fossils are pelmatozoan debris and peloids. Fresh surface is a light olive gray (5 Y 6/1).	0.4

Total measured thickness of the Paradise Formation: 133.2m

#### *Base of Paradise Formation*

Contact with underlying Escabrosa Group is sharp and conformable. It is place where the thick-bedded cherty, pelmatozoan-rich grainstones change to thinly-bedded, silty, cross-bedded limestones of the basal Paradise Formation.

## Chaney Canyon Measured Section, Big Hatchet Mountains

(NW 1/4, Sec. 6, T31S, R15W) Hidalgo County, New Mexico

This section is located high up along the southern side of Chaney Canyon on the northwestern side of the Big Hatchet Mountains. Strata strike N-57-W and dip 11° to the southwest. Dip increases to 32° up section with the strike remaining constant. Section was measured using 1.5m Jacob's staff and brunton compass.

### *Top of Section*

Horquilla Limestone not measured

*Top of Paradise Formation.* Contact with overlying Horquilla Limestone is sharp and disconformable.

Unit	Description	Thickness(m)
Unit 12	Partially covered, slope forming, medium gray (N 5) weathering siltstone. Unit is void of primary sedimentary structures. Both the upper and lower contacts are sharp. Fossils include brachiopods and pelmatozoans. There is no evidence suggestive of an erosional surface between this unit and the overlying Pennsylvanian Horquilla Limestone. Fresh surface is a dark greenish gray (5 GY 4/1).	0.4
Unit 11	Partially covered, slope forming, medium gray (N 5) weathering, dolomitic lime mudstone. Unit is void of any sedimentary structures. Both upper and lower contacts are sharp. No macrofossils. Fresh surface is an olive gray (5 Y 6/1).	0.3
Unit 10	Ledge forming, olive gray (5 Y 6/1) weathering, highly indurated very fine-grained sandstone. Unit contains abraded and broken fossil fragments. Both upper and lower contacts are sharp. Recognizable fossils are brachiopods and pelmatozoan fragments. Fresh surface is an olive black (5 Y 2/1).	0.8
Unit 09	95% covered, slope forming, medium gray (N 5) weathering lime mudstone. No macrofossils or sedimentary structures. Fresh surface is a dark gray (N 3).	2.5
Unit 08	Ledgy, pale yellowish brown (10 YR 6/2) oolitic grainstone. Unit is very distinctive. Lower surface is slightly irregular, but appears conformable. No visible macrofossils or sedimentary structures. Fresh surface is a brownish gray (5 YR 4/1).	0.3
Unit 07	Cliff forming, medium light gray (N 6) weathering, thick-bedded lime mudstone. Fresh color is dark gray (N 3).	2.4
Unit 06	Mostly covered, medium light gray (N 6) weathering, nodular lime mudstone. No macrofossils. Upper surface is slightly irregular with unit 07. Fresh surface is a medium dark gray (N 4).	1.0
Unit 05	Ledge forming, light olive gray (5 Y 6/1) weathering, silty, biotubated packstone. Fossils include pelmatozoans, brachiopods, and mollusks. Fresh surface is an olive gray (5 Y 4/1) color.	0.8

Unit	Description	Thickness(m)
Unit 04	Mostly covered, slope forming, olive gray (5 Y 4/1) weathering, lime mudstone. Slight hint of horizontal laminates in the exposed beds. No macrofossils. Fresh surface is an olive black (5 Y 2/1).	3.9
Unit 03	Ledge forming, light olive gray (5 Y 6/1) weathering grainstone. Unit is fossiliferous with abundant pelmatozoan debris, brachiopods, and rare tabulate corals. The upper 1/3 of the unit is distinctly striped with herringbone cross-stratification. Fresh surface is a dark greenish gray (5 GY 4/1).	1.45
Unit 02	Somewhat covered, ledgy, light olive gray (5 Y 6/1) weathering pelmatozoan packstones. Fossils are dominated by pelmatozoan debris with rare brachiopod fragments. No distinctive sedimentary structures. Fresh surface is an olive gray (5 Y 4/1).	2.0
Unit 01	Mostly covered, slope forming, light gray (N 7) weathering, wackestones and packstones. Fossils include pelmatozoan debris, brachiopods, and fenestral bryozoans. Fresh surface is a dark gray (N 3).	1.6
Total measured Paradise Formation:		17.45 m

*Base of exposed Paradise Formation*

Contact with underlying Escabrosa Group is covered. Section begins in a craggy, covered arroyo due south of the termination of Chaney Canyon road.

## **APPENDIX C**

### Thin Section Point Count Data

## **APPENDIX C**

Thin Section Point Count Data

## APPENDIX C

Abundance data from thin section point counts for samples collected from the Paradise Formation in the Big Hatchet Mountains, Hidalgo County, New Mexico are given as a percent volume of the whole rock.

The following names and abbreviations are used throughout the following tables:

**Pelm**-Pelmatozoans; **Im**-Impunctate Brachiopods; **Pn**-Punctate Brachiopods; **Ps**-Pseudopunctate Brachiopods; **Tbrachs**-Total Brachiopods; **Fen**-Fenestrate Bryozoa; **Arch**-*Archimedes* Bryozoa; **En**-Encrusting Bryozoa; **TBry**-Total Bryozoa; **Bi**-Bivalve; **G**-Gastropod; **C**-Cephalopod; **TMol**-Total Mollusks; **Tri**-Trilobite; **Pel**-Pellet; **Oo**-Ooids; **Int**-Intraclasts; **For**-Foraminifera; **Cal**-Calcisphere; **Q**-Detrital Quartz; **Sp**-Sparite Cement; **M**-Micrite; **PsM**-Pseudospar; **TLM** Total Lime Mud; **Dol**-Dolomite; **Ch**-Chert; **Op**-Opaque; **Ot**-Other





Table C-1 - Continued

Slide	Brachiopods										Bryozoans										Mollusks										
	PeIn	Im	Ph	Ps	TBrachs	Fen	Arch	En	Tw	TBy	Bi	G	C	TMol	Tri	Pel	Oo	Int	For	Cal	Q	Sp	M	PsM	TLM	Dof	Ch	Op	Ot		
HP-39	1.43	0.29	0.00	0.00	0.29	3.14	0.00	0.00	0.00	3.14	0.00	0.00	0.00	0.00	0.00	35.71	0.00	0.00	0.00	0.00	55.43	4.00	0.00	0.00	0.00	0.00	0.00	0.00	0.00	0.00	0.00
HP-40	64.86	3.71	0.00	0.00	3.71	23.14	0.00	0.00	0.00	23.14	0.00	0.00	0.00	0.00	0.00	0.00	0.29	0.00	0.00	0.00	tr	7.71	0.00	0.00	0.00	0.00	0.00	0.00	0.00	0.00	0.00
HP-40*	1.14	0.86	0.00	0.00	0.86	4.57	5.71	0.00	0.00	10.29	0.00	0.00	0.00	0.00	0.00	77.43	0.00	0.00	0.00	0.29	6.86	0.00	2.29	0.86	3.14	0.00	0.00	0.00	0.00	0.00	
HP-41	4.57	4.57	0.00	0.00	4.57	0.00	34.57	0.00	0.00	34.57	0.00	0.00	0.00	0.00	0.00	9.71	0.00	0.00	0.00	0.00	5.43	0.00	41.14	0.00	0.00	0.00	0.00	0.00	0.00	0.00	
HP-42	28.86	6.86	0.00	0.00	6.86	4.57	0.00	0.00	0.00	4.57	0.29	0.00	0.00	0.29	0.00	0.00	19.71	33.71	0.00	0.00	5.43	0.00	0.00	0.00	0.00	0.00	0.00	0.00	0.00	0.00	
HP-43	2.86	0.57	0.00	0.00	0.57	0.00	0.00	0.00	0.00	0.00	0.29	0.00	0.00	0.29	0.00	0.00	60.00	5.43	0.00	0.00	0.00	30.86	0.00	0.00	0.00	0.00	0.00	0.00	0.00	0.00	
HP-45	17.71	8.00	0.00	0.00	8.00	10.00	0.00	0.00	0.00	10.00	2.00	0.00	0.00	2.00	0.00	6.00	3.14	3.43	6.86	0.00	0.29	0.00	11.71	30.86	42.57	0.00	0.00	0.00	0.00	0.00	
HP-47	9.71	1.71	0.00	0.00	1.71	9.14	0.00	0.00	0.00	9.14	0.57	0.00	0.00	0.57	0.00	0.00	41.14	28.29	0.00	0.00	0.00	0.00	0.00	0.00	0.00	0.00	0.00	0.00	0.00	0.00	
HP-47a	36.57	0.29	0.00	0.00	0.29	2.29	0.00	0.00	0.00	2.29	0.00	0.00	0.00	0.00	0.00	0.00	12.57	42.57	0.00	0.00	0.00	9.43	0.00	0.00	0.00	0.00	0.00	0.00	0.00	0.00	0.00
HP-49	3.58	2.99	0.00	0.00	2.99	2.09	0.00	0.00	0.00	2.09	0.00	0.00	0.00	0.00	0.00	0.00	0.00	0.00	0.00	0.00	1.49	0.00	85.67	4.18	89.85	0.00	0.00	0.00	0.00	0.00	
HP-50	26.29	0.57	0.00	0.00	0.57	18.57	0.00	0.00	0.00	18.57	0.57	0.00	0.00	0.57	0.00	0.29	1.14	5.71	0.29	0.00	0.86	26.86	17.71	0.00	0.00	0.00	0.00	0.00	0.00	0.57	
HP-50a	20.57	3.43	0.57	0.00	4.00	5.71	0.00	0.00	0.00	5.71	1.71	0.00	0.00	1.71	0.00	0.00	30.57	17.14	0.00	0.00	0.00	20.29	0.00	0.00	0.00	0.00	0.00	0.00	0.00	0.00	
HP-51	22.29	6.00	0.00	0.00	6.00	6.00	0.00	0.00	0.00	6.00	5.71	0.29	0.00	6.00	0.29	9.43	4.86	2.29	0.00	0.00	15.43	25.71	1.71	0.00	1.71	0.00	0.00	0.00	0.00	0.00	
HP-51a	0.57	0.57	0.00	0.00	0.57	0.29	0.00	0.00	0.00	0.29	0.00	0.00	0.00	0.00	0.00	0.00	50.86	0.00	0.00	0.00	47.71	0.00	0.00	0.00	0.00	0.00	0.00	0.00	0.00	0.00	
HP-52	13.71	3.43	0.00	0.00	3.43	1.71	0.00	0.00	0.00	1.71	0.00	0.00	0.00	0.00	0.00	0.00	72.00	0.00	tr	0.00	4.86	4.00	0.00	0.00	0.00	0.00	0.00	0.00	0.00	0.00	0.00
HP-54	0.00	0.00	0.00	0.00	0.00	0.00	20.29	0.00	0.00	20.29	0.00	0.00	0.00	0.00	0.00	0.00	0.00	0.00	0.00	0.00	0.00	0.00	79.71	0.00	0.00	0.00	0.00	0.00	0.00	0.00	
HP-55	0.57	0.00	0.00	0.00	0.00	0.00	0.00	0.00	0.00	0.00	0.00	0.00	0.00	0.00	0.00	0.00	0.00	0.00	0.00	0.00	0.00	0.00	0.00	0.00	0.00	0.00	0.00	0.00	0.00	0.00	
HP-56	0.00	0.00	0.00	0.00	0.00	0.00	0.00	0.00	0.00	0.00	0.00	0.00	0.00	0.00	0.00	0.00	42.86	0.00	0.00	0.00	0.00	0.00	1.71	47.14	48.86	0.00	0.00	0.00	7.71	0.00	
HP-57	7.14	2.57	0.00	0.00	2.57	5.71	0.29	0.00	0.00	6.00	4.00	0.29	0.00	4.29	0.00	0.00	67.14	0.00	0.00	tr	0.00	0.00	9.71	23.14	32.86	0.00	0.00	0.00	0.00	0.00	
HP-58	0.00	0.00	0.00	0.00	0.00	0.00	0.00	0.00	0.00	0.00	0.00	0.00	0.00	0.00	0.00	0.00	37.14	1.71	0.00	0.00	4.00	0.00	0.00	37.14	37.14	0.00	0.00	0.00	0.00	0.00	
HP-59-2	0.00	0.00	0.00	0.00	0.00	0.00	0.00	0.00	0.00	0.00	0.00	0.00	0.00	0.00	0.00	0.00	0.00	0.00	0.00	0.00	100.00	0.00	0.00	0.00	0.00	0.00	0.00	0.00	0.00	0.00	
HP-60-2	3.71	4.29	0.00	0.00	4.29	1.43	0.00	0.00	0.00	1.43	0.86	0.00	0.00	0.86	0.00	0.00	57.86	0.00	0.29	0.00	1.14	0.00	13.43	26.00	39.43	0.00	0.00	0.00	0.00	0.00	
HP-60-2a	2.57	1.14	0.00	0.00	1.14	0.00	0.00	0.00	0.00	0.00	0.29	0.00	0.00	0.29	0.00	0.00	0.00	0.00	0.00	0.00	76.86	12.00	0.00	0.00	0.00	0.00	0.00	0.00	0.86	0.00	
HP-61-2	0.00	0.00	0.00	0.00	0.00	0.00	0.00	0.00	0.00	0.00	0.00	0.00	0.00	0.00	0.00	0.00	0.00	0.00	0.00	0.00	63.43	25.43	0.00	0.00	0.00	0.00	0.00	0.00	0.00	7.14	
HP-61-2	0.00	0.00	0.00	0.00	0.00	0.00	0.00	0.00	0.00	0.00	0.00	0.00	0.00	0.00	0.00	0.00	0.00	0.00	0.00	0.00	4.00	0.00	0.00	96.00	96.00	0.00	0.00	0.00	0.00	0.00	









## **APPENDIX D**

Tabulated Diversity Data From Thin-Section Analysis











**APPENDIX E**  
Stable Isotope Data

Table E-1 Stable isotope data, Paradise Formation, Big Hatchet Mountains. (wh-Whole rock, Cal- Calcite, Dol-Dolomite)

Sample	$\delta^{18}\text{O} \text{ ‰}$ (Corrected PDB)	$\delta^{13}\text{C} \text{ ‰}$ (PDB)	Material	Sample	$\delta^{18}\text{O} \text{ ‰}$ (Corrected PDB)	$\delta^{13}\text{C} \text{ ‰}$ (PDB)	Material
CH-1	-5.496	2.463	wh/Cal	HP-17b	-5.667	2.285	Pelmatzoan
CH-2	-7.567	1.470	wh/Cal	HP-5	-6.178	-5.613	Pelmatzoan
CH-3	-8.119	1.678	wh/Cal	HP-23	-10.027	1.101	Brachiopod
CH-4	-9.189	1.752	wh/Cal	HP-17b	-3.091	1.817	Brachiopod
CH-5a	-6.935	1.982	wh/Cal	HP-17a	-3.387	2.511	Brachiopod
CH-5b	-7.177	0.514	wh/Cal	HP-24b	-6.597	-1.203	Pelmatzoan
CH-6	-5.329	3.231	wh/Cal	HP-17a	-11.193	-1.593	Brachiopod
CH-7	-5.625	2.198	wh/Cal	HP-24b	-5.366	3.097	Brachiopod
CH-7	-5.637	2.120	wh/Cal	HP-24b	-4.226	-3.566	Pelmatzoan
CH-7b	-5.495	0.970	wh/Cal	HP-17a	-7.386	1.724	Ooid
CH-8	-6.149	1.727	wh/Cal	HP-17a	-5.086	1.689	Ooid
CH-10	-6.673	0.928	wh/Cal	HP-23	-15.397	-3.376	Spar Cement
CH-12	-6.770	0.932	wh/Cal	HP-3c	-17.423	-5.309	Spar Cement
CH-13	-6.220	1.783	wh/Cal				
HP-1	-5.109	0.611	wh/Cal				
HP-1a	-5.153	0.667	wh/Cal				
HP-2	-4.847	0.457	wh/Cal				
HP-3	-5.100	0.263	wh/Cal				
HP-3a	-4.862	0.364	wh/Cal				
HP-3c	-4.955	-0.820	wh/Cal				
HP-4	-5.724	-1.942	wh/Cal				
HP-5	-4.860	-3.047	wh/Cal				
HP-6	-5.592	-2.852	wh/Cal				
HP-7	-5.510	-0.257	wh/Cal				
HP-8	-6.181	0.074	wh/Cal				
HP-8b	-2.781	-1.020	wh/Dol				
HP-9a	-2.487	-1.222	wh/Dol				
HP-9	-5.816	-0.538	wh/Cal				
HP-9a	-5.830	-0.010	wh/Cal				
HP-11a	-4.679	-0.195	wh/Cal				
HP-11b	-6.015	-1.379	wh/Cal				
HP-11c	-5.884	-3.985	wh/Cal				
HP-12	-5.917	-4.861	wh/Cal				
HP-13	-5.356	-0.174	wh/Cal				
HP-14	-6.346	-1.605	wh/Cal				
HP-15	-5.653	1.420	wh/Cal				
HP-17a	-6.732	0.977	wh/Cal				
HP-17b	-5.648	1.575	wh/Cal				
HP-18	-6.880	1.006	wh/Cal				
HP-19	-5.851	2.083	wh/Cal				
HP-20	-6.064	2.351	wh/Cal				
HP-21'	-6.342	1.682	wh/Cal				
HP-21	-6.456	1.877	wh/Cal				
HP-23	-6.649	1.602	wh/Cal				
HP-23a	-5.783	-0.961	wh/Cal				
HP-23b	-5.538	-2.498	wh/Cal				
HP-24	-6.262	-0.683	wh/Cal				
HP-24b	-5.868	-3.430	wh/Cal				
HP-25	-6.065	-3.204	wh/Cal				
HP-27	-6.906	1.783	wh/Cal				
HP-28	-5.131	1.761	wh/Cal				
HP-32	-8.240	1.145	wh/Cal				
HP-32a	-6.355	1.690	wh/Cal				
HP-33	-6.304	-1.686	wh/Cal				
HP-34	-7.675	0.459	wh/Cal				
HP-36	-7.237	0.305	wh/Cal				
HP-37	-5.969	2.518	wh/Cal				
HP-38	-6.415	2.373	wh/Cal				
HP-39	-7.343	1.596	wh/Cal				
HP-40	-5.362	2.177	wh/Cal				
HP-41	-6.253	2.198	wh/Cal				
HP-41a	-6.085	1.907	wh/Cal				
HP-42	-6.446	2.435	wh/Cal				
HP-43	-6.315	2.215	wh/Cal				
HP-45	-5.827	2.528	wh/Cal				
HP-47	-5.940	2.118	wh/Cal				
HP-47a	-4.070	2.095	wh/Cal				
HP-49	-4.849	2.432	wh/Cal				
HP-50	-6.337	1.837	wh/Cal				
HP-50a	-5.699	2.134	wh/Cal				
HP-51	-5.944	1.665	wh/Cal				
HP-51a	-9.079	0.724	wh/Cal				
HP-52	-7.749	0.779	wh/Cal				
HP-54	-5.720	3.639	wh/Cal				
HP-55	-5.974	1.326	wh/Cal				
HP-56	-6.377	1.148	wh/Cal				
HP-57	-7.184	-1.030	wh/Cal				
HP-59-2	-6.822	0.433	wh/Cal				
HP-60-2a	-7.436	-0.191	wh/Cal				
HP-61-2	-7.065	0.577	wh/Cal				

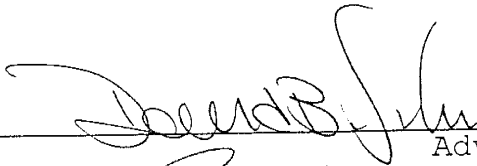
## VITA

David John Sivils was born in Columbus, Ohio, on March 2, 1960, to Dr. Jimmy C. Sivils and Marcia E. Sivils. After completing high school at Coronado High in El Paso, Texas he entered The University of Texas at El Paso in the fall of that year. He received both a Bachelor of Science and a Master's of Science degree with majors in geology from The University of Texas at El Paso. Following completing his Master's degree he entered the Ph.D. program at the University of Georgia and attended that institution for a year before transferring to the Geoscience Department at New Mexico Institute of Mining and Technology and entering the Ph.D. program. He has been employed as a development and exploration geologist with ARCO Oil and Gas Co., Unocal Oil and Gas Co., and Occidental International Exploration and Production Co. He is currently employed as a geologist with Texaco Exploration and Production Inc. in Midland, Texas.

Current address: Texaco Exploration and Production Inc.  
P.O. Box 3109  
Midland, Texas 79702

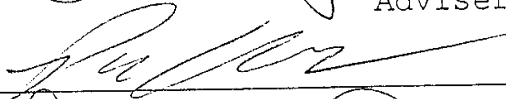
Permanent address: 659 Road Runner Lane  
Albuquerque, New Mexico 87122

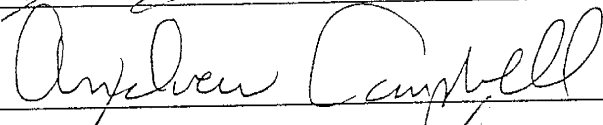
This dissertation is accepted on behalf of the faculty  
of the Institute by the following committee

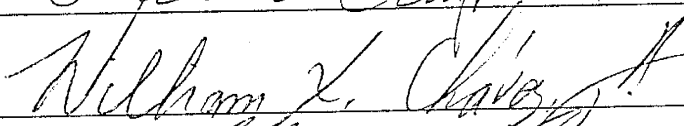


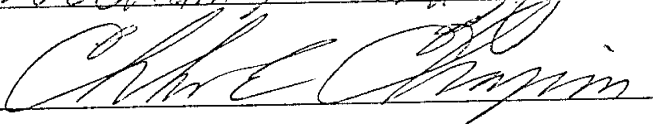
Adviser

12/18/97



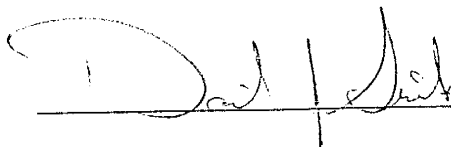


 90 December, 1997

 12/9/97

Date

I release this document to New Mexico Institute of Mining  
and Technology.



Student's Signature

12/15/97

Date